ETH zürich

Diss. ETH No. 30202

NAVIGATING CELLULAR COMPLEXITY IN PLASMONIC PHOTOTHERMAL THERAPY: A STANDARDISED *IN VITRO* PROTOCOL

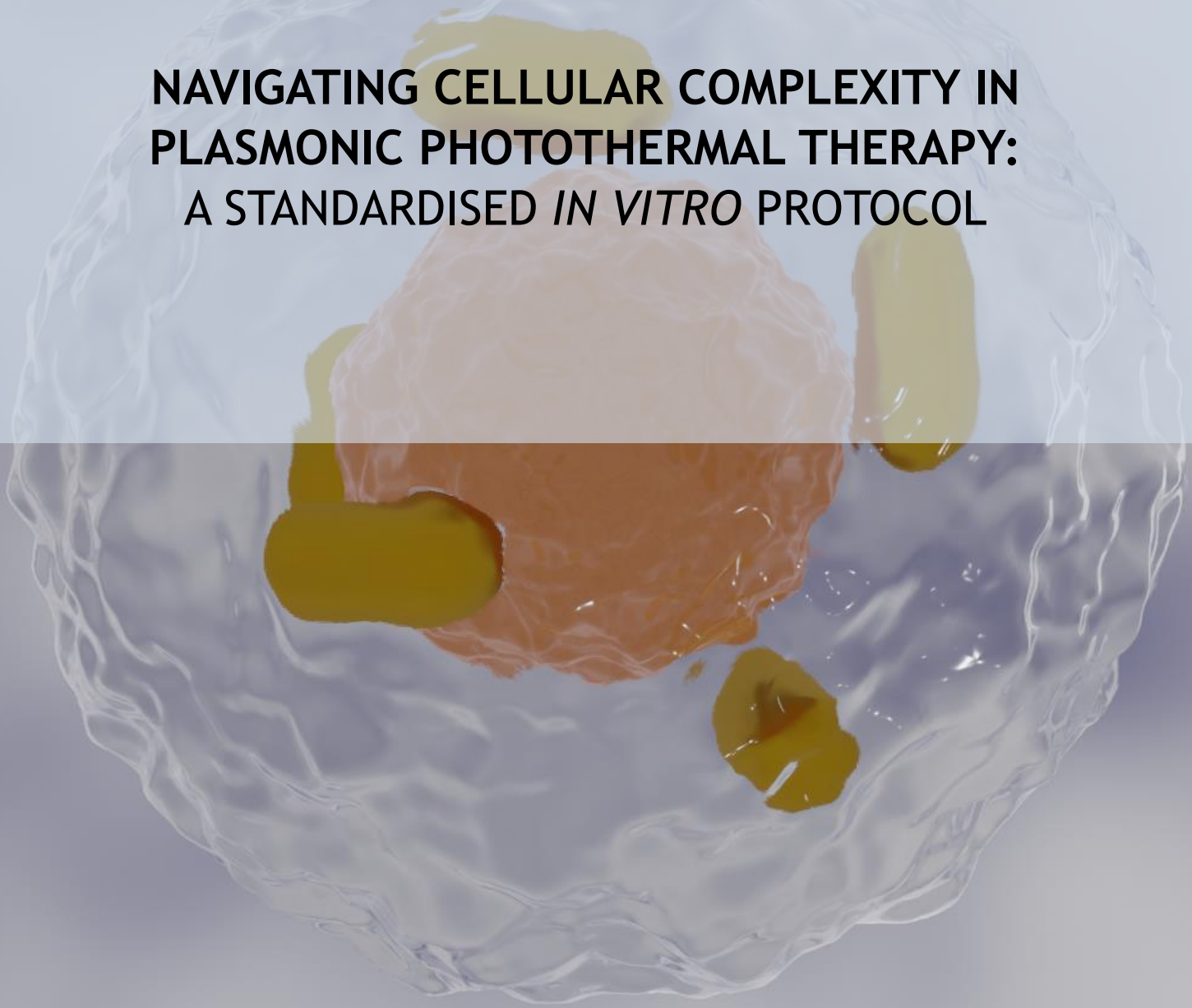

Helena Villuendas Garcia

Zürich 2024

Diss. ETH No. 30202

Navigating cellular complexity in plasmonic photothermal therapy: a standardised *in vitro* protocol

A thesis submitted to attain the degree of

DOCTOR OF SCIENCES

(Dr. sc. ETH Zurich)

Presented by

Helena VILLUENDAS GARCIA

MSc in Translational Medicine, Universitat de Barcelona

Born on 17.06.1995

accepted on the recommendation of

Prof. Romain Quidant (Examiner)

Dr. Clara Vilches (Co-examiner)

Prof. Inge Herrmann (Co-examiner)

2024

Abstract

Plasmonic photothermal therapy (PPTT) emerges as a transformative approach for cancer treatment at the intersection of nanophotonics, biotechnology and cell biology, promising to overcome the limitations of conventional cancer treatments. In PPTT, gold nanoparticles are illuminated to induce localised heating, selectively targeting malignant cells in a minimally invasive treatment. However, despite its potential, the lack of comprehensive data and clarity on the reporting of crucial parameters of PPTT hampers its adoption into clinical settings. Moreover, while PPTT is strongly dependent on the cell line, available data are sparse.

To address this gap, we established a standardised guideline for *in vitro* PPTT experimentation, covering the main aspects of research, including nanomaterials, biological samples and comprehensive pre-, during and post-irradiation characterisation. Adhering to this framework, our study systematically investigated the cytotoxicity and uptake of gold nanorods (AuNRs) across various cancerous and non-cancerous cell lines derived from diverse tissues. Our findings revealed differences in uptake and cytotoxicity across cell lines, with AuNR concentration demonstrating a direct link with toxicity. After PPTT, the cell death mechanism triggered depended on the intensity of the irradiated light, and the resulting temperature increase, placing importance on monitoring cell viability over time. We observed a preferential activation post-PPTT of programmed cell death, prompting the evaluation of the involvement of specific proteins in the apoptotic pathway, and a comparative analysis with conventional heating methods. Additionally, we evaluated the cytokine secretion capacity in immune cells, to reveal possible pro-inflammatory signals after PPTT.

Our systematic approach to study *in vitro* PPTT highlighted significant variances in the susceptibility of different cell lines and tissues to targeted plasmonic hyperthermia, with the added value of simultaneous evaluation of viability in different cell times with complementary approaches at more than one timepoint, underscoring cell death as a dynamic process. This dissertation offers valuable insight into the efficacy and mechanisms underlying PPTT, laying the foundations to refine the therapy, e.g. optimising laser dosage and nanoparticle delivery strategies, enhancing therapeutic control and broadening applications beyond cancer treatment.

Zusammenfassung

Plasmonische Photothermale Therapie (PPTT) etabliert sich als ein innovativer Ansatz für die Krebsbehandlung an der Schnittstelle von Nanophotonik, Biotechnologie und Zellbiologie und verspricht, die Grenzen herkömmlicher Krebstherapien zu überwinden. Bei der PPTT werden Goldnanopartikel beleuchtet, um eine lokalisierte Erwärmung zu induzieren und somit bösartige Zellen gezielt in einer minimalinvasiven Behandlung anzusprechen. Trotz ihres Potenzials behindert der Mangel an umfassenden Daten und Klarheit bei der Berichterstattung über wichtige Parameter der PPTT deren Einführung in klinische Umgebungen. Darüber hinaus sind die verfügbaren Daten zur PPTT stark von der Zelllinie abhängig, jedoch spärlich.

Um diese Lücke zu schließen, haben wir eine standardisierte Richtlinie für in-vitro-PPTT-Experimente entwickelt, die die wichtigsten Aspekte der Forschung abdeckt, einschließlich Nanomaterialien, biologischer Proben und umfassender Charakterisierung vor, während und nach der Bestrahlung. Unter Einhaltung dieses Rahmens untersuchte unsere Studie systematisch die Zytotoxizität und Aufnahme von Goldnanorods (AuNRs) in verschiedenen Krebs- und nicht-krebsartigen Zelllinien verschiedener Geweben. Unsere Ergebnisse zeigten Unterschiede in der Aufnahme und Zytotoxizität zwischen den Zelllinien, wobei die Konzentration von AuNR eine direkte Verbindung mit der Toxizität aufwies. Nach der PPTT hing der ausgelöste Zelltodmechanismus von der Intensität des Lichts und dem resultierenden Temperaturanstieg ab, was die Überwachung der Zellviabilität im Laufe der Zeit wichtig macht. Wir beobachteten eine bevorzugte Aktivierung des programmierten Zelltods nach der PPTT, was die Bewertung der Beteiligung bestimmter Proteine im apoptotischen Signalweg und einen Vergleich mit herkömmlichen Erwärmungsmethoden nahelegt. Darüber hinaus bewerteten wir die Fähigkeit zur Zytokinsekretion in Immunzellen, um mögliche proinflammatorische Signale nach der PPTT aufzudecken.

Unser systematischer Ansatz zur Untersuchung der in vitro PPTT zeigte signifikante Unterschiede in der Anfälligkeit verschiedener Zelllinien und Gewebe für die gezielte plasmonische Hyperthermie auf, wobei der zusätzliche Wert der gleichzeitigen Bewertung der Viabilität in verschiedenen Zellzeiten mit ergänzenden Ansätzen zu mehreren Zeitpunkten den Zelltod als einen dynamischen Prozess betonte. Diese Dissertation bietet wertvolle Einblicke in die Wirksamkeit und Mechanismen der PPTT und legt damit die Grundlagen zur Verfeinerung der Therapie, z. B. zur Optimierung der Laserdosierung und der Nanopartikel-Lieferstrategien, zur Verbesserung der therapeutischen Kontrolle und zur Erweiterung der Anwendungen über die Krebsbehandlung hinaus.

Contents

List of Figures

List of Tables

Acknowledgements

During the completion of this PhD, several people have played a decisive role in its success, and I would like to take this opportunity to thank them.

I would like to start by thanking Prof. Romain Quidant, for giving me the opportunity to do my master thesis and that its results granted me access to pursue a PhD in a project that really suited my interests. I also would like to thank the Institute of Photonic Sciences (ICFO) for providing, together with the group of Prof. Quidant (Plasmon Nano Optics), a very welcoming environment, full of scientific and social activities that expanded my scientific horizons and allowed me to participate in outreach activities of all types. I fondly remember my small contributions to the Women in Science month and participation in 100tifiques.

I also would like to thank everyone in the current group of Prof. Quidant at ETH, the Nanophotonic Systems Laboratory. Especially those with whom I have shared an office, coffee, or tabletop game, which must be everyone at this point. The spontaneous breaks, coffees and conversations were highlights of very busy days. I truly appreciated everyone that brought sweets and snacks, game changers when the sun didn't shine in Zürich for weeks. Some special thanks go to:

Alexia, for introducing me to hiking, brunch and Switzerland. You are one of my closest friends and I do not even mind that every excursion with you has turned into an adventure, I really enjoy the controlled craziness you can bring into a normal hike in the beautiful Swiss scenery. I cannot wonder how the PhD would have been without meeting you, but I am happy I do not have to think about it. Thanks for everything, the rants, the science and knowing that I am not good with words.

Marc S and Rebecca, for being excellent friends and colleagues, and for sharing the joy of free snacks. I hope you enjoyed the entertainment I brought, even if my jokes occasionally came at one of your expenses (from the bottom of my heart). Together with Alexia, forming the Daily Rant Squad, we were able to let out our frustrations and talk about failed experiments.

To the office E17.2, aka the Gossip Office, for always closing the door.

No puedo olvidarme de agradecer el apoyo recibido por parte de mi familia, incluyendo cuando me mudé a Suiza, en medio de un doctorado y una pandemia, cuando nadie se lo esperaba. Gracias por escuchar cada día mis mil y una historias, por dejarme la salita durante toda la cuarentena, por los tuppers, comidas y cenas, y por recogerme del trabajo más de un fin de semana. Eternamente agradecida a las maletas llenas de jamón, queso, aceite y galletas, que siempre hacen las vueltas a Zúrich más amenas. Al fin llega una doctora a la familia, y está en los Alpes ;) Y en los Alpes tengo que dar las gracias a Ian, por dejarme hablar y hablar, y escucharme. Estos meses han sido mucho más fáciles a tu lado.

I Clara, et deixo la última perquè no se com agrair-te tot el que has fet en els últims anys, des de que vaig començar el projecte del Màster en el que no sabia res de cultiu cel·lular, fins al dia d'avui. Crec que la sort que he tingut amb tu de supervisora no la té tothom. Ets una persona todoterreno, que em motiva per seguir fent la feina ben feta, però també em recorda que hi ha coses més enllà del lab. Aquesta tesis no estaria aquí sense tu. Gràcies!

Finally, and a bit against the tradition of acknowledging everyone that has helped in the completion of this dissertation, I would like to thank my past self. As I revisit this thesis in the years to come, I would like to remember all the ups and downs of these many years of PhD. To myself, for stepping out of the comfort zone and relocating to a new country in the middle of a pandemic. In hindsight, I do not recommend anyone to start a laboratory from scratch whilst trying to get a PhD, in the middle of a plastic shortage and with zero experience talking with vendors. Nonetheless, I am grateful for the experience gained and to everyone that has accompanied me in this journey. Next time, I will try to leave out the stress, anxiety, and imposter syndrome. Please, enjoy this dissertation.

“Those who cannot be cured by medicine can be cured by surgery.

Those who cannot be cured by surgery, can be cured by fire.

Those who cannot be cured by fire, are indeed incurable.”

-Hippocrates (479-377)

1

Introduction

The human body operates optimally within a defined range of temperatures, ensuring the correct functioning of physiological processes at their maximal capacity. With an average temperature of 37ºC, the body retains its ability to function within slight deviations below and above this threshold.[1] However, prolonged exposure to extreme temperatures can impact specific molecular processes and induce irreparable damage to body tissues, leading to cellular demise, and death.

The significance of human temperature regulation has long been known, prompting historical applications of heat and cold as therapeutic modalities for certain diseases. Notably, the human body exhibits fever as a natural defence mechanism where temperature elevation, in response to bacterial and viral infection, is employed to combat and eliminate these. Heat for therapeutic purposes extends for more than five centuries,[2,3] and nowadays it is used as a treatment for rheumatic diseases (such as arthritis or fibromyalgia), sepsis and cancer.[4–6]

Hyperthermia, defined as an elevation in body temperature, encompasses a spectrum ranging from moderate increases (39-42ºC) to lethal levels (>42°C).[2] When used in a clinical scenario, hyperthermia can be broadly categorized into whole-body hyperthermia and localised hyperthermia. The latter is particularly preferable, as temperature elevation and its secondary effects are confined to a specific region of the body.

In oncology, heat is commonly used as an adjunct to conventional methods of treatment,[7] as it enhances the effectiveness of other treatment modalities. Notably, hyperthermia and radiotherapy can act synergistically.[8] But the method of application of heating for cancer treatment can delimit its uses. For instance, ultrasound hyperthermia is suitable for both superficial and deep regional tumours, while microwaves have higher effectivity for superficial tumours on certain regions.[2]

Hyperthermia for cancer treatment can be categorized into different modalities: thermal ablation (temperatures above 47°C, usually employed as a standalone therapy), thermal sensitisation (range of 41-45°C, as a sensibilisation technique for other methods), and as nanoparticle and drug delivery enhancement.[9,10] The latter involves locally increasing the temperature of a region of interest to increase blood blow and facilitate targeted delivery of nanoparticles or drugs,[10] whereas as a standalone modality, hyperthermia has demonstrated success in causing tumour shrinkage and, in some cases, complete eradication.[11–14]

The impact of hyperthermia is based on its thermal effects on tumours. Therefore, controlled heating is a crucial aspect to consider, requiring specialised equipment with sufficient power and steering capability to control the area of treatment. Additionally, precise measurement and control of heat distribution during treatment is essential.[15]

Given that cancer is the second leading cause of global mortality, with almost 10 million deaths in 2020,[16] improving treatments that selectively target cancerous cells is essential for reducing the secondary effects usually associated with more conventional methods of treatment. An innovative and targeted approach is plasmonic photothermal therapy (PPTT).

In recent years, the field of nanomedicine has been harnessing the unique properties of materials at the nanoscale. Many materials exhibit distinct characteristics at the nanoscale compared to when observed in bulk, opening avenues for many applications. Notably, the interaction between nanoparticles and light

has become a significant area of research. At first, heat losses produced with nanoparticle illumination were perceived negatively associated with their original application.[17] However, the potential of using localised heat generation for therapeutic purposes shifted engineering to deliberately enhance light to heat conversion.

The increasing interest in plasmonic nanoparticles led to their application in cancer therapy, specifically in PPTT. PPTT strategically exploits the enhanced optical absorption of noble metal nanoparticles, such as gold nanoparticles, to induce therapeutic hyperthermia in malignant cells upon exogenous illumination.[18,19] By irradiating the nanoparticles at their localised surface plasmon resonance (LSPR), there is controllable temperature generation, facilitating targeted and localised therapeutic effects.[20,21]

Gold nanoparticles (AuNPs) have attracted special attention in PPTT due to their unique combination of physical and chemical properties.[22,23] AuNPs exhibit robust light absorption in a specific range of wavelengths. The results of the interaction of nanoparticles with light, inducing their LSPR, relies on the coherent oscillation of free electrons of the metal. LSPR is strongly dependent on the illumination wavelength, nanoparticle shape and size.

Nanoparticles can be fashioned in a variety of shapes based on their intended applications. In the context of PPTT, rod-shaped gold nanoparticles (AuNR, gold nanorods) are advantageous due to their two absorption bands along the two axes of the rod. Controlling the aspect ratio of the rods enables shifting the excitation wavelength to the near-infrared (NIR) region,[21] aligning with the optical biological window, which extends from 700 to 980 nm. This trait makes AuNRs attractive for *in vivo* applications, as tissues have minimal light absorption at the NIR region.[24–26] When AuNRs are photoexcited at their LSPR resonance, they can efficiently convert photon energy into heat, whilst the use of a NIR laser light allows performing a minimally invasive therapy due to its deeper tissue penetration, reducing the risks associated with extensive surgery.

Nonetheless, nanoparticles are foreign bodies when introduced into the body, and this raises concerns regarding the consequences of potential adverse effects.[27–31] Importantly, the method of administration influences the observation of secondary effects. Intravenous (IV) administration distributes the nanoparticle throughout the entire body via the bloodstream, reaching the target tissue as well as healthy cells.[32–34] In contrast, intratumoral (IT) administration minimises the delivery of nanoparticles to undesired areas, but the nanoparticle distribution within the tumour is very confined to the insertion place.[35–37] The inherent toxicity of nanoparticles relies on factors such as shape, size, material and manufacturing. Accordingly, nanoparticle toxicity must be carefully considered and evaluated.

The prevalent method in AuNR synthesis is the seed-mediated method, developed by Nikoobakht *et al*.[38] and modified many times to better accommodate the specific requirements of each study.[33,38,39] This method involves the use of cetyltrimethylammonium bromide, most commonly known as CTAB, a highly toxic surfactant.[40,41] To mitigate its toxicity, CTAB can be replaced with more biocompatible moieties, including polyethylene glycol (PEG) or mercaptoundecanoic acid, or encapsulation methods.[41] PEGylation, for instance, not only improves biocompatibility but produces hydrophilic nanoparticles and increases blood circulation time, reduces recognition by the mononuclear phagocyte system (MPS) and helps evade the immune system, overall improving the status of nanoparticles to be administered *in vivo*. However, PEG can diminish overall cellular internalisation efficiency.[42,43]

Additional moieties can be fixed into nanoparticles to target specific body locations and cellular types.[44,45] Surface modifications with antibodies or peptides can provide specific biochemical interactions with tumour cells while avoiding healthy ones, improving targetability. However, nanoparticle functionalisation and targeting can be rendered invisible by the formation of a protein corona that covers these modifications.[30,46] Further studies on IV administration and protein corona formation are highly requested.

In the context of PPTT, other factors beyond nanoparticle toxicity can also be lethal to cells. Laser irradiation possesses a highly cytotoxic potential dependent on laser dosage (power density and time of

irradiation). Monitoring both nanoparticle and light toxicity, independently of each other, is a must. Moreover, laser power density should remain viable for healthy and cancerous cells in the absence of nanoparticles, preventing temperature elevation or cell damage in those regions where there is no overlap of plasmonic nanoparticles and laser irradiation.

In PPTT, the damaging effects of heat are localised at the intersection of plasmonic nanoparticles and light, resulting in selective destruction of specific cells. Only where the laser light strikes the nanoparticle LSPR there will be a local increase of temperature that triggers a series of molecular events that cause the demise of cancer cells. With precise control over illumination and temperature measurements, secondary effects are confined to specific regions, minimising overall damage.

While initially applied to cancer, PPTT holds the potential for various biomedical applications. Gold nanoparticles have already been tested in models of Alzheimer's disease to produce structural changes to αβ amyloid plaques. The introduction of PPTT could potentiate the unfolding effect of these gold nanoparticles and reduce the neuropathological effects of Alzheimer.[47,48] PPTT has been tested as a proof-of-concept for treatments ranging from retinal degenerative diseases,[49] hepatic fibrosis,[50] biofilm inhibition,[51] acne therapy and hair removal, on top of cancer treatments.[52–54] In addition, applications of PPTT will be manyfold when used as an adjuvant to other technologies.

Importantly, PPTT has already been employed for the treatment of prostate cancer in clinical trials in 2016, showing promising results with a significant percentage of the patients experiencing total ablation 12 months after irradiation.[55] However, the number of clinical trials on PPTT remain considerably lower compared to the extensive research performed on the topic at the pre-clinical level. To close this gap, and further advance PPTT, rigorous studies on various cell types, with high standards and reproducibility, are essential. Well-performed PPTT research at the pre-clinical stages, in addition to understanding the cellular reactions activated during treatment, will catapult its transition to clinical studies.

This dissertation aims to underscore the significance of *in vitro* studies as a fundamental basis for building strong pre-clinical models, identifying potential PPTT candidates and affected death molecular pathways. The objectives of this dissertation were to:

1. Determine non-toxic laser powers and irradiation times for non-cancerous cells and cells without nanoparticles.
2. Identify differences in the response to PPTT among different cell lines, focusing on uptake, nanomaterial cytotoxicity and response to treatment.
3. Examine differences at the molecular level, emphasizing the apoptotic pathways.
4. Detect distinct patterns of cytokine expression on immune T-cells after PPTT-induced hyperthermia.
5. Establish guidelines for the standardisation of *in vitro* PPTT studies for better understanding and development of the technique.

This comprehensive approach aims to propel PPTT research towards effective clinical applications, from the bench to the bedside.

2

Plasmonic photothermal therapy: past, present, and future challenges

Plasmonic photothermal therapy (PPTT) is a very interdisciplinary research topic where a landscape of disciplines work together with the same purpose: to develop a novel technique to treat cancer and other diseases with precision. The background of researchers involved in PPTT extends from physics, chemistry and material science to biology and medicine, and each discipline holds expertise in a specific area of PPTT. Communication and clarity in reporting key parameters and results from experimentation in PPTT are important to ensure comprehensive understanding between disciplines.

This chapter will explore some key concepts of PPTT, tracing its recent past, rapid evolution and future challenges. As research on PPTT involves various distinct factors, we will delve into hyperthermia, the development of nanotechnology and nanomedicine, the expansion of plasmonic gold nanoparticles, and PPTT. This will be done with a focus on human disease and emphasis on the goal of comprehension to a diverse array of disciplines.

2.1. Hyperthermia

Hyperthermia is the increase of body temperature over 39°C. It can be a natural process during a viral or bacterial infection as part of fever, raising the body temperature enough to eliminate those microorganisms.[5] This increase of temperature is very controlled, but prolonged periods of fever, or fevers higher than 40.5°C, can have serious side-effects and medical attention should be provided.

Therapeutic hyperthermia, on the other hand, is defined as raising the temperature of the entire body or a specific region above normal temperature for a defined duration.[2] In this case, temperature elevation in the body is induced externally. Given that maintaining normothermia is typically recommended for the patient well-being, whole-body hyperthermia is generally discouraged, and more targeted approaches have been developed. Habash[2] provides an extensive review detailing the classification of various types of therapeutic hyperthermia.

The method employed to induce hyperthermia have distinct advantages and disadvantages that will limit their application. Additionally, each heating approach results in different types of cellular damage. Traditional methods include ultrasound hyperthermia[56], radiofrequency and microwaves.[57,58] These are usually applied in combination with conventional cancer therapies to enhance the effectiveness of each other. For instance, ultrasound hyperthermia is a great sensitiser to radiotherapy, whereas radiofrequency and magnetic hyperthermia are usually combined with chemotherapy.[59]

Numerous combinations of hyperthermia and cancer treatments exist. Breast, bladder, head and neck and prostate cancer have been effectively treated with hyperthermia or combinations of elevated temperatures with other methods.[9,55,60] With the development of nanobiotechnology, the methods to induce hyperthermia continue to expand, consequently the range of cancers being successfully treated using these approaches continues to grow.

Hyperthermia can induce changes in cellular metabolism that can either produce a stress response that reduces cellular functionality, but cells are still viable, or if the heat stress is strong enough, trigger the cellular death mechanisms.

2.1.1. Molecular mechanisms triggered by hyperthermia

The mechanisms in which hyperthermia can impair cellular viability are manyfold and depend on the method of application, temperature, and exposure time, among others. One of the most detrimental effects of hyperthermia at the molecular level is the unfolding and aggregation of proteins. Protein denaturation causes the loss of the three-dimensional arrangement of amino acids in a protein, exposing hydrophobic regions to the medium. This loss of quaternary, tertiary and secondary structures lead to interactions with other proteins and aggregation. When protein structure is lost, its functions are inhibited, and cellular functionality and viability are vastly affected.

To prevent this, cells have a certain tolerance to heat stress dictated by the presence of basal levels of heat shock proteins (Hsps). Nonetheless, Hsps only offer a certain amount of protection to the negative effects of elevated temperatures. If heat is too elevated, instead of initiating the heat shock response and affecting molecular events inside the cells, the cell death program will be activated. Other important cellular alterations are described in the following sections.

2.1.1.1. Mitochondrial damage

Mitochondria are one of the most important organelles in the cell. They generate most of the energy required to produce the biochemical reactions needed in a cell. This energy is generated through oxidative phosphorylation in the mitochondrial respiratory chain. Alterations in their membrane potential and electron transport chain result in reduced production of ATP and cellular impairment. Moreover, loss of mitochondrial permeability and release of cytochrome C to the cytosol serve as inductors for apoptosis.[61,62] Nanoparticles that can heat up when irradiated are being specifically designed to target mitochondria (in particular tumour cell mitochondria) to increase cellular damage,[63] and many research papers report on mitochondrial damage and increased production of reactive oxygen species (ROS) after hyperthermia.[59,64,65]

Generation of ROS in the cell is necessary for many physiological processes and is closely associated to oxidative phosphorylation during cellular respiration in mitochondria. However, elevated production of ROS radicals renders cells reactive to oxidative stress and promotes apoptosis.[62,66]

2.1.1.2. Cell adhesion

Cellular architecture is a very important feature, *in vivo* and *in vitro*, as it governs the way cells move and interact. Epithelial cells have two main types of interactions, through cell-cell junctions as well as cell-matrix interactions. These connections control the orientation and behaviour of the cytoskeleton, which at the same time affect the intracellular location of organelles and can dictate cellular division.[67]

In the case of cancer, cellular adhesion is crucial, as the dissemination of cells from a primary tumour can result in metastasis and the formation of secondary tumours elsewhere in the body. Heat stress can affect the cytoskeleton and induce cellular rearrangements.[64,68] It was observed in hyperthermia-treated platelets, which experienced reduced adhesion under flow conditions.[69] Neuroblastoma cells also showed reduced cellular adhesiveness and integrin expression after an hyperthermic treatment in a water bath at 43°C, reporting “floating cells” after the heat stress.[70]

In fact, targeting of adhesion molecules with hyperthermia has been reported for cancer treatment. Integrins are transmembrane proteins that provide a physical linkage between the cytoskeleton and the extracellular matrix (ECM). They are found to be over-expressed in many cancer types and this has been exploited to target drugs and nanoparticles specifically to the tumour. Integrins have a highly conserved binding motif, the Arg-Gly-Asp (RGD),[71] and the idea is that by adding this peptide to the drug it will preferentially accumulate in regions with high density of integrins, such as tumours.

By targeting integrins with gold nanoparticles (AuNR-RGD) and irradiating them with 5.8 W/cm^2 for 1 minute, temperatures reached 42°C and cancer cell migration was stunted.[72] The studied human oral squamous cell carcinoma (HSC-3) saw their cytoskeleton affected after this mild increase in temperature, observing changes in downstream regulators of integrin signalling. However, the authors

also reported that the exposure to AuNR-RGD alone had an inhibiting effect on cell adhesion and migration, only that NIR light exposure enhanced this result.[72]

This is of particular interest, as another research studied the promotion of cancer cell migration by nanoparticles. This study showed the potential of titanium oxide, gold and silica nanoparticles to produce nanomaterial-induced endothelial leakiness (NanoEL).[73] In this case the presence of the nanomaterial designed to kill the tumour could be producing gaps in the endothelium by binding to adherens junctions. This enabled metastasis of cancer cells, by facilitating cellular intravasation and extravasation.[73]

Promotion of metastasis by nanoparticles is an undesirable effect and further studies on the combination of nanoparticles and hyperthermia on cellular adhesion must be considered to determine if this is an effective cancer treatment that will not induce metastasis. Both papers described here convey different valid results on the migration abilities of cancer cells after nanoparticle and heat exposure. Of course, nanoparticle and cellular type are playing an important role in the conclusion of the study, but for these reasons, further investigation on this topic is crucial.

2.1.1.3. Cellular communication

Intercellular communication has evolved to allow the collaboration and coordination of cellular functions. Cellular signalling is mediated mainly by extracellular signal molecules. These molecules can work in close contact with surrounding cells from the emitting cell (paracrine signalling) or reach further destinations via the bloodstream (endocrine signalling).

Extracellular signal molecules encompass a wide range of molecules, including hormones, growth factors, ROS, cytokines, and extracellular vesicles. The information they convey determines the fate of the recipient cell, prompting survival, cell death, mitosis, or differentiation.[74]

Whole body hyperthermia induces an increased expression of cytokines IL-1β, IL-6, IL-8 and TNF-α on peripheral blood around 3 hours after the event.[75] Increased expression of cytokines after elevated temperatures can trigger an immune response to induce an anti-cancer immune reaction. Moreover, hyperthermia targeting the tumour microenvironment can induce the formation of danger signals and promote the formation of extracellular Hsp. This enhances the activation of the immune system: increased production of inflammatory cytokines (such as IL-1β and IL-6) and overexpression of PD-L1 help lymphocytes to infiltrate the tumour microenvironment and attack solid tumours.[76] Nonetheless, the profile of cytokine expression and communication with other cells is complex.[77]

Hyperthermia creates a favourable tumour microenvironment for cancer treatment and synergies with conventional treatments. Interestingly, mild hyperthermia enhances the efflux of exosomes in breast cancer cells and macrophages.[78,79] The size and content of exosomes varied under different hyperthermic stress.[79] This is of importance as exosomes can carry antioncogenes that reduce the resistance to certain drugs in breast cancer cells.[78] Exosomes are important mediators of intracellular communication and carry specific information from their progenitors. Understanding exosome secretion during hyperthermia and the potential of exosomes to carry antitumour molecules[80] is important for targeted therapy.

2.1.1.4. Cell cycle

The cellular cycle is characterised by having two different phases: the interphase (which comprises the S phase and the two gap phases, G_1 and G_2) and the M phase (in which cellular division is accomplished). Although the S and M phases are critical due to the importance of DNA synthesis (chromosome duplication) and production of two identical copies in mitosis, the gap phases function as more than pauses that give time for the cell to grow.

During G_1 and G_2 the cell monitors the internal and external microenvironment to decide if it can commit to cellular division. If the conditions are favourable, the cell will continue with the cell cycle and division. However, if unfavourable circumstances are detected, the cell may arrest the cell cycle and

enter G_0. This state, also known as quiescence, is non-proliferative and is characterised by lower metabolic activity. Many cells leave G_0 when conditions are favourable again, but many others stay permanently in quiescence.

The cell cycle control system has several restriction points, or transition checkpoints, that allow the cell to continue with cellular division. The G_1/S checkpoint allows the cell to start duplicating their genetic content. The G_2/M transition checks the alignment of the chromosomes in the mitotic spindle and if DNA replication is completed before committing to mitosis. The last checkpoint is during the metaphase to anaphase transition, where chromosomes must be attached to the spindle before sister-chromatid separation.

The control of the cell cycle is done through a variety of cyclins and cyclin-dependent kinases (Cdks). Their activity and levels cycle during the process of cellular division and they themselves are controlled by many other enzymes and signalling cascades. During cancer, the rules of cell cycle and cell growth are transgressed, and cells grow and proliferate out of control.

Hyperthermia is closely related to the cell cycle and heat sensitivity varies during the different phases of the cycle.[7,64] The M phase seemed to be the most sensitive phase of cell cycle, as elevated temperatures showed damage of the mitotic spindle, indicating inefficient mitosis. Different sensitivity to hyperthermia at different phases can indicate that different molecular signalling pathways are being activated.[7]

Treatment of uterine cervical cancer cell line CaSki with heat (43°C, 45°C and 47°C) lead to heat shock arrest of cells in the S phase.[81] Moreover, cells at the S phase have increased thermal hypersensitivity,[82] which could be exploited in synergistic treatment of hyperthermia with gene therapy.

2.1.1.5. Cell death

Cellular death has a vital role during development, damage, or infection.[74] In most cases, cells follow a programmed cell death mechanism, apoptosis, in which the cell loses many of its characteristics and dies. Apoptosis is characterised by several morphological changes, including membrane blebbing, cellular shrinkage, chromatin condensation, DNA breakage, and formation of apoptotic bodies, among many others. Importantly, on *in vivo* situations, apoptotic cells express "eat me" signals to macrophages, that engulf these dying cells. All these events are not associated with an inflammatory response, as cells do not spill their constituents into the extracellular environment and they are quickly phagocytosed by scavenger cells.[83]

Many stimuli can determine if a cell must undergo apoptosis, but not all cells will respond equally to the same stimulus. Stimuli can have a physiological origin in case the cell must die (e.g. during development). However, in the adult, the inductors of apoptosis are mainly pathological and have diverse origins: heat, radiation, hypoxia or cytotoxic drugs, among others.[83] The dose at which these stimuli are perceived will dictate if the cell undergoes apoptosis, or on the contrary, endures the degradative process of necrosis. As a rule, low doses of pathological stimuli trigger apoptosis, whereas higher doses or acute insults induce necrosis.

Apoptosis depends on a proteolytic cascade mediated by caspases. Caspases cleave proteins and lead to inappropriate activation or disablement of key proteins and enzymes.[84] Initiator caspases have the role to activate executioner caspases when an apoptotic signal triggers the apoptotic cascade. When executioner caspases are activated, they cleave downstream effectors of the apoptotic cascade and many other proteins. This execution phase is activated through the intrinsic or extrinsic pathway. The latter is mediated by death membrane receptor proteins, which contain a death domain (DD). In many instances of activation via the extrinsic pathway, upon binding of the death signal to the receptor, there is a clustering of receptors that recruit and activate a death-inducing signalling complex (DISC) that activates initiator caspases.[74] On the other hand, the intrinsic apoptotic pathway detects intracellular stimuli, such as free radicals, hyperthermia or radiation.[83] During activation of the intrinsic pathway,

changes to the permeability of the outer mitochondrial membrane allow cytochrome C to flow to the cytosol and form and activate the apoptosome, leading to caspase activation. A whole family of proteins, the inhibitors of apoptosis (IAPs), are in charge of controlling their activation and avoiding an undesired proteolytic cascade.

Necrosis is different from apoptosis in that it is an energy-independent form of cell death. Necrotic cells experience swelling and their membranes lose integrity, spilling their molecular contents into the extracellular space and eliciting an inflammatory response.[74] On special cases where no scavenger cells are present to remove apoptotic cells, the cell completes the cell death process through secondary necrosis.[85,86] This is a case in which kinetics of cell death are important to determine the cell death mechanism occurring. An initial apoptotic scenario may be incorrectly labelled as necrosis because of the observation of secondary necrosis features (membrane permeabilization and swelling). Nonetheless, secondary necrotic cells still present apoptotic features that are distinguishable, such as release of caspase 3.[85] Many other cell death mechanisms have been reported, an extensive review of them can be found in Galluzi *et al*.[87]

Activation of apoptosis rather than necrosis for cancer treatment would be preferable for the lack of an inflammatory response. During hyperthermia, apoptosis is predominantly activated rather than necrosis.[2,64,70,88–90] However, this is modulated by the temperatures achieved and the method of application of hyperthermia, among other considerations. In many instances, lower temperatures promote apoptosis, whereas acute temperature elevations cause necrosis.[91]

The application of hyperthermia may also play a role in the molecular events triggered during and after heating, as in the case of PPTT the laser effects and properties of the gold nanoparticles may induce different mechanisms.[92]. Zhou *et al*.[81] reported that in hyperthermia induced with a water bath, 45°C induced apoptosis, while 47°C activated necrosis. Ali *et al*.[92] reported that temperatures over 44°C with PPTT induced apoptosis, whereas over 46°C, necrosis would be activated. However, the time exposed to the elevated temperatures where different. Adjusting the treatment parameters, it is possible to modulate the cell death activated.

2.1.2. Thermotolerance

Thermotolerance, or heat tolerance, refers to the cellular capacity to withstand temperatures beyond the normal homeostatic range without significant disruption to metabolism. Heat susceptibility is dependent on the cellular type, environmental conditions, pH levels, and expression of molecular chaperones. Thermotolerance can have multiple origins, but non-lethal increases of temperature (38-42°C) are associated with increased levels of Hsps, and are key in rendering cells resistant to therapeutic hyperthermia.[7,91,93,94]

Hsps prevent misfolding of proteins and concede higher resistance to elevated temperatures and other cellular stressors that trigger protein unfolding. They first received their name after being observed in experiments on *Drosophila* flies experiencing hyperthermia.[93] Some Hsps are constitutively expressed to allow rapid responses to cellular stress and increase their expression in response to an insult, whereas others are uniquely expressed to respond to a physiological stress.[95]

Hsps are closely related to apoptosis, regulating many of the downstream effectors of the apoptotic pathway. Hsps maintain cellular survival by inhibiting caspase activity and blocking pro-apoptotic Bcl-2 proteins to prevent mitochondrial permeabilization.[96] The regulation of apoptotic pathways by Hsps is a pivotal point for reducing cellular sensitivity to damaging stressors, allowing cells to escape apoptosis.[96] Thermotolerance is associated with higher drug resistance,[7] and this could be one of the reasons.

To increase the effectiveness of cancer treatments, approaches to inhibit Hsps have been tested to enhance the cytotoxic effects of anti-cancer drugs.[97–99] Moreover, the activity of Hsps on cancer cells is altered and many tumour cells depend on their function, so they become a potential therapeutic target

that could be exploited together with hyperthermia.[100] Targeting of Hsp90 and other important Hsps can be the gateway to improve the effect of drug- and heat-resistant cells.[97–99]

2.2. Nanomedicine and nanotechnology

Nanotechnology encompasses various areas of science and technology focused on products and phenomena at the nanometre scale. The potential of working at the nanoscale stems from the unique phenomena that occurs at this scale, which are not observable at larger dimensions. These arise due to changes in the surface-to-volume ratio, resulting in distinct material properties, obtaining new functions and enhanced phenomena.[101]

The design, production, and application of materials with precise control at the nanometre scale offers almost limitless possibilities for various sectors, including industry, energy technology, communication, food industry and healthcare. For instance, in healthcare, nanotechnology has led to advancements on targeted drug delivery systems, medical imaging techniques and disease detection methods. Moreover, emerging nanotechnologies develop tools such as microfluidic devices, droplet microfluidics and labs-on-a-chip that are revolutionising bio-nanomedicine.[102,103] These technologies allow precise manipulation and analysis of nano-sized components and small volumes of sample, improving imaging, analyte capture and diagnostics.[104]

However, despite its promising prospects, nanotechnology can pose significant risks to humans, animals, and the ecosystem due to their small scale. Their application will determine the health hazards the nanomaterial can cause, and to control this, numerous organisations oversee nanotechnology-associated particles and conduct risk analysis.[105,106]

Nanomedicine, a subset of nanotechnology, refers to the application of nanotechnology in medical products and healthcare. It holds the potential of transforming disease detection and prevention, novel drug development and medical imaging techniques. Nanomedicine has the capacity to address unmet medical needs and overcome challenges that traditional medicine struggles to fix. It can modernise healthcare towards precise medicine, with personalised therapies tailored to individual patients, pathologies, or preferences.[107,108]

The field of nanomedicine is propelled by various types of nanoparticles, including organic materials like liposomes and micelles, and inorganic materials such as gold nanoparticles and quantum dots.[108,109] Liposomal nanoparticles are usually employed together with chemotherapy drugs, as they are biocompatible and have low antigenic effects. But these drug-loaded nanoparticles are easily sequestered by the mononuclear phagocyte system (MPS) and must be coated with stealth moieties, such as polyethylene glycol (PEG), albumin and hydrogels.[110] Liposome-based nanoparticles are the most common type of nanoparticle found in clinical trials.[110] Two very well-known examples are doxorubicin[111] and paclitaxel.[112]

Inorganic nanoparticles have unique qualities that make them more attractive to diagnosis, imaging and light-based therapies.[113] They fill purposes that organic nanoparticles cannot account for, but their application is also limited because they tend to have lower biocompatibility and solubility, and are more difficult to metabolise.[109] Nonetheless, their unique electrical, magnetic and optical properties make them very valuable nanotools. Inorganic nanoparticles are flexible enough to be tuneable for specific applications, as many of their features (shape, size, material, conjugation, etc.) are adaptable, and their functions manyfold.[108]

Among these, gold nanoparticles are particularly noteworthy due to their unique combination of physical and chemical properties. They have the ability to strongly absorb and scatter light, which makes them especially attractive for photothermal therapies, light-based biosensors, surface-enhanced Raman spectroscopy (SERS) and as bright contrast agents for two-photon luminescence.[92,114,115]

Despite the potential of nanomedicine, significant challenges still stand on the path for translating many nanoparticle-based therapies into clinical practice.[116] Nanoparticles as multifunctional agents that carry multiple clinically relevant functions have higher versatility, but are faced with more scrutiny from regulatory agencies due to concerns about the safety of each novel component and their combined effects.[117,118] Balancing innovation with safety in nanotechnology and nanomedicine is paramount for clinical translation. Interdisciplinary collaboration and early involvement of clinicians, together with robust and standardised assessment methodologies and protocols are crucial for the effective utilisation of nanomedicine in healthcare.[117,119,120]

The development of new technologies that allow manipulation of nano-sized molecules and unravelling of the complexity of phenomena at the nanoscale will only increase in the coming years, allowing precise medicine based on nanotechnology to address unmet clinical needs with minimal side effects.

2.2.1. Gold nanoparticles

Gold nanoparticles have attracted special attention in nanomedicine due to their unique combination of physical, chemical and biological properties, as well as their low associated toxicity due to the inert nature of gold, ease of functionalisation, colloidal stability and scalable synthesis.[26,30,31,121,122] Their unique plasmonic capabilities, stemming from their localised surface plasmon resonance (LSPR), make them ideal for several applications, including hyperthermia and sensing applications.[23,114,123]

The LSPR is an optical phenomenon driven by the collective oscillations of free electrons on the metal surface upon incident light. The oscillation of electrons on nanostructures is spatially confined to the size of the nanoparticle and it rapidly decays away from the nanoparticle.[9,21,48] The LSPR is highly dependent on the nanoparticle shape, size, and composition, and can be tuned by changing these parameters. Multiple particle designs allow to have gold nanoparticles with peak absorption at many wavelengths, including the near-infrared (NIR) region.[48]

The exploitation of the plasmonic characteristics of gold nanoparticles has found applications in fields that range from solar harvesting and fluid control to cancer treatment and biosensing.[124] LSPR-based biosensors depend on the gold nanoparticle to shift their refractive index LSPR upon binding of a target of interest.[114,125] These LSPR-biosensors are very sensitive to detect small changes in the dielectric environment of the nanostructure.[114] Gold nanoparticles, specially gold nanorods, are great contrast agents for imaging thanks to their two-photon luminescence,[115,126] simplifying imaging procedures.

Many gold nanoparticles, when illuminated, scatter part of the light to their surroundings, but their enhanced optical absorption of light is transformed into heat, known as thermoplasmonics. Thermoplasmonics can be applied for biophysical manipulation and biomedical applications, being plasmonic photothermal therapy (PPTT) for cancer treatment the most recognisable.[23,48,124] Polymerase chain reaction (PCR)-chips are one of the applications of gold nanoparticles and thermoplasmonics, in which heat generated by illumination and rapid cool off upon turning it off, is used to allow efficient, rapid and small volume PCR assays.[127]

Specifically gold nanorods (AuNR), in which we focus during this dissertation, are ideal candidates for PPTT because of their tuneable peak of absorption. AuNRs possess different absorption bands (longitudinal and transversal), and modifying their aspect ratio can tune the longitudinal LSPR to the NIR region.[21] In this region, AuNR match the biological optical window and ensures that there is minimum light absorption by the tissue.[20]

Interestingly, AuNRs are also ideal candidates as their shape can easily be modified by changing the concentration of their reagents during synthesis. By modifying the concentration of Au seed, cetyltrimethylammonium bromide (CTAB), gold, ascorbic acid and silver nitrate it is possible to modify the anisotropic growth of gold nanorods and obtain different shapes and functions.[28]

Within the group, studies on the optimum morphology of AuNR were conducted to determine the optimal aspect ratio of AuNR that provided the most efficient heat generation upon illumination, high

cellular uptake and low *in vitro* cytotoxicity.[128] The chosen candidate were AuNRs of 11×44 nm, with their LSPR localised at 808 nm, right at the centre of the biological transparency window.

Importantly, the use of CTAB as a surfactant during AuNR synthesis is an inconvenience for their use on *in vivo* settings, as CTAB is highly cytotoxic, so several steps must be taken to remove this moiety from the nanoparticle surface.[40,129] The approaches to remove CTAB are usually based on their substitution by other stabilising molecules, such as polyethylene glycol (PEG) or human serum albumin.[130,131] Nanoparticle functionalisation improves biocompatibility and maintains AuNR colloidal stability.

On top of the concerns of cytotoxicity of nanoparticles during *in vivo* uses, another difficulty is the sterilisation of nanomaterials for clinical use. Sterilisation is a requirement for nanoparticles tested in animals and clinical applications.[132] For *in vitro* settings, sterilisation is crucial during assessment of the cytotoxicity of nanomaterials to prevent cross-contamination and ensure accurate results.[133] The sterilisation process must be carefully chosen to avoid spoiling the AuNR shape, so freeze-drying and formaldehyde cycles and filtering are the most popular methods.[40,132,133]

2.2.1.1. Passive vs active targeting

The extravasation of nanoparticles into the target tissue is crucial for their effective application. Extravasation is heavily affected by the nanoparticle characteristics, such as size: smaller nanoparticles can more readily leave blood vessels and reach tissues than large nanoparticles.[113]

The process of nanoparticle uptake can be divided into passive and active methods. Although both are different, they rely on the extravasation capacity of the nanoparticle. The nature of tumours and their leaky vasculature promised advantageous accumulation of nanoparticles into the tumour. This effect, termed enhanced permeability and retention (EPR), implied that due to the chaotic growth of tumours and their associated new blood vessels, these would be more porous and prone to leakage, allowing molecules to be accumulated in tumours.[134,135] The lack of a lymphatic system on tumours would improve their retention.[20] However, this EPR effect, firstly observed in animals, is not a universal consequence of tumour growth and is not present in most human solid tumours.[118] Therefore, solely relying on the EPR effect for justifying enhanced accumulation in tumours is a highly controversial topic in nanomedicine.

To improve tumour accumulation and enhance the specificity of nanoformulations, researchers turned to active targeting strategies for nanoparticles. Gold nanoparticles are well-suited for conjugation with targeting moieties via gold thiol-chemistry.[136] This approach involves fixing a molecule, usually an aptamer, peptide or antibody, to the surface of the nanoparticle to direct them to target tissues or cells.[130] These targeting moieties are designed against specific biomarkers that are upregulated in the tissue of interest. For example, and as described before, the peptide RGD has been added to nanoparticles to target the increased expression of integrins found in cancer.[71]

Unfortunately, regardless of the functionalisation strategy used for nanoparticles, whether passive or active targeting, more than 99% of the administered *in vivo* nanoparticles ultimately accumulate in the mononuclear phagocytic system.[137] A meta-analysis on nanoparticle delivery to tumours found that the delivery efficiency of active-targeting nanoparticles was only 0.3% higher than passive strategies, and in total, only 0.7% of the injected dose reached the tumour, independently of the conjugation.[138]

Indeed, our group determined that *in vitro* there was higher binding affinity for AuNR-RGD in 786-0 cancerous kidney cells compared. However, studies on *in vivo* accumulation revealed no statistically improvement using RGD-targeted AuNRs in comparison to passive AuNR-PEG, as pointed out in the literature.[11,44]

The inefficiency of active targeting on *in vivo* experimentation may be attributed to the formation of a protein corona upon contact of gold nanoparticles with a biological medium, altering the nanoparticle

identity.[137] The protein corona is far from being completely understood and its dynamics change over time. Adsorption of proteins to the nanoparticle surface is time dependent. First, the more abundant proteins with higher mobility, like albumin, encounter the nanomaterial and interact with it. Over time, smaller and less abundant molecules, but with higher affinity, such as lipids and immunoglobulins, compete with albumin and change the composition of the protein corona.[139,140]

The formation of the protein corona is dependent on many factors: the nanoparticle (surface charge, functional groups and ligands, hydrophobicity vs hydrophilicity, etc.), the biological media (proteins, acids and bases, salts and ions, etc.), and the nano-bio interface, to mention some.[141] The adsorption of proteins can cause nanoparticle agglomeration, change the hydrophilicity and charge, and influence the uptake pathway.[113,142] The protein corona facilitates the recognition and uptake of gold nanoparticles by macrophages,[113,137] and generally, improve their biocompatibility at the cost of reduced uptake.[143]

Understanding the protein corona is crucial for predicting the biological fate, behaviour, uptake and potential therapeutic effects of nanoparticles in nanomedicine. However, the multitude of cell types and microenvironments found *in vivo* challenge the study of the interaction of nanoparticles with biological systems.[143] Further investigation on the protein corona effect will improve clinical use of nanoparticles by achieving useful and effective targeting.[144]

2.2.2. Plasmonic photothermal therapy (PPTT)

In the realm of cancer therapy, gold nanoparticles are the ideal tool to induce hyperthermia in a controlled and specific manner. In PPTT, the intrinsic plasmonic properties of gold nanoparticles are used to transform photon energy into heat for selective tumour ablation.[23,26,92,121,145] PPTT can be used to treat malignant cells, inducing localised hyperthermia in response to an exogenously applied laser light, with minimal side effects.

Gold nanorods stand out for PPTT due to their good biocompatibility, ease of functionalisation, and scalable synthesis. Moreover, their tuneable light absorption, achieved by modifying their aspect ratio, enables the shift of their LSPR towards the NIR. This feature grants PPTT access to the optical biological window, eliminating the need for surgical intervention as the laser light will be able to penetrate the tissue.[145] Consequently, PPTT is a targeted approach that reduces invasiveness compared to more conventional therapies against cancer.

PPTT is a highly localised cancer treatment capable of selectively target and destroy cancer cells while minimising the damage to healthy tissue. This occurs because with the correct nanoparticle and laser, increases of temperature and damage will only occur at the interface of the laser with the nanoparticle.[26] This spares all tissue that is not being illuminated. The specific targeting of the tissue of interest occurs by directing the nanoparticles to the tumour (via the above-mentioned methods or intratumoural injections) and directing the laser light only to the region of interest. This minimises side effects and improves the precision of the therapy.

Recent advancements in PPTT have demonstrated the potential of this therapy. Clinical trials for prostate cancer have shown sustained remission (12 months) in patients treated with gold-silica nanoshell particles and repeated laser exposures (25 excitations ranging from 4.5 to 6.5 W).[55] The same gold nanoparticles have been tested for lung metastatic tumours and head-and-neck tumours, but the results have not yet been published.

However, the clinical translation of PPTT still faces several challenges, as can be seen from the difference on numbers between pre-clinical and clinical studies. Optimisation of the nanoparticle design for enhanced photothermal conversion efficiency and ensuring precise tumour targeting, whilst controlling protein corona formation is crucial for improving the translation of PPTT. The protein corona influences the behaviour of the nanoparticles and conceals active targeting strategies. Overcoming these tasks demands comprehensive understanding of bio-nano interactions and the subsequent development of improved targeting strategies.

Innovative particle designs with tuneable plasmonic properties offer opportunities to enhance treatment efficacy and expand therapeutic applications. Combinations of plasmonic hyperthermia with other modalities, such as chemotherapy or immunotherapy, hold promise for synergistic effects and improved treatment outcomes.[3] An example of this is the development of multifunctional nanoparticles. Chen *et al*. developed AuNRs functionalised with moieties for the specific targeting of CD44 and hyaluronic acid, together with diclofenac, an inhibitor of Glut1. The sequence of action required AuNR to reach target cells and hyaluronidase to release diclofenac, which depleted Glut1 in the cell and triggered a cascade of intracellular events that rendered cells sensitised for photothermal therapy upon laser irradiation of those same AuNRs.[146]

Another synergistic effect that is highly sought after is photothermal therapy in combination with photodynamic therapy (PDT). Dual plasmonic nanoparticles that can locally increase the temperature upon laser illumination and produce ROS highly decreased viability in cancerous HeLa cells.[147] The challenges of combining both anti-cancer modalities are numerous, as both PPTT and PDT require oxygen, but PDT depletes oxygen during operation. A very extensive review on this topic, by Overchuk *et al*.,[10] emphasises on all the combinations and roles that PTT+PDT can adopt to increase the therapeutic effectiveness of both types of modalities.

The challenge lies in multifunctional nanoparticles offering additional capabilities to standard plasmonic nanoparticles also introduce complexities that hinder their clinical translation. Simply adding extra functionalities to nanoparticles does not necessarily help developing PPTT.[117] Nanoparticles need to be designed to prioritise efficiency and efficacy.[117] In the context of PPTT, this entails plasmonic nanoparticles that can efficiently convert light-to-heat, with high biocompatibility and targetability, within the NIR region in the target tissue, may be more desirable than overly complex nanoparticles with multiple functions. Regulatory agencies examine new drugs and techniques for human use, and as mentioned above, obtaining their approval requires more preclinical and clinical data for each element of the multifunctional nanoparticle.[117,118] In the case of the clinical trials with PPTT and gold nanoshells (Aurolase®Therapy), the Food and Drug Administration (FDA), branded the modality as a medical device instead of as a drug because the nanoshells are metabolically inert unless irradiated.[34] Their effect is physical, not biological or chemical. Nanoparticles with multiple functions, may be metabolically active without laser activation, and may result in other regulatory protocols.

The shortages of conventional cancer therapies, particularly in addressing drug resistance, create a niche where PPTT could prove its potential.[99] Solid tumours usually have an acidic microenvironment that renders them particularly susceptible to hyperthermia, whereas normal cells with their normal pH levels will exhibit greater resistance to elevated temperatures.[148] This differential sensitivity leaves cancer cells more vulnerable to treatment with PPTT, sparing healthy tissues. In its most basic form, PPTT relies solely on the plasmonic nanoparticles, such as AuNR in our project, exposed to NIR laser light to induce hyperthermia. The resulting heat generation can produce a range of cellular damage, dependent on the applied temperature.[118,136] PPTT-induced heat can also be applied to activate the release of a drug, trigger different functions, or make the drug work at different rates, as the drug response can be different at elevated temperatures than at 37°C.[148]

In conclusion, gold nanoparticles and PPTT represent a paradigm shift in cancer therapy. The outlook of PPTT is offering targeted and local treatment modalities with minimal off-target side effects. Because of its relative simplicity and facility to combine it other therapies, it holds great potential for cancer therapy and other diseases, including opportunistic use on veterinary medicine. Continued research on PPTT, elucidating its molecular mechanisms, refining nanoparticle design and optimising targeting, is a collaborative effort of researchers from different disciplines, crucial to harness the full potential of PPTT for clinical applications.

2.3. Study limitations

2.3.1. *In vitro* vs *in vivo* experimentation

The differences between *in vitro* and *in vivo* experimentation are readily apparent. Both research methods have their own advantages and disadvantages. *In vitro* models are key in basic research as they provide great information on biological responses and allow for high-throughput drug screening, without elevated costs nor ethical concerns. However, they lack dimensionality and the complexity and interactions of *in vivo* tissues. The limitations of *in vitro* cell culture must be acknowledged, as they serve as a representative model of a real complex situation.

Development of stablished cell lines, as well as primary cell lines, is central in laboratory and medical research and are highly dependent on it. It helps extensively in the development of nanotechnology and nanomedicine, ensuring nanoparticles are suitable for *in vivo* usage, with minimal risk for the animal models, although the *in vitro*-*in vivo* translation is sometimes deficient. A hypothesis theorises that this deficient translation could be due to the different protein corona formed in both situations,[144] but many other factors are crucial in the jump from the bench to the bedside. In PPTT, *in vitro* experimentation allows to test and validate many of the factors and variables that make plasmonic hyperthermia, but keeping up high standards is essential to validate all newly developed nanotools.[149] Moreover, there is high variability on the cell death effects of hyperthermia depending on the tumour type and cellular line.[7] All this highlights the importance of the need to replicates and standardisation of protocols for nanomedicine, specifically for PPTT.

2.3.2. PPTT: thousands of possibilities

In PPTT the combination of possibilities is endless. It is possible to manipulate the laser source and power, the time of irradiation, temperature reached and the nanoparticle type. PPTT can be used in synergy with other therapies or as a standalone technique. It can be used to treat cancer, but other maladies as well.

If the reader is familiar with a Rubik cube, they will know that to solve it, many times the already completed colours must be scrambled to finish the Rubik cube. In PPTT many factors are considered in each of the faces. An experimental protocol may determine the best material, size, and shape of nanoparticle, but when laser power and viability are considered, these already tested components of PPTT may become outdated. Even when PPTT's Rubik cube is solved, different types of cubes (e.g. laser settings) and colours (e.g. nanoparticle types) may have been developed, and the protocol defined may not be appropriate anymore.

This is not discouraging for PPTT, in fact, it opens the possibilities of hyperthermia for many cancer types and diseases, including their combination with chemo- and radiotherapy. PPTT can be used to enhance drug delivery and sensitise tissues.[3,10]

This endless combination possibilities difficult the comparison of experiments. Standardisation on reporting data, results, and protocols on PPTT, nanomedicine and nanotechnology are key for their development and translation to clinical settings. It is a thought process that requires expertise from researchers in very different fields working simultaneously.

This study has been performed with the same AuNR-PEG concentration, laser power density and time of irradiation, selected to study the effect of PPTT on seven different cell lines at the same times after treatment. Both cancer and healthy cell types were picked to determine differences between both conditions. However, this arrangement excluded other cell types and nanoparticle models that have also been studied for PPTT. This is to show that results may vary among different cell lines, as observed in the cells studied in this dissertation. The studied cancerous cells were derived from human kidney, lung, and liver cancers. Lung cancer, together with breast and colorectal cancers, comprise one third of all new diagnosed cancers worldwide. Liver cancer, on the other hand, was the third leading cause of cancer mortality in 2020, and kidney cancer accounts for 4 % of all cancer cases in Europe.[16]

This research shows that systematic approaches can be used to assess similar models.[150] Here, we compared the response to PPTT across various cell types, as well as delving into the molecular effects triggered. This was possible by adhering to a systematic methodology for studying the effects of PPTT *in vitro*. The merit of this dissertation is not on determining which cell type is a better fit for PPTT or which powers and concentrations are better suited to treat cancer cells, but on comparing different outcomes resulting from the same treatment.

3

General methods and instrumentation

3.1. Gold nanorods

Nanoparticles made of noble metals possess certain physicochemical characteristics that when exploited, are well-suited for medical application. The choice of material for nanofabrication is critical to determine their utility. Most materials were initially chosen as they were deemed inert at the macroscale, but when reduced to the nanoscale their properties undergo important changes.[151] For instance, silver is commonly used in jewellery, but in nanoquantities it produces reactive oxygen species (ROS), inducing toxicity to cells and rendering them more sensible to other aggressions.[141]

Gold is typically considered biocompatible in bulk, but at the nanoscale it can trigger disruption on protein conformation and lethal effects within the cell.[141] AuNRs are desired for biomedical applications due to the optical assets, like the presence of a LSPR, as well as their physical advantages such as the modification of their aspect ratio, and chemical attributes, such as easy functionalisation.[26]

In our case, previous studies conducted within the group allowed to optimise the synthesis of gold nanorod (AuNRs) to create *in-house* nanoparticles. These previous studies determined the optimum morphology[128] to reduce AuNR toxicity, which proved to be associated to the quantity of nanomaterial and independent of shape and size. This line of research also set the ideal aspect ratio and size for optimum light-to-heat conversion in the field of *in vitro* PPTT.

3.1.1. AuNR synthesis

AuNRs of 11 × 44 nm were synthetised *in-house* using a slightly modified seed mediated method[33,38,39] optimised by Dr. Ignacio de Miguel. The aspect ratio and volume of AuNRs produced was controlled by the quantity of silver nitrate ($AgNO_3$) and gold seed size added to the growth solution containing cetyltrimethylammonium bromide (CTAB, H5882, Sigma-Aldrich). Controlling the aspect ratio determined the position of the LSPR. Synthetised AuNRs following this method are chemically and morphologically stable for several months at 31ºC.

The CTAB chains allow to sculpt the seed into a rod-shape nanoparticle by acting as a stabiliser that hampers nanoparticle growth in one axis, encouraging growth in the other.[41] CTAB forms a bi-layer structure on the surface of the nanoparticle that promotes their stability in aqueous solution and prevents sedimentation. Unfortunately, CTAB is a highly cytotoxic component that can reduce their applicability *in vitro* and *in vivo*.[41] For these reasons, it is imperative to remove CTAB chains from the AuNRs after synthesis.

3.1.2. PEGylation

Polyethylene glycol (PEG) was used to enhance stability and biocompatibility of AuNRs after elimination of CTAB moieties. PEGylation – coupling PEG chains to a molecule – is one of the many methods and coatings that can be employed to improve nanoparticles for clinical settings. Mitigation of CTAB in seed-mediated synthesis is still a problem for the development of biomedical nanoparticles. An extensive review on the current methods being employed was produced by Shi *et al*.[41]

PEGylation increases the biocompatibility of AuNRs by replacing CTAB on the nanoparticle surface, thereby improving their stability and preventing the sedimentation of the AuNR.[42] However, it does not entail specific tumour targeting.

Following the method detailed in Morales *et al*.,[128] AuNRs suspended in CTAB were concentrated by ultra-centrifugation for 25 min at 30ºC at 23708 x g (Avanti J-E rotor JA-25.50, Beckman Coulter) and 90% of supernatant discarded. The substitution of CTAB by PEG occurred by mixing ultra-purified water (MilliQ, Merck KGaA), 50 % v/v of citrate 0.1 M pH 4 (C3434, Sigma Aldrich), 3 kDa PEG (PEG1099, Iris Biotech) at 1 mg/mL and the concentrated suspension of AuNR at 0.25 OD/mL. The mixture was sonicated for 30 min and stored overnight at 30ºC to allow the ligand exchange reaction to occur. The following day, the pH of the functionalised solution of AuNR-PEG was adjusted to 7-7.4 to prevent aggregation and sedimentation of the nanorods in the next steps.

3.1.3. Dialysis and purification

PEGylation removes CTAB from the nanoparticle surface and reduces AuNR clusters, but CTAB remains in the solution, therefore, its removal is a priority for their use in clinical settings. In our case, the AuNR-PEG solution was ultra-centrifuged (25 min, 30ºC, 23708 x g), the supernatant discarded and the pellet containing the AuNRs redispersed in MilliQ water. These AuNR-PEG were dialysed (Spectra/Por™ Standard RC Dialysis, 1-50 kDa, Spectrum™) in a bucket containing 5 L of purified water with 0.1 M phosphate buffered saline (PBS). PBS induced CTAB to flow outside, whilst the dialysis membrane acted as a net that trapped the nanoparticles inside. Water was exchanged a minimum of 2 times in a period of 2 days.

After dialysis, the AuNR-PEG suspension was filtered (25 mm RC syringe filter, 0.2 µm pore size, Corning Inc.) to remove impurities such as bacteria. Finally, the AuNR-PEG were centrifuged as described above and concentrated in ultra-purified water.

3.1.4. Spectra measurement

The spectral characterisation with UV-VIS spectroscopy allowed us to determine the final AuNR suspension concentration. Clear flat 96-well plates (polystyrene, Nunc MicroWell, Thermo Fisher Scientific) were used to measure the optical density (OD) between 400 and 999 nm with a Synergy H1 multi-mode microplate reader (BioTek Instruments Inc.). For each sample, 250 µL of volume and a 0.69 cm path length was used. Triplicates of each sample were taken, and water spectrum measurements were subtracted. AuNR-PEG concentration was obtained as:

$$c = OD\,\frac{l}{\epsilon}$$

were molar concentration (c) is expressed as mol/L, OD (a.u.) is the optical density, l (cm) is the path length, and ϵ ($l/$(cm × mol/L)) is the AuNR-PEG molar extinction coefficient. More detailed instructions on the method are described in Morales *et al*.[128]

3.2. Cell culture

Cellular culture is a cornerstone of biomedical research, providing a controlled environment for cell manipulation and experimentation for the investigation of disease, treatment, and diagnosis exploration. It is a reliable and cost-effective platform for screening drug testing before advancing to more complex and representative animal models and human trials. Cell culture allows the meticulous examination of a wide range of specific parameters and testing the reproducibility of experiments, key aspects in scientific research. The extensive availability of primary and established cell cultures (also known as immortalised or transformed) provides researchers with an enormous opportunity to work with a diverse array of cells, considering their origin, type, and source.

Animal experimentation has higher resemblance to the human organism than *in vitro* experimentation. However, it is associated with soaring ethical concerns and high experimental costs. In this regard, cellular culture has the advantage of providing a preliminary alternative for parameter screening before resorting to *in vivo* experimentation. Nonetheless, it is also crucial to acknowledge the limitations of cell culture. The reduction of the inherent complexity of whole organisms and complex tissues to simpler models must be ascertained, as outcomes can bring discrepancies, particularly with changes in

physiological characteristics.[152] With careful control and consideration of all factors during data generation, cell culture results can be reliable and serve as a model for understanding potential consequences in animal models.

Despite these limitations, cell culture remains indispensable in nanomedicine to assess the safety and efficacy of nanomedicines and nanoparticles.[106,153] Well-judged cell culture use, in combination with other techniques, is vital for drug approval and unravelling the associated complexities of cellular processes.

In this dissertation, seven different cell lines were used, six of them grown as adherent cell cultures and one of them in suspension. All cellular cultures were always manipulated under strict sterile conditions, as well as manipulated individually to prevent cross-contaminations, ensuring the integrity and reliability of the research.

3.2.1. Cellular lines

Following the manufacturer instructions, each cell line was maintained in a 37ºC and 5 % CO_2 humidified environment (Table 3.1). Culture medium was supplemented with 5 or 10 % (v/v) foetal bovine serum (FBS, 10270106, Gibco) and 1 % (v/v) penicillin-streptomycin (PS, Pen-Strep, Gibco).

From here on, the culture medium supplemented as detailed in the provided table will be denoted as "complete medium". In contrast, the culture medium without the addition of FBS will be referred to as "fresh medium".

3.2.2. Subculture and maintenance

All cell lines were cultured as per the manufacturer instructions to maintain the cells at an optimal density for proliferation. Routine subculture of cells was modified based on cellular needs, usually when cells in the flask reached an 80-90 % confluence, but always a minimum of two to three times per week. Cells were controlled under the microscope daily to split cells before they reached confluence.

For all adherent cells, complete medium was removed by aspiration and cells were washed with fresh medium to remove traces of FBS that could reduce the action of the desired dissociation reagent. After aspirating the washes, 1x Trypsin-EDTA 0.05 % (Gibco 25300-062, Thermo Fisher Scientific) was added to cover the surface of the flask and briefly incubated at 37ºC to encourage cellular detachment. Once cells could be seen detached under the microscope, pre-warmed complete medium was added to stop the dissociation reagent and cells were recovered to a 15 mL Falcon tube to be centrifuged at 200 x g for 5 minutes. Supernatant containing trypsin was removed and the cellular pellet was diluted in growth medium, ready to be reseeded at the desired concentration.

The lung non-cancerous cell line NL20 was subcultured as described above. However, instead of the conventional use of trypsin, cell dissociation buffer (#13150016, Gibco, Thermo Fisher Scientific) was used following the instructions provided by ATCC©.

Non-adherent Jurkat T cells do not require the use of dissociation reagents. Cell cultures were maintained by adding a portion of the volume from the original flask to a new flask with pre-warmed complete medium. Depending on the volume moved, cellular splits allowed to maintain cellular concentrations between 1×10^5 and 2×10^6 cells, never exceeding higher concentrations for the viability of the cells.

Table 3.1. Outline of the specific cell lines used in this dissertation. Specific information for each cell line, including cell line reference, seeding density and incubation conditions.

Cell line	Reference	Tissue-Type	Type of culture method	Culture medium	Supplements	Precoating	Cellular dissociation	Freezing medium
786-0	CRL-1932 (ATCC©)	Kidney - Cancer	Adherent	RPMI 1640	10 % FBS, 1 % PS	None	Trypsin-EDTA 0.05%	10 % DMSO
A549	CCL-185 (ATCC©)	Lung - Cancer	Adherent	DMEM	10 % FBS, 1 % PS	None	Trypsin-EDTA 0.05%	10 % DMSO
HepG2	HB-8065 (ATCC©)	Liver - Cancer	Adherent	EMEM	10 % FBS, 1 % PS	None	Trypsin-EDTA 0.05%	10 % DMSO
Hek293	CRL-1573 (ATCC©)	Kidney - Healthy	Adherent	EMEM	10 % FBS, 1 % PS	None	Trypsin-EDTA 0.05%	10 % DMSO
NL20	CRL-2503 (ATCC©)	Lung - Healthy	Adherent	Ham's F12	1.5 g/L sodium bicarbonate, 2.7 g/L glucose, 2.0 mM L-glutamine, 0.1 mM nonessential amino acids, 0.005 mg/ml insulin, 10 ng/ml EGF*, 0.001 mg/ml transferrin, 500 ng/ml hydrocortisone, 4% FBS	None	Cell dissociation buffer (#13150016, Gibco)	5 % DMSO
THLE-3	CRL-11233 (ATCC©)	Liver-Healthy	Adherent	BEGM + Bullet kit (Lonza-Clonetics, CC3170)	Add all separate additives provided in the kit expect GA† and Epinephrine. Add 5 mg/mL EGF, 70 ng/mL Phosphoethanolamine, 10 % FBS	Mixture of 0.01 mg/mL fibronectin, 0.03 mg/mL bovine collagen type 1, 0.01 mg/mL BSA dissolved in BEBM medium	Trypsin-EDTA 0.05%	5 % DMSO
Jurkat	ACC 282 (DMSZ)	T cell lymphoblast	Suspension	RPMI 1640	10 % FBS, 1% PS, 25 mM HEPES, 2mM L-glutamine	None	None	70 % RPMI, 20 % FBS, 10 % DMSO

*EGF: Epidermal growth factor, †GA: Gentamycin/Amphotericin, BSA: Bovine Serum Albumin, EDTA: Ethylenediaminetetraacetic acid, DMSO: dimethyl sulfoxide

3.2.3. Cryopreservation and thawing

Many experiments require considerable numbers of cells, and it is critical that these cells are at low passage number. Each cellular replication can be subject to genetic modifications, which are passed to daughter cells. To adhere to good laboratory practises, long-term storage of cells is crucial. Cryopreservation requires the use of a cryopreservant that avoids the formation of crystals, preventing membrane disruption and reduction of viability. However, many cryopreservants used, as dimethyl sulfoxide (DMSO), are very toxic to cells at room temperature, so freezing cells quickly after adding it to the medium is imperative.

The process of cryopreservation starts by trypsinising cells as described in section 3.2.1. After cell counting, cells are centrifuged at 200 x g for 5 minutes. Supernatant is discarded and replaced with cryopreservation medium, consisting of complete growth medium and DMSO. The quantity of DMSO is specific to each cellular type and are outlined in Table 3.1. Cellular pellets were resuspended, and 1 mL aliquots containing 1×10^6 cells were prepared in specialised freezing vials. Cryovials were transferred to a dedicated container (Frosty, Nalgene Inc.) and placed inside an ultra-freezer to controllably reduce temperature overnight before being transferred to a liquid nitrogen tank.

Cellular thawing is as critical as cell freezing. The typical procedure is applicable across cell types to achieve a good survival rate. As DMSO is toxic, good planning and timing is key. Before starting the thawing process, it is recommended to prepare a 15 mL Falcon tube with pre-warmed complete medium. Subsequently, place the cryovial containing the cells in a water bath at 37ºC for 1-2 minutes. When no ice is observed, promptly transfer the cells into the previously prepared falcon tube under a cellular safety cabinet and immediately centrifuge them for 5 minutes at 200 x g. Remove supernatant and gently resuspend the cellular pellet to transfer it to a T25 flask. Place the cells in an incubator and monitor them daily to ensure attachment and survival. After 24 hours, medium was replaced to remove any DMSO impurities and non-attached cells, preventing potential reduction of viability.

3.3. Bio-nano interactions

In experiments that entail the interaction of nanoparticles with biological systems, such as cells, tissues, or organisms, is important to understand their interaction for applications spanning medicine, diagnostic and environmental sciences.[143] As scientists continue to harness the unique properties of materials at the nanoscale, ensuring the safety and efficacy of these interactions is crucial. Key considerations regarding bio-nano interactions will depend on the application they are intended for, but will have to encompass biocompatibility and toxicity, cellular uptake, and surface modifications.

To better understand the intricate connection between biological and nanoengineered components, the MIRIBEL guidelines[119] (Minimum information reporting in bio-nano experimental literature) provide a framework for designing and reporting bio-nano experiments. To do so, it establishes a framework of research guidelines, reporting standards, and checklists to create robust and reproducible research in the field of bio-nano interactions.

This dissertation followed the MIRIBEL recommendations with the objective to improve the quality of the research and improve the accessibility and quality of the data. Building upon these guidelines, the upcoming chapter will examine standardisation of the minimum information to be reported, tailored for PPTT.

3.3.1. Nanoparticle cytotoxicity

In vitro cytotoxicity assays include a range of approaches that evaluate crucial factors influencing cell viability. These assays are fast, convenient, and cost-effective, offering advantages over more specific methods that target specific markers. Assays that measure cytotoxicity may be classified as enzymatic, metabolic, reactive, and staining techniques.[27]

Given than the interaction between nanoparticles and cells can lead to undesirable effects, studying cellular viability upon contact with nanomaterials is a critical aspect for their use in food and health

applications. Cytotoxicity may arise from the shape and size of the nanoparticle, as well as their materials.[28,141,154] Most nanoparticles are produced with materials which in bulk are considered non-toxic for humans, but their cytotoxicity is different at the nanoscale. Therefore, it is important to check viability of cells on nano-interactions.

3.3.1.1. MTT assay

To study the cytotoxic potential of AuNR-PEG and laser irradiation, thiazolyl blue tetrazolium bromide (MTT) was used in cancerous and non-cancerous cell lines upon contact and incubation with the nanoparticle suspension. MTT measures the metabolic activity of cells, directly dependent on mitochondrial respiration, interpreted as a measure of cellular viability. Considered a quantitative colorimetric test, the MTT assay relies on the metabolic conversion on viable cells of MTT into insoluble formazan crystals. Unviable or dying cells do not retain their redox potential and are unable to transform MTT.

The MTT assay allows to rapidly quantify the metabolic activity of cells, but some considerations must be taken. This assay is very susceptible to the number of cells, concentration of MTT added to the cellular suspension, and time the MTT salt is in contact with the cells.[155] By controlling all these parameters and making them highly reproducible, including replicates and internal controls, we ensure that analysis of AuNR-PEG cytotoxicity with MTT is a robust method. Nonetheless, the MTT assay measures only one aspect of cellular viability, so complementary methods that observe other parameters are highly encouraged to perform simultaneously.

3.3.1.2. Trypan blue staining

The trypan blue assay studies the membrane integrity of cells. Trypan blue is a non-permeable dye that requires membrane permeabilization or fractures to travel inside the cell. It relies on the nuclear-exclusion principle in which membrane-impermeable trypan is excluded from viable cells but can enter cells whose membrane integrity has been compromised. However, trypan blue is inherently toxic to cells. Consequently, viable cells may eventually stain after long exposures to the dye, potentially impacting measurements if time of exposure changes between analysis. To mitigate this, the exact same short incubation times (1 to 2 minutes) and immediate counting is crucial to prevent the dye from permeating to viable cells.

This assay, characterised by its simplicity and rapidity, measures viability exclusively by observing dye exclusion in cells placed inside a haemocytometer or cell counter. Nevertheless, and similarly to the MTT assay, it has the limitation to measure viability based exclusively on membrane integrity.[156] Thus, viability may have been compromised through other means that this assay cannot evaluate. Employed with complementary viability assays trypan blue can be an indispensable tool to AuNR-PEG, and PPTT toxicity.

3.3.2. Nanoparticle uptake

Studying the uptake of gold nanoparticles is crucial, particularly in the context of PPTT, where differences observed between cells irradiated with or without nanoparticles can be attributed to their presence or absence during irradiation. Namely, only cells that have internalised the plasmonic nanoparticles will efficiently convert light to heat and increase their temperature.

The process of cellular internalisation is widely affected by the size of the nanoparticle, and understanding how different cell lines internalise them is important for nanotoxicology and drug development. The intricacies of cellular uptake are not only associated to the size, but also to the shape, material and functionalisation that the nanoparticle may have. Various factors urge to investigate the internalisation of nanoentities by cells.[157,158] One example that becomes more apparent *in vivo* than *in vitro* is the protein corona. This layer of proteins that adsorb to the nanoparticle surface upon contact with biological fluids can impact uptake and cellular distribution. Therefore, models that incorporate

these and other complexities, such as an immune system, whilst studying uptake are essential for a complete understanding of the internalisation process.[154,159,160]

In vitro uptake studies, nonetheless, are efficient approaches to obtain valuable insights and preliminary understanding of potential differences in uptake between cell lines, nanoparticles, and specific targeting.

3.3.2.1. TPL microscopy

Two-photon luminescence (TPL) microscopy enabled the measurement of AuNR-PEG concentrations in cell culture. The unique light scattering properties of gold nanorods eliminate the necessity for specialised staining or use of fluorophores to quantify AuNR uptake. AuNR are attractive for TPL as they possess TPL at the near-infrared, where minimal scattering by biological molecules and tissues occurs.[161] TPL from the absorption of two photons by AuNR provides a robust signal that is resistant to photobleaching.[126,162]

When compared to confocal microscopy, both techniques remove out-of-focus light, improving the signal and making it clearly distinguishable from tissue background. However, in TPL microscopy, photodamage and toxicity in biological samples is reduced, still providing deep imaging capabilities.[33,115,126,161] AuNR excited at their LSPR enhance two-photon absorption and are suitable for bright, stable and long-term tracing. Correlation between TPL signal and concentrations of AuNR-PEG is built on the linear relationship between both factors by using calibration factors.

3.3.2.2. Microscope calibration

Following the calibration between TPL signal and AuNR-PEG concentration performed previously in the group by Morales *et al*.[33] we were able to determine the uptake of AuNR-PEG by the different cell lines. Details for obtaining the calibration factors entailed the acquisition and characterisation of the point spread function (PSF) for the specific studied nanoparticle. The PSF served as the acquisition voxel for all TPL images and was maintained stable for all future measurements. For establishing the correlation between the mean TPL signal and AuNR concentration, TPL images of suspensions of 100 µL of AuNR dispersed in dH_2O were measured at different molar concentrations. By extracting the slope from the linear fit between the drak-substracted TPL in each voxel of the image, and the concentration of AuNRs, the calibration factor was obtained. This method was repeated in triplicate to eliminate uncertainties.

3.3.2.3. Imaging system

TPL images for AuNR-PEG *in vitro* quantification were obtained using a confocal microscope (Leica TCS SP5, Leica Microsystems) coupled to a Kerr lens, mode-locked, Ti:sapphire laser with a 200 fs pulse duration (Mira900, Coherent) tuned around the absorption peak of the used AuNR-PEG (810 nm).

3.4. Platform for *in vitro* PPTT

AuNR-PEG have their peak absorbance where their LSPR is. To optimise the conversion of light to heat during irradiation, the light source illuminating the nanoparticles should align with their maximum peak of absorbance. In the context of *in vitro* applications, ideally, the laser emission wavelength and nanoparticle LSPR should align with the optical biological window (700 to 980 nm). In this range of wavelengths, NIR lasers encounter lower absorption by water, blood and haemoglobin.[22,25,26,163,164] These characteristics that are advantageous for *in vivo* irradiation, prove also valuable on *in vitro* experiments, where models simulating tissues, such as with 3D structures, skin-like models and cellular phantoms, can benefit from deeper tissue penetration lasers.[165–167]

The platform that was developed in the group for *in vitro* PPTT allowed us to irradiate cells in a semi 3D-like situation, where cells were not attached to a surface, with the possibility to control the laser power density and time of irradiation. Moreover, the addition of a thermal bed and IR thermal camera granted us the possibility to control and observe temperature generation before, during and after irradiation.

3.4.1. Illumination source

For this project, a continuous wave (cw) collimated laser beam from a Ti:sapphire laser (LU0808D 180 diode laser, LuOcean Mini, Lumics GmbH) with a 808 nm wavelength was used to illuminate the samples. With an original maximum output power of 18 W, the laser was coupled to a 400 µm fibre (NA=0.22) to reach a collimating lens (F810SMA-780, NA=0.25, Thorlabs) fixed to a graduated diaphragm or iris (SM1D12C, Thorlabs) to control the irradiation beam diameter and power density output (Figure 3.1- A). The control of the aperture of the iris allowed us to change the diameter of the collimated laser beam between 0 and 12 mm.

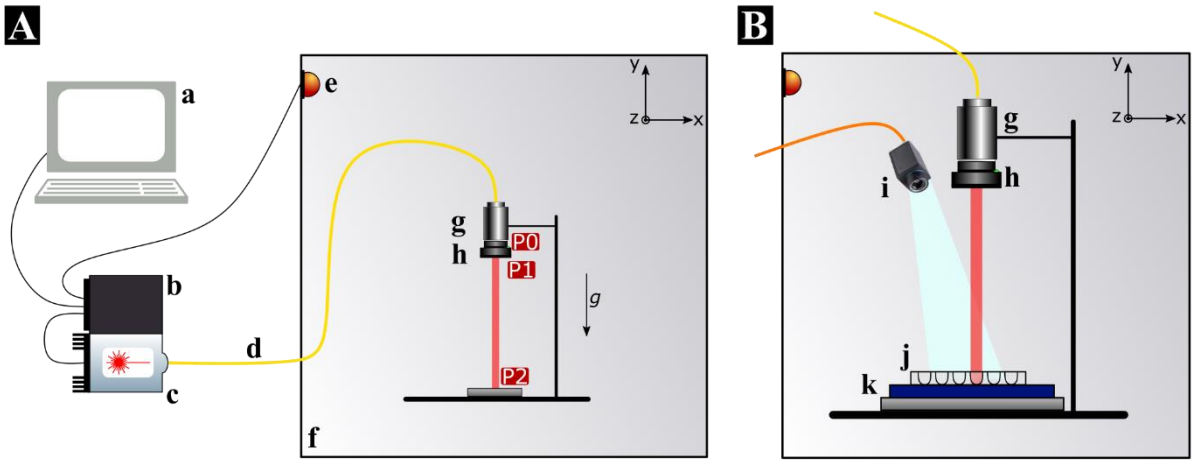

Figure 3.1 Schematic representation of the in vitro PPTT laser irradiation platform. A) Interior and exterior components of the Hyperbox. B) Close-up of the elements inside the Hyperbox. The components listed are: a: Computer/External controlling software, b:Laser power supply, c: Laser and cooling block, d: Optical fibre, e: Interlock, f: Hyperbox, g: Collimating lens, h: Iris, i: Thermal camera, j: 96-well plate with samples, k: heating bed, P0,P1: Laser power before and after collimating lens, P2: Laser power density at sample.

For the *in vitro* PPTT experiments discussed, and unless otherwise specified, the laser characteristics were adjusted to a 3 mm laser beam diameter, single laser power of 3 W/cm^2 and 3 minutes time of irradiation. Prior to the selection of these parameters, several power densities and time of irradiation were tested on the 786-0 cell line. These results are briefly discussed in Chapter 5.

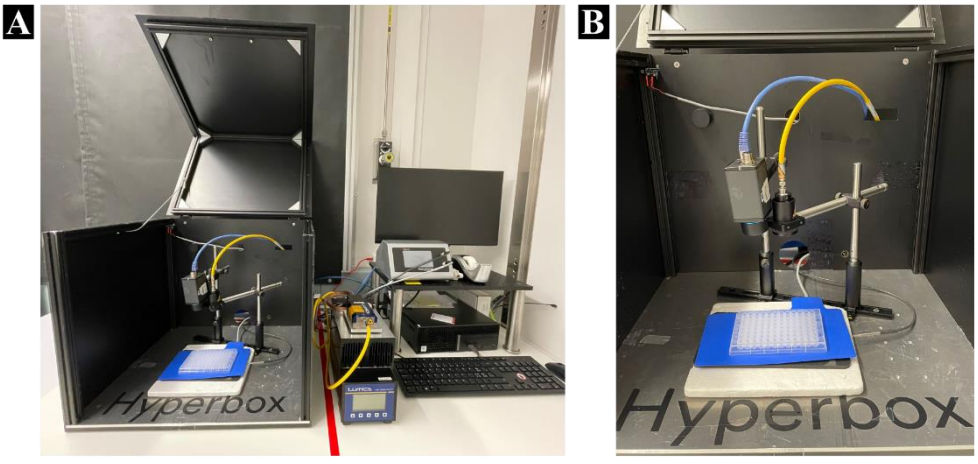

Figure 3.2. Images showcasing the schematic representation of Figure 3.1. A) Hyperbox overview illustrating the structural design and external features. B) Close-up of Hyperbox contents. Zoomed-in view showcasing the only items contained inside the box during irradiation.

3.4.2. Laser irradiation platform

To safely illuminate the samples without the risk of getting into direct contact with either the laser or the irradiated cells, all components needed for PPTT and measurements were contained inside a black box, from here on named Hyperbox. This box was kept closed during irradiation (Figure 3.2-A). The box contained the laser collimator and diaphragm (Figure 3.1-B, g and h), the thermal camera (i), a heating bed (k, homeothermic monitoring system, 55-7020, Harvard Apparatus) and the 96-well plate with U-bottom that contained the samples during irradiation (j).

3.5. Experimental workflow

To maximise the output of each of our experiments and maintain high reproducibility and standardise the process, we followed for all experiments a similar protocol: first cells were seeded in the most appropriate vessel, then incubated with AuNR-PEG and, finally, the experiment of interest was performed. For each experiment, the details are written in the following sections. In Figure 3.3 it is possible to observe the experimental details for the uptake, cytotoxicity and PPTT experiments regarding number of cells, nanoparticle concentrations and timings.

This experimental workflow was repeated for all attached cells without additional variations. Exceptionally, and detailed in their specific section, Jurkat cells required of specific changes to the protocol to fit their specificities (suspension culture).

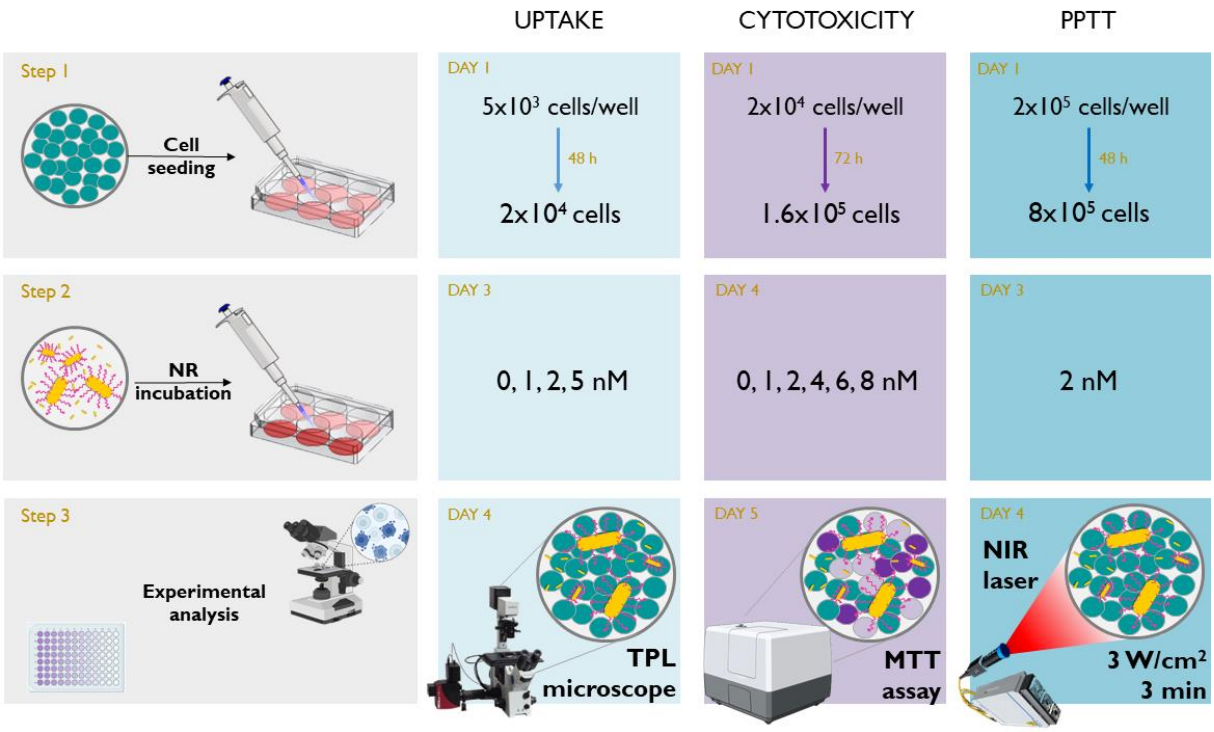

Figure 3.3. Schematic representation of sample preparation process. Schematic overview illustrating variations in the number of cells seeded, AuNR-PEG concentrations and experimental setups. Each column is a distinct experiment. The different timelines are also represented.

3.5.1. Sample preparation

As shown in Figure 3.3, for each experiment a different total number of cells were used. For uptake quantification, 5000 cells were seeded in 96-well plates (polystyrene clear flat bottom, Thermo Fisher Scientific) and allowed to expand for two days. For cytotoxicity assays, 2×10^5 cells were seeded in 24-well plates (polystyrene clear flat bottom, Thermo Fisher Scientific) and allowed to grow for 3 days. For PPTT, 2×10^6 cells were seeded in 6-well plates (polystyrene clear flat bottom, Thermo Fisher Scientific) and allowed to grow for 2 days, eventually containing 8×10^6 cells in each well.

Prior to incubation with AuNR-PEG, wells were washed with appropriate cell culture medium without supplements and AuNR-PED were added diluted in culture medium without FBS at the desired concentration to each well. In the case of non-cancerous cell lines (Hek293, NL20 and THLE-3) incubation with AuNR-PEG had to be performed with medium containing FBS due to the delicate nature of the cell lines, as 24 hours without FBS proved to be highly lethal.

3.5.2. *In vitro* quantification of uptake

AuNR-PEG were incubated with all cell lines at four different molar concentrations (0 nM, 1 nM, 2 nM and 5 nM) for 24 hours. Before imaging, excess AuNR-PEG was removed, and all wells washed twice in PBS. Cells were fixed with 4 % paraformaldehyde (PFA) for 5 minutes, washed twice with PBS, incubated with 2 % PFA for 15 minutes, washed and let in 1 % PFA. Bright field (BF) and TPL images of two random positions from each well, and triplicates for each concentration, were taken. Six images per cell line and concentration were obtained, except for controls (0 nM) where only three images were taken.

A calibration curve of the TPL signal of the AuNR-PEG in each cell line was acquired using different concentration of AuNR-PEG diluted in purified water. Image processing of TPL and BF images was done using open-source Image J software. Borders of cells were delimited in BF images to detect TPL signal coming only from internalised AuNR-PEG.

3.5.3. *In vitro* quantification of cytotoxicity

AuNR-PEG cytotoxicity was analysed at six different molar concentrations (0 nM, 1 nM, 2 nM, 4 nM, 6 nM and 8 nM) after 24 h of incubation by the addition of MTT (M2128, CAS 298-93-1, Sigma Aldrich) to a final concentration of 0.5 mg/mL. Plates were incubated at 37°C for 30 minutes. MTT solution was removed and formed formazan crystals were dissolved in 300 µL DMSO. Plates were read at 550 and 750 nm on a microplate reader (Synergy H1, BioTek Instruments). Every cell line had appropriate alive controls (0 nM) and four replicas per condition. Viability was calculated as a percentage of the alive group.

3.5.4. Photothermal irradiation

For PPTT effects on cellular lines, a suspension of 8×10^6 cells in 20 µL on a 96-well plate with round bottom (polypropylene, round bottom, costar3879 Corning Inc.) was irradiated from the top with a 3 mm diameter cw collimated laser beam from an illumination source according to the description above. A single laser power density and time of irradiation (3 W/cm^2 – 3 minutes) were used throughout the experiments.

Baseline well plate temperature was controlled with an auto-regulated thermal bed to keep constant starting temperatures, as well as not allowing cell temperature to drop below 34°C during irradiation.

After irradiation, viability was studied at two different timepoints (Figure 3.4). Immediately after illumination, cell suspensions were recovered in 1 mL of appropriate cell culture medium without FBS and the sample was divided into two equal parts (500 µL) to examine viability immediately after treatment (TAT 0 h) or 24 hours later (TAT 24 h). For the TAT 24h the cell suspension was reseeded in a 6-well plate with 1 ml complete cell culture medium and let it rest at 37°C in a 5 % CO_2 incubator. The remaining 500 µL cellular suspension of the TAT 0h is analysed with two complementary cell viability assays: MTT assay and trypan blue staining. For the trypan blue staining, 50 µL of the sample was stained with 12.5 µL trypan blue solution (0.4 %, Gibco, Thermo Fisher Scientific), and counted in a haemocytometer under an inverted microscope. For the MTT assay, 50 µL MTT 5 mg/mL were added to the remaining 450 µL cell suspension and incubated 30 minutes at 37°C. After incubation, samples were centrifuged to pellet cells and formazan crystals and 90 % of supernatant removed before adding 1 mL DMSO and read samples as with the cytotoxicity studies.

For the TAT 24h assessment of viability, cell culture medium and attached cells were recovered from each well and centrifuged to pellet cells and were re-suspended in 500 µL of appropriate culture medium

without FBS. The same protocol than in the TAT 0h sample was implemented for the analysis of the TAT 24h (Figure 3.4).

Viability was calculated as a percentage of the alive control group (without AuNR-PEG and not irradiated) for the MTT assay. In the case of trypan blue, results are the percentage of cells, dead and alive, for each condition.

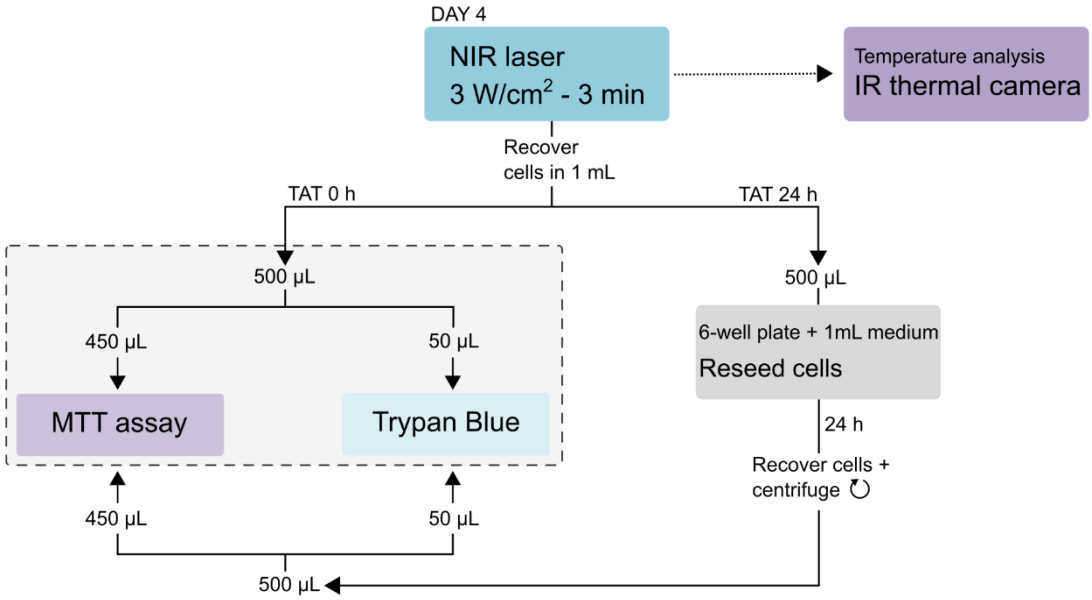

Figure 3.4. Experimental workflow of PPTT. Schematic overview of the workflow for laser irradiation and post-irradiation procedures. This representation outlines laser application and cell recovery after irradiation, as well as visual organisation of the methodology used to analyse viability after treatment.

3.5.5. Statistical analysis

Statistical analysis was performed using R studio (R Core Team, 2020) and Graphpad Prism (Graphpad Software Inc.). All data are expressed as mean ± SEM (standard error of mean). SEM was the preferred method to express error as the number of samples per experiment was equal between groups. The number of samples (n) used is provided in each experiment, meaning the standard deviation (SD) is easily extractable. For comparisons between multiple groups, one-way ANOVA or Kruskal-Wallis tests were used (depending on the normality of the data), followed by a post-hoc test for multiple comparisons. For all statistical analyses, significance level is 0.05 (*p<0.05, **p<0.01, ***p<0.001).

3.6. Molecular responses to PPTT

Exploring the effects of PPTT on cellular viability provided a lot of insight on what is occurring to cells after irradiation, with and without AuNR-PEG. In tandem with these findings, a closer examination of molecular events that could be triggered can unravel the intracellular processes occurring after locally increasing the temperature via PPTT.

3.6.1. Human apoptosis protein array

The decrease in viability observed during the MTT assay with irradiated cells, in contrast to the unaffected membrane integrity spotted during trypan blue staining, suggested that apoptosis rather than necrosis was being triggered during *in vitro* PPTT. This aligned with the findings from previous studies, described in Chapter 5.

For a comprehensive apoptotic cellular response analysis post-irradiation, the protein profiler for human apoptotic proteins was employed. It is a rapid and sensitive test capable of detecting the relative expression of 35 proteins on each membrane. Each membrane was used to study a single sample. The samples were obtained in triplicates for controls, cells irradiated with AuNR-PEG, without AuNR-PEG

and heated in an oven. For irradiated samples (with and without AuNRs) two different timepoints were studied.

Following irradiation as detailed in section 3.5.4., cells were recovered and reseeded in 6-well plates until 6 and 24 h after treatment. After the specified duration, cells from three wells under the same condition and treatment were recovered together and centrifuged at 300 x g for 5 minutes to pellet cells. Supernatant was removed and the cell pellet washed with 1 mL PBS. Cells were centrifuged again and supernatant discarded. The pelleted sample – containing the cells of 3 irradiated samples, approximately 2.4×10^6 cells – was stored at -80°C until the proteome profiler experiment.

As a control to hyperthermia, cells heated in an oven were used to compare them to PPTT-induced heating. To do so, cellular pellets as described in section 3.5.4. (800,000 cells in 20 µL), were placed in a pre-heated oven at 60°C for 5 minutes. After this, cellular pellets from three wells were recovered and resuspended in 3 mL of medium and centrifuged at 300 x g for 5 minutes to pellet them, obtaining a sample with approximately 2.4×10^6 cells. This sample was washed in 1 mL PBS, centrifuged and supernatant discarded. The oven-cells pelleted sample was stored at -80°C until the proteome profiler experiment.

After sample collection, cellular pellets were thawed and solubilised in 240 µL Lysis Buffer, following the kit manufacturer instructions. The lysates were gently rocked at 2-8°C for 30 minutes and briefly sonicated 2 seconds before centrifugation at 14000 x g for 5 minutes. The resulting supernatant was transferred into a clean test tube and total protein quantification was performed (Pierce™ BCA Protein Assay Kit, Thermo Fisher Scientific). It's crucial to use cell lysates immediately, working with them on ice or storing them at -80°C. For the array, 220 µg of total protein were used for each experiment, using the same total concentration to ensure uniformity for relative quantification comparisons. Subsequent steps were performed in accordance to the manufacturer instructions.

Membranes were read on a chemiluminescence reader (Chemidoc XRS+ System, Bio-Rad Laboratories Inc.) immediately after mixing with the chemiluminescence detection reagents. Image analysis was performed with Image Lab software (Bio-Rad Laboratories Inc.).

3.6.1.1. Data analysis

The mean values of each protein spot signal were used to analyse the data. To ensure uniformity, the same amount of data pixels was used for each spot, even across samples. Duplicate values of each membrane repeated spot were averaged and normalised to reference spot values. Reference spot values should be consistent across all membranes and were used for data normalisation between samples. This involved the average of the reference spots of all membranes, comparing them to the reference spots of control samples (cells without AuNR-PEG and not irradiated), and creating a factor to which they correct to. The signal values of each membrane were multiplied by their respective correction factor.

To create a ratio of relative expression, we averaged the values of controls samples as the standard protein expression. We then divided the protein signal values against the same protein control signal value. This way, we were able to obtain the relative expression for each of the 35 proteins against controls, and it allowed us to do a meaningful comparison of protein expression between conditions.

For statistical analysis, the normalised values after correcting for membrane differences were used. We assessed normality with the Shapiro-Wilk. An ANOVA or Kruskal-Wallis test was performed, depending on the normality of the data. A post-hoc multiple comparison test was performed a posteriori. All statistical data and graphs were created with Graphpad Prism (Graphpad Software Inc.). Statistical information is presented in tabular format, highlighting relevant comparisons for clinical needs. Graphs depict ratioed values against controls.

3.6.2. Cytokine expression

To determine if PPTT stimulated the cytokine expression of human immune Jurkat cells, we first defined the experimental conditions. After irradiation of cells as described in section 3.5.4., each of the 8×10^5 cells sample was recovered in 1 mL. After recovery, 10 samples from the same condition were combined, and 100 µL of this mixture was reseeded in well of a 96-well plate. At each desired timepoints (30 minutes, 60 minutes, 90 minutes, 2 hours, 3 hours, 4 hours and 6 hours) contents of the wells were recovered. Cells were centrifuged and the supernatant was transferred to another tube, which was then frozen at -80°C until the moment of analysis.

Cytokine expression was studied using an uncoated ELISA kit (Thermo Fisher Scientific) for cytokines of interest IL-1b, IL-2, IL-6 and TNF-α. Following the manufacturer's instructions, the capture antibody was applied to the ELISA microplates overnight at 4°C. The next day, plates were blocked, followed by a 3-hour incubation with the samples. To obtain a calibration curve for cytokine concentration values, serial dilutions of cytokine standards were introduced for each cytokine assay. The detection antibody was added to the microwells, followed by incubation with Avidin-HRP and substrate solution for colour development. After the recommended incubation times, stop solution was introduced and the ELISA microplate was read at 450 and 570 nm. Between all incubation steps, several washes with PBST (Phosphate Buffered Saline- 0.05 % Tween) were done.

For data analysis, replicates for each condition and time analysed to obtain the mean expression and standard deviation of the mean. Statistical analysis was performed using Tukey's multiple comparison test, comparing first the expression differences at different time points for each condition, and testing the differences between control samples and samples irradiated with and without nanoparticles at each different timepoint.

4

Standardisation of *in vitro* studies for plasmonic photothermal therapy

This chapter was published in ACS Nanoscience Au 2023, 3 (5), 347-352 with DOI: 10.1021/acsnanoscienceau.3c00011

As we have learned in Chapter 3, the methodologies and techniques used in studying *in vitro* plasmonic photothermal therapy (PPTT) are pivotal for achieving high accuracy and reproducibility. Translation from preclinical to clinical stages faces great challenges that impact the application of nanomaterials for human use. Drug regulatory agencies, including the FDA (US Food and Drug Administration) and the EMA (European Medicines Agency), are responsible for granting licenses for diagnostic and therapeutic nanomaterials,[110] setting high standards to guarantee the safety and effectiveness of nanoformulations. Their rigorous regulatory framework, combined with a lack of systematic experimentation in nanomedicine and challenging data comparison from different studies, affects the approval process for nanoparticles.[119,153,154]

Standardisation addresses the commercial, academic, and societal concerns[119] associated with scientific research by creating experimental protocols that produce robust and reproducible data, easily accessible by researchers and allowing comparisons between different studies and groups.[154,168] Obtaining and presenting data through standardised procedures improves the validity of the results, accelerating the approval process with regulatory authorities.

Guidelines that outline the minimum information to be reported improve our understanding of acquired data. In the bio-nano experimental literature, the MIRIBEL guidelines[119] (Minimum Information Reporting in Bio-nano Experimental Literature) improve the development of novel technologies for biomedical use by encouraging the application of methodical approaches for material characterisation, risk assessment and experimental design. For animal experimentation, the ARRIVE guidelines[169] (Animal Research: Reporting of In Vivo Experiments) stablish the items that must be reported on *in vivo* experiments. All in all, adhering to these guidelines ensures reproducibility and comparability across scientific studies, cultivating a robust foundation for the transition from preclinical to clinical settings.

In PPTT, lack of standardisation is one of the main hindrances for the development of the therapy, as already pointed out by Sharifi *et al.*[122] Albeit the many obstacles present on the translation to clinical practice, following methodical approaches improves the creation of robust and comprehensive data. At the same time, standardisation facilitates the evaluation of different types of nanoparticles, biological systems -their interaction- as well as identification of sources of variability by using systematic studies and keeping reference standards.[149] Systematic *in vitro* PPTT studies will push the field forward by addressing concerning questions about biocompatibility, delivery and effectivity.

PPTT can be useful as a standalone treatment for cancer treatment or by locally combining it with more conventional treatment methods. The potential of this therapy has been repeatedly proven *in vitro*, and has been performed with success in clinical human pilot studies.[55] Nonetheless, validation *in vivo* is challenging due to the ethical concerns and increased costs than animal experimentation impose. On the other hand, *in vitro* studies have a limited ability to replicate complex *in vivo* environments, limiting the reflection of results on what happens in organisms. Moreover, the heterogeneity of cell lines, nanoparticles and protocols used by researchers, render preliminary conclusions that are difficult to contrast and hinder data comparison.[159]

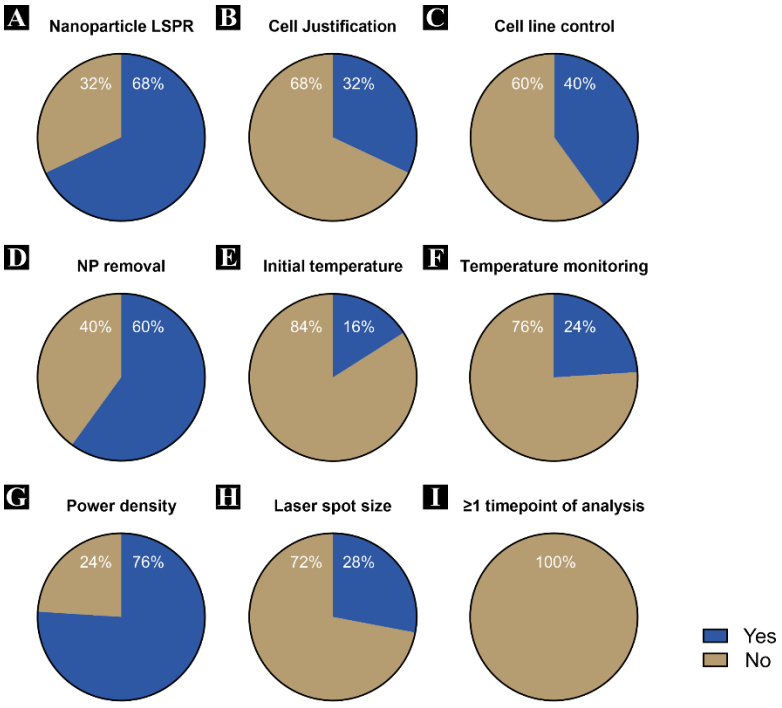

Figure 4.1. Pie charts depicting the answers across 25 articles that carry out PPTT in response to the following questions (A-I). A) Does it mention the nanoparticle LSPR? B) Do the authors explain why the used cell lines were selected? C) Is there a cell line used as a control for the results? D) Are the nanoparticles removed prior to irradiation? E) Is the initial temperature before irradiation reported? F) Is the temperature monitored continuously or intermittently during irradiation? G) Is the power given as power density? H) Is the laser spot size reported? I) Is more than one timepoint after irradiation analysed? Each chart represents the proportion of articles that answered "yes" or "no" to the question, as indicated in the legend.

The ability to contrast findings after an experiment is important for the outcome of the research. This work was motivated by the observation of the large discrepancy on the data reported in the literature. A 25-article sample on papers carrying PPTT was carefully examined, and key aspects of the therapy were recorded to obtain information on what, and how, each researcher was reporting when performing *in vitro* PPTT. Figure 4.1 illustrates the disparity observed when reporting PPTT information. A striking example is the lack of clear mention of removal of nanoparticles prior to irradiation (Figure 4.1-D). From the 25-article sample, 40 % of the authors do not specify the removal, giving the impression that increases of temperature experienced by cells during illumination is the result from the irradiation of suspended nanoparticles in the medium, not of internalised nanoparticles.

This exhaustive analysis of published papers, focusing on key parameters for the field of PPTT, led to the work published in ACS Nanoscience Au.[120] Given the broad spectrum of the community, a didactic and synthetic format of communication was chosen to reach a wider audience, making it accessible to everyone in the field, independently of their level of expertise and scientific background. Within the published work, we proposed a series of best laboratory practices along with a checklist of minimum data to be reported (Figure 4.2and Table 4. 1). Detailed explanations are given on how to easily improve various aspects of *in vitro* PPTT. This guideline format is fully complementary with in-depth reviews available in the field for the numerous topics involved in PPTT.[9,10,14,26,135,163,170]

4.1. Material characterisation

4.1.1. Nanoparticle purification

The goal of nanoparticle purification is to remove the cytotoxic fraction of nanoparticle synthesis, remove medium-related impurities and obtain sample homogeneity for enhancing biocompatibility. Seed-mediated growth synthesis, one of the most versatile methods to produce gold nanoparticles (AuNPs), uses cetyltrimethylammonium bromide (CTAB) as a stabilising agent. CTAB has shown high cytotoxicity levels, and several strategies have been adapted to remove this moiety from nanoparticles after synthesis.[159]

Ligand exchange and functionalisation improves biocompatibility and reduces the formation of clusters, however, CTAB remains in the medium and washes by centrifugation do not eliminate it completely. To further increase biocompatibility of nanoparticles, dialysis can be used to eliminate CTAB in solution.[171] Dialysis is an effective, but time-consuming method, in removing unbound moieties and organic

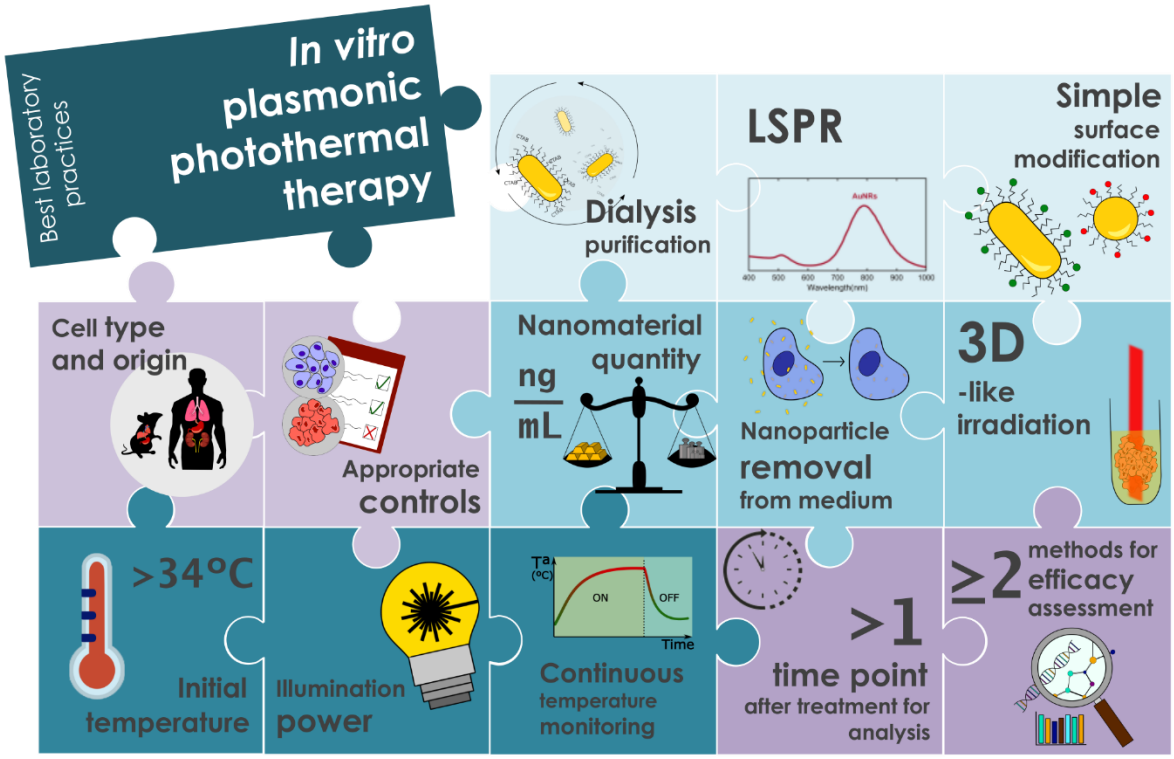

Figure 4.2. Schematic representation of the main key aspects to ensure meaningful and reproducible data for in vitro PPTT.

solvents used during functionalisation or synthesis, thereby reducing the overall cytotoxicity. The dialysis membrane acts as a net, trapping the nanoparticles inside while allowing CTAB to flow outside.

Other high-yield processes can also be used for nanoparticle functionalisation, such as tangential flow filtration and salt/buffer-exchange columns. Each method presents distinct advantages and disadvantages to remove medium-related impurities in nanoparticle solutions.[43] Considered a highly useful method for reducing large quantities of unbound moieties from the supernatant, ultracentrifugation has the challenge of removing the supernatant closer to the nanoparticles without disturbing the pellet. This challenge can be overcome by combining several ultracentrifugation cycles with other methods. In our case, the presence of traces of CTAB in the pellet after centrifugation affected the sterilisation process by filtration, resulting in sample loss due to the gold nanorods (AuNR-PEG) adhering to the filter. This risk can be mitigated by doing several centrifugation cycles, followed by dialysis and posterior filtration.

The most suitable purification method will depend on the specific requirements of each type of nanoparticle. Considerations of time, cost and scalability are crucial to select the most appropriate technique.

4.1.2. Simple surface modifications

Nanoparticle functionalisation has three main objectives: targeting, increasing colloidal stability, and reducing cytotoxicity. Surface modifications are essential in many nanoparticle types to increase their biocompatibility. A myriad of molecules, ranging from inorganic moieties to antibodies, can be conjugated to nanoparticles to produce multifunctional nanostructures e.g., to target specific tissues.

However, the complexity of multiple functionalisation nanoparticles can lead to increased costs of production and less consistent large-scale batches, posing challenges in commercialisation and approval by regulatory agencies. [10,105,116–118,122] When combining a nanoparticle with a functionalisation, targeting or drug, it is necessary to test the toxicity of all excipients in both bound and released states, considering all potential combinations.[105,118] Regulatory agencies often demand more rigorous testing for complex

	Representative units	Information
Material Characterisation		
Method of purification		Dialysis, ultracentrifugation…
Conjugation-stabilizer		
Laser wavelength	nm	
Nanoparticle LSPR	nm	
Nanoparticle type and ligand information		MIRIBEL guidelines*
Biological Characterisation		
Cell culture details		MIRIBEL guidelines*
Cell type and origin		Epithelial, human, cancerous…
Appropriate controls		
Experimental Protocol		
Nanomaterial quantity	ng/mL, µg/µL	Amount of material in the nanoparticle samples
Time of incubation	min, h	
Nanoparticle removal prior to irradiation	Yes, no	
Irradiation dimension		2D, 3D, organoid, suspension…
Type of well plate		Flat bottom, U-bottom, cuvette…
Time between administration and therapy	min, h	
Irradiation Protocol		
Temperature		
Initial temperature	°C	
Final temperature	°C	
Temperature increase	°C	Difference between initial and final temperature
Temperature recording		
Type		IR thermal camera, probe…
Time period		Continuous, intermittent…
Position		Position regarding the sample (top, lateral, bottom…)
Baseline and cool-off	s, min	Temperature recorded before and after irradiation
Laser		
Type		Collimated, divergent
Position	cm	Position and distance to the sample (top, lateral, bottom…)
Beam diameter/Area	mm, mm^2	
Power density	W/cm^2	
Time of irradiation	s, min	
After Irradiation		
Method of assessment		Techniques used to assess viability, toxicity…
Time after treatment	min, h	Time between the end of irradiation and viability assessment

Table 4. 1. Summary and checklist of parameters to be reported on *in vitro* PPTT experiments. This table provides a summary of the parameters to be included on *in vitro* PPTT experiments. We provide representative units to use when reporting results. *MIRIBEL guidelines[119] complete the proposed table for characterization of bio-nano interactions.

nanoparticles, resulting in additional protocolary steps.[105,116] Simple surface modifications overcome this, offering more scalable synthesis, less time-consuming and more cost-effective formulations.

A study conducted by Wilhelm *et al*.[138] performed a meta-analysis of 117 research papers regarding *in vivo* delivery of nanoparticles to target tissues. On average, AuNPs had only 1 % delivery efficiency to target cells. For all types of nanoparticles, findings showed that active targeting, although slightly better that passive targeting for tumour accumulation of nanoparticles (0.9 % and 0.6 % delivery efficiency, respectively), still had low delivery efficiency to the target tissue. A head-to-head comparison between both methods revealed a lack of significant differences in tumour accumulation.[44,138,172] As of today, strategies developed to enhance nanoparticle delivery have not effectively addressed the challenges of sequestration and targeting. Therefore, targeting modifications are still debatable on their efficacy to target certain tumours or cellular regions.

This phenomenon of lack significant differences in tumour accumulation between targeting types is partially attributed to the formation of the protein corona when nanoparticles interact with biological fluids. This dynamic process changes the physiochemical properties of the nanoparticle and their interaction with the cell membrane.[141] The protein corona formation on the nanoparticle obscures the targeting strategies, reducing the distinctiveness between passive and active targeting. The complexity introduced with the protein corona highlights the challenge in achieving precise control of nanoparticle behaviour *in vivo*.[46] Understanding its formation can be useful to pre-functionalise the nanoparticles to better suit the method of administration and specific target objective.[160,173] This knowledge can be used to improve nanoparticle design and customisation for specific biological environment. Nonetheless, characterisation of nanomaterial behaviour within a biological fluid cannot be fully assessed *in vitro*.

4.1.3. Localised surface plasmon resonance

Plasmonic nanoparticles have attracted special interest in nanomedicine due to their unique combination of physical and chemical properties.[22,174,175] They feature unique photophysical properties, which endow them the capacity to strongly absorb light at their localised surface plasmon resonance (LSPR). The LSPR is based in the coherent oscillation of free electrons of the metal and is strongly dependent on the constitutive material and geometry of the nanoparticle.

Non-symmetrical nanoparticles, like gold nanorods (AuNR), feature different absorption bands (longitudinal and transversal). Modifying the aspect ratio of AuNRs is used to tune the longitudinal LSPR to the near-infrared region (NIR),[176] to match the biological optical window, ensuring minimal light absorption by the tissue.[177] The points exemplified with AuNR are also applicable to other types of nanoparticles.

Optical properties of nanoparticles can be varied by changing their properties and the surrounding environment.[178] Measuring the detuning of the laser wavelength with respect to the LSPR peak of nanoparticles is important as it directly affects the efficiency of light-to-heat conversion.

4.2. Biological characterisation

4.2.1. Cell type and origin

Cell line selection for *in vitro* experimentation must account for their different behaviours. Immortalised cell lines will conduct themselves differently to primary cell lines and will have unique limits to what can be characterised with them. The choice of cell type (epithelial, fibrotic, tumoral…), source of origin (lung, kidney, skin…) and organism (human, mice…) affects the outcomes of *in vitro* PPTT and determines follow-up research based on these results. Cell type and cellular manipulation have an important effect on the outcomes of *in vitro* variability,[149,151,154] which will impact interpretation of PPTT data. As an example, nanoparticle internalisation depends not only on the properties of the nanomaterial and experimental protocol, but also on the cellular type, observing different trends between type and origin of cells.[158,179]

Extreme precaution should be taken when selecting the cell line to study the effects of PPTT *in vitro*. Data comparisons and future research will be heavily influenced by the chosen cell line, and therefore, justification of cell line selection is essential to fully comprehend the outcomes of the therapy.

4.2.2. Appropriate controls

The use of appropriate controls ensures the validity and robustness of scientific research. Studies across different cell types and their correlation with *in vivo* data provides the consistency needed to advance to clinical settings.[180] Currently, researchers have at their disposal thousands of cell lines available to perform *in vitro* experiments.

PPTT aims to eliminate malignant cells that have internalised the nanoparticles of interest. However, non-malignant cells will also be exposed to both laser and nanoparticles. It is important to study the influence of both factors -and their combination- will have on the viability of non-malignant cells. Non-carcinogenic cell lines used as a control should be from the same type, tissue, and organism, to confirm data robustness and safety of the nanomaterial. These characteristics are applicable to any research that involves the elimination of malignant cells, where the drug or nanomedicine will also encounter non-cancerous cells.

In addition, during systemic administration of nanoparticles, such as intravenous (IV) administration, only 1% of the administered dose reaches target cells,[138] observing a lot of off-target interactions of nanoparticles with cells.[118] Therefore, it is important to conduct experiments on malignant and non-malignant cells from different tissues.[151,153] Investigation in a myriad of cell lines provides information regarding effectivity of PPTT in different cancers, and it is possible to identify possible side effects on off-target cells, setting limits for light and nanoparticle dose safety.

4.3. Experimental protocol

4.3.1. Nanomaterial quantity

Nanomaterial cytotoxicity is assessed by performing sequential dilutions of nanoparticle concentrations and studying, by one or more methods, the viability after exposure at different endpoints. Concentrations are usually reported in molar concentration or as optical density, which becomes an obstacle to compare different studies, as the material, size, and geometry of the particle, among other factors, could also be responsible for the cytotoxicity of nanoparticles.

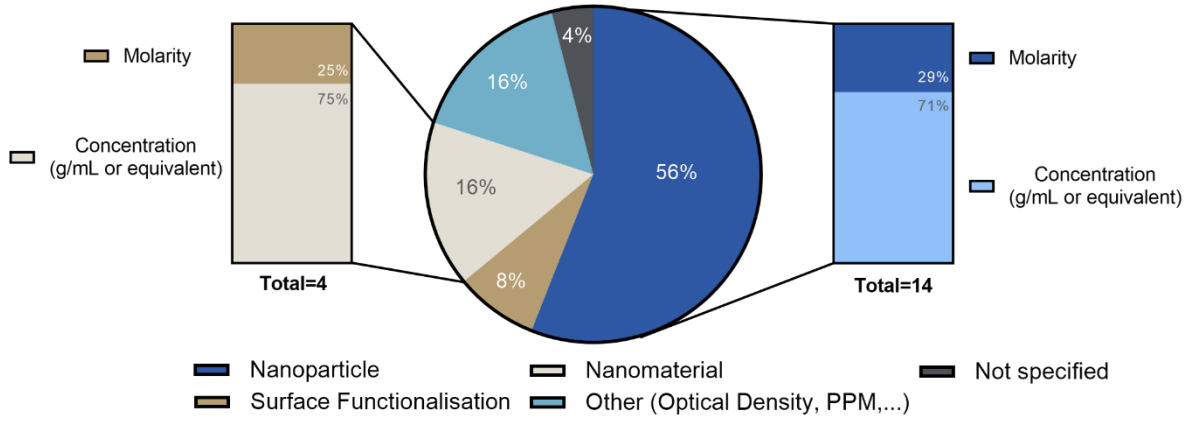

Figure 4.3. Pie chart representing the vocabulary employed to describe the concentration of nanoparticles used in experiments. Some authors prefer to refer to the concentration of nanoparticles used, whereas others opt to report the amount of nanomaterial. Nonetheless, there are discrepancies in the use of molarity or concentration (grams per millilitre or equivalent). Other authors report concentrations used of surface functionalisation or the optical density of the nanoparticles.

Lack of standardisation regarding nanoparticle concentrations makes it difficult to obtain consensus regarding cytotoxicity of nanoparticles (Figure 4.3), as reported by Jauffred *et al*.[145] Providing the concentration of the nanomaterial (e.g. mg/mL of gold, in AuNRs) is essential to assess the biocompatibility of nanoparticles.

Owing to their high biocompatibility, stability and photothermal efficiency, AuNRs are of the most used nanoparticles for PPTT. For AuNRs, cytotoxicity increased with the total gold concentration in the suspension, and was found to be independent of the shape.[128] Defining the nanomaterial quantity in a ng/mL format helps contrasting data between researchers and determining which factors govern the toxicological events of plasmonic nanoparticles. Similarly, internalised doses of the nanomaterial should be specified to obtain direct definitions of toxicity of nanoparticles, in contrast to exposure doses.[154]

4.3.2. Nanoparticle removal from the medium

For PPTT to be a valid therapy to treat cancers as a minimally invasive technique, it is important that cells can incorporate the nanoparticles and that they are equally distributed inside tumours. Ideally, non-target cells would not incorporate them. Moreover, it is critical that internalised nanoparticles can be irradiated externally. The efficacy of PPTT depends on the combination of biocompatibility, cellular uptake, and heat generation efficiency.

When studying *in vitro* PPTT, cells are exposed to plasmonic nanoparticles, so they are internalised, and later irradiated. Between these two steps, most protocols require several washes to remove nanoparticles not incorporated by the cells. Omitting the removal of unbound nanoparticles from the medium can have an impact on temperatures achieved during laser irradiation, consequently leading to incorrect conclusions about the efficacy of PPTT to eliminate targeted cells.

Some protocols omit the washing step and irradiate cells in a suspension of nanoparticles. This leads to measurement of temperature of nanoparticle suspensions, and not of internalised nanoparticles. Specifying the removal of non-incorporated nanoparticles from the medium prior to irradiation is key to ensure reproducibility between experiments and detecting differences in the final temperature achieved.

4.3.3. 3D-like irradiation

In vitro research encounters a significant challenge due to the lack of dimensionality of conventional cell culture methods. Nowadays, this challenge is often addressed by working with spheroids, organoids, or cellular scaffolds. While these approaches improve the physiological relevance of the cell culture, they are difficult to master, and manipulation of cells is more complex.

In the context of *in vitro* PPTT, most research is performed in 2D settings, where cells in a single attached layer are being illuminated. An alternative to 2D irradiation was described by Yang *et al*.,[181] where cells grown and incubated with nanoparticles in standard 2D conditions, were detached from the surface and illuminated in suspension. This irradiation in a 3D-like arrangement increases the collective thermal effects, hence increasing the homogeneity of the temperature profile, as well as maximum temperature increments. Moreover, it reduces heat dissipation with the surrounding environment.

Experiments on medium droplets containing high cell concentrations are better mimicking *in vivo* scenarios, where cells are in a disorganised distribution, and not uniformly irradiated. The effect of light and temperature is better reproduced than for 2D attached cells, as a thermal gradient to the outskirts of the irradiated area can impair the viability study after treatment. In a typical cell culture irradiated in an attached 2D cell culture, it is possible to distinguish the illuminated area from the region kept in the dark.[182] The creation of 3D models and phantoms that mimic tissue environments are useful to study laser penetration and obtaining more *in vivo* relevant temperature measurements. Laser penetration depth is crucial to ensure the accurate irradiation of the laser to the region of interest. Numerous papers address these concerns computationally by simulating photothermal therapy,[183] whilst *in vitro* efforts focus their aim in recreating human skin with phantoms.[166] These are useful methods to translate bio-optics to the clinical settings, as well as reducing racial bias by understanding different skin tones. Irradiation of cells briefly mimicking a 3D arrangement as proposed by Yang *et al*.,[181] and used throughout this dissertation, better defines laser illumination than irradiation of a single layer of cells.

Selecting suitable cell lines for 3D culture is important, considering varying resistance to external sources of stress, which may affect viability. Importantly, 3D cell arrangements increase the density of

irradiated cells, influencing the accumulation of signalling molecules (such as cytokines, growth factors and proteins) that impact cellular biology.[149] Besides, spatial organisation and cell interactions differ from 2D models, consequently affecting the outcomes of the therapy.

While not inherently superior, the move towards 3D culture methods in PPTT increases the predictability of *in vivo-in vitro* comparisons,[184] and improves clinical translation by better representing tissue and tumour environments. 3D methods present their own disadvantages, but more focus should be deposited in developing these procedures. The addition of dimensionality and complexity to the model will report more realistic tissue environments for PPTT.

4.4. Irradiation protocol

4.4.1. Initial temperature

Cell culturing requires, in most mammalian cell lines, maintaining a temperature of 37°C for optimal cell growth and maintenance. Nonetheless, typical laboratory temperatures are usually between 20-25°C and cells are commonly manipulated for prolonged periods of time in mild hypothermia conditions, hence influencing the cellular stress response.[178]

PPTT relies on increases of temperature to decrease cellular viability by introducing cells in a hyperthermia environment in a controlled manner. Therefore, it is essential that cells are maintained in a homoeothermic state closer to 37°C, so increases of temperature achieved during light-to-heat conversion are biologically and therapeutically meaningful by reaching temperatures over 42°C.

Cells that are originally at room temperature (20-25°C), eventually experience lower temperatures when irradiated and any impact observed on viability could be the effect of light irradiation and not of temperature increase. Recorded temperatures with a temperature sensing device will also be skewed. By maintaining a starting temperature over 34°C, all starting conditions are over mild hypothermia, hence the stress response only starts upon irradiation.

4.4.2. Illumination power

When it comes to illumination, relevant parameters are laser power, dosage and irradiation time.[118] Laser power and laser beam diameter indicate the amount of energy per unit of area (W/cm^2, commonly known as power density) delivered to the cells. Providing power intensity without informing of the illuminated area or beam diameters can lead to confusions and misleading data. Standardising the format in which laser power is reported will make it easier to note similarities or discrepancies with data from other researchers.

Distance of the light source to the sample can affect the efficacy of the treatment. Indeed, in the case a non-collimated laser is used to illuminate the sample, it becomes highly important to report distance to determine the real light power experienced by the cells. For collimated laser beams, the divergence that occurs between the laser output and the sample for intermediate beam diameters (e.g. 3 mm) is not of relevance to produce changes in noise and temperature calculations.

Control of the laser beam power enables researchers to precisely control temperature generation in cell lines,[185] to study similarities and differences of heat generation efficacy and the outcomes it has on cells.

4.4.3. Continuous temperature recording

Light-induced heat generation in plasmonic nanoparticles can be measured by using thermal imaging or temperature probes. Temperature monitoring allows studying the photothermal conversion efficiency and photothermal stability of the nanomaterial. Bulk measurements of temperature of nanoparticles in a concentrated solution are not equivalent to measuring the temperature increase arising from internalised nanoparticles in cells. As mentioned above, specifying the removal of nanoparticles before irradiation is important in these cases, as different uptake process by different cell lines exposed to the same nanoparticle concentration will lead to different degrees of internalisation, and hence different

hyperthermia levels. Temperature estimation in nanoparticle suspensions lead to false assumptions and have an impact on the proper interpretation of results.

Additionally, continuous real-time recording of temperature provides better understanding of heat generation and insight into differences between irradiated cells. Indeed, continuous measurements help identify laser power settings that do not increase temperature in absence of nanoparticles and detect the appearance of temperature gradients[186] of cells in a 2D arrangement. The collection of this data, together with viability assessments after treatment, increases the possibility to tune temperatures, reaching and maintaining certain values for determined periods of time via feedback mechanisms.

4.5. After irradiation

4.5.1. More than one timepoint for analysis

Broadly speaking, cell death is classified as necrosis and apoptosis. The former is a mechanism that occurs almost immediately after the heat-induced damage, producing loss of membrane integrity and leading to pro-inflammatory responses. The latter leads to a delayed demise, producing eat-me signalling to favour phagocytosis and avoid the activation of inflammatory signals.[180] An increase of temperature initiated by PPTT can cause both mechanisms to be activated depending on the power, exposure time and heating dose. Cell death is a dynamic process and evaluating viability at a single timepoint can miss events occurring on the cellular level. Studying at several timepoints the molecular mechanisms activated after treatment provides more reliable data and crucial information to differentiate between necrosis, apoptosis, ferroptosis, pyroptosis and other cell death types by characterising early and late stages of cell death pathways.[187] Findings in an experiment performed with radiofrequency ablation, a non-invasive thermal treatment for hepatocellular carcinoma, showed how different temperatures during different exposure times results in different patterns for early and late apoptosis in irradiated cells.[186] Characterisation at more than one timepoint provides new insights into cytotoxicity of nanomaterials and new possibilities of PPTT.

In this line, analysing viability of different cell lines after *in vitro* PPTT we observed different levels immediately and 24 h after irradiation. The drops in viability after 24 h of irradiation were not equivalent between cell lines, highlighting the importance of evaluating cellular mortality at more than one timepoint, and in more than one cell line.[179]

4.5.2. Two or more methods to assess cellular viability

Different cell death mechanisms activate different molecular machinery, therefore, evaluating cellular viability with more than one read out system is as important as assessing viability at different timepoints.

Complementary assays that provide insight into different cellular parameters can be used to evaluate the activation of a cell death mechanism over another. It is essential to identify the information provided by the viability assay, as different experimental readouts can be interpreted in various ways.[149] The most common assays measure metabolic active cells (MTT, WST-1, ROS generation assays) or membrane integrity (trypan blue staining and LDH assay). Integrating methods that assess different end points simultaneously will provide a more comprehensive readout and can reveal discrepancies that could otherwise not be observed.[188] It is critical to systematically use multiple methods to assess viability at multiple timepoints.

4.6. Conclusions

As research in nanomedicine is foreseen to keep growing, involving new nanoparticles and drugs towards improved treatments, establishing criteria on experimental protocols should simplify contrasting data sets and allow for greater reproducibility of results. The adoption of these best practises can be generalized to other diseases beyond cancer, allowing PPTT to benefit a broader range of clinical scenarios. Likewise, reporting the items enumerated in the checklist will allow better comparison of results and more synergetic contributions from different laboratories.

5

Determination of main experimental parameters

The research project for determining which parameters are crucial for *in vitro* plasmonic photothermal therapy (PPTT) originated during my master's thesis and served as the basis for this dissertation. In this phase of the project, we focused on establishing the laser optimal conditions (laser power density and time of irradiation) for plasmonic hyperthermia. Previous work in the group already set a concentration of nanoparticles of 2 nM as non-toxic for 786-0 cell line. Our primary work was to identify a laser power density that selectively induced hyperthermia and affected cellular viability in 786-0 cells that had incorporated gold nanorods (AuNR-PEG). We considered time of irradiation and post-treatment duration within the hypothesis and observed their effects on both types of conditions, cells previously incubated with and without AuNR-PEG.

Additionally, we aimed to discriminate the cell death mechanism triggered by hyperthermia by evaluating the activation of caspase-3 (Ca-3) as a key apoptosis indicator. These findings provided insight into the molecular effects of *in vitro* PPTT and laid the groundwork for the experiments elaborated in this dissertation, while also laying the foundation for standardisation of PPTT and improving its future prospects for cancer treatment.

5.1. Heating behaviour validation

An important aspect of hyperthermia with PPTT is how different the temperature profile is in cells being irradiated with and without nanoparticles. During the preface of this dissertation, we were able to test different irradiation protocols, in which we irradiated cells in a 2D conformation (attached to a well plate) and 3D-like format (in suspension). We observed that when cells were attached to the well, increases of temperature were not substantial, in contrast to cells irradiated with AuNR-PEG in a 3D-like conformation. Moreover, in this conformation we were able to irradiate many more cells (8×10^6 cells in a 20 µl volume) than when they are attached, where the laser diameter limits the space of cells that can be irradiated at the same time.

Additionally, the incorporation of a heating bed during irradiation allowed us to maintain stable starting irradiation temperatures of the well plate, over 34°C. As mentioned in Section 4.4.3, laboratories are kept between 20 and 25°C[178] and cells should be maintained around 37°C to maintain physiological conditions. By adding a thermal bed under the well plate being illuminated, we were able to measure physiological relevant increases of temperature, as we avoided initial cellular temperatures of 21-22°C. Using a thermal IR-camera, allowed us to record bulk increases of temperature, validating which powers and times of irradiation cells need to be illuminated for to reach mild hyperthermia conditions.

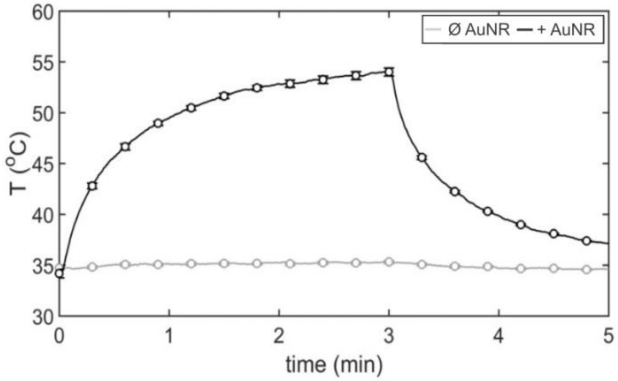

Figure 5.1.Temperature behaviour in cells with and without AuNR-PEG during laser illumination. 786-0 cells irradiated with a power dosage of 3 W/cm² and 3-minute irradiation. Mean ±SD

The temperature elevation in cells irradiated with AuNR-PEG was higher than in control groups, up to 20 times more elevated with the higher laser power densities and longer irradiation times (Table 5.1 and Figure S.5. 1). Temperature increase occurred rapidly at the onset of irradiation, swiftly stabilising, and slowing the initial temperature increment. In many cases, the stabilisation of the temperature increase during irradiation is influenced by the exchange at the air-medium interface.[189] Once laser irradiation is stopped (minute 3), a rapid dispersion of heat to the air was observed and temperature dropped to temperatures pre-irradiation (Figure 5.1).

			Viability (%)		ΔT^a(°C)		
			Median	**SEM**	**Median**	**SEM**	**n**
1W/cm²	**3min**	**+AuNR-PEG**	115.40	30.56	4.50	0.52	3
		ØAuNR-PEG	107.03	18.12	0.73	0.35	3
		p-value	*0.7000*		*0.07652*		
	8min	**+AuNR-PEG**	127.17	14.47	6.10	1.01	3
		ØAuNR-PEG	123.48	33.58	0.93	0.40	3
		p-value	*1.0000*		*0.0765*		
3W/cm²	**1min**	**+AuNR-PEG**	66.99	16.23	9.08	4.39	8
		ØAuNR-PEG	95.22	14.67	0.60	0.29	8
		p-value	*0.0111**		*0.0004****		
	3min	**+AuNR-PEG**	58.32	17.85	15.27	3.18	17
		ØAuNR-PEG	99.03	16.23	1.13	0.41	17
		p-value	*5.86E-07*****		*1.37E-13*****		
	8min	**+AuNR-PEG**	33.54	7.73	19.13	2.06	3
		ØAuNR-PEG	76.55	16.02	2.33	0.15	3
		p-value	*0.1000*		*0.1000*		
4W/cm²	**1min**	**+AuNR-PEG**	58.88	6.64	15.77	1.33	3
		ØAuNR-PEG	100.02	10.79	0.87	0.21	3
		p-value	*0.1000*		*0.1000*		
	3min	**+AuNR-PEG**	31.65	11.04	19.47	3.21	6
		ØAuNR-PEG	73.96	10.88	1.30	0.28	6
		p-value	*0.0022***		*0.0050***		
	8min	**+AuNR-PEG**	21.09	10.68	20.80	14.96	4
		ØAuNR-PEG	75.67	28.89	1.55	0.84	4
		p-value	*0.0286**		*0.02856**		
6.3W/cm²	**3min**	**+AuNR-PEG**	19.70	0.58	24.70	1.47	3
		ØAuNR-PEG	46.75	6.40	3.40	1.95	3
		p-value	*0.1000*		*0.1000*		
	8min	**+AuNR-PEG**	7.20	1.91	34.63	1.12	3
		ØAuNR-PEG	58.59	9.16	6.37	0.70	3
		p-value	*0.1000*		*0.1000*		

*Table 5.1. Cellular viability (%) and temperature increase (°C) of cells with (+AuNR-PEG) and without (ØAuNR-PEG) irradiated. Cellular viability (%) was measured with MTT relative to controls (not irradiated, ØAuNR-PEG). Temperature increase calculated as difference from initial temperature to maximum temperature achieved. SEM: standard error of the mean. n: number of samples. P-values indicate statistical differences between cells irradiated with and without AuNR-PEG under the same laser power and time of irradiation: *<0.05, **<0.01, ***<0.001, ****<0.0001.*

5.2. Exposure time and laser dosage analysis on cellular viability

The data obtained from assessing the impact of different laser dosages and exposure times in temperature and cellular viability let us identify the optimal experimental conditions toward decreasing viability exclusively in irradiated cells that contained AuNR-PEG.

Four different laser power densities ranging from 1 W/cm^2 to 6.3 W/cm^2 were tested, as well as three different times of irradiation: 1, 3 and 8 minutes (Table 5.1 and Figure S.5. 1). As expected, with cells incubated with AuNR-PEG, as laser dosage and time of irradiation increased, temperature augmented with the consequent loss of viability. Low laser dosage and times of irradiation (e.g. 1 W/cm^2 - 3 min) didn't significantly increase temperature compared to cells without AuNR-PEG ($\Delta T = 4.5°C$, $p = 0.077$) and viability was not significantly affected ($p = 0.700$), therefore, we discarded the lowest power density for posterior experiments.

On the other hand, in irradiated cells without AuNR-PEG, no remarkable changes in temperature could be observed. Maximum temperature increases were around 1°C for tested low to medium laser powers and times of irradiation (e.g. 3 W/cm^2 - 3 minutes), whereas for the higher laser powers and times of irradiation (e.g. 6.3 W/cm^2 - 8 minutes) a maximum increase of temperature of 6°C was observed. In these cases, viability was decreased down to 46.75 % and 58.59 % (6 W/cm^2, 3 and 8 minutes, respectively) (Table 5.1). The international organisation for standardisation (ISO) defines a substance as cytotoxic if cell survival is less than 70 %. Therefore, a power of 6.3 W/cm^2 was discarded. Moreover, the decline in viability observed in cells without AuNR-PEG after illumination indicated that laser light was too toxic for the cells. For these reasons, 4 W/cm^2 and ≥ 3 minutes of irradiation (e.g. 73.96 %) were discarded as cellular death approached the 70 % viability boundary.

After these experiments, we defined a power density of 3 W/cm^2 and 3 minutes of irradiation as the ideal illumination conditions to harness the light-to-heat potential of AuNR-PEG and locally increase temperature (15.27°C) and reduce viability (58.32 %), without risking harming cells that had not been exposed to nanoparticles prior to illumination (99.03 % viability) (Table 5.1).

To further validate viability in 786-0 cells after PPTT, we analysed cells under an automated fluorescence microscope with the help of the CellEvent® Caspase3/7 Green Detection Reagent kit (C10427, Invitrogen) and Hoechst solution (Hoechst33528, Sigma-Aldrich). Staining of the nucleus (blue stain in Figure 5.2) and of activation of caspase-3 (red stain), allowed the measurement of caspase activity and the area of the nuclei. Measurements were taken at four different timepoints (2, 4, 6 and 24 hours). Thereby, the ratio of cells expressing caspase-3 activity was derived from dividing the number of active caspase-3 cells to the nuclei count. Results showed an increase in the ratio of activation of caspase in cells, indicating the activation of apoptosis in irradiated cells with AuNR-PEG, with up to a 5-fold increase in expression after 24 hours (Figure 5.3-A).

In parallel, the cellular morphology after irradiation was examined (Figure 5.3-B). Cells with AuNR-PEG after irradiation had decreased their well plate attachment compared to the other conditions. By measuring the nuclei area changes at the different studied timepoints we were able to observe a significant shape change in control cells (from spherical, to flattened structures). Two hours after irradiation, cells were not yet attached to the surface, translating to spherical nucleus shapes for all conditions (similar nucleus areas, around 150 μm^2). As duration after treatment increased, cells adhering to the surface expanded, translating to a grow of their nuclei area (flattening, over 200 μm). AuNR-PEG cells did not reattach at the same capacity, keeping spherical shapes and maintaining a constant nuclei area throughout the experiment.

Once this information was collected and analysed, we confirmed the validity of the used power density and time of irradiation to exclusively induce apoptosis in cells irradiated that contained AuNR-PEG, but not on 786-0 cells without nanoparticles. Our light settings were not toxic to cancerous kidney cells; however, the open question was to understand how non-cancerous cells and cell lines from different tissues reacted to PPTT under these same parameters: testing their toxicity to AuNR-PEG,

internalisation efficiency, and response to irradiation. Observing the effects of PPTT in different cell types is important for clinical settings, as irradiation can reach non-tumorous tissues and PPTT could be applied to many cancer types.

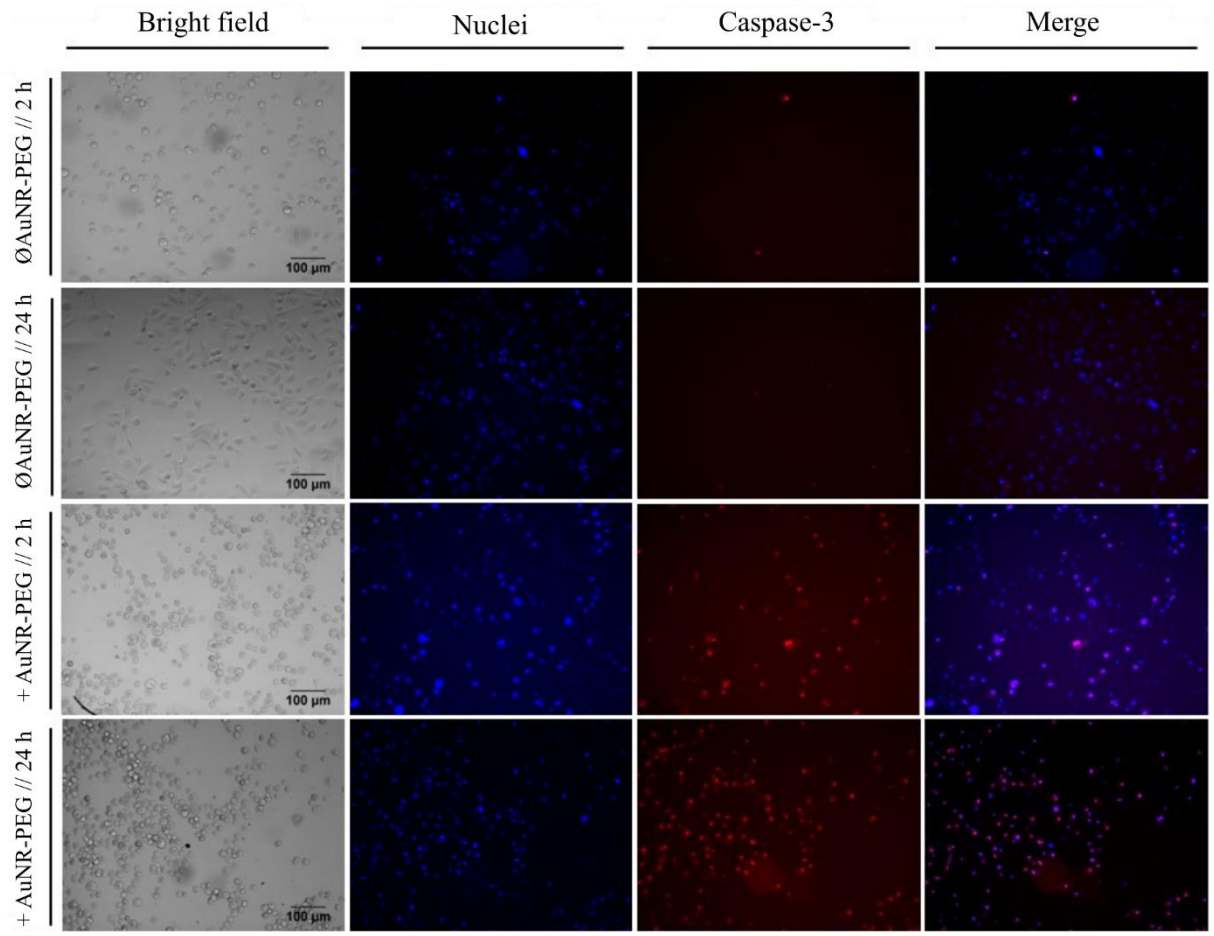

Figure 5.2. Representative images of cells irradiated with (+AuNR-PEG) and without at 2 and 24 hours after treatment. Hoechst (blue, nuclei staining) and activated caspase 3 (red) staining of 786-0 cells irradiated (3 W/cm^2-3 minutes). Upper panels show cells irradiated without AuNR-PEG (ØAuNR-PEG) 2 and 24 hours after illumination. Lower panels show AuNR-PEG cells (+AuNR-PEG) 2 and 24 hours after illumination. 10x augmentation. Scale bar: 100 µm.

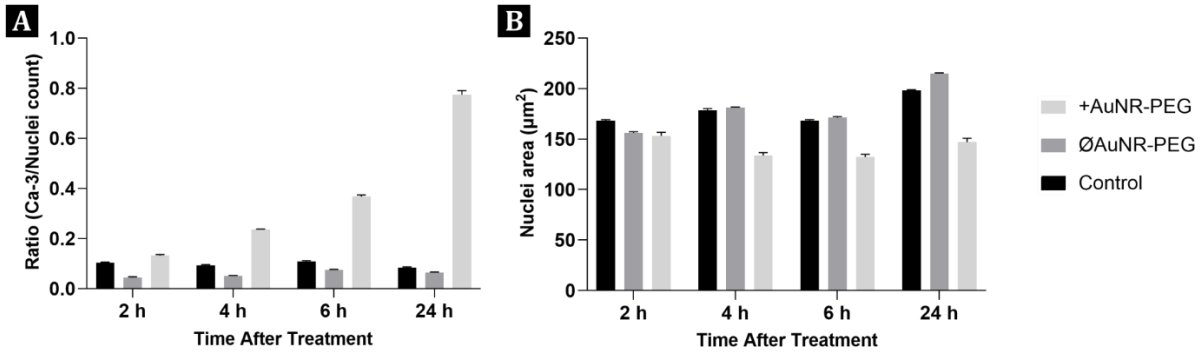

Figure 5.3. Analysis of Caspase-3 (Ca-3) activation and Nuclei size. A) Quantification of caspase-3 activation per cell (nuclei count). B) Measurement of nuclei area size (µm^2).

6

Influence of cell type on the efficacy of plasmonic photothermal therapy

This chapter was published in ACS Nanoscience Au 2022, 2 (6), 494-502 with DOI: 10.1021/acsnanoscienceau.2c00023

6.1. Introduction

The significance of selecting the appropriate laser and laser conditions for plasmonic photothermal therapy (PPTT) using gold nanorods (AuNR-PEG) is important for both *in vitro* and *in vivo* applications. The combination of the laser used with the nanoparticle type should allow for high efficiency regarding light-to-heat conversion, meaning that the laser should have an emission wavelength on the peak of absorbance of the nanoparticle.[21] Moreover, the laser wavelength would ideally fit within the optical biological window (700 to 980 nm) to allow deeper laser penetration with minimal light absorption by the tissue.[24–26,190] Regarding nanoparticle delivery, the method of administration will determine the distribution of the nanomaterial throughout the body, either clustered within the tumour site injection in the case of intratumoral injection (IT)[36,191] or disseminated throughout a multitude of body tissues and organs in the case of intravenous administration (IV).[32,34,192]

The nature of PPTT implies that when administering the therapy, several cellular types will be in contact with AuNR-PEG during administration (e.g. in the case of IV delivery), and during laser irradiation. For example, target cells, as well as their microenvironment and surrounding tissues are illuminated to ensure that tumour cells are destroyed and cannot escape death. Nonetheless, when addressing the existing literature of PPTT, a gap was identified regarding the understanding of how different cell lines react to PPTT and its multiple components. Most papers examined a single cancerous cell line during the experimental section, disregarding comparing the effects of PPTT, nanoparticle toxicity and laser illumination in healthy cells and cells from different tissues. Certainly, it is essential to understand and address the differences between cell types, particularly considering the implication during *in vivo* irradiation. In the context of therapeutic applications of PPTT, potential exposure of non-cancerous cells to treatment and nanoparticle presence is a critical factor for comprehensive pre-clinical assessments.

To bridge this gap, this chapter delves into understanding at the *in vitro* level, the differences in cytotoxicity and uptake of AuNR-PEG across various cell types and tissues, as well as assessing the effects laser light treatment had in cellular viability. Recognising the differences of these elements of PPTT between cell types can contribute to more robust and accelerated translational efforts from pre-clinical to clinical applications.

In vitro studies allow biomedical research to work within the principle of the 3R framework (replacement, reduction and refinement)[193,194], avoiding the unnecessary use of animals for experimentation in pre-clinical phases of development of drugs and therapies. However, particular care must be taken when selecting the appropriate cell lines for the study of *in vitro* PPTT, as they must be suitable to compare them to each other.

This pivotal aspect of cell line selection for PPTT led us to report on lung cancer cell lines as an example of a target tissue for therapy. Lung tissues are generally exposed to external aggressions (virus, bacteria, changes in air temperature, etc.)[195] and lung cancer was the second most diagnosed cancer in the world in 2020.[16,196] At the same time, liver and kidney derived cell lines were chosen as they will, as part of the mononuclear phagocytic system and renal clearance, respectively, be responsible for a high

sequestering of nanoparticles during IV delivery of nanoparticles.[138] Moreover, liver was the third cause of cancer mortality in 2020.[16] For each tissue, both cancerous and non-cancerous human cell lines were selected, to establish differences between healthy and cancer cell types.

Validity of laser illumination conditions was done by testing different power densities and time of irradiation on 786-0 cells (epithelial cancerous kidney cell line) (Chapter 5), establishing a protocol that impaired viability of cells irradiated with AuNR-PEG under 70 %, but did not alter cellular viability of cells irradiated without nanoparticles.

To further endorse PPTT, subsequent experiments reported the effects of PPTT – from the cytotoxicity of the nanoparticle to the outcomes of hyperthermia – in cancerous and non-cancerous cell lines of three different tissues. Epithelial human kidney, lung and liver cell lines were used to determine differences in the efficacy of PPTT in eradicating cancer cell lines, whereas non-canceorus cell lines were used as controls to determine the safety of AuNR-PEG, as well as evaluating the consequences of collateral uptake and illumination. Cytotoxicity was assessed by means of mitochondrial activity, whereas uptake was quantified with two-photon microscopy. PPTT was evaluated at two different time-points by studying their mitochondrial activity and membrane integrity. With this systematic study, we demonstrated the safety and efficacy of PPTT in an *in vitro* set up, highlighting the importance of creating reliable, reproducible, and meaningful data sets that are comparable between studies and groups that use different types of nanoparticles or laser irradiation.

6.2. Results and discussion

6.2.1. *In vitro* quantification of AuNR-PEG uptake

Quantification of AuNR-PEG internalised by various cell types and tissues was performed to explore uptake performance differences. Uptake is dependent on the type and surface charge of nanoparticles used,[197] but their functionalisation and cell type will also have a role in the process of internalisation. Uptake (AuNR-PEG/cell) was measured over a fixed incubation time (24 hours) and increasing AuNR concentrations (0, 1, 2, and 5 nM). The objective of this experiment was to determine the highest uptake while maintaining cellular viability, not to obtain the maximum uptake possible, as higher concentrations than 5nM could have been used.

Cancer cell lines had a statistically higher uptake per cell compared to non-cancerous cells of the same tissue ($p \leq 0.04$) for incubations with 2 and 5 nM (Figure 6.1 and Figure S.6. 1). It has been described that cancer cells more readily incorporated AuNP with higher concentrations compared to healthy cells[198] but we remark that for all cell types there was an increase in uptake with concentration. The lower uptake of normal cell lines is consistent with the incubation of AuNRs in cell culture medium containing 5 to 10 % FBS, compared to FBS-free medium in cancer cell lines. The protein-containing medium presence during AuNR incubation can decrease the surface reactivity and uptake of AuNP by cells.[199,200] These *in vitro* findings on uptake underscore the complexity of nanoparticle uptake dynamics, emphasizing the multifaceted interplay between nanoparticle characteristics, cell type and the surrounding environment.[42,141,196]

786-0 cell line had a statistically lower uptake than A549 for all studied concentrations ($p \leq 0.04$), and lower than HepG2 at 5 nM ($p < 0.03$). Hek293 also had lower uptake than the other non-cancerous cell lines studied, showing a trend in kidney cells of lower uptake of AuNR-PEG *in vitro* than lung or liver cell lines under the same conditions.

Among the studied concentrations, the highest uptake observed was obtained with a AuNR-PEG concentration of 5nM (Figure 6.1-A and Figure S.6.2). However, higher concentrations of gold also presented the lowest viabilities (Figure 6.2). For non-toxic concentrations of gold (viability >70 %, ≤ 2 nM, Figure 6.2-A), incubations with 2 nM meant higher uptake for all studied cell lines without compromising cellular viability under 70 % (Figure 6.1-B).[201] Selecting the correct concentration for incubation will determine the cytotoxicity of AuNR-PEG and impact their performance during irradiation, as temperature generation will be influenced by the presence of AuNR-PEG in cells.

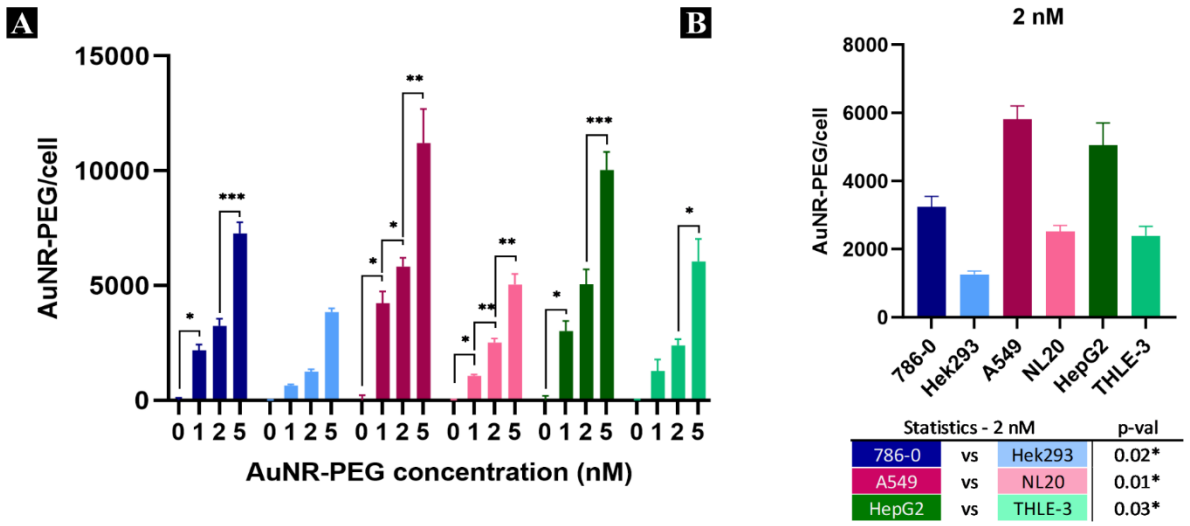

*Figure 6.1. Uptake of AuNR-PEG as a function of concentration for different cell lines. A) Increase of uptake for different cell lines with the increase of concentration. B) Uptake of AuNRPEG at 2 nM (104 µg/mL gold). *p<0.05, **p<0.01, ***p<0.001. Error bars represent SEM (n=3-6). No statistical differences were observed between all conditions for Hek293.*

Overall, under the same conditions, cancerous and non-cancerous epithelial cell lines have different uptake capability, which is also seen between different tissues, compromising the efficacy of PPTT, and highlighting the importance of studying more than one cell type to determine the uptake of nanoparticles.

6.2.2. *In vitro* determination of AuNR-PEG toxicity

Nanoparticle toxicity can originate from the size and shape of the nanoparticle, their biological activity and interactions, and the surface functionalisations,[199] but the cellular type and endpoint examined play an important role in determining the biocompatibility of nanoparticles for PPTT. Several papers have tried to find the optimal nanoparticle for increased light-to-heat conversion and minimal toxicity.[26,128,199] In the case of our AuNR-PEG,[128] viability was found to be affected by the quantity of gold and not by the size of the nanoparticles.

To assess nanomaterial cytotoxicity, thiazolyl blue tetrazolium bromide (MTT) was used to determine the toxic potential of AuNR-PEG in cancerous and non-cancerous cell lines of three different tissues. Results showed how exposure to low AuNR-PEG concentrations (≤ 2 nM) equivalent to lower than 104 µg/mL of gold were not toxic to cells, whereas increases in concentration decreased the survival rate below 70 % after 24h of exposure (e.g. THLE-3 had 84 % viability at 2 nM, but lowered down to 58 % at 4nM, Figure 6.2. and Figure S.6.3). As stated by Kim *et. al*, and according to the International Organisation for Standardisation (ISO), if the cell survival rate is less than 70 %, a substance is defined as cytotoxic. In this particular case, cytotoxicity is both concentration and cell type dependent.[201] The impact of high gold concentrations was more pronounced in non-cancerous NL20 and THLE-3 cell lines, while Hek293 showed high resistance to various gold concentrations (65 % viability at 8nM, compared to values ≤30 % for the other normal cell lines) (Figure 6.2), indicating dissimilarities between healthy cells from different tissues. Between cancerous cell lines, no statistical relevant differences were found at any of the concentrations evaluated ($p \geq 0.05$). Regarding differences between same tissue cell types, only at concentrations ≥ 4 nM statistical differences were observed (Figure S.6.3). Non-cancer cell lines had statistically lower survival rates than cancerous cell lines; however, Hek293 had statistically higher viability than cancer kidney cell line 786-0 ($p \leq 0.034$, at > 4 nM).

To determine sensitivity of the different cell lines to AuNR-PEG, the inhibitory concentration (IC_{50}) was calculated (Figure 6.2-B). The concentration at which the survival rate dropped to 50 % was around 7 nM for all three cancer cell lines, confirming they have a similar response to the toxic potential of AuNR-PEG in the absence of light. Normal NL20 and THLE-3 had lower IC_{50}, around 5 nM, being the least resistant to higher gold concentrations. On the other hand, Hek293 had an IC50 of almost 15 nM,

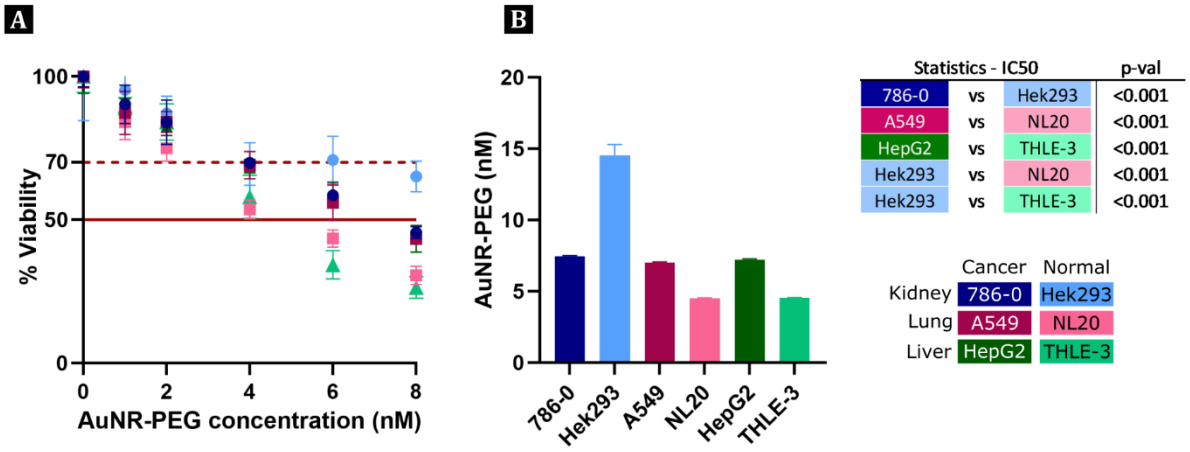

Figure 6.2. Effect of AuNR-PEG concentration on cellular viability. A) Viability of cell lines for all studied concentrations shown and percent of controls (0 nM). B) IC_{50} of cell lines. Only statistically relevant data is shown. Error bars represent SEM (n=4).

showing high resistance to AuNR-PEG. The synthesis of non-intrinsically toxic nanoparticles is crucial for ensuring their safety.[202]

Remarkably, no statistically relevant differences between the two lowest concentrations used (52 and 104 µg/mL, 1-2 nM, $p \geq 0.05$) were found for any of the cell lines. This is relevant as cell survival is elevated with the highest non-toxic concentration of 2 nM, and at the same time, more uptake is observed when studying internalisation for all cell lines after the same incubation time. For this reason, maintaining a constant incubation of AuNR of 2 nM (104 µg/mL gold) and 24h was ideal to further study the effects of PPTT in different cell types at different times after treatment.

Nanomaterial cytotoxicity will greatly influence clinical translation of PPTT. Resistance to different doses or exposure times will be cell type dependent, but most nanotoxicology studies focus their efforts on targeting cells, disregarding the impact on non-target cells.[203,204] *In vitro* PPTT data focuses mostly on the cellular response of cancer cells, but the differences in uptake shown above confirm the need to study cytotoxicity in off-target tissues, as the mechanisms triggered after contact with the nanomaterial may differ between cell types. Zhao *et al*. determined non-cancerous cell line HK-2 is more resistant than 786-0 cancer kidney cell line to spherical AuNPs of different sizes at increasing concentration, as the autophagy mechanism employed to incorporate the nanoparticles seemed to protect them from harm,[205] and agree with our findings that cancer 786-0 cell line is more susceptible to high concentrations of AuNRs than normal cells. Moreover, increased susceptibility of non-cancerous hepatic L02 cells compared to HepG2 with spherical AuNPs,[198] is also in good agreement with our results showing lower IC50 for normal THLE-3 than cancer HepG2 hepatic cells.

6.2.3. Photothermal irradiation

The temperature of all six cell lines irradiated at a fixed power density (3 W/cm^2) and time of irradiation (3 minutes) are shown in Figure 6.3. The rise of temperature followed a quasi-exponential increase until it stabilised for cell lines with AuNR-PEG. After 3 minutes, when laser irradiation stopped, a rapid diffusion of heat to the air and medium was observed, which translated into a drop of temperature.

Differences in final temperatures achieved were detected among cell lines (Figure 6.3-B). Cancer cell lines (786-0, A549 and HepG2) experienced larger increases in temperature compared to non-cancerous ones (Hek293, NL20 and THLE-3). For non-cancerous cell lines, PPTT treatment resulted in maximum temperatures around 42°C, while for cancer cell lines, maximum temperatures were over 47°C. In the case of 786-0, the increase of temperature (over 53°C) was statistically significant compared to A549 and HepG2 cells ($p \leq 0.026$).

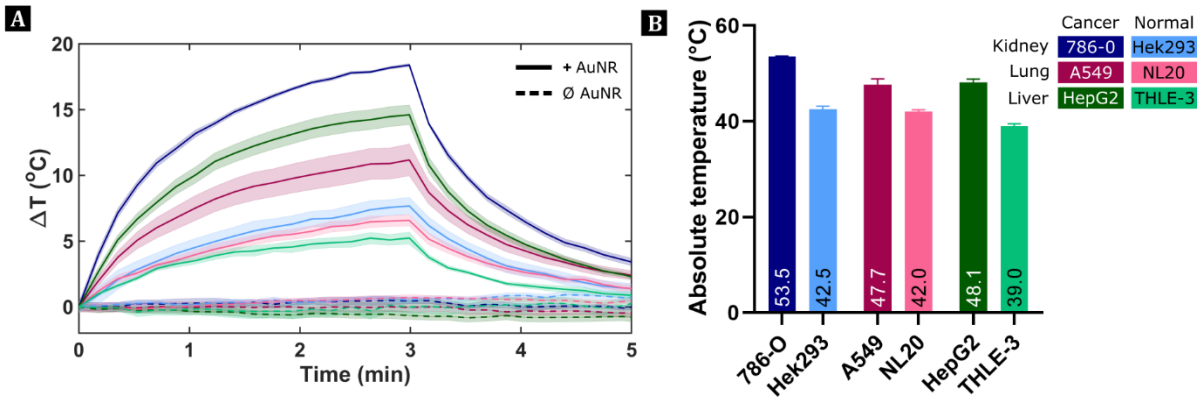

Figure 6.3. Temperature dynamics in +AuNR-PEG and ⌀AuNR cells upon irradiation. A) Increase in temperature as a function of time for cell lines irradiated 3 min with an 808 nm laser light at 3 W/cm². Continuous line indicates cells with AuNR-PEG (+AuNR-PEG) and dotted line cells without AuNR-PEG (⌀AuNR-PEG). Shaded line represents the SEM. B) Averaged absolute increases of temperature of cells irradiated + AuNR-PEG.

For cells irradiated without AuNR-PEG (Fig. 3), no statistically relevant increase of temperature was detected ($p \geq 0.05$). Namely, an average increase of 0.28°C, up to a maximum temperature of 34.58°C, was observed for all six cell lines studied (Figure S.6.6).

This data allows us to observe the dynamics of light-to-heat conversion inside cells by AuNR-PEG, emphasizing the importance of recording the temperature of the different cell lines being irradiated. In all cases, cancer cell lines achieved statistically higher temperatures than non-cancerous cell lines in the presence of AuNR-PEGs. At the same time, we confirm that increases of temperature are caused by the interaction of AuNR-PEGs with laser light, as cells irradiated in the absence of nanoparticles did not experience light-to-heat conversion. The addition of a third dimension during irradiation has two main consequences: collective thermal effects increase while heat dissipation with the surrounding gets reduced. Eventually both effects contribute to increase the temperature experienced by the cells.[206] Differences in the increase of temperature can be the result of the different amount of internalised nanoparticles and the total amount of gold in the suspension[207] which will elicit different responses from the cells.

Viability after irradiation was assessed at two different timepoints after treatment (0 and 24 hours) with two complementary methods (MTT assay and trypan blue staining), shown in Figure 6.4 and Figure 6.5, respectively. The MTT assay studied mitochondrial activity as a reporter of cellular viability, whereas trypan blue staining reported on the loss of membrane integrity, labelling cells as non-viable. The assessment of multiple endpoints with more than one method[208] allows to identify the molecular pathways activated by PPTT in both target and non-target tissues.

For the MTT assays, cells without AuNR-PEG and not irradiated were used as a viability control (CTL). Irradiated cells without AuNR-PEG (labelled as ØAuNR) maintained their viability over 70 %, immediately and 24 hours after treatment (Figure 6.4, A-F). Following the cytotoxicity evaluation of AuNR, we established > 70 % viability of cell lines as a criterion to determine if laser light conditions were toxic to cell lines. Altogether, we show that the laser parameters used (c.w. 808 nm, 3 W/cm², 3 minutes irradiation) can be considered non-toxic for all 6 cell lines studied.

Cells irradiated that contained AuNR-PEG (+AuNR) experienced in some cases pronounced increases of temperature (Fig. 3), which severely impaired their viability after irradiation (Figure 6.4). High temperatures impaired mitochondrial activity, reducing viability of cell lines drastically, occasionally, down to 50 % immediately after treatment. This initial drop of cellular viability could be observed in all cell lines except for Hek293, which even after 24 hours, the mild increase of temperature experienced (maximum of 42°C) seemed not to impair mitochondria (viability ≥ 90 %). All non-cancerous cell lines had higher viabilities after irradiation compared to their diseased counterparts (Figure S.6.5). In the case of kidney cell lines, these differences between cancer and non-cancer cell line were very pronounced,

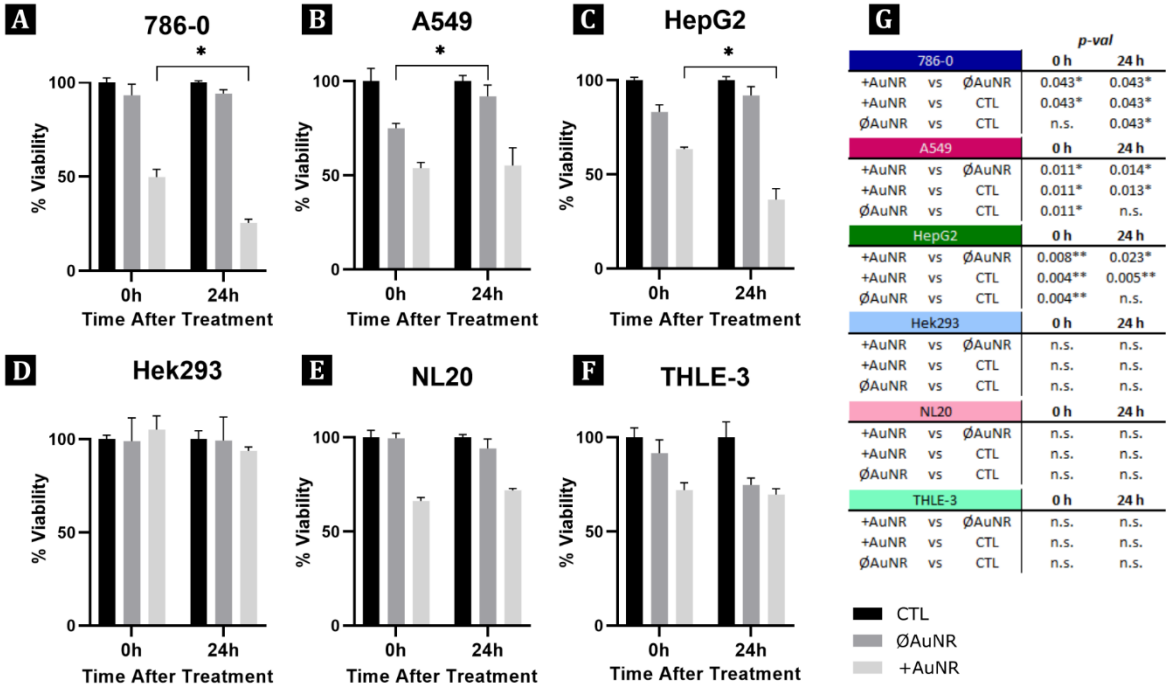

Figure 6.4. Cellular viability (%) after treatment assessed with MTT assay. A–F) Viability at 0 and 24 h after irradiation in control (CTL) and in cells irradiated with AuNR-PEG (+AuNR-PEG) and without (⌀AuNR-PEG). G) Statistical comparison for each cell line at different timepoints between conditions from panels A to F. Differences between 0 and 24 h are shown in the graphs. Statistical comparisons were made using Tukey/Wilcox post hoc tests. *p ≤ *0.05;* **p ≤ *0.01;* ***p ≤ *0.001; ns, not significant.*

being 786-0 much less viable than Hek293 (24 hours after irradiation, 25 % and 93 % viability respectively, p=0.03*). This difference could be explained by the different temperatures reached during irradiation. However, large changes in temperature were also recorded for lung and hepatic cells, but in this case, differences in viability were much less pronounced. Both lung cell lines seemed to recover some mitochondrial activity 24h after irradiation (between 2-5% increase in viability), and the differences found immediately after treatment faded after 24 hours. In contrast, hepatic cell lines had very similar viabilities immediately after treatment, but after 24 hours significant differences were found after a drop in viability of HepG2 cells (decrease of > 25 % of viability, $p < 0.05$).

We also studied viability with trypan blue staining (Figure 6.5). For cancer cell lines with AuNR-PEG, the increase of temperature had an impact on membrane integrity. All three cell lines had lower viabilities 24 hours after irradiation than immediately after treatment (Figure 6.5, A-C), although this decline of viability was only significant for 786-0 cells. On the other hand, A549 cells appeared to have more resistant membranes to hyperthermia and laser irradiation, with viability over 90% (Figure 6.5-B).

In the case of non-cancerous cell lines, no differences were found between the different conditions (CTL, ØAuNR, +AuNR) at any timepoint after treatment ($p \geq 0.05$) (Figure 6.5-G). Hek293 showed high resistance to either light or light + AuNR-PEG, immediately and after 24h (viability ≥ 92%), whilst NL20 cells seemed to be more affected by the increase of temperature (87% after 24 hours of irradiation). On the other hand, THLE-3 cells lost membrane integrity by the application of light alone, and its impairment increased with the presence of AuNR-PEG (66 % viability after 24 hours).

When comparing cell types irradiated with AuNR-PEG, 786-0 and Hek293 reach the highest temperatures when compared to cancerous and non-cancerous cell lines, respectively, however they showed opposite responses (786-0 decreased their viability down to 50 % after 24 hours of irradiation, whereas Hek293 was close to 100 %, this difference was statistically significant ($p = 0.03$). 786-0 cells were less viable than A549 and HepG2, although not statistically significant (Figure S.6.4). However, Hek293 had statistically significant higher resistance to hyperthermia than NL20 and THLE-3 ($p \leq 0.05$).

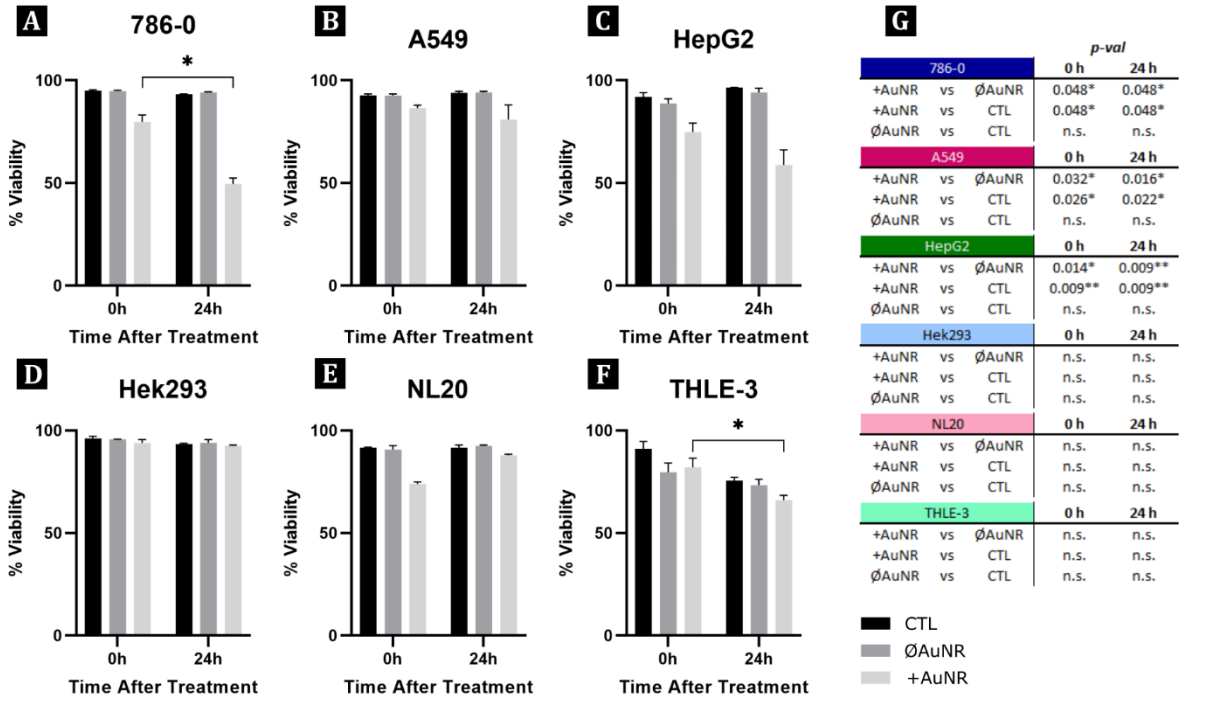

G

			p-val	
786-0			0 h	24 h
+AuNR	vs	ØAuNR	0.048*	0.048*
+AuNR	vs	CTL	0.048*	0.048*
ØAuNR	vs	CTL	n.s.	n.s.
A549			0 h	24 h
+AuNR	vs	ØAuNR	0.032*	0.016*
+AuNR	vs	CTL	0.026*	0.022*
ØAuNR	vs	CTL	n.s.	n.s.
HepG2			0 h	24 h
+AuNR	vs	ØAuNR	0.014*	0.009**
+AuNR	vs	CTL	0.009**	0.009**
ØAuNR	vs	CTL	n.s.	n.s.
Hek293			0 h	24 h
+AuNR	vs	ØAuNR	n.s.	n.s.
+AuNR	vs	CTL	n.s.	n.s.
ØAuNR	vs	CTL	n.s.	n.s.
NL20			0 h	24 h
+AuNR	vs	ØAuNR	n.s.	n.s.
+AuNR	vs	CTL	n.s.	n.s.
ØAuNR	vs	CTL	n.s.	n.s.
THLE-3			0 h	24 h
+AuNR	vs	ØAuNR	n.s.	n.s.
+AuNR	vs	CTL	n.s.	n.s.
ØAuNR	vs	CTL	n.s.	n.s.

Figure 6.5. Cellular viability (%) after treatment assessed with Trypan Blue staining. A–F) Viability at 0 and 24 h after irradiation in control (CTL) and in cells irradiated with AuNR-PEG (+AuNR-PEG) and without (⌀AuNR-PEG). (G) Statistical comparison for each cell line at different timepoints between conditions from panels A to F. Differences between 0 and 24 h are shown in the graphs. Statistical comparisons were made using Tukey/Wilcox post hoc tests. *p ≤ *0.05;* **p ≤ *0.01;* ***p ≤ *0.001; ns, not significant.*

This seemingly higher thermotolerance of low hyperthermia of Hek293 could be an adaptative response of the embryologic nature of this cell line. In any case, 24h after irradiation, viabilities for non-cancerous cell lines with AuNR-PEG were higher than their diseased counterparts.

Our results indicated that increases of temperatures favoured an apoptotic cell death mechanism (loss of mitochondrial function) over a necrotic one (membrane rupture) with low power density irradiation. Other studies showed how high temperatures achieved with higher laser powers favour the induction of necrosis,[209] although apoptosis can be triggered with the combination of different types of nanoparticles and laser irradiation.[210–213] Under the laser conditions used, we can confirm that the laser irradiation settings employed are non-toxic for these cell lines *in vitro*, but in cells with AuNR-PEG, maximum temperature, mitochondrial activity and membrane integrity differed between cell types. Our findings are in good agreement with the use of low AuNR concentration, laser power and exposure time to promote apoptosis.[214]

6.2.3.1. Correlations

Studying the variables of PPTT in parallel can be used to observe associations between them. Nanoparticle toxicity, together with cellular uptake, can provide a lot of information regarding cellular resistance to nanoparticles and their materials. Bhamidipati *et al.*[203] studied the correlation of uptake of AuNRs, gold nanostars and gold nanospheres in U87 cells (human glioblastoma) and fibroblasts, but no correlation could be stablished between the two factors for the values reported. Our results, disagreeing with the outcomes of Bhamidipati, found a negative correlation between the number of nanoparticles incorporated and cytotoxicity (r = -0.83). Higher uptake by cells agreed with a decrease of cellular viability when studied with the MTT assay, the gold standard assay for cytotoxicity.[204] Discrepancies between studies highlight the importance of studying cytotoxicity for different cell types, tissues and nanoparticles individually, almost erasing the possibility of extrapolating results.

Cellular uptake will also impact the temperatures reached during irradiation. Although this correlation will be prone to fluctuations depending on the laser set up, with the settings used throughout our research (3 W/cm^2, 3 minutes, 808 nm), a positive correlation was established between the number of AuNR-PEG incorporated and temperature (r = 0.85) (Figure 6.6). Additionally, cell size and exocytosis rate also have a role on cellular uptake and photothermal heating.[215] Different cell sizes denote different cell volumes, which influences the location and distribution of internalised nanoparticles. Two cell lines may have similar number of internalised nanoparticles when the used metrics are nanoparticle/cell, however, a bigger cell will have a larger dispersion of nanoparticles inside the cell, affecting the collective thermal effects and intra-cellular heat dissipation. This is a limitation of the dose metrics typically used to express uptake, and a factor to consider during results extrapolation and standardisation. Moreover, different cell size affects biocompatibility of the material due to changes in mass concentration inside the cell.

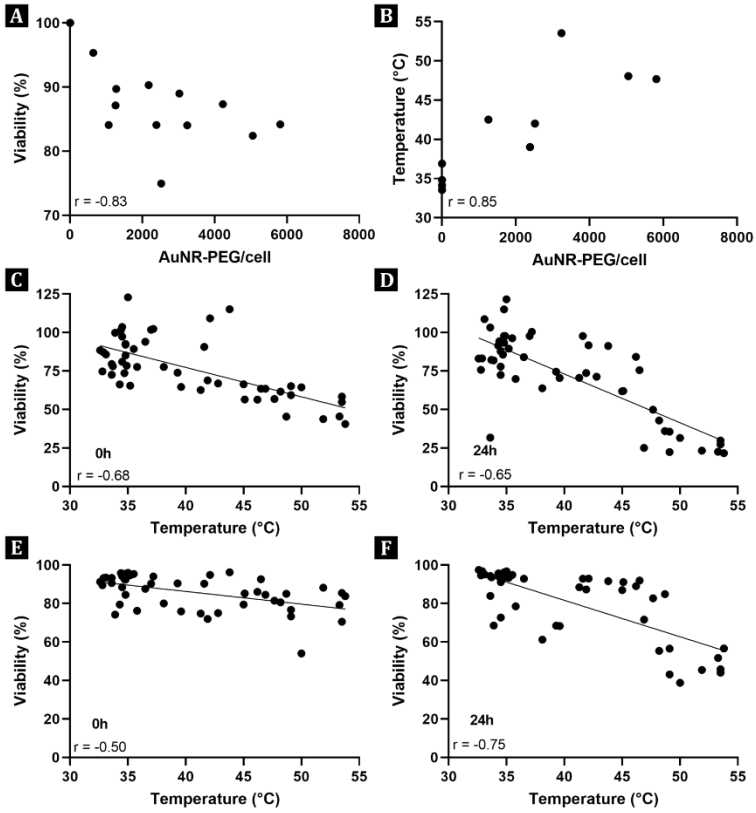

Figure 6.6. Plots showing the correlation between the different parameters studied in all cell lines. A) Correlation between uptake and cytotoxicity. B) Correlation between uptake and averaged maximum temperature. C and D) Correlation between maximum temperature and cellular viability with the MTT assay at 0 (C) and 24 hours (D) after treatment. E and F) Correlation between maximum temperature and cellular viability studied with trypan blue staining at 0 (E) and 24 hours (F) after treatment.

Increases of temperature should be inversely correlated with viability. Both immediately and 24 hours after treatment, high temperatures agreed with a decrease in viability studied by mitochondrial activity. Although the correlation coefficients are similar between the two timepoints (r = -0.68 and r = -0.65), a trending line emphasises a more pronounced decrease of viability 24 hours after irradiation (Figure 6.6). As previously mentioned, this further decrease of viability might be the result of a dynamic cell death process, instead of a single event. Loss of membrane integrity shows slightly different results compared to mitochondrial activity, as immediately after irradiation high temperatures do not strongly correlate with loss of viability (r=-0.50). However, this trend changes after 24 hours (r = -0.75), indicating that the effects of temperature on cell lines are not immediate and studying viability at two different timepoints, with different methods, is recommended. The approaches selected should look at different markers of viability: metabolic activity (e.g. MTT, XTT), membrane permeability (e.g. trypan blue or Propidium iodide staining), enzymatic activity (e.g. LDH) or DNA synthesis/replication.[216]

6.3. Conclusions and outlook

Nowadays, there is a remarkable imbalance between the large number of pre-clinical studies on photothermal therapy and the few clinical trials conducted to date. There are multiple and varied factors underlying this disproportion, from nanoparticle-related issues to technical hurdles of the treatment itself.[217] At this stage of maturity of PPTT, animal experimentation is unavoidable, but *in vitro* models play a key role in the reduction and refinement of the number of animals required. Identifying potential

obstacles at the *in vitro* level of development, such as toxicity to non-target organs either from the nanomaterial or from light treatment, allows for changes and refinements of the technique without need for large cohorts of animals.

The current work highlights the differences in cellular uptake, toxicity, and viability after treatment with PPTT for different cell types and tissues while maintaining the parameter space constant through the experiment. This study selected a single nanoparticle type, power, and time of irradiation to be tested against six different cell lines as a systematic approach to directly compare PPTT on different cellular types.

This study showed differential uptake and sensibility to AuNR-PEG, translating to different cell type susceptibility to PPTT. Hence, *in vitro* experiments should be thoroughly designed to produce robust and reliable data to set a solid basis for further *in vivo* experiments. Using more complex *in vitro* systems, like co-cultures and 3D cell culture methods, can give key information on communication between neighbouring cell types and help unravel different behaviours cells can have in PPTT. Moreover, the combination of such cellular systems with lab-on-a-chip technologies would provide PPTT research with a powerful tool for high throughput analysis, where many variables and outcomes can be tested in a more realistic tumour environment allowing for a better understanding of all biological process involved in PPTT, from nanomaterial uptake to cell death mechanisms.

By systematically reporting the results on the application of *in vitro* PPTT and engaging in a discussion of the possible effects PPTT has on different cell lines, we aimed to bring insight into the complex interplay of AuNR-PEG, cell type and treatment conditions. Altogether, improving and standardizing *in vitro* research will undoubtedly guide *in vivo* studies, which will, in turn, adjust the overall efficacy of PPTT, produce more quality on pre-clinical data, and ultimately favour the clinical translation of PPTT.

7

Apoptotic activation after hyperthermia

7.1. Introduction

The previous chapter covered the reactions of different cell types to plasmonic photothermal therapy (PPTT) and their viability after treatment. The significant decrease in mitochondrial activity, in contrast to the stability of membrane integrity, led to the conclusion that apoptosis was being activated rather than necrosis. Moreover, in the preliminary studies discussed in chapter 5, progressive activation of caspase-3 was observed, a clear indication of the activation of apoptosis.

Many hallmarks of apoptosis can be used to determine if a cell has activated its programmed cell death mechanisms. Cells undergoing apoptosis show chromatic condensation, membrane blebbing, DNA fragmentation and phosphatidyl-serine exposure on their membrane.[83] These characteristics allow to recognise apoptosis through mechanisms such as microscopic examination, DNA-gel electrophoresis, cytochrome C release and annexin V staining. To obtain more information on the events being triggered at the molecular level, protein arrays offer high throughput analysis, useful to determine which molecular cascades have been triggered after the death signal activation.

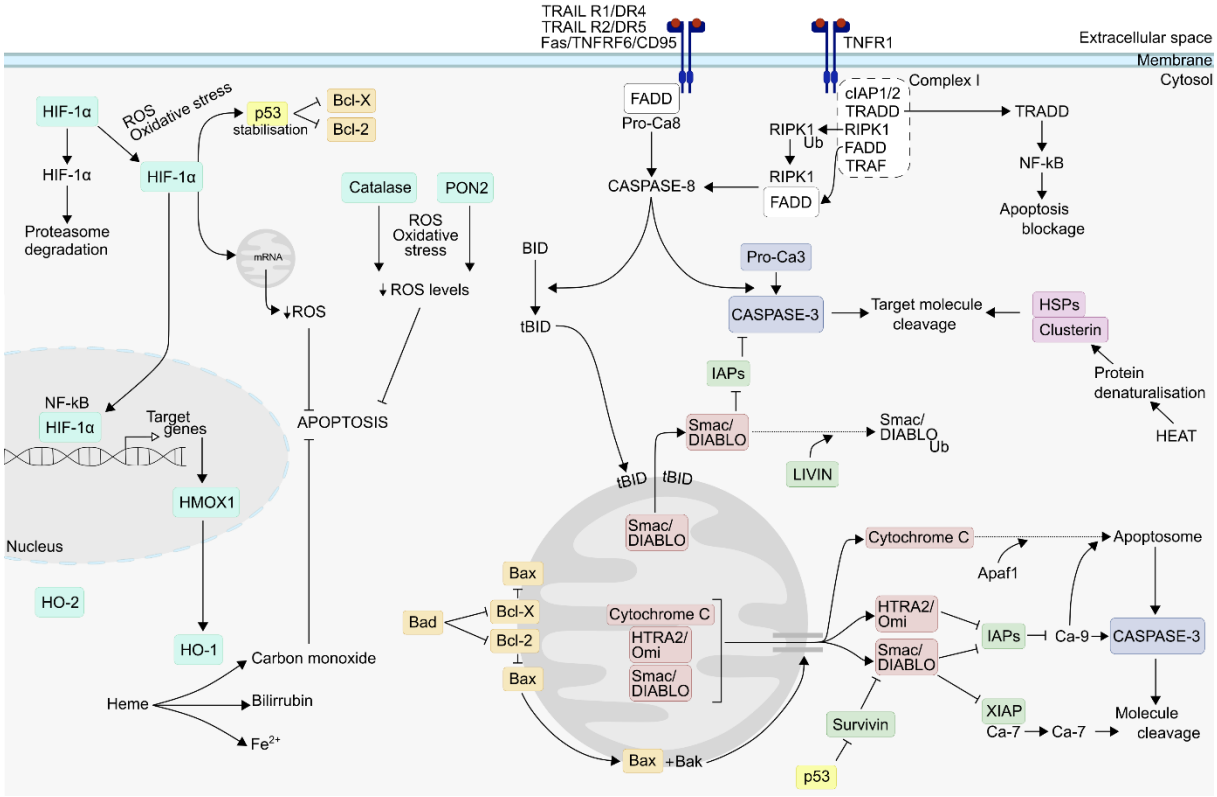

Figure 7.1. Overview of proteins studied with apoptosis proteome array. Schematic representation illustrates the interactions and functions of all 35 studied proteins using the apoptosis proteome array. The diagram highlights key apoptotic events and the interplay between proteins, providing a comprehensive overview of their roles in apoptotic pathways and interaction with each other. Studied proteins are colour coded by their functions. Blue: caspases, red: proapoptotic, green: anti-apoptotic, pink: heat shock proteins, cyan: oxygen related proteins, white: receptors, yellow: cell cycle proteins. Proteins involved in the cell cycle were omitted for sense of clarity.

Our previous data suggested the stimulation of the apoptotic cascade, therefore we decided to analyse its activation at 6 and 24 hours after PPTT. Additionally, cells irradiated without nanoparticles and cells not treated were used as controls. Moreover, traditionally induced hyperthermia (60°C for 5 minutes in the oven) was used to compare the differential expression of certain proteins between PPTT-induced and conventional hyperthermia.

A protein array containing 35 proteins involved in the apoptosis pathway was used. To better understand the interaction between all examined proteins, Figure 7.1 provides an overview of the engagement of these proteins with each other to activate, or inhibit, the apoptotic cascade. Many proteins are key factors in the commitment of cells to apoptosis, necrosis, or survival. This dance, although highly understood, still is susceptible to the intensity in which each of the cell death stimulus initiate or deter programmed cell death.

Although all proteins were simultaneously examined, we categorised them based on their functions and involvement in specific pathways. This approach was taken to enhance the clarity and interpretability of the findings. The classification scheme is outlined as follows: caspases, heat shock proteins, Bcl-2 protein family, proapoptotic proteins, anti-apoptotic proteins, extrinsic pathway of apoptosis, oxygen-related proteins, and cell cycle-related. To simplify the explanation provided in the main text and allow for a more focused discussion, detailed descriptions of some protein functions and explanations will be available in Annex C.

7.2. Results

7.2.1. The caspase executor: caspase 3

Caspases are cysteinyl-aspartate specific proteases that cleave proteins to either activate or inactivate substrates.[96] They are expressed as inactive proteases, namely pro-caspases, in most cells. Their activation occurs upon apoptotic signalling by cleavage of the pro-caspase form, allowing them to dimerise, aggregate and cleave other proteins. (Figure 7.2-A) Caspase activation leads to a proteolytic cascade that amplifies the apoptotic signal.

In apoptosis, caspase 3 is the dominant executor of the apoptotic signalling cascade. Many elements within the apoptotic cascade aim to activate executioner caspases, that trigger the cleavage of target molecules. Activated caspase 3 is the mediator of many of the biochemical and morphological characteristics of apoptosis, such as DNA fragmentation and membrane blebbing.[86] Caspase 7, another executioner caspase, regulates cellular detachment during programmed cell death.[218]Pro-caspase 3 is activated by initiator caspases that cleave at specific domains in the protease, allowing its subunits to dimerise and start mediating the cleave of key proteins. Measuring both, pro- and cleaved- caspase 3 provides first grade information on the execution of the apoptotic pathway.

The relative expression of pro-caspase 3 and cleaved caspase-3 after PPTT irradiation is shown in Figure 7.2-B. Between cells experiencing PPTT, with or without nanoparticles, and controls, no significant differences were observed at 6 or 24 hours after irradiation ($p > 0.05$). Basal expression of pro-caspase 3 was maintained at these timepoints, however, for cells experiencing hyperthermia through conventional methods (800,000 cells in a 20 µL pellet incubated at 60°C for 5 minutes) -from here on referred to as “oven-cells”- pro-caspase 3 expression was sharply increased in comparison to all other samples ($p \leq 0.03$). This is interesting, as it shows differences in the incidence of hyperthermia between PPTT-induced and conventional hyperthermia for basally expressed pro-caspases.

On the other hand, cleaved caspase 3 expression was increased almost 4-fold compared to control samples 6 hours after irradiation ($p < 0.0001$). After 24 hours, the signal from cleaved caspase was halved in samples that experienced hyperthermia but was still statistically higher than controls ($p = 0.0245$). The peak in expression at 6 hours strongly indicates the initiation of apoptosis following temperature elevation during PPTT. The subsequent decline in expression is likely attributed to all events leading to caspase cleavage having been completed, resulting in cell death activation slowing down. Most cells will have already undergone apoptosis and self-destructed.

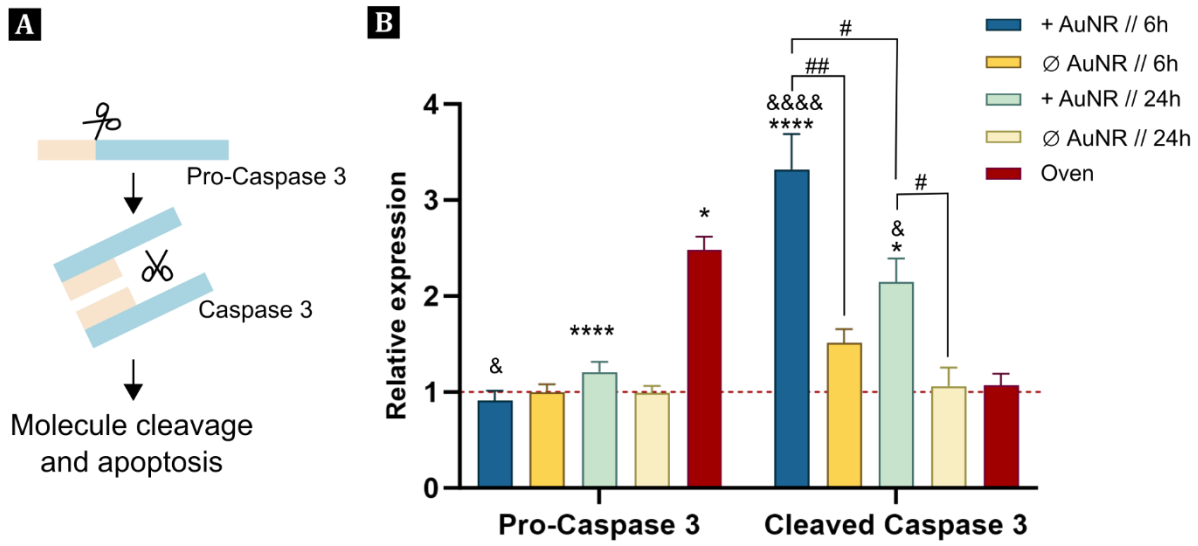

*Figure 7.2. Activation mechanism and expression levels of caspase. A) Schematic depiction of pro-caspase cleavage into its active form, leading to molecule cleavage and apoptosis. Scissors represent caspase cleavage activity B) Relative expression levels of caspase compared to controls. Dotted line represents mean expression of control samples. Statistical significance is denoted by symbols: * indicates significance vs control samples, & indicates significance vs oven samples, and # denotes significance vs other samples. *p<0.05, **p<0.01, ***p<0.001, ****p<0.0001*

Oven-cells did not increase the expression of cleaved caspase after hyperthermia. This absence of apoptosis activation following a thermal insult, despite a sharp increase in expression of pro-caspase, may be attributed to the protein expression kinetics after hyperthermia. Oven cell samples were recovered immediately after heating. This suggests that cells prepare to activate programmed cell death mechanisms by increasing the expression of pro-caspase during hyperthermia, but have not yet cleaved the protease for activation, as there were non-detectable changes. In the case of PPTT-cells, any pro-caspase increase in expression immediately post-treatment, would likely have been cleaved by the 6-hour mark.

Differences in the upregulation level of pro-caspase and caspase 3 depend on the temperature and time elapsed after hyperthermia.[81] Programmed cell death is a very time-dependent process, being the events that lead to cellular demise sequential.

Cells irradiated without AuNR-PEG were not subjected to hyperthermia and did not present significant changes in the expression of both forms of the protein. This indicates that, in the absence of AuNR-PEG, our laser irradiation settings (3 W/cm^2, 3 minutes) are insufficient to activate the apoptotic cell death mechanisms. Interestingly, research has shown that the presence of gold nanoparticles alone can activate caspase 3, but this occurred after several hours of treatment.[219] However, this does not affect our results, as incubation with AuNR-PEG occurs 24 hours previous to irradiation, ensuring any caspase 3 activation finished before sample irradiation.

7.2.2. Heat shock proteins: the stress-response guardians

One of the main events triggered during hyperthermia is protein denaturation. Denaturation consists in the breakage of bonds within proteins, producing a loss of secondary, tertiary and quaternary structure. Protein function is strongly associated with its 3D structure, therefore losing its structure leads to function loss. If denaturation exceeds the cellular capacity to recover and refold proteins, cells will commit to cellular death.

Heat shock proteins (Hsps) are a family of highly conversed proteins, synthetised by cells in response to a cellular stress (pH changes, heat, physical stress, etc.). They act as molecular chaperones, aiding on protein folding and stability, and protecting transport and aggregation of proteins.[97] Hsps expressed at their basal levels are involved in the correct folding of proteins during homeostatic conditions in crowded cellular environments.[220] However, they are upregulated upon cellular stress, where they adopt

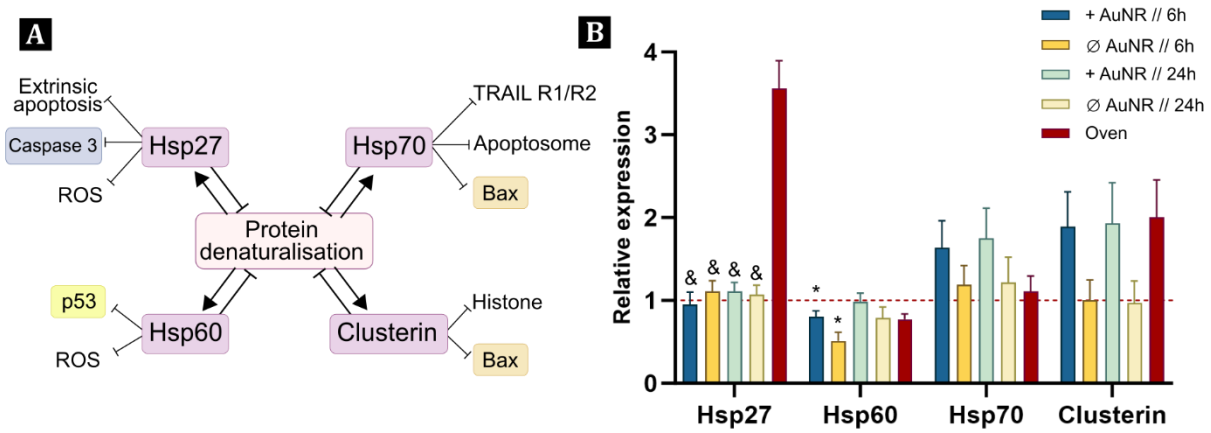

*Figure 7.3. Role of heat shock proteins and expression levels. A) Schematic representation illustrating the main activation and inhibition roles of Hsps. The figure highlights the dynamic interplay between Hsps and protein denaturalisation upon cellular stress. B) Graph depicting the relative expression levels of Hsps. Only statistically and clinically relevant differences are shown. Statistical significance is denoted by symbols: * indicates significance vs control samples, and & indicates significance vs oven samples. *p<0.05, **p<0.01, ***p<0.001, ****p<0.0001*

a cytoprotective role, regulating the apoptotic cell machinery.[96,97] Hsps are importantly also upregulated in cancer cells, so it is possible to target Hsps to improve anti-cancer therapies.[97,98] Unfortunately, many Hsps have functional redundancy, which challenges the exploration of anti-Hsp drugs for cancer treatment.[98]

During our experiments, four different Hsps were studied: Hsp27, Hsp60, Hsp70 and Clusterin. They are usually classified by their molecular weight, as the number accompanying their name indicates. Their main functions can be seen in Figure 7.3-A.

7.2.2.1. Hsp27

The Hsp27 provides thermotolerance on *in vivo* situations and increased survival of cells in cytotoxic conditions.[95] It functions on several cellular signalling pathways, integrating the different apoptotic pathways as an anti-apoptotic molecules.[95,97] Moreover, it regulates redox homeostasis and mitochondrial stability, both initiators of apoptosis.[97,221] Hsp27 binds to cytochrome C after its mitochondrial release and to pro-caspase 3, preventing downstream mitochondrial damage and formation of the apoptosome.[222] For additional details on function, please refer to Annex C. Hsp27 works very closely with Hsp70 and Hsp90, and their interactions are crucial for their functionality.

In PPTT-cells, both with and without AuNR-PEG, no statistically relevant changes in the relative expression of Hsp27 were observed (Figure 7.3). The expression of Hsp27 on all irradiated samples was very similar to the expression in control cells ($p \geq 0.05$). However, on cells experiencing hyperthermia on the oven, an almost 4-fold increase in expression of Hsp27was observed (Figure 7.3-B).

The increased expression in oven-cells immediately after treatment, together with the consistent expression pattern observed in Hsp27 at 6 and 24 hours after PPTT, could be attributed to its rapid response to stress. Hsp27 is rapidly phosphorylated after the exposure to stress, leading to an increase in expression levels.[95] However, this surge in expression is transient and upon removal of the stressor, levels return to baseline. Our stressors, namely heat and laser illumination, may induce short-lived changes in expression that we may have not captured by assessing the protein expression at 6 and 24 hours after irradiation. However, we did observe these changes in oven-cells, as they were examined immediately after heat exposure. Short time periods at high temperatures in the macroscopic scale induce overexpression of Hsp27.

The observation of no changes between PPTT and irradiated cells at two different timepoints, together with the detected overexpression in oven-cells underscores the importance of studying kinetics in apoptosis-related proteins. The significance of studying viability and molecular events at multiple

timepoints is crucial, as analysing cells at single static point of time may overlook many decisive molecular events.

The differences between *in vitro* and *in vivo* may also play a role in understanding the apoptotic process post-hyperthermia. Chen *et al*.[223] determined that in immunosuppressed mice, hyperthermia induced after intratumoral high-frequency ultrasound (1 W, 30 seconds) expression of Hsp27 was elevated in the experimental group in comparison to the control group 18 hours after irradiation. This is positive for anti-cancer purposes, as the expression of Hsp27 and its phosphorylation is inversely correlated with progression of hepatocellular carcinomas.[224] Mild heat shock is enough to induce the expression of Hsp27, but prolonged non-lethal exposure to heat may render the cells thermotolerant.[91]

7.2.2.2. Hsp60

Hsp60 main activity is performed together with co-chaperone Hsp10 binding to newly synthesized proteins and facilitating their correct folding.[93,225] Its anti-apoptotic functions are mainly performed by providing a folding chamber for unfolded denature proteins, protecting surviving and modulating p53.[226] Hsp60 modulates p53 by inhibiting its migration towards the nucleus, preventing the invalidation of the G2/M checkpoint during cell cycle.[226]

The function of Hsp60 on apoptosis is highly discussed in healthy vs cancerous cells, being considered anti-apoptotic in the former, but apoptotic in the latter. In Jurkat cells, Hsp60 acts as a pro-apoptotic proteins by leading to the maturation of caspase 3,[98,226] whereas in clear cell renal carcinoma, Hsp60 is downregulated and causes tumour progression.[227] For additional details, please refer to Annex C.

Our observations of Hsp60 expression detected a significant decrease of relative expression of irradiated cells, with and without AuNR-PEG, against control cells 6 hours after illumination ($p < 0.048$). This reduction on Hsp60 expression was more pronounced for cells irradiated without AuNR-PEG that did not experience elevated temperatures (Figure 7.3). The other analysed samples showed no statistically significant decreases in relative expression of this chaperonin, including oven-cells, that had very similar expression levels to AuNR-PEG samples 24 hours after irradiation.

The initial decrease observed six hours after PPTT treatment seemingly indicates the cellular predisposition to damage by apoptotic signals and protein denaturation. However, this could be a red herring, as ccRCC cells, such as the studied 786-0 cell line, express abnormal levels of Hsp60. Further studies on the effect of hyperthermia on ccRCC cells, both *in vitro* and *in vivo*, are needed to explain the further reduction of expression of Hsp60. Cells irradiated without AuNR-PEG do not drastically see their viability decreased, indicating that Hsp60 function in irradiated 786-0 cells is not essential for viability or mortality after PPTT.

This observation is a clear example of why results obtained from a single cell line should be taken with great consideration, as other cell types may exhibit similar, or opposing, reactions in terms of protein expression. For 786-0, it would be prudent to observe the relative expression of Hsp60 at additional timepoints and compare those to healthy renal cell lines, to gain a more comprehensive understanding of the role of Hsp60 on PPTT-induced hyperthermia.

7.2.2.3. Hsp70

Hsp70 is a constitutively expressed chaperone that plays a pivotal role in heat and stress response. It aids in protein assembly and folding processes is almost all cellular compartments, as well as facilitating protein traffic.[225] Hsp70 has high binding affinity for non-native proteins, able of recognising hydrophobic surfaces in proteins.

Mild stress can induce an increase in the expression of Hsp70, having the important role of associating with different co-chaperones to allow to refold aberrantly folded proteins. Hsp70 hinders the apoptotic cascade by preventing the interaction of Apaf-1 with caspase 9 to form the apoptosome.[96] It also associates with Bax, preventing its oligomerisation and cytochrome C release from the mitochondria.[97,98]

Under stress, Hsp70 interacts and suppresses Bcl-2 family members apoptotic signals.[96] Hsp70 is largely considered an anti-apoptotic protein. For additional details on protein function, please refer to Annex C.

After PPTT-induced hyperthermia, 1.5-fold increases in the expression of Hsp70 could be observed in cells with AuNR-PEG at 6 and 24 hours after illumination (Figure 7.3). Upon exposure to mild heat shock, the expression of Hsp70 is usually induced,[91] but the changes observed were not statistically significant ($p \geq 0.05$).

Expression in cells irradiated without AuNR-PEG also had slight increases of Hsp70 expression compared to controls, similar to oven-cells, but none of the changes were statistically significant. Nonetheless, and from a clinical perspective, the higher increase in expression in PPTT-cells at 6 and 24 hours, compared to oven-cells immediately after treatment is an indication that the processes by which PPTT and conventional hyperthermia elevate temperature differ. With an additional timepoint for oven-cells, we would be able to determine if Hsp70 is activating cellular survival mechanisms upon thermal heating.

On *in vivo* experiments, Chen *et al*. found increases of Hsp70 expression in hepatic tumours 18 hours after irradiation-induced hyperthermia.[223] Experiments that modulated Hsp70 expression *in vitro* found out that down-regulation of Hsp70 in oral (HSC), breast (MCF-7) and liver (Huh7.5) produced a significant reduction in viability, increasing apoptosis after PPTT.[35] By conjugating anti-Hsp70 drugs to gold nanoparticles, the efficacy of PPTT-induced hyperthermia is enhanced.[35] Silencing Hsp70 may have a cytotoxic effect on tumour cells, but not on healthy ones.[98]

7.2.2.4. Clusterin

Clusterin is a secreted multifunctional protein that upon stress-induced precipitation of unfolded proteins, it acts as a chaperone by associating with Hsp70 and interfering with Bax activation, blocking its pro-apoptotic effects.[228–230] During chemical or heat-induced stress, clusterin avoids protein segregation of slowly aggregating proteins, indicating that clusterins act as chaperons that preferentially recognise particularly unfolded proteins.[220] For additional details on the role on clusterin on protein folding and during efferocytosis (removal of dying cells by macrophages), please refer to Annex C.

After PPTT and oven-induced hyperthermia, clusterin had a mean 2-fold increase in expression compared to control cells and cells irradiated without AuNR-PEG, however, none of these increases were statistically significant ($p \geq 0.05$) (Figure 7.3). Although this lack of statistical relevance, it is possible to define a clinical change in the expression on the relative expression of clusterin after thermal stress.

Clusterin is a very resistant protein to heat-induced stress. When heated to 60°C for 30 minutes, it did not experience precipitation, but could protect other proteins (Catalase and GST) when heated at the same temperatures. However, the protection provided by clusterin was only physical, as these proteins experienced loss of function.[228] Nonetheless, the increase in expression of clusterin after all hyperthermic effects (PPTT and oven) reinforces its interaction with slowly aggregating proteins after hyperthermia.[220]

7.2.3. The Bcl-2 protein family: orchestrators of cellular fate

The Bcl-2 protein family has dual roles in the balance between cellular survival and apoptosis. All proteins within the family share the same Bcl-2 homology (BH)-domain, the BH3-domain, that allows proteins of the family to interact with each other.[231] The other BH-domains that the proteins have will indicate their role in cellular death, as pro- or anti-apoptotic.

The Bcl-2 protein family is classified into three subgroups: BH3-only (proapoptotic, e.g. Bad), effectors or pore-former (proapoptotic, e.g. Bax) and anti-apoptotic (e.g. Bcl-2 and Bcl-x). Their binding interactions regulate the formation of the mitochondrial outer membrane pore (MOMP), setting an apoptotic threshold for the mitochondrial release of cytochrome C and other proapoptotic proteins.[232,233]

As shown in Figure 7.1 and Figure 7.4, anti-apoptotic proteins in homeostasis are mutually sequestering pore-forming proteins (Bax and Bak), and BH3-only proteins, preventing the formation of a mitochondrial pore. Upon apoptotic signalling, BH3-only proteins capture anti-apoptotic proteins Bcl-2 and Bcl-X, allowing Bax and Bax to oligomerise and the formation of the MOMP, marking the activation of apoptosis.[232–234]

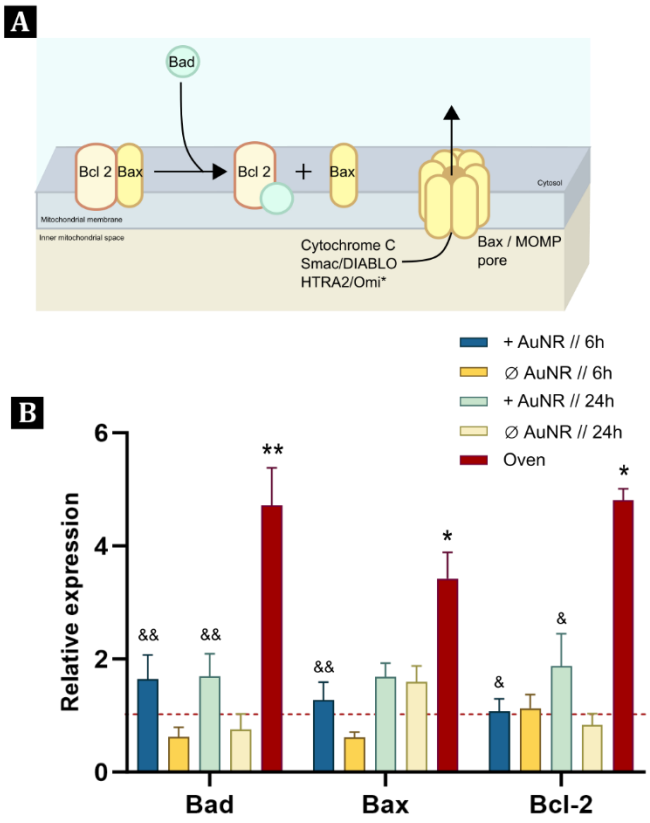

*Figure 7.4. Bcl-2 protein family in apoptosis activation. A) Schematic representation of the interaction between members of the Bcl-2 protein family. Bad sequesters Bcl-2, liberating Bax, that can form the MOMP and allow mitochondrial proteins to flow to the cytoplasm. B) Graph depicting relative expression of Bad, Bax and Bcl-2. Only statistically and clinically relevant differences are shown. Statistical significance is denoted by symbols: * indicates significance vs control samples, and & indicates significance vs oven samples. *p<0.05, **p<0.01, ***p<0.001, ****p<0.0001*

The apoptosis array used to test the expression of apoptotic-related proteins allowed us to test for Bad, Bax, Bcl-2 and Bcl-X, however, the data of only three of these proteins could be analysed. In the array, Bcl-X spot-antibodies were located next pro-caspase 3- During imaging, the signal intensity from the expression of pro-caspase 3 was strong enough to influence the neighbouring spot (Bcl-x). As a consequence, of both replicate antibody spots for Bcl-x, one had higher intensity than the other. This discrepancy between replicates within the membrane could add a lot of error in data analysis, and therefore, it was decided to forego its analysis and discussion. Nonetheless, functional redundancy of anti-apoptotic proteins Bcl-2 and Bcl-x, regarding mutual sequestration of Bax, allowed us to analyse the Bcl-2 protein family role on cellular fate after PPTT.

7.2.3.1. Bad

Bad is a proapoptotic protein. Its main role is engaging with anti-apoptotic proteins and liberate Bax to form a MOMP and promote apoptosis. Bad displaces Bax from mutual sequestration and allows it to translocate to the mitochondrial membrane. It acts as a sensitiser protein, recognizing intrinsic and extrinsic triggers of apoptosis (DNA damage, endoplasmic reticulum damage, oxidative and metabolic stress).[233,235] Bad is therefore an initiator protein that neutralises the effect of Bcl-2 protein.

After a hyperthermic event, the expression of Bad was increased 1.5 times compared to controls in cells irradiated with AuNR-PEG, at 6 and 24 hours after the event (Figure 7.4). In the case of cells irradiated without AuNR-PEG, a slight decrease in the relative expression of Bad could be detected. However, none of these changes were statistically significant ($p \geq 0.05$). On the other hand, cells experiencing 60°C for 5 minutes in an oven displayed a more than 4-fold increase in the expression of Bad, and this was statistically significant compared to all other samples and controls ($p < 0.0124$). Overexpression of Bad induces sensitization to TRAIL-induced (extrinsic) apoptosis, as well as increasing apoptosis due to loss of cellular adhesion.[235,236]

7.2.3.2. Bax

Bax is a proapoptotic protein and one of the main components of the mitochondrial outer membrane pore (MOMP). In homeostasis, Bax is usually mutually sequestered by Bcl-2 or Bcl-x. Upon apoptotic activation, Bax is released from Bcl-2 and can retro-translocate within the mitochondrial membrane and form the MOMP. This pore allows cytochrome C and other pro-apoptotic proteins to escape from the inner mitochondrial space to the cytosol, where they will active downstream apoptotic effectors.[232,233]

Oligomerisation of Bax, with itself or together with Bak, is a crucial aspect for the development of apoptosis. After PPTT, the expression of Bax was dysregulated. On cells irradiated with AuNR-PEG, relative expression of Bax was upregulated, being slightly higher 24 hours after hyperthermia. However, in the case of cells irradiated without AuNR-PEG, 6 hours after illumination, expression was halved compared to controls, whereas 24 hours after irradiation Bax expression had increased (Figure 7.4). None of these changes were statistically significant. This increase in expression in cells illuminated that did not experience hyperthermia could indicate the late effects of laser irradiation in activating some apoptotic processes.

Oven hyperthermia cells had on the other hand, a clear increase in the relative expression of Bax immediately after treatment, indicating a drastic increase in the formation of mitochondrial pores after a thermal event. Bax overexpression sensitises cells to apoptosis and anti-cancer drugs, indicating the potential of hyperthermia to enhance the effect of anti-cancerous drugs. More investigation in the effects of PPTT for Bax overexpression should be done, as our results at 6 and 24 hours after the hyperthermic effect did not show significant increase, but perhaps the effect had already passed.

7.2.3.3. Bcl-2

Bcl-2 is a pro-survival protein that prevents the oligomerisation of Bax and inhibits BH3-only proteins.[233] Overexpression of Bcl-2 increases the signalling threshold required to trigger apoptosis.[232] However, downregulation of Bcl-2, unless accompanied by downregulation of anti-apoptotic proteins, such as Bcl-x and MCL1, does not result in an increase in apoptosis because of its functional redundancy.

Expression of Bcl-2 wasn't changes compared to controls 6 hours after irradiation for both cells with and without AuNR-PEG. However, 24 hours after irradiation, the relative expression of cells after PPTT-induced hyperthermia experienced a 2-fold increase, however it was not statistically significant. On the other hand, immediately after the hyperthermic event, oven-cells had a 5-fold increase in expression compared to controls. This rise was statistically higher than the increase observed in AuNR-cells 24 hours after illumination.

7.2.3.4. Bcl-2 family: game of affinities

The result of apoptotic signalling within the Bcl-2 family of proteins is a game of affinities between pro-survival and pro-apoptotic proteins. The concentrations and affinities of each of the members of the protein family dictate which protein is interacting with which another, mutually sequestering proteins to either induce or suppress apoptotic signalling.

Our relative expression levels of the Bcl-2 protein family indicate apoptosis is being triggered over cellular survival for PPTT-cells, as Bad and Bax expression were slightly increased at both timepoints after hyperthermia, but anti-apoptotic Bcl-2 protein only experienced a rise in expression 24 hours after elevated temperatures. This late pro-survival reply could be the cellular response of remaining cells to persist after the initial thermal event. The differences observed between the different timepoints analysed could also indicate that more apoptotic events are happening 6 hjours after treatment compared to 24 hours later. To confirm this, mRNA expression levels should be analysed as the same timepoints as protein expression was checked. Moreover, studying the expression of Bcl-2 proteins immediately after PPTT treatment could better explain the speed at which the apoptotic events are occurring. For all oven-cells, protein expression was more heavily induced compared to PPTT-induced hyperthermia, this could be the results of a more aggressive thermal insult (higher temperature, 60°C, and 5 minutes exposure).

7.2.4. Cellular apoptotic activators: mediators of cell demise

Cellular apoptotic activators are tightly regulated by their location in the cell and their ability to interact with cytosolic proteins. The fine balance between apoptotic activators and inhibitors is distorted during apoptosis. Formation of the MOMP allows mitochondrial proteins to flow to the cytosol and interact with downstream effectors of apoptosis, (Figure 7.1 and Figure 7.5) either antagonising anti-apoptotic proteins or forming pro-apoptotic complexes. The release of Smac/DIABLO, HTRA2/Omi and cytochrome C from the mitochondria are key events for testing the induction of apoptosis.

7.2.4.1. Smac/Diablo

Smac/Diablo, during homeostasis, is found inside the mitochondria, but when an apoptotic signal is detected by the cell, and the MOMP is formed, it is released into the cytoplasm. Smac neutralises the effect of inhibitor of apoptosis (IAP) proteins, preventing their interaction with caspases and releasing them to form the apoptosome and activate executor caspase 3.[237] This reduces the targeting and destruction of caspases, therefore, an increase in the expression of Smac/Diablo is representative of apoptosis, as it lowers the apoptotic threshold for cells after a death stimulus.[238] Overexpression of Smac/Diablo sensitises cells to chemotherapeutic drugs.[239] For additional details on the method of action, please refer to Annex C.

Our observations, 6 and 24 hours after PPTT irradiation did not detect an increase in the expression of Smac/Diablo, but a sharp decrease in the relative expression 6 hours after illumination in cells with AuNR-PEG. Although this drop in expression was not statistically relevant, it allows IAPs free to block the formation of the apoptosome. Nonetheless, this decrease was neutralised 24 hours after PPTT, with expression levelling to the one of cells irradiated without AuNR-PEG. On the other hand, oven-cells experienced a sharp increase in the expression of Smac/Diablo immediately after hyperthermia. This increase indicates that 60°C for 5 minutes applied macroscopically is enough to activate the apoptotic mechanisms and release Smac/Diablo.

In the case of studied renal cell carcinoma, the expression of Smac/Diablo is controversial, as several studies have found a lower expression level of this pro-apoptotic protein, inversely correlating with progression and prognosis of cancer.[237] This results, compared to the outcomes of the relative expression of Smac/Diablo after hyperthermia indicate that for conventional methods, hyperthermia can sensitise tumours to chemotherapeutic drugs, but that PPTT-induced hyperthermia may have to deal with Smac/Diablo not being easily inducible 6 and 24 hours after treatment.

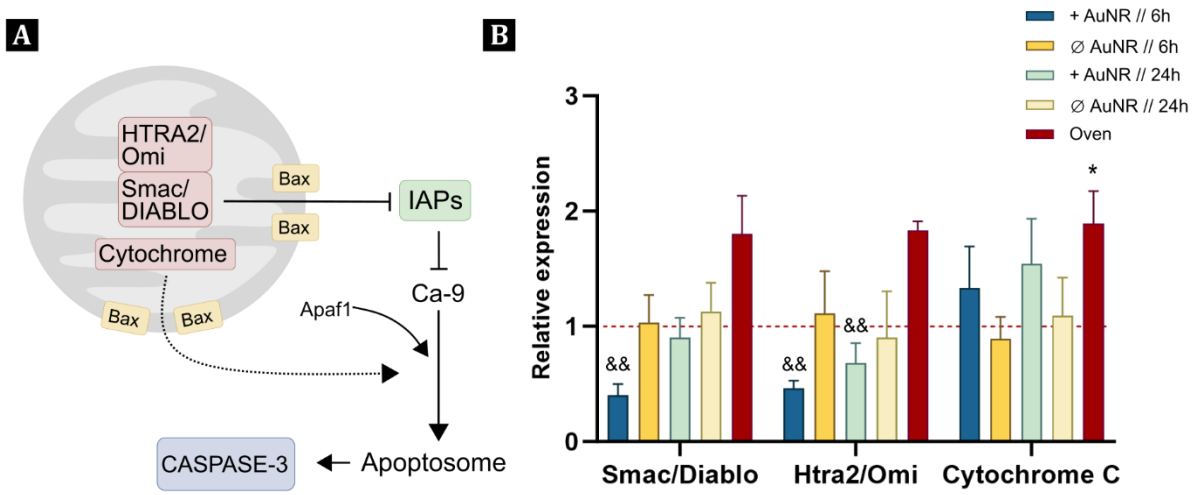

*Figure 7.5. Cytochrome C and Smac/Diablo release and expression levels of pro-apoptotic proteins. A) Image depicting the effects of pro-apoptotic proteins release from the mitochondria. B) Graphs depicting the relative expression of Smac/Diablo, Htra2/Omi and cytochrome c. Only statistically and clinically relevant differences are shown. Statistical significance is denoted by symbols: * indicates significance vs control samples, and & indicates significance vs oven samples. *p<0.05, **p<0.01, ***p<0.001, ****p<0.0001*

7.2.4.2. Htra2/Omi

Htra2/Omi, or high temperature requirement protein A2, is a pro-apoptotic protein that reduces the activity of IAPs by incapacitating them. Htra2/Omi is a serine protease that can cleave IAPs, reducing their capacity to inhibit caspases (Figure 7.5-A).[240,241] Increases of Htra2/Omi are associated with apoptosis promotion, as it efficiently removes their inhibitors, rendering cells susceptible to death signals and drugs.[240,241]

The observation of the relative levels of Htra2/Omi showed a similar expression profile to Smac/Diablo despite its more assertive function against IAPs. After 6 hours of irradiation with AuNR-PEG, its expression was halved compared to controls, but this change was not statistically significant ($p \geq 0.05$). In contrast to Smac/Diablo, Htra2/Omi expression is not completely recovered 24 hours after hyperthermia, but still exhibits an increase ($p \geq 0.05$) (Figure 7.5). In oven-cells, close to a 2-fold increase in the expression of Htra2/Omi could be observed after hyperthermia. This increase would logically be followed by a decrease in the expression of IAPs, but as we will see in the next section, IAP expression is also elevated after hyperthermia.

7.2.4.3. Cytochrome C

Cytochrome C is a major protein in the apoptotic cascade. Generally, it resides within the inner mitochondrial membrane, where it participates in the electron-transport chain, accepting electrons from complex III and transferring them to complex IV.[242,243] During apoptosis, cytochrome C is released from the mitochondria into the cytoplasm, where it binds into Apaf-1 (Apoptosis protease-activating factor-1).[61]

Apaf-1, in the absence of cytochrome C resides as a monomer, uncapable of recruiting and activating caspase-9. Upon binding of cytochrome C to Apaf-1 it forms the characteristic ring-like formation, uncovering the caspase recruitment domains (CARD), enlisting pro-caspase 9 (initiator caspase) and forming the apoptosome. The completed apoptosome can activate executioner caspases 3 and 7, orchestrating the cleavage of specific molecules and determining cellular fate (Figure 7.5).[61,242–244]

Cytochrome C release is a turning point in apoptosis activation, often used as an apoptotic marker during the study of programmed cell death mechanisms. After hyperthermia, through PPTT or in the oven, cells experienced a general increase on the relative expression of cytochrome C compared to controls, however none of these increases were statistically significant ($p \geq 0.05$). In comparison, the mean expression of cells irradiated without AuNR-PEG was similar to those of controls. We observed high variability for all samples after treatment, reducing the statistical relevance of comparisons. However, the larger increase in expression of cytochrome C in cells experiencing hyperthermia, compared to those that do not, suggests, though not definitely, that apoptosis has been triggered.

Hsp27, on top of blocking the interactions mentioned above, is able to prevent cytochrome C interaction with Apaf-1 and pro-caspase 9.[222] Therefore, the increase of cytochrome C, together with the increase of Hsp27 indicates an effort of cells heated in the oven to protect against heat-induced apoptosis. However, the lack of change on Hsp27 after PPTT, together with cytochrome C increase, suggest that 6 and 24 hours after irradiation, programmed cell death is induced in 786-0 cells after hyperthermia.

7.2.5. Cell survival defenders: IAPs

To maintain cellular homeostasis, apoptotic inhibitors regulate programmed cell death in most mammalian cells.[245] Inhibitors of apoptosis (IAPs) hold a key position as controllers of programmed cell death when apoptotic signals are considered to be sublethal and cellular recovery and survival is plausible. This may occur when the stress-inducing event that triggers the death mechanism rapidly disappears or lacks the required intensity to surpass the apoptosis threshold.

The inhibitors of apoptosis are a highly conserved protein family, sharing the baculovirus-IAP-repeat (BIR) domain, allowing them to bind caspases and block them.[245] Together with other domains they present, it determines how IAPs exert their anti-apoptotic functions: directly inhibiting caspases with

physical interactions, targeting caspases for ubiquitination and proteasomal degradation, or interacting with pro-apoptotic proteins, such as Smac/Diablo (Figure 7.6-A).[246,247]

The downregulation of IAPs does not result in the activation of apoptosis, but rather it indicates that cells are sensitised to apoptotic stimuli, reducing the threshold for activation of programmed cell death.[248] Moreover, functional redundancy within the IAP protein family renders deletion and downregulation of certain inhibitors of apoptosis unremarkable.[249] To find further details on the action of IAPs and analysis of additional anti-apoptotic proteins examined during the proteome array, please consult Annex C.

7.2.5.1. c-IAP1, c-IAP2 and XIAP

Cellular IAP1 and IAP2 (c-IAP1 and c-IAP2) and X-linked IAP (XIAP) are negative regulators of apoptosis in a different number of pathways, including the intrinsic mitochondria-mediated pathway and the death receptor-mediated pathway.

c-IAP1 and c-IAP2 cannot directly inhibit caspases, but they help on the ubiquitination of caspase 3 and caspase 9, targeting them both for proteasomal degradation.[246] Moreover, due to the putative redundancy of c-IAP1 and c-IAP2, the combined absence of both proteins rendered cells sensitive to extrinsic TNFα-receptor cell death signalling.[250] cIAPs mediate TNFR1-TRAF-RIP1-Caspase 8 activation, ultimately leading to the activation of apoptosis.[247] c-IAP1 is known to promote oncogenesis by promoting the degradation of a negative regulator of Myc.[251]

XIAP can directly bind to caspase 3 and 7 and prevent their interaction with their substrate for cleavage effectively blocking caspase function.[248] Additionally, they possess E3-ubiquitin ligase activity, tagging caspases with ubiquitin for subsequent proteasomal degradation.[247,248,252] XIAP is direct target of Smac/Diablo, displacing XIAP-bound caspases and reactivating molecular cleavage.[252]

The results obtained after analysing the relative expression of IAPs after PPTT compared to controls showed decreases on the expression of all three IAPs after PPTT-induced hyperthermia (Figure 7.6-B). These changes were not statistically significant ($p \geq 0.05$). Cells irradiated with NIR light without AuNR-PEG had not significant increases of IAPs 6 hours after illumination. On the other hand, oven-cells had a 3-fold increase of c-IAP1 compared to controls ($p < 0.0031$), and 1.5-fold increase for c-IAP2 ($p < 0.0473$). XIAP expression after hyperthermia in the oven did not significantly change ($p \geq 0.05$).

The lack of relevant changes in the expression of any of these three inhibitors of apoptosis after laser irradiation indicates that our laser setting, by itself, does not increase the susceptibility of cells to

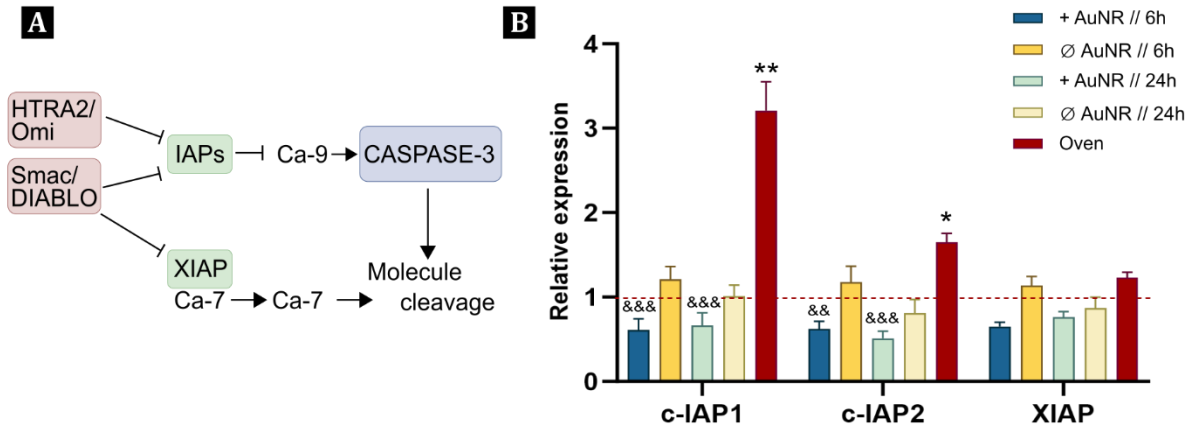

*Figure 7.6. Inhibitors of apoptosis role in apoptosis. A) Schematic representation of the interaction between pro-apoptotic and anti-apoptotic proteins. B) Graph depicting relative expression of Bad, Bax and Bcl-2. Only statistically and clinically relevant differences are shown. Statistical significance is denoted by symbols: * indicates significance vs control samples, and & indicates significance vs oven samples. *p<0.05, **p<0.01, ***p<0.001, ****p<0.0001*

apoptosis. However, the modest downregulation of IAPs after PPTT treatment could be a marker of plasmonic hyperthermia rendering cells more susceptible to apoptotic stimuli. Oven-cells immediately after treatment express high percentages of IAPs. It would be interesting to observe the expression kinetics of these inhibitors after oven hyperthermia, because if a drop in expression was observed, it would indicate that cells can initially protect themselves against the apoptosis signal triggered by elevated temperatures, but these protection decays with time, as more death signals could have been produced by the cells (ROS production or damage-associated molecular patterns (DAMPs)).

Interestingly, the reduction in the expression of c-IAP1 after PPTT may be beneficial for cancerous cells, as its role on oncogenesis in the Myc pathway will be reduced.[251] Evasion of apoptosis is a hallmark of cancer, and reduction of IAPs can indicate a decrease in tumour development and progression, including lower therapeutic resistance after PPTT.[248]

7.2.6. The extrinsic pathway: death receptors and associated proteins

Apoptotic cell death receptors and their associated proteins fulfil a central role in the activation of the extrinsic pathway of apoptosis. The signals they transmit accelerate the activation of the common downstream effectors of apoptosis where intrinsic and extrinsic apoptosis converge, such as Bid, a protein from the Bcl-2 family, with similar functions to bad.[253,254]

Of the four receptors analysed in the human apoptosis kit, three of them (TRAIL R1/DR4, TRAIL R2/DR5 and Fas/TNRFRSF6/CD95) are considered to be direct activators of apoptosis upon binding of their respective ligands, TRAIL (TNF Receptor Apoptosis-Inducing Ligand) and FasL. On the other hand, TNF R1/TNFRSF1A (TNFR1 for short) can exert both pro- and anti-apoptotic effects depending on which downstream proteins are activated or stabilised.[83,87,253] For additional details on the receptor functions during apoptosis, please refer to Annex C.

TRAIL R1 and TRAIL R2 are type II transmembrane proteins. TRAIL R1 and R2 are type II transmembrane proteins. Binding of TRAIL results in trimerization of R1 and R2, forming the DISC complex (death-inducing signalling complex), capable of FADD (Fas-associated protein death domain) recruitment and posterior activation of initiator caspases, such as caspase 8 (Figure 7.1), leading to caspase 3 activation.[254,255] The activation of both TRAIL receptors involve the enrolment of FADD, having functional redundancy upon binding of their respective ligands.[255] Their expression increases with stress and with the upregulation of transcriptional factor p53, sensitising cancer cells to apoptosis.[256] On the other hand, lack of TRAIL receptors render cells insensitive to extrinsic apoptosis.

Fas receptor activates upon binding of FasL (Fas Ligand), recruiting FADD and allowing the formation of the DISC together. FADD is therefore a key mediator for death receptor apoptosis, acting as a bridge between receptors being activated after ligand binding and recruitment of initiator caspases and other associated proteins (Figure 7.1 and Figure 7.7).[257,258]

FADD is also involved in the activation of TNFR1-mediated apoptosis. Binding of TNFα activates receptor trimerization and creation of a platform for recruitment of several proteins (Figure 7.7-A), forming complex I. Within this complex, TRADD can activate an anti-apoptotic program, but if RIPK1 is deubiquitinated, complex I shifts to complex II, recruiting FADD and leading to apoptosis activation.

After irradiation, the expression of all receptors and FADD lacks consistency to determine if the extrinsic apoptotic pathway has been activated (Figure 7.7 and Figure S.7. 2). TRAIL R1 experienced a 2-fold increase in expression compared to controls 6 hours after irradiation, for both cells with and without AuNR-PEG ($p \geq 0.05$). However, after 24 hours, expression rocketed with a 10-fold increase for cells with AuNR-PEG ($p < 0.0001$) and almost 5-fold increase in cells without AuNR-PEG ($p < 0.0394$). On the other hand, TRAIL R2 showed no change in expression in samples that experienced hyperthermia 6 hours after irradiation, but the next day, relative expression compared to controls reached a 5-fold increase ($p < 0.0003$). On the other hand, cells illuminated without AuNR, that did not suffer elevated temperatures, had close to a two-fold increase compared to controls, but this was not statistically significant.

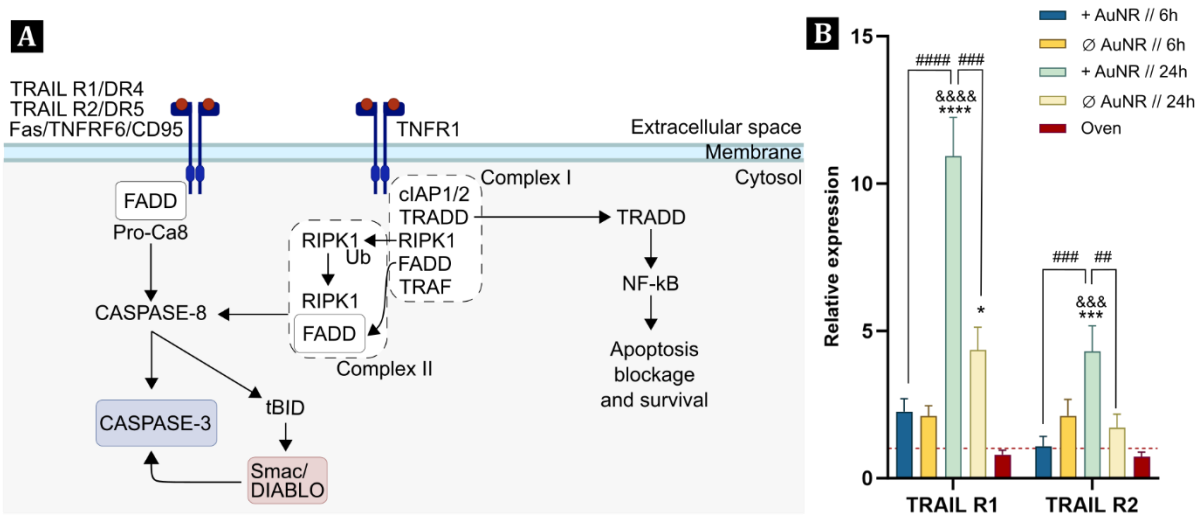

*Figure 7.7. Extrinsic apoptosis activation. A) Schematic representation illustrating the key steps involved in activation of extrinsic apoptosis. B) Graphs depicting the expression levels of TRAIL R1 and R2. Only statistically and clinically relevant differences are shown, with symbols denoting significance: * indicates significance vs control samples, & indicates significance vs oven samples, and # indicates significance vs other samples. *p<0.05, **p<0.01, ***p<0.001, ****p<0.0001*

For all other receptors, no relevant changes in their expression could be observed after PPTT, 6 and 24 hours after illumination, nor for cells experiencing hyperthermia through conventional heating in an oven (Figure S.7. 2). The lack of changes in the expression of Fas and FADD is surprising together with the excess of expression detected for TRAIL R1 and R2.

Upregulation of TRAIL R1 and R2 can induce apoptosis in renal cancer cells.[259] Moreover, hyperthermia promotes TRAIL-induced apoptotic death upon binding of their ligand.[260–262] The timely increase in expression of these two receptors after PPTT determines that hyperthermia can induce extrinsic activation of apoptosis. However, hyperthermia is known to activate TNF-induced apoptosis, but only decreases were observed for TNFR1.[260] All in all, the expression and activation kinetics of death receptors after PPTT can determine the cellular sensitivity to heat-induced cell death, and further research on this topic is of interest, as specific drugs targeting these receptors and associated proteins can be attractive for synergistic cancer therapies.

7.2.7. Hypoxia and oxidative stress: role in apoptosis

Hypoxia and oxidative stress are potential triggers of programmed cell death. Cellular life depends on the presence of oxygen, but lack of oxygen or excessive incidence of reactive oxygen species (ROS) can affect cellular mechanism and, in some instances, activate the apoptotic process.[62,83]

Different proteins are involved in maintaining correct cellular pathways and removing the products generated after the electron transport chain, such as ROS, superoxide anion, hydrogen peroxide and hydroxyl radicals. These cause oxidative stress and damage to cell components if not correctly neutralised.[62] The increase in expression of antioxidant systems can be an indicator of cells experiencing oxidative stress. Downregulation of these proteins can indicate that cells are becoming more vulnerable to oxidative stress and affecting the correct cellular metabolism.[263]

Hyperthermia and production of ROS are closely related. Many instances have been reported in which PDT (photodynamic therapy) and PPTT are combined to obtain synergistic anti-cancerous effects.[10,146,264] Heat stress induces ROS production, but the precise mechanism for how elevated temperatures produce ROS are still undetermined.[69]

7.2.7.1. HIF-1α

The hypoxia inducible factor 1 α-subunit (HIF-1α) is the oxygen-dependent subunit of the heterodimeric transcription factor, HIF-1, that allows cells to adapt to low oxygen levels.[265,266] In normal conditions, oxygen is used as a substrate to hydroxylate HIF-1α, tagging the protein to be recognised and

ubiquitinated, targeting it for proteasomal degradation. During hypoxia, HIF-1α hydroxylation is not possible, allowing the protein to accumulate since it is not ubiquitinated and degraded. The stabilisation of this factor allows it to translocate to the nucleus, joining its other subunits and generating a transcription factor that can promote target gene expression by binding onto the HRE elements (hypoxia response elements),[265] promoting the expression of pro-apoptotic genes.[267] The roles of HIF-1α after stabilisation during apoptosis are complex, with opposing accounts regarding its role as pro- or anti-apoptotic. Additional details on HIF-1α as an anti-apoptotic protein can be found in Annex C.

After PPTT-induced hyperthermia (Figure 7.8), the expression levels of HIF-1α were slightly reduced compared to controls. However, this reduction was not statistically different from the expression levels after irradiation without AuNR-PEG or the reduction observed in oven-cells. HIF-1α is regulated at the protein level, and during homeostasis, its mRNA expression remains stable and is ubiquitination which regulates its degradation. In hypoxia, levels would be expected to increase due to the lack of oxygen that allows hydroxilation and posterior ubiquitination. After these results, we can conclude that cells after PPTT have similar access to oxygen levels and no hypoxic conditions are triggering cell death, however, careful consideration must be taken, as HIF-1α can interact with wild-type p53, but not with mutant p53 found in some cellular types.[266]

7.2.7.2. HO-1 and HO-2

Oxygen levels are not the only responsible for oxygen-mediated apoptosis. Oxidative stress can induce the expression of antioxidant proteins to balance the metabolic state of the cell in favour of normal physiological activities. If pro-oxidative circumstances arise, a series of pathological processes can be triggered that can result in apoptosis.

To avoid this, heme oxigenase-2 (HO-2/HMOX2) is constitutively expressed in a wide variety of cells, contributing to heme metabolism and redox equilibrium.[268] On the other hand, heme oxygenase 1 (HO-1/HMOX1/HSP32) is stress inducible. Upon pro-oxidant stimuli detection, the cell upregulates its expression.[269–271] Encoded in gene HMOX1, a variety of signals can induce its expression, including HIF-1 stabilisation due to hypoxia.[272]

HO-1 provides multiple cytoprotective functions by its antioxidant and anti-apoptotic effects. It can remove hypoxia induced ROS as well as catalysing the breakdown of haem, a highly cytotoxic component that must be rapidly metabolised when in a free form. Heme catabolism by HO-1 produces three products: Carbon monoxide (CO), bilirubin and Fe^{2+}. CO and bilirubin have antioxidant and cytoprotective effects within the cell. Importantly, the metabolic state of the cell can indicate how it will react to CO, mostly producing pro-apoptotic effects in cancer cells, and anti-apoptotic effects on normal cells (Figure 7.1).[272] Absence of HO-1 produces higher levels of ROS, activated caspase 3 and 9 and induction of apoptosis.[269,270,272]

The results obtained from the human apoptotic array clearly show that expression of HO-1 is inducible in contrast to the constitutive expression of HO-2 (Figure 7.8), for which we observed non-significative changes in its expression. HO-1 experienced up to 3-fold increase in its relative expression compared to controls 6 hours after PPTT, expression slightly reduced after 24 hours ($p < 0.0361$). The increase in HO-1 on cells irradiated without AuNR-PEG suggests that the reaction of light with cells could be promoting the production of ROS and oxygen radicals, nonetheless, the differences between controls and samples without AuNR-PEG were not statistically significant.

7.2.7.3. Catalase

Catalase is an enzymatic scavenger that detoxifies the cell from ROS molecules. It catalyses hydrogen peroxide decomposition to water and oxygen.[66] Catalase is stored in peroxisomes (single membrane organelle) and in a similar manner to mitochondria, oxidative stress can induce pore formation in the peroxisome and release catalase to the cytosol. In contrast, to pore formation in mitochondria and the

release of apoptogenic factors, catalase release to the cytosol produces an anti-apoptotic effect, prompting its catalytic effects on oxidators and decanting the balance again towards cellular survival.[273]

After PPTT, catalase expression peaked 6 hours after irradiation in cells with AuNR-PEG and maintained its 2-fold increase compared to controls until 24 hours after illumination (Figure 7.8). However, due to the increased variability in the expression these increases were not statistically significant ($p \geq 0.05$). Nonetheless, the increase in expression together with the results of HO-1 indicate the presence of ROS in the cellular environment, activating its protection mechanisms against oxidative stress. Interestingly, no increase in expression after exposure to the laser light was observed for catalase, suggesting that catalase expression in triggered after hyperthermia (as also observed in oven-cells), but not with laser illumination.

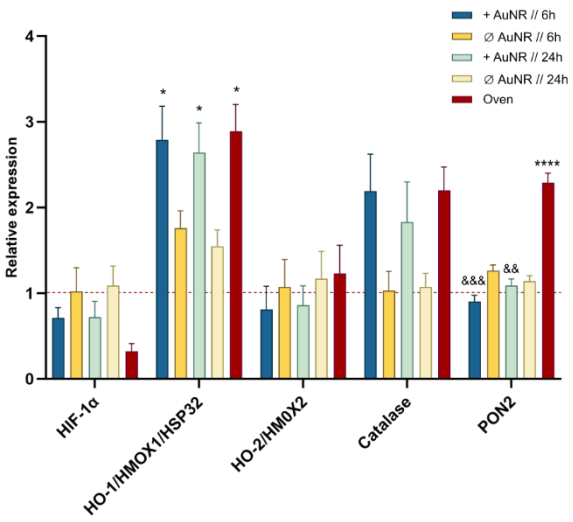

*Figure 7.8. Expression of oxygen-related proteins. Graphs depicting the expression levels of HIF-1α, HO-1 and HO-2, Catalase and PON2. Only statistically and clinically relevant differences are shown, with symbols denoting significance: * indicates significance vs control samples and & indicates significance vs oven samples. *p<0.05, **p<0.01, ***p<0.001, ****p<0.0001*

7.2.7.4. PON2

Human paraoxinase-2 (PON2) has two main activities inside the cell: lactonase activity and antioxidant. Its lactonase activity works as defence from pathogen infection, but its antioxidant activity reduces oxidative stress and inhibits apoptosis. In contrast to PON1, PON2 is exclusively expressed intracellularly, having no impact on the extrinsic apoptotic pathways. PON2 reduces intrinsic apoptosis by preventing cytochrome C release, caspase activation and superoxide formation. This influence on redox signalling and on the intrinsic pathways, promotes cell survival.[274–276]

Although it can reduce oxidative stress from the mitochondria, PON2 expression protects cells specifically from endoplasmic reticulum (ER)- induced apoptosis. We did not detect changes in cellular expression after PPTT, suggesting that we are not inducing ER-related apoptosis after PPTT (Figure 7.8).[276] Treatment at 43°C for one hour induced apoptosis through ROS production and ER-stress.[90] PON-2 expression had a 2-fold increase in oven-cells ($p < 0.0025$) indicating that conventional hyperthermia may impact more severely the ER than PPTT-induced hyperthermia.

7.2.8. Cell cycle and apoptosis

A cell that encounters a cellular stress may experience DNA damage, which activates the cellular checkpoint mechanisms. During checkpoints, the cell assesses DNA integrity and prepares for cellular division. G_1/S checkpoint allows the cell to duplicate their genetic content, whereas G_2/M checks the correct alignment of chromosomes before mitosis. During favourable conditions, cells continue their cycle and commit to cellular division. However, if damage is detected, the restriction points are activated and cell cycle may be restricted to the G_0 phase. If the damage poses a risk to the cell, the apoptotic process may be triggered to avoid the distribution of damaged DNA to daughter cells.[277]

Several proteins are protagonists during these checkpoints to assess the cellular condition. Their interaction with the DNA during each phase of the cell cycle dictates the cellular future. Many of these proteins are regulated not only by their active or passive role or their protein concentration, but controlled by their phosphorylation state. Post-translational modifications determine the functionality and tasks of the transcription factor during a stressful event. For further information on the role of cell cycle-related proteins, please refer to Annex C.

7.2.8.1. p21/CIP/CDKN1A

p21/CIP/CDKN1A (p21) is a tumour suppressor protein that inhibits cell cycle progression at the G_1/S checkpoint. Phosphorylated p53 is the main modulator of p21, it upregulates p21 expression and causes cell growth arrest by associating with cyclin and cyclin-dependent complexes (Cdk) to inhibit kinase activity, stopping the cell cycle at the G_1 phase (Figure 7.9-A).[277–279] Although p21 has growth arrest and apoptotic functions, it can also suppress apoptosis depending on the damage and cell type.

p21 is involved in DNA damage repair. Irradiation induces DNA breakage, which up-regulates p53 activity and overexpression of p21. This increase in expression after irradiation has the aim of arresting the cellular cycle to allow the cell machinery to repair the DNA.[279] Therefore, downregulation of p21 is an enhancer for irradiation-induced cytotoxicity and apoptosis.

After PPTT irradiation with AuNR-PEG, no changes in the expression levels of p21 were observed. On the other hand, cells irradiated without AuNR-PEG saw a moderate increase in the expression of p21. None of these changes were statistically significant ($p \geq 0.05$) (Figure 10B), however it suggests that light irradiance may be causing some potential DNA damage and p21 is being upregulated to stop the cell cycle and allow time for the cell to recover. The lack of change after PPTT-induced hyperthermia, even if they are irradiated with the same laser conditions, can be due to the masking effect that the increase of temperature has on other proteins, supporting the trigger of other molecular pathways.

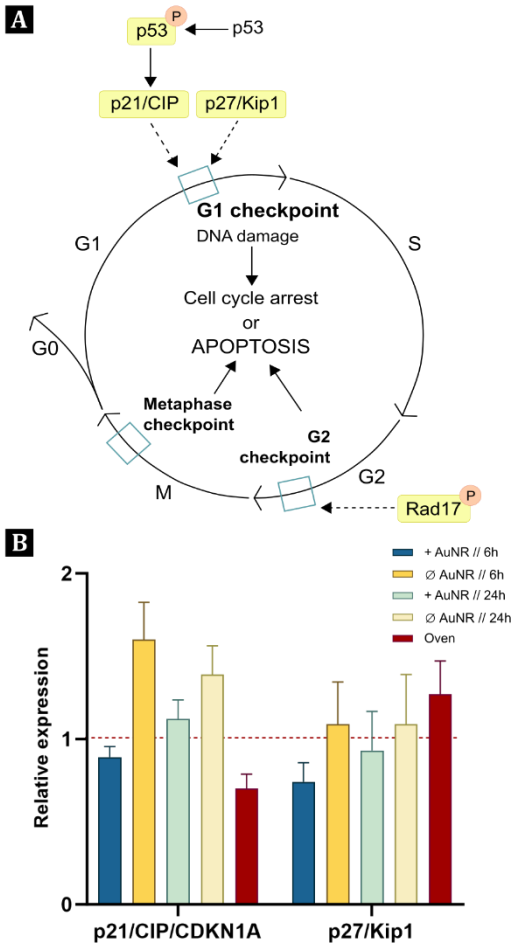

Figure 7.9. Cell cycle checkpoints and protein expression levels. A) Schematic representation illustrating the interaction of the key checkpoints of the cell cycle and the studied proteins. The dotted line represents an indirect effect on the checkpoints. B) Graphs depicting the expression levels of p21 and p27. No statistically or clinically relevant differences were obtained.

7.2.8.2. p27/Kip1

p27 has proliferation-inhibition functions, similar to p21, by interaction with cyclin-dependent kinase (Cdk) inhibitors.[280,281] Its main target is Cdk2, restricting the G_1 checkpoint during cell cycle progression. Overexpression of p27 induces growth arrest and apoptosis, but their relationship is still unclear,[282] as excessive p27 presence can also protect the cell from apoptosis.[281] The significance of p27 in apoptosis remains uncertain depending on the cell type and their origin (tumoral or healthy).[277]

For 786-0 cells, induction of p27 expression resulted in proliferation inhibition and apoptotic stimulation.[283] After PPTT irradiation in cells with and without nanoparticles, and in oven-cells, no significant changes in p27 expression was observed for any time point ($p \geq 0.05$) (Figure 7.9).

7.2.8.3. Phospho-p53

The p53 tumour suppressor protein and its gene, TP53, are among the most studied components in cancer biology due to their high mutation rate in most human cancers.[284] Regulation of p53 is mainly performed by ubiquitin ligase Mdm2, targeting p53 for proteasomal degradation in normal homeostatic conditions.[284–287] Non-mutated phosphorylated p53 (pp53) avoids Mdm2 and increases its half-life and

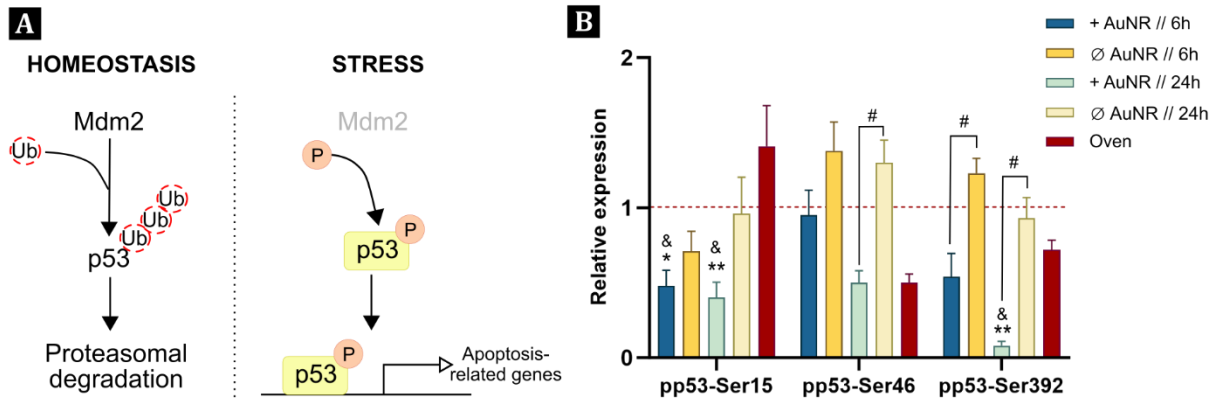

*Figure 7.10. p53 activation by phosphorylation in apoptosis. A) Scheme illustrating the different states of p53. During homeostasis, Mdm2 ubiquitinates p53, tagging it for proteasomal degradation. However, under stress, Mdm2 cannot ubiquitinate p53, allowing its phosphorylation and stabilisation to induce the transcription of apoptotic related genes. B) Graph depicting the expression levels of phosphorylated p53 at Ser15, Ser46 and Ser392. Only statistically and clinically relevant differences are shown, with symbols denoting significance: * indicates significance vs control samples,, & indicates significance vs oven samples, and # indicates significance vs other samples. *p<0.05, **p<0.01, ***p<0.001, ****p<0.0001*

acting as a transcriptional factor in the nucleus (Figure 7.10-A), activating pro-apoptotic genes and inhibiting cellular proliferation.[284–287] However, phosphorylation of p53 at different sites modulates their interactions with the cell cycle and apoptosis. Phosphorylation at Ser15 (pp53-Ser15) avoids Mdm2 ubiquitination and stabilises p53 expression,[286] whereas phosphorylation at Ser392 (pp53-S392) impacts the growth suppression function of p53, its DNA binding affinity, and its transcriptional activation.[288] More importantly, pp53-Ser46 dictates the ability of p53 to activate apoptosis.[286,289]

PPTT and laser irradiation significantly impacted the phosphorylation patterns of p53. For Ser15, phosphorylation was halved for cells irradiated with AuNR-PEG at both, 6 and 24 hours after irradiation ($p < 0.0134$), whereas cells only illuminated showed a slight decrease in Ser15 phosphorylation after 6 hours ($p \geq 0.05$) (Figure 7.10). Oven-hyperthermic samples experienced an increase in expression that was only statistically different from PPTT + AuNR-PEG cells ($p = 0.0345$). The differences between both PPTT-irradiated samples, and conventional hyperthermia suggests that the effects of heat, light+heat and light alone differently activate the kinases responsible for Ser15 phosphorylation. However, the different timepoints studied in oven and PPTT-cells must be considered during analysis. All in all, PPTT-induced hyperthermia does not avoid p53 ubiquitination by Ser15 phosphorilation.

Phosphorylation at Ser46 differs between cells irradiated with and without nanoparticles. Cells without AuNR-PEG increased pp53-Ser46 expression 6 and 24 hours after irradiation, but these were not statistically significant compared to controls ($p \geq 0.05$) (Figure 7.10). This increase improves the chances of cells to activate apoptosis if the apoptotic signal is strong enough. On the other hand, phosphorylation in cells irradiated with AuNR-PEG was only affected 24 hours after treatment. This decrease in phosphorylation was statistically significant compared to samples irradiates with nanoparticles ($p < 0.019$) but not to controls. Cells heated in the oven also experienced a decrease in expression, but this was immediately after heating, but this was not statistically different compared to controls ($p \geq 0.05$). All in all, these are indicators that apoptosis after hyperthermia is not being activated through p53-Ser46 phosphorylation.

Regarding Ser392 phosphorylation, its levels were maintained in cells irradiated without nanoparticles, but drastically lowered in cells illuminated with AuNR-PEG 24 hours after irradiation ($p < 0.0038$) (Figure 7.10). This indicates that after PPTT-induced hyperthermia, kinase activity in 786-0 is greatly reduced. Oven-cells did not have significant changes in expression of pp53-Ser392 after hyperthermia ($p \geq 0.05$).

Nonetheless, in clear cell renal carcinoma, of which 786-0 cell line is an *in vitro* model, p53 can be functionally inhibited, meaning that phosphorylation of p53 and its overexpression may be incapable of activating apoptosis.[290]

7.2.8.4. Phospho-Rad17

Rad17 is a cell cycle checkpoint protein required for cell cycle arrest and DNA damage repair at the G_1/S checkpoint. At this transition, phosphorylated Rad17 can interact with claspin and regulates its phosphorylation by Cdk1. Ionising radiation (IR), ultraviolet light (UV), DNA damage and disruption of the replication fork activates phosphorylation at Ser635, enhancing its interaction with other proteins, among them, claspin. Rad17 phosphorylation is essential for its function and is necessary to activate the G2/M arrest, via Chk1 (Figure 7.9 and Figure 7.11).[291,292]

Cells irradiated without AuNR-PEG experienced an increase in the phosphorylation of Rad17, with a 2-fold increase after 24 hours of illumination (Figure 7.11). However, these changes were not statistically significant ($p \geq 0.05$) as control samples had high variability on their phosphorylation levels. Nonetheless, these results suggest that NIR laser light can activate phosphorylation at Ser635, like it has been shown for IR and UV light. The lack of change in irradiated samples with AuNR-PEG or in oven-cells can be a secondary effect of temperature increase, in which kinases responsible for its phosphorylation have been downregulated.

7.2.8.5. Claspin

Claspin is a checkpoint protein deeply involved in apoptosis and cellular response to replication stress and DNA damage. It is a tightly regulated protein, having high instability because its constant ubiquitination, displaying various levels of expression throughout the cell cycle. When replication stress is detected, claspin binds to the DNA and is phosphorylated, acting as an adaptor protein that passes the replication stress signal to Chk1 to facilitate a checkpoint arrest.[293,294] If apoptosis has been triggered, claspin can be cleaved by Caspase-7, influencing the decision between cell cycle arrest and apoptosis.[295] An unphosphorylated claspin cannot activate the checkpoint arrest and cells will undergo apoptosis (Figure 7.11-B).[295,296]

Six hours after PPTT, neither sample irradiated with or without nanoparticles experienced any change in claspin expression compared to controls ($p \geq 0.05$) (Figure 7.11). However, 24 hours after illumination, both samples experienced an increase in claspin expression, with a 2-fold increase compared to controls in PPTT-induced hyperthermia ($p < 0.0125$). This increase in claspin 24 hours after hyperthermia can be the result of the time requirements for claspin activation after genotoxic damage, however, claspin concentration is regulated at the mRNA and protein levels.[294] Nonetheless,

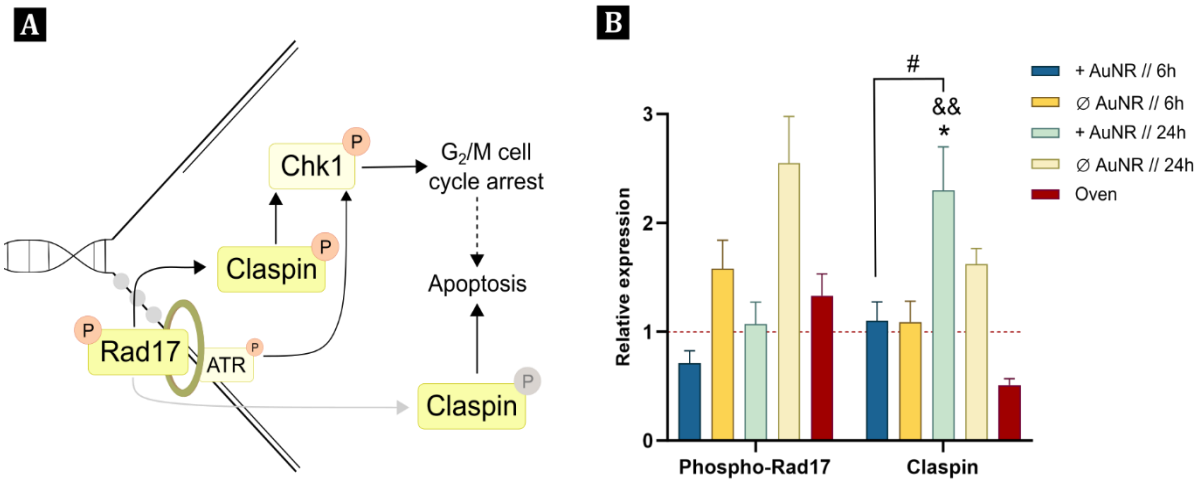

*Figure 7.11. Replication fork under stress. A) Schematic illustration depicting the proteins studied involved in resolving replication stress. Phosphorylated Rad17 aids in phosphorylating Claspin, which via Chk1 induced cell cycle arrest. If claspin is not correctly phosphorylated (grey line), upon replication stress the cell may induce apoptosis. At the same time, an unresolved G_2/M transition can develop into apoptosis (dotted line). B) Graph depicting the expression levels of phosphorylated Rad17 and claspin. Only statistically and clinically relevant differences are shown, with symbols denoting significance: * indicates significance vs control samples, & indicates significance vs oven samples, and # indicates significance vs other samples. *p<0.05, **p<0.01, ***p<0.001, ****p<0.0001*

the phosphorylation of Rad17, known to activate claspin, does not impact the expression of claspin after PPTT.

7.3. Discussion

The interplay between conventional hyperthermia and cellular death has been extensively documented, particularly concerning the activation of programmed cell death pathways. The most important directors of apoptosis (Caspases, Hsps, and cytochrome C release) are well studied on their effect on the activation of apoptosis. Understanding how these, and other apoptotic-related proteins, are influenced by PPTT-induced hyperthermia, can shed light on the potential applications of heat-based treatments, especially for cancer treatment.

Programmed cell death is a desired outcome after PPTT induction, with lower immunogenic and inflammatory responses compared to necrosis. However, the intensity of the hyperthermic stimulus is crucial in determining the cellular response. Mild temperature increases activate apoptosis, but the specific temperature at which this occurs is highly cell dependent.[35,81,90,297,298] On the other hand, most cells share a similar temperature threshold in which they overpass the apoptotic molecular pathway and activate necrosis.[298] This poses a more significant threat on *in vivo* situations, as an inflammatory response could be triggered.

Timing on the application of PPTT and its analysis are also key factors for the outcome of the therapy. Apoptosis is a dynamic and temporally regulated death process, wherein cellular events unfold in a sequential manner, encompassing initiation, execution, and resolution phases. This temporal aspect underscores the importance of studying the events occurring after PPTT at more than one timepoint. By doing this, it is possible to observe the activation or inhibition of certain molecular pathways, being able to time them to second doses of PPTT and multimodal therapeutic strategies combining heat with chemotherapy and radiotherapy to enhance their pro-apoptotic effect.

Additionally, monitoring the molecular mechanisms activated after PPTT can determine the induction of thermotolerance after an hyperthermic event. Understanding the fundamental mechanisms of thermotolerance and their relationship to drug resistance can inform of the development of tailored therapeutic approaches to overcome this problem.

Thermotolerance is often associated with the presence of Hsps.[91] Temperature elevation increases the expression of Hsp27 and 70,[223] and their downregulation is often induced to enhance the effectiveness of heat-based anti-cancer therapies.[35,98] Downregulation of Hsp70 is associated with a cytotoxic effect on tumour cells, but not on healthy cells, underscoring the role of Hsps in cancer therapies.[98] The role of Hsps in thermotolerance is often associated with sub-lethal heat stress during treatment. Further studies, particularly involving reapplication of hyperthermia in various doses, should investigate the correlation between Hsp expression and other anti-apoptotic protein levels and therapeutical outcomes.

The connection between Hsp expression and hyperthermia also extends on their interaction with p53. Some studies provide evidence of Hsp70 and mutant versions of p53 having higher affinity to each other than to wild type p53 (wt-p53). Hsp70 interaction with mutant versions of p53, often found in cancer cells, provides more thermal resistance and reduction of apoptosis than on healthy cells presenting wt-p53.[7] Although these findings are highly discussed, our results detect increases in Hsp70 are accompanied by decreases in p53 phosphorilation, suggesting that on cancerous kidney cell line 786-0, the interaction between Hsp70 and p53 post-hyperthermia may be a plausible method for the cell to try escape apoptotic cell death.

At the same time, Hsp27 expression can block cytochrome C from effectively joining the apoptosome, preventing apoptotic cell death.[96,222] After PPTT, Hsp27 levels were not altered 6 and 24 hours after illumination, but cytochrome C levels were also not significantly increased. However, on oven-cells, Hsp27 expression was highly induced, probably as a way to try to block the increased release of cytochrome C (2-fold increase compared to controls) in 786-0 cells after the thermal event. The

differences between both types of hyperthermia can be due to the distinct modalities in which heat is applied (nanoscopic vs macroscopic), or to the different timepoint at which they were analysed.

Interestingly, the expression of anti-apoptotic proteins that actuate after the release of pro-apoptotic proteins from the mitochondria were mostly downregulated 6 and 24 hours after PPTT. c-IAP and XIAP lowered their expression after hyperthermia (non-significant changes). These proteins are blocked by pro-apoptotic Smac/Diablo and Htra2/Omi proteins (Figure 7.12). If the expression of these pro-apoptotic proteins was increased, we would expect a decrease in IAPs. However, we also detected a decrease in Smac/Diablo and Htra2/Omi highlighting the complexity of understanding the apoptotic cellular pathway after PPTT. Oven-cells, on the other hand, experienced increases in the expression of both pro- and anti-apoptotic proteins (Figure 7.13), underscoring the belief that the trigger of the apoptotic pathway can resolve into its activation or inhibition.[7,83]

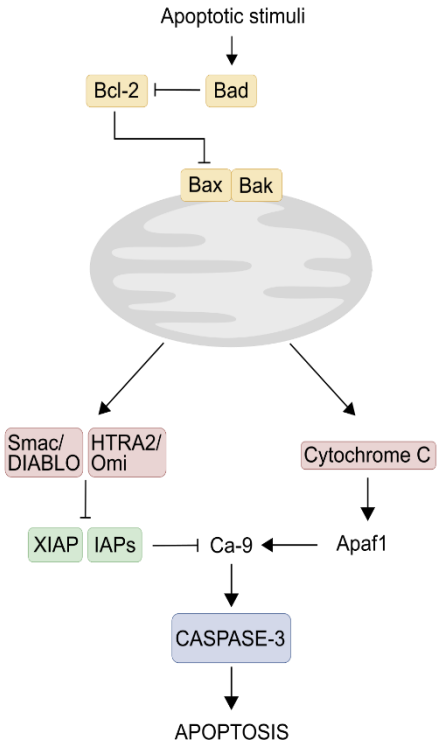

Figure 7.12. Diagram illustrating the main pathway of intrinsic apoptosis. Highlighted are the studied proteins and their interplay.

The effects of hyperthermia on the tumour microenvironment also require further investigation, as the effects they have may be detrimental or beneficial for resolving an anti-cancerous treatment. The production of ROS, cytokines, chemokines or damage-associated molecular patters by cells irradiated or that have experienced elevated temperatures may be transmitted to neighbouring cells and the tumoral microenvironment.[77,79,83,265,299]

The induction of ROS production seems to occur both with PPTT and hyperthermia treatments, regardless of the observation period. This is supported by the upregulation of antioxidant proteins such as HO-1, Catalase, or PON2, suggesting an attempt to mitigate ROS levels in response to the treatment effect (Figure 7.13). Excess levels of ROS can damage proteins, DNA production and membrane integrity[66] after an hyperthermic event. Hypoxia, on the other hand, does not seem to be a problem after PPTT, as HIF-1α expression is not triggered after treatment. Hypoxic cells, as well as those with acidic pH or deficient nutrient supply are more thermosensitive to heat-based therapies.[7]

Cytokine expression can also be elevated or decreased under heat stress, and exosome production is higher after mild hyperthermia, being capable of transporting Hsp70 and inducing an immunogenic response in other cancer cells. [77,79,265,299] Understanding ROS production and cellular communication after PPTT-induced hyperthermia is important to determine if an inflammatory or immune response will be triggered after treatment, as well as to recognise their contribution to apoptotic signalling cascades.

PPTT-hyperthermia can cause detrimental effects on the DNA due to the combination of elevated temperatures and NIR-irradiation. This can cause DNA strand breakages and ceasing of the cellular division machinery. Hyperthermia by itself can cause the inhibition of DNA synthesis and introduction of the cell to a senescent state,[7] in which cells halt their metabolic processes to recover from protein denaturation and DNA damage, without risking apoptosis. Senescence, like apoptosis, is closely related to mitochondrial protein leakage, ROS production and release of extracellular DAMPs [300] so it would be really interesting to observe what occurs in quiescent cells after PPTT-induced hyperthermia.

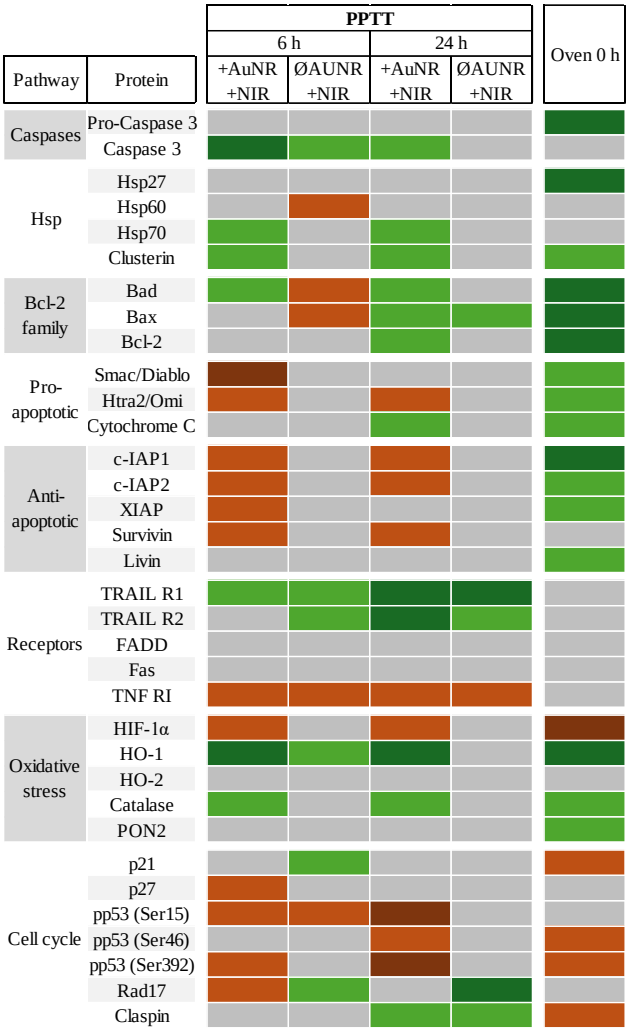

Figure 7.13. Expression of apoptotic proteins. Summary of all studied proteins in a heatmap-like view of results presented in Figures 7.2 to 7.11. Colours represent relative expression compared to controls. Dark green: ≥2.5; Light green:1.5 to 2.5; Grey: 0.75 to 1, Orange: 0.4 to 0.75, Dark orange: ≤0.4.

Briefly, although the interaction between hyperthermia and apoptosis is much more complex than what we can describe here, we can conclude that after PPTT-induced hyperthermia we are favouring the activation of apoptotic mechanisms, as well as of proteins that try to protect the cells from programmed cell death. These dual complex molecular mechanisms observed can be because of some cells experiencing a complete apoptotic death process, passing through the initiator, executor, and resolution phases, whereas other cells may be receiving sub-lethal signalling, where the apoptotic stimulus received fails to reach the necessary threshold. Nonetheless, the observation of differential expression of pro- and anti-apoptotic proteins between different timepoints and methods of hyperthermia application can facilitate the development of more effective hyperthermia-based therapies – either alone or in synergy with other anti-cancer treatments- and improve the patient's outcomes.

8

Cytokine expression after plasmonic photothermal therapy

8.1. Introduction

Cytokines are small extracellular proteins that facilitate cell-cell communication by binding to specific receptors on cellular membranes. Produced by various cell types, cytokines act as local mediators playing important roles in immune response regulation and maintaining homeostasis.[74]

The study of cytokines expression after plasmonic photothermal therapy (PPTT) is of particular interest due to the widespread presence of cytokine producing cells throughout the body. T cells, for example, coordinate the immune system against pathogens and tumours, as well as helping maintaining the body homeostasis when faced with an instability.[301]

T cells are distributed across most tissues, including lymphoid and mucosal tissues (e.g. lungs and intestines), but also blood and the tumour microenvironment.[301] The Jurkat cell line, derived from leukemic immune T cells, serves as a valuable model to study intracellular signalling, T cell activation and cytokine production, making it ideal for immunotherapy testing.[302,303]

The induction of key inflammatory cytokines following PPTT-induced hyperthermia is intriguing to understand the potential of inducing pro-inflammatory effects after treatment. Additionally, obtaining insight into nanoparticles contributing to produce inflammatory signals through cytokine production is essential for the development of nanoparticle-based therapies, given the significant role of cytokines in health and disease.[304] Understanding the activation of cytokine expression can advance multimodal cancer treatments combining immunotherapy, nanomedicine and hyperthermia.[305]

Fever and hyperthermia can induce increased cytokine production in Jurkat cells,[306] with thermal stress increasing the expression of pro-inflammarory proteins such as IL-1β, IL-2, IL-6, IL-8, TNFα and IFN-γ, both *in vitro* and *in vivo*.[11,306–308] Although these observations, the impact of PPTT on cytokine expression still remains poorly understood.

Examining cytokine expression after PPTT is important as it can impact neighbouring cells and affect the tumour microenvironment.[309,310] By focusing on the production of cytokines by Jurkat cells we aim at determining if an inflammatory response may be triggered post-PPTT.

Before assessing the cytokine production of Jurkat cells following PPTT irradiation, the cytotoxicity of gold nanorods (AuNR-PEG), as well as the viability after NIR irradiation, was evaluated. This assessment was crucial to ensure that AuNR-PEG were not toxic on Jurkat cells and to test the efficacy of our experimental setup on this suspension cell line. This preliminary evaluation is necessary to integrate all results with the subsequent analyses.

8.2. Results

8.2.1. Plasmonic photothermal therapy on Jurkat cells

To evaluate the effectiveness of PPTT in Jurkat cells, the cytotoxicity of AuNR-PEG was initially assessed to determine the appropriate nanoparticle concentration for this cell type. Thiazolyl blue tetrazolium bromide (MTT) was used to evaluate nanomaterial toxicity and compare it with previously tested cell types.

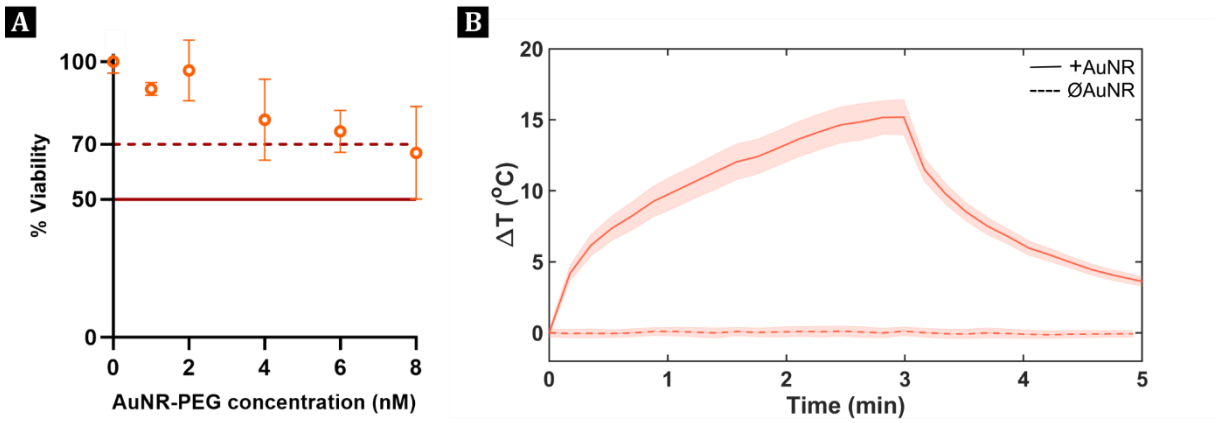

Figure 8.1. Cytotoxicity of AuNR-PEG and temperature dynamics after PPTT on Jurkat cells. A) Effect of AuNR-PEG concentration on cellular viability. Viability shown as percent of controls (0 nM). Error bars represent SEM (n=4). B) Temperature dynamics in + AuNR-PEG and Ø AuNR-PEG during irradiation for 3 minutes with an 808 nm laser light at 3 W/cm². Continuous line indicates cells with AuNR-PEG (+) and dotted line without AuNR-PEG (Ø). Shaded line represents the SEM. n=7.

Results demonstrated minimal cytotoxicity in Jurkat cells even at the higher concentration of AuNR-PEG tested, with a viability of 66.8% ± 16.8 at 8 nM (Figure 8.1-A). Jurkat cells had high compatibility with the nanoparticle type, estimating an IC_{50} of 17 nM. These findings highlight the resilience of immune T cells to high nanoparticle concentrations, compared to cancerous and healthy cells.

At the concentration used for PPTT and cytokine expression experiments, 2 nM, Jurkat cell viability exceeded 95 % (Figure 8.1-A). No statistically significant changes were observed between the studied concentrations and control samples (0 nM) ($p \geq 0.05$), indicating that any difference observed during the illumination of Jurkat cells with AuNR-PEG is attributable to the combined presence of light and nanoparticles, inducing elevated temperatures.

Temperature profile after irradiation of Jurkat cells with a fixed power density (3 W/cm^2) and time of irradiation (3 minutes) are shown in Figure 8.1-B. The temperature increase exhibited a similar profile to that observed in cells studied in Section 6, with a rapid rise immediately upon laser irradiation, followed by a steady increase after the first seconds. Temperature declined rapidly to initial temperatures post-irradiation.

The mean maximum temperature reached 49.8°C, with a mean temperature increase of 14.9°C. While this increase was not statistically different compared to adherent cancer cell lines (786-0, A549, HepG2) ($p \geq 0.05$), it was statistically higher compared to healthy cell lines (Hek293, NL20 and THLE-3) ($p < 0.007$).

This indicated the robust capacity of Jurkat cells to effectively incorporate AuNR-PEG, with low toxicity associated, and high light-to-heat conversion. The increase of temperature led to reduced viability, assessed at two different timepoints (0 and 24 hours after irradiation) using the MTT assay and trypan blue (TB) staining.

For the MTT assay, Jurkat cells not illuminated and without AuNR-PEG were used as controls (CTL). Cells irradiated without AuNR-PEG (dark grey) and with AuNR-PEG (light grey) showed decreased viability compared to controls immediately after treatment (Figure 8.2-A, $p < 0.0032$). This rapid viability declines in both irradiated cell lines suggested that the employed laser settings impaired mitochondrial function immediately after treatment. The absence of statistically significant differences between both conditions ($p \geq 0.05$) suggests that temperature had no effect on this initial decrease in viability.

In contrast, 24 hours after irradiation, cells irradiated without AuNR-PEG showed a recovery of mitochondrial activity compared to immediately after treatment ($p < 0.0091$). The increase in viability post-irradiation suggests that the toxic effect of NIR irradiation on Jurkat cells was temporary, allowing cells to recover their metabolic activity after 24 hours. On the other hand, cells irradiated with AuNR-PEG and that experiences temperatures over 49°C further decreased their viability 24 hours post-illumination ($p < 0.0036$) (Figure 8.2-A), indicating that Jurkat cells treated with hyperthermia were unable to recover their mitochondrial activity.

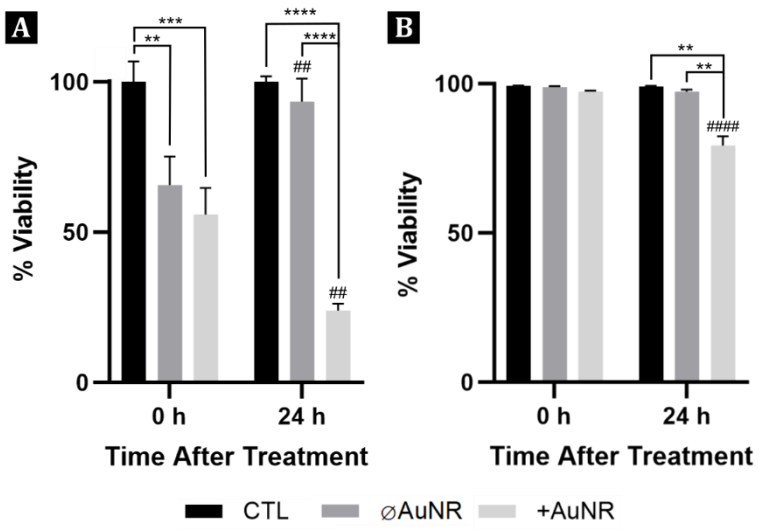

*Figure 8.2. Cellular viability (%) immediately and after 24 hours of treatment for controls (CTL) and cells irradiated without (ØAuNR-PEG) and with AuNR-PEG (+AUNR-PEG). A) Viability measured with the MTT assay. B) Viability measured with the trypan blue assay. Statistical significance is denoted by symbols: * indicates significance between conditions (same timepoint), # indicates significance vs 0 hours (same condition). *p ≤ 0.05; **p ≤ 0.01; ***p ≤ 0.001, ****p < 0.0001. n=7.*

The evaluation of membrane integrity post-irradiation on Jurkat cells with TB staining revealed that cell membrane was not compromised immediately after treatment for any of the studied conditions ($p \geq 0.05$) (Figure 8.2-B). After 24 hours, the cellular membrane of cells irradiated with AuNR-PEG showed some impairment compared to controls and cells without AuNR-PEG ($p < 0.01$) and to immediately post-irradiation ($p < 0.0001$).

The decrease in viability observed with the MTT assay, as opposed to the stable viability observed with the TB assay, suggests that PPTT predominantly induced apoptotic cell death (characterised by loss of mitochondrial activity), rather than necrosis (marked by membrane integrity impairment) in Jurkat cells. This is consistent with the findings observed in adherent cell lines, both cancerous and healthy. Moreover, our results indicated that under the laser conditions used, PPTT temporarily affected mitochondrial function, but it is recovered after 24 hours, whilst membrane integrity is not affected in cells without AuNR-PEG. This aligns with the use of a low power and exposure time to exclusively induce apoptotic cell death on cells containing plasmonic nanoparticles.

8.2.2. Cytokine expression after PPTT

To determine if PPTT stimulated cytokine expression in human immune Jurkat cells, enzyme-linked immunosorbent assays (ELISA) were performed for interleukin-1β (IL-1), IL-2, IL-6 and tumour necrosis factor α (TNFα). These cytokines were selected based on their known pro-inflammatory functions and documented elevated expression in serum from murine models after PPTT-induced hyperthermia.[11,307]

The decision to evaluate cytokine expression in Jurkat cells over a 6 hours period was informed by hyperthermia studies effect on cytokine expression performed by Israelsson *et al*.[308] and Oh *et al*.[311] The group of Israelsson *et al*. investigated cytokine expression following conventional hyperthermia (incubation at 42°C for 1 hour) and monitored viability and cytokine concentration at various intervals between 6 and 24 hours after hyperthermia in Jurkat cell lines.[308] Similarly, Oh *et al*. studied cytokine production after chemical stimulation during a time period of 2 hours in a multiplexed microchip.[311]

After PPTT, supernatants from irradiated Jurkat cells, with and without AuNR-PEG, were collected at multiple timepoints (30 minutes, 60 minutes, 90 minutes, 2 hours, 3 hours, 4 hours and 6 hours). The

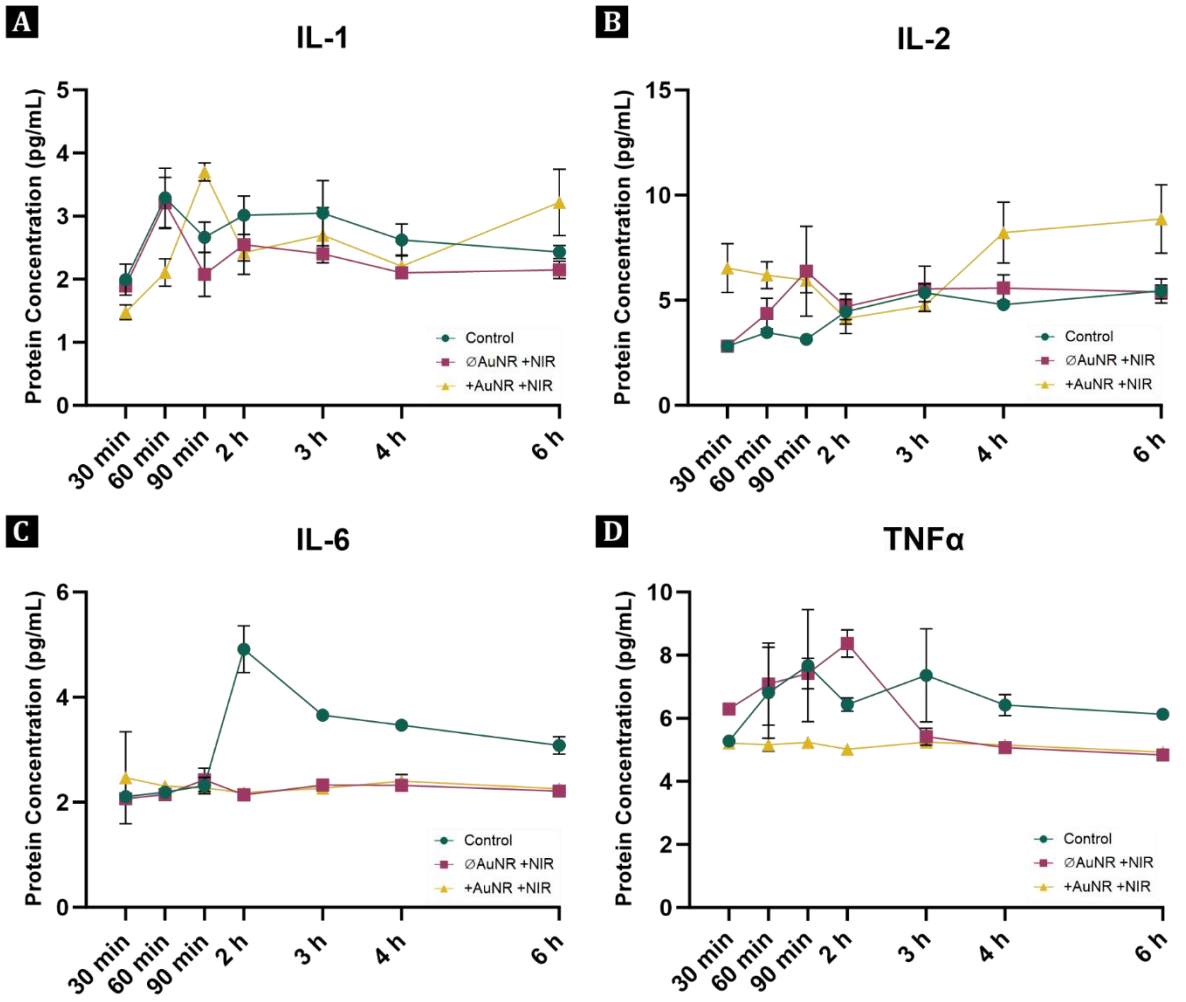

Figure 8.3. Cytokine expression (pg/mL) in + AuNR-PEG and Ø AuNR-PEG cells as a function of time. Concentration of cytokines A) IL-1, B) IL-2, C) IL-6 and D) TNFα studied at several timepoints for cells irradiated 3 minutes with a 808 nm laser at 3 W/cm2, with AuNR-PEG (+AuNR+NIR) and without (ØAuNR+NIR). n=3, error bars represent the SEM.

results, shown in Figure 8.3 revealed significant variations on the concentration of each evaluated cytokine across the duration of the experiment.

For IL-1, a similar expression pattern was observed for control cells (cells without AuNR-PEG and not irradiated) and cells irradiated without AuNR-PEG (Ø AuNR-PEG). A peak of expression was observed for both conditions 60 minutes after treatment, with statistically higher concentrations compared to cells irradiated with AuNR-PEG (+AuNR-PEG) that experienced hyperthermia ($p < 0.035$) (Figure 8.3-A and Table 8.1). However, 90 minutes after PPTT, the concentration of IL-1 in cells subjected to PPTT-induced hyperthermia was statistically higher than cell irradiated without AuNR-PEG ($p < 0.0013$), but not compared to controls ($p \geq 0.05$). The erratic variability in IL-1 concentration post-PPTT in Jurkat cells suggests that there is no differential induction of this interleukin following PPTT-induced hyperthermia or NIR laser irradiation, compared to controls.

The expression of IL-2 in +AuNR-PEG samples displayed an alternating pattern post-PPTT. Immediately after irradiation, the concentration of IL-2 was higher than in control samples or samples illuminated without AuNR-PEG ($p < 0.011$). However, this difference was offset after 2 hours, where IL-2 expression was the same for all conditions ($p \geq 0.05$). At 4 hours post-PPTT, IL-2 concentration increased again and at the last studied timepoint it was higher for cells having experienced hyperthermia than for controls or samples only irradiated ($p < 0.0201$) (Figure 8.3-B and Table 8.1).

Following PPTT, the expression of IL-6 remained unchanged for all irradiated samples, with and without nanoparticles, across all evaluated timepoints (Figure 8.3-C). Only 30 minutes post-illumination,

samples containing AuNR-PEG showed an increased variability in IL-6 concentration, indicated by the standard deviation of the mean. On the other hand, control samples expressed a rapid increase in IL-6 expression between the 90 minutes at 2 hours timepoints ($p < 0.0001$, Table S 1-Annex D). It is important to note that control samples are manipulated as the other conditions but lacked the irradiation treatment or AuNR-PEG incubation. This shows that cellular manipulation at the *in vitro* level can evoke stress responses in Jurkat cells that trigger cytokine expression. This emphasises the importance of using appropriate controls during *in vitro* experimentation.

Similarly, the expression of TNFα after PPTT-induced hyperthermia is also unchanged for the duration of the experiment (Figure 8.3-D). However, in control samples and cells irradiated without AuNR-PEG, TNFα expression steadily increased for the first 90 minutes to 2 hours, stabilising after that for control conditions, and reducing for samples without nanoparticles. The variability exhibited in control samples underscores the stress of cellular manipulation, whereas illuminated conditions expressed more consistent concentrations.

For all studied cytokines we observed unpredictable wavering patterns on the concentrations. However, around the 90 minutes to 2 hours mark, changes in concentration, either up- or downregulating expression, were observed for all cytokines. At these timepoints it was possible to observe the biggest differences in concentration between the studied conditions and compared to other timepoints (Table 8.1and Table S 1-Annex D). This suggested that following cellular manipulation and treatment, cells undergo an adaptation period during which expression patterns may be affected and show erratic variability. Furthermore, the lack of evident differences in cytokine expression between samples experiencing PPTT-induced hyperthermia, irradiated cells and control samples stops us from confirming a clear expression pattern of cytokines after treatment.

			IL-1			**IL-2**			
			60	90	360	30	90	240	360
CTL	vs	ØAuNR	ns	ns	ns	ns	0.0294*	ns	ns
CTL	vs	+AuNR	0.0220*	ns	ns	0.011*	ns	0.0201*	0.0201*
+AuNR	vs	ØAuNR	0.0350*	0.0013**	0.0428*	0.011*	ns	ns	0.0183*

			IL-6				**TNFα**	
			120	180	240	360	90	120
CTL	vs	ØAuNR	<0.0001****	0.0006***	0.0032**	0.0293*	ns	ns
CTL	vs	+AuNR	<0.0001****	0.0003***	0.0063**	0.0414*	0.0431*	ns
+AuNR	vs	ØAuNR	ns	ns	ns	ns	ns	0.0037**

Table 8.1. Statistical analysis results after PPTT at significant timepoints. These tables present the results of the statistical analysis comparing different conditions (controls, samples irradiated with AuNR-PEG and irradiated without AuNR-PEG) at various timepoints. Only statistically significant differences are shown, highlighting timepoints where differences were observed for any of the studied conditions. The corresponding graphs and detailed data can be found in Figure 4.

8.3. Discussion

Jurkat cells serve as an excellent model to study T cell activation and cellular signalling.[302] Following cellular stress whether chemical or physical, these cells can regulate the expression of certain cytokines to initiate an inflammatory response and communicate with neighbouring cells.

After an hyperthermic stress, changes in IL-1, IL-2, IL-6 and TNFα concentration were observed.[11,307,308] The studies by Bear *et al*.[307] and Morales[11] found increased expression of the studied cytokines 24 hours after performing PTT in murine *in vivo* models. Both studies employed similar testing parameters as we used to evaluate cytokine production: Bear *et al*. employed the same laser power density and time of irradiation than us (3 W/cm^2, 3 minutes, spot diameter=8 mm, temperatures not specified) to externally

illuminate the tumour, whereas Morales laser settings induced temperatures over 60°C after 5 minutes of irradiation with the same nanoparticles we employed (3 W/cm^2, 5 minutes, spot diameter=12 mm).

These observations, together with the increase in mRNA expression of cytokine proteins detected by Israelsson *et al*. in OVCAR-3, SKOV-3 (ovarian cancer cell lines) and Jurkat cell line after thermal stress (incubation at 42°C for 1 hour), led us to study *in vitro* cytokine production in Jurkat cells after PPTT-induced hyperthermia.

Understanding cytokine production after PPTT is crucial not only for the development of combined synergistic techniques, such as PPTT with immunotherapy, but also for comprehensively assessing the inflammatory response and potential systemic effects of the therapy.

Overall, expression levels of cytokines are notably low, typically in the range of picograms per millilitre (pg/mL). Non-stimulated T cells have a mean cytokine expression of 27±22 pg/mL for IL-2, 49±56 pg/mL for IL-6 and 15±18 for TNFα.[312] These values show the low concentration and considerable degree of variability in cytokine expression for T cell concentrations of 1000 cells/µL. Upon chemical stimulation, Sullivan *et al*.[312] detected that T cells exhibited substantial increases in the secretion of IL-2 and IL-6, with 49-fold and 22-fold increases, respectively, 24 hours after stimulation. The study of IL-2 and TNFα after Tacrolimus stimulation by Oh *et al*.[311] revealed concentration increases of 8-fold, reaching concentrations of 1500 to 2000 pg/mL for each cytokine, respectively.

In comparison we were observing a range of expression for all conditions and cytokines between 2 and 10 pg/mL for Jurkat concentrations of 900 cells/mL. After PPTT, we anticipated an increase in secreted cytokine concentration following PPTT-induced hyperthermia. However, we observed both upregulation and downregulation in the expression of all four cytokines across all conditions, including control samples. Controls were used to establish the basal expression levels of all cytokines after cell manipulation, excluding the effects of AuNR-PEG or NIR laser irradiation. Surprisingly, rather than accumulation of secreted cytokines, or no change at all, as described in Heled *et al*.[77] we observed elevation and decreases in expression.

Interestingly, around the two-hour timepoint after the last manipulation we could observe a sudden surge in IL-6 concentration for control samples, a rapid increase in IL-1 expression for AuNR-PEG irradiated samples and elevated TNFα levels for cells irradiated without AuNR-PEG. The inconsistency in results and kinetic expression throughout these experiments prevents us from drawing any definitive conclusions regarding the statistical significance of the observed differences. However, they strongly suggest that we are inducing cellular stress during the PPTT process by the alterations in the expression of all conditions, as well as indicating that chemically induced cytokine secretion is much stronger compared to physical stimulation.

Nonetheless, it's worth noting that cytokines are unstable proteins susceptible to the action of proteases and serum metalloproteinases. After irradiation of Jurkat cells, we did not use a protease inhibitor during the studied period of 6 hours. This was done to avoid the blockage of caspase 3 activation (protease dependent) and other cleavage processes involved in apoptosis post-PPTT. This could have led to an increased expression of extracellular proteases that may have degraded secreted cytokines during the duration of our experiment.

Furthermore, T cell activation through the T cell receptor (TCR) relies on intracellular calcium (Ca^{2+}) levels. TCRs function by mobilising transmembrane calcium and altering the calcium potential within the cells.[302] Calcium signalling plays a critical role in regulating differentiation proliferation, activation and cytokine production in T lymphocytes.[313] Without these intracellular potential changes, proximal signalling cannot occur, leading to a lack of induction in cytokine production, at both mRNA and post-transcriptional levels.[302] Observations of intracellular calcium deposits after conventional and PPTT-induced hyperthermia show differential calcium localisation between both types of thermal stress. These suggest that the agglomeration of calcium after PPTT may be impacting cytokine secretion.

The described changes observed at the *in vivo* level,[11,307] may stem from a systemic response to the tumour treatment or to cytokine expression associated to potential skin burns resulting from the external illumination of tumours during treatment.[314,315] It's crucial to note that these dynamics may significantly differ *in vitro*, as it is an isolated system, devoid of complex interactions between the different tissues and organs present in whole body organisms. Moreover, *in vitro* systems, while invaluable for studying cellular responses, lack the capability to continuous monitor cytokine expression due to their macroscopic nature. However, the arrival of microchips integrating cell culture present an exhiting opportunity to facilitate uninterrupted and continuous measurement of cytokine secretion by the cultured cells, providing real-time data into cytokine expression dynamics, without the constraints of specific timepoints.

In parallel, the low concentration of cytokines produced by unstimulated cells,[308,312] necessitates detection methods with higher sensitivity. While multiplexing nanoplasmonic biosensors have reduced the required sample volume, their sensitivity remains on the lower end of the spectrum for basal expression levels of secreted cytokines, which can be below the detection limit of the chip,[311] but it allows for multiple measurements and the possibility to remeasure the same sample repeatedly. It's important for the development of new detection technologies to align with the specific requirements of the biomedical community.

Additionally, it's essential to study cytokine production at both the protein and mRNA levels. There is a delay between transcriptional activation and protein secretion,[308] indicating that the kinetics of cytokine secretion into the extracellular space may not align perfectly with the timing of transcriptional activation. This complexity, with multiple parameters and sometimes unpredictable behaviour, underscores the need for careful consideration when studying cytokine production kinetics.

9

Conclusions

Plasmonic photothermal therapy (PPTT) exploits the physicochemical properties of gold nanorods (AuNRs) to convert NIR light into heat, inducing localised cell death. This approach capitalises on the capacity of AuNR to efficiently absorb light and convert it into heat thanks to their localised surface plasmon resonance, thereby selectively targeting and damaging cancer cells, while sparing healthy surrounding tissue.[23]

The multidisciplinary nature of PPTT raises questions across research fields, from bionanomedicine to nanophotonics. Knowledge in all steps of the therapy is crucial to advance towards clinical models, but further research is needed to assess treatment effectiveness and molecular events triggered within cells after treatment, to pave the way for personalised PPTT, tailored to target specific cellular pathways and conditions. Information obtained at the molecular level will direct the therapy towards specific cell lines, tissues, and diseases.

To address these gaps, we focused on investigating the *in vitro* effects of PPTT to build a strong pre-clinical model and identify potential candidates for treatment with this technique. This dissertation lays the groundwork for developing such a model by defining the minimum information to be reported for experiments involving nanoparticles and laser irradiation, emphasizing reporting standards and the use of representative units. We determined the optimal parameters for inducing damage selectively to cells containing AuNRs and irradiated, comparing six different cell lines sensitivity to PPTT conditions. We focused on the activation of the apoptotic cell death mechanisms, exploring differences between PPTT-induced and conventional hyperthermia. Additionally, we studied cytokine production on immune T cells after PPTT to determine if *in vitro* models can be used to predict the production of inflammatory cytokines.

This dissertation successfully examined its initial objectives, providing valuable insight into optimising PPTT *in vitro* efficacy and offering standardisation recommendations for future clinical translation.

1. **Determine non-toxic laser powers and irradiation times for non-cancerous cells and cells without nanoparticles.**

As shown in Chapter 5, many different laser power settings and times of irradiation were tested on kidney cancer cell line 786-0. Following the international organisation for standardisation (ISO) definition of cytotoxicity, we considered a viability over 70% to be acceptable after laser irradiation. If cellular survival after irradiation without AuNRs was less than 70%, those laser settings were discarded.

Following this definition, we determined the optimal laser power density, and time of irradiation to cause damage specifically to irradiated cells containing AuNRs, sparing cells that had not been previously exposed to the nanomaterial. These settings (AuNR concentration = 2 nM, laser power density = 3 W/cm^2, time of irradiation = 3 minutes, spot diameter = 3mm) were used throughout the dissertation, as they were found to be tolerable for all studied cell lines (Chapter 6).

2. **Identify differences in the response to PPTT among different cell lines, focusing on uptake, nanomaterial cytotoxicity and response to treatment.**

After systematically studying the parameters involved in PPTT across three cancerous cell lines and three healthy cell lines derived from kidney, lung, and liver, we observed distinct responses to AuNR

uptake, cytotoxicity, and viability after treatment. The findings revealed differences between malignant and normal cell lines from the same tissue, as well as among different cancerous cell lines and normal cell types.

Uptake of AuNRs for the studied concentrations was higher for all cancerous cell lines compared to their healthy counterparts. While these differences hold promise for cancer treatment, suggesting preferential accumulation of AuNRs on cancerous tissues, they require careful due to experimental design constraints. Incubation of AuNR with normal cell lines required the use of foetal bovine serum (FBS) to maintain cellular viability during the 24 hour incubation period, which is known to impact cellular uptake.[199,200]

All cancer cell lines exhibited similar decreases in viability with increasing concentrations, with an IC50 of approximately 7.5 nM across all cancer cell lines independently of the tissue of origin. In contrast, normal cell lines from lung and liver displayed greater sensitivity to higher AuNR concentrations compared to normal kidney cell line Hek293, which had an IC50 of 15 nM. This difference in the sensitivity of Hek293 to the cytotoxic effects of high AuNR concentrations may be attributed to the embryonic origin of this cell line.

At a concentration of 2nM, all cell lines maintained viability over the ISO-established limit for cytotoxicity of 70%. At this concentration, we maximize the number of nanoparticles incorporated by the cells without compromising cellular viability prior to NIR irradiation. Together with the laser settings defined in Chapter 5, PPTT was evaluated with these parameters.

Due to the lower uptake of AuNR by healthy cell lines, maximum temperature reached during laser irradiation ranged between 39-42°C, whereas cancer cell lines with greater nanoparticle uptake experienced temperatures exceeding 47°C. These differences in temperature translated to different decreases in viability following treatment.

Viability was assessed studying mitochondrial activity using the dimethyl tetrazolium bromide (MTT) assay and membrane integrity with trypan blue staining. Mitochondrial activity was reduced after PPTT compared to control samples and cells irradiated without AuNR, with a more pronounced decreased in viability 24 hours post-irradiation, indicating the temporal progression of cell death. Membrane integrity was less compromised compared to mitochondrial activity for all conditions and studied timepoints. These findings indicate a preferential activation of the apoptotic cell death pathway compared to necrosis, evidenced by the absence of membrane disruption, and reduced mitochondrial activity following PPTT-induced hyperthermia. More importantly, across cell lines different responses to PPTT were triggered, highlighting the relevance of using more than one cell line and appropriate controls to determine the effectiveness of hyperthermia against cancer cells.

3. Examine differences at the molecular level, emphasizing the apoptotic pathways.

The differences observed between the reduction in mitochondrial activity and integrity of the cellular membrane in Chapter 6 suggested the activation of apoptosis after PPTT. A protein array was used for a high throughput analysis of key proteins implicated in the apoptotic cell death pathway.

Results underscored the different activation of the intrinsic vs extrinsic pathway of apoptosis after PPTT-induced hyperthermia. Moreover, it also highlighted the different time required for the activation of certain molecular pathways within the apoptotic cascade. The observed differences in the activation kinetics of both pro- and anti-apoptotic proteins stress the complexity of the interaction occurring within programmed cell death.

The pivotal apoptotic executor, caspase 3, was strongly activated 6 hours after PPTT-induced hyperthermia, triggering a cleavage cascade that will lead to cellular demise. However, the steps required for activation of pro-caspase 3 to its active form were altered after irradiation. Both, apoptotic inhibitors (IAPs) and inducers (Smac/Diablo and Htra2/Omi) demonstrated decreased expression after elevated

temperatures induced by PPTT. Interestingly, cytochrome c was elevated for all hyperthermia types. These results, together with increased expression of Bad and Bax after hyperthermia, suggest a preferential activation of the intrinsic pathway of apoptosis. The extrinsic pathway intensified 24 hours after irradiation, indicating the potential for the cell population to produce extracellular signals detected by death receptors, thereby increasing their expression.

The expression of heat shock proteins (Hsp) during hyperthermia serves as an indicator of protein denaturation and loss of functionality. Following PPTT and conventional hyperthermia, the expression of certain Hsps increased, suggesting a cellular response aimed at preserving structural integrity and functionality. In parallel, the expression of proteins involved in the regulation of oxidative stress increased, indicating that elevated temperatures generate reactive oxygen species (ROS).

An experimental constraint was the examination of protein expression of irradiated cells and cells incubated at high temperatures at different timepoints. Nonetheless, the results obtained yielded valuable insights into the contrast between inducing thermal stress through different mechanisms and how important is to evaluate cell death at more than one timepoint. After evaluating the results of all 35 evaluated proteins we observed a general upregulation of proteins for oven treated cells, compared to more distinct patterns observed after PPTT.

4. **Detect distinct patterns of cytokine expression on immune T cells after PPTT-induced hyperthermia.**

Cytokine expression was evaluated to determine if, after PPTT, immune T cells could be inducing pro-inflammatory signals to the environment. The results, shown in Chapter 8, described a high resistance of Jurkat cells to increasing AuNR-PEG concentrations. After reaching maximum temperatures of almost 50°C during irradiation, viability of Jurkat cells dropped immediately after treatment, declining its mitochondrial activity even further 24 hours after irradiation with nanoparticles. On the other hand, membrane integrity was not altered after irradiation, and only 24 hours post-irradiation an increase in membrane impairment could be observed.

The expression of four different cytokines whose concentration was known to be augmented after conventional hyperthermia were studied. Protein concentration for IL-1, IL-2, IL-6 and TNFα was found to be low for all four cytokines. An irregular pattern of expression was observed, with no apparent increase or decrease in concentration for neither control samples or irradiated cells, with or without nanoparticles.

The lack of relevant differences between conditions or cytokines prevented us from drawing conclusions on the effectiveness of PPTT to induce cytokine expression in Jurkat T cells. However, the experimental protocol only conceived a period of 6 hours after irradiation, with no proteases inhibitors during this time to prevent cytokine cleavage. The unstable nature of cytokines, together with their low basal expression, entails that a change of protocol (e.g. increasing the number of cells to double the concentration of cytokines) and period of observation may be beneficial for the detection of changes after irradiation. On top of that, we consider that evaluating mRNA levels, in parallel to protein concentration, will provide more information on the induction of cytokine secretion and its kinetics after PPTT-induced hyperthermia.

5. **Establish guidelines for the standardisation of *in vitro* PPTT studies for better understanding and development of the technique.**

During the elaboration of a literature review for this project, we recognised a significant gap in the literature concerning PPTT. Information being reported by researchers on the field was not consistent on which data was described and how it should be conveyed, hindering comparison our results with those obtained by other researchers. In response to this challenge, and in alignment with the MIRIBEL guidelines (Minimum information reporting in bio-nano experimental literature) initiative, we

developed our own checklist outlining the minimum information to be conveyed on *in vitro* PPTT experimentation, as detailed in Chapter 4.

To achieve rigorous and reproducible results in PPTT research, we proposed a series of parameters to be included on *in vitro* PPTT. These parameters, complementary to existing guidelines for bio-nano interactions, place particular emphasis on the unique combination of nanoparticles, laser irradiation and biological entities that occurs in PPTT. The proposed guidelines cover material and biological characterisation to provide precise information on experimental setups These include cell type justification, appropriate selection of controls and nanoparticle purification, among others. Consideration of experimental design during data collection is also a valuable item to consider during PPTT, as nanoparticle removal prior to irradiation and viability evaluation at more than one timepoint will provide more valuable information for future research on the field.

The challenges hindering the advancement of clinical trials of PPTT are multifaceted. However, it is widely acknowledged that improving preclinical models will refine the transition from the bench to the bedside. This improvement requires a criteria establishment for experimental protocols that facilitates contrasting data from different researchers. By enabling data comparison, ensuring reproducibility, and advocating for the report of essential data, we can foster not only cancer directed PPTT, but also benefit numerous other clinical scenarios that can gain from the synergistic application of plasmonic nanoparticles and light.

9.1. Outlook

As biotechnology and plasmonics continue advancing at a very fast pace, it is essential to reflect on the strides that have been made in the progression of PPTT and the open avenues ahead for this promising therapy, not only against cancer, but also other maladies.

PPTT overcomes the current limitations of conventional cancer therapies by offering a minimally invasive treatment with high precision. This approach confines the therapeutic efficacy of hyperthermia treatments to the intersection of plasmonic nanoparticles and light.[23,118]

Recent years have witnessed significant progress in nanoparticle design, leading to the development of versatile platforms for cancer diagnosis and treatment, attributed to the particular optical properties of nanoparticles.[123,124] In the case of PPTT, innovation on nanoparticle synthesis has improved their light-to-heat conversion efficiency., biocompatibility and targetability. Gold nanorods have proven to be the ideal candidate for plasmonic hyperthermia as they fulfil most conditions required, as described by Zhou et al.[316]: uniform in size, good aqueous dispersibility, excitation within the NIR range, photostable and exhibit low or none cytotoxicity. In addition, gold nanorods are easily scalable, with facile synthesis, high surface-to-volume ratio, easy surface modifications and targeting, as well as their capacity to be combined with other forms of treatment.[163]

Yet, the actual knowledge on gold nanoparticles will undoubtedly continue to advance with the development of novel surface modifications and the incorporation of new targeting ligands to improve tumour-specific targeting. While nanoparticle design optimisation is an ongoing pursuit, attention must also be directed towards understanding and controlling the formation of the protein corona, as neglecting its implications can render the efforts to improve nanoparticle biocompatibility and targetability pointless.[143]

Enhancing biocompatibility will be pivotal to define better safety standards for PPTT, extending beyond nanoparticle design alone. Safe nanoparticles in PPTT entail the inertness of the nanoparticle outside their target tissue, or when not subjected to irradiation. But off target effects of laser illumination and heat-induced immune responses, are also required to be considered during PPTT to minimise secondary effects compared to conventional techniques for cancer treatment.

The main challenges for PPTT rely on the scalability of the process and regulatory approval processes. The integration of PPTT into existing treatment paradigms could facilitate increased clinical trials done on PPTT, propelling its development.[105] Therefore, the future of PPTT relies on its combination with other therapeutic approaches and the maturation of personalised medicine. The combination of PPTT-based heat therapies could enhance drug delivery and activate drug effects and release upon illumination. Synergistic strategies of PPTT will be pivotal for improving therapeutical outcomes whilst mitigating side effects. Biomarker discovery for resistance to thermal stress or enhanced response to PPTT-induced hyperthermia can tailor treatment parameters for specific needs or individual patients, maximizing the therapeutical benefits.[3,10]

Embracing emerging technologies, such as the development of imaging technologies (e.g. observation of nanoparticle accumulation within the body) and computational modelling, can illuminate the underlying mechanisms of PPTT, refining PPTT personalisation and optimising its outcomes. Moving towards 3D *in vitro* settings and organ-on-chips diagnostic platforms during nanoparticle assessment and study of PPTT effects will provide more relevant data for clinical settings.[154,167,317]

In conclusion, PPTT stands as a well-established yet innovative alternative to conventional cancer treatment, propelled by the rapid development of bionanotechnology and plasmonics. Multidisciplinary collaborations are essential to tackle the challenges that divide the number of preclinical and clinical research being done on PPTT. Moreover, the expertise from various fields will offer new insights into potential application of PPTT beyond cancer treatment.

This dissertation aimed to underscore the importance of standardising PPTT studies *in vitro* and stress the importance of cell type during experimentation.

Bibliography

(1) Derrickson, Bryan; Tortora, Gerard. *Principles of Anatomy and Physiology*, 13th Edition.; 2011.
(2) Habash, R. W. Y. Therapeutic Hyperthermia. In *Handbook of Clinical Neurology*; Elsevier B.V., 2018; Vol. 157, pp 853–868. https://doi.org/10.1016/B978-0-444-64074-1.00053-7.
(3) Bettaieb, A.; Wrzal, P. K.; Averill-bates, D. A. Hyperthermia: Cancer Treatment and Beyond. *Cancer Treat. Innov. Approaches* **2013**, *Book 2* (Chapter 12), 257–283. https://doi.org/10.5772/55795.
(4) Lin, A. Y.; Yang, E.; Rink, J. S.; Xu, D.; Miller, S.; Gordon, L. I. Photoablation with the Aurolase System Reduces T Cell Exhaustion and Synergizes with Immunotherapies in Lymphoma. *Blood* **2023**, *142* (Supplement 1), 2825. https://doi.org/10.1182/blood-2023-185400.
(5) Markota, A.; Kalamar, Ž.; Fluher, J.; Pirkmajer, S. Therapeutic Hyperthermia for the Treatment of Infection—a Narrative Review. *Front. Physiol.* **2023**, *14*, 1215686. https://doi.org/10.3389/fphys.2023.1215686.
(6) Jeziorski, K. Hyperthermia in Rheumatic Diseases. A Promising Approach? *Reumatologia* **2018**, *56* (5), 316–320. https://doi.org/10.5114/reum.2018.79503.
(7) Hildebrandt, B.; Wust, P.; Ahlers, O.; Dieing, A.; Sreenivasa, G.; Kerner, T.; Felix, R.; Riess, H. The Cellular and Molecular Basis of Hyperthermia. *Crit. Rev. Oncol. Hematol.* **2002**, *43* (1), 33–56.
(8) Jha, S.; Sharma, P. K.; Malviya, R. Hyperthermia: Role and Risk Factor for Cancer Treatment. *Achiev. Life Sci.* **2016**, *10* (2), 161–167. https://doi.org/10.1016/j.als.2016.11.004.
(9) Beik, J.; Abed, Z.; Ghoreishi, F. S.; Hosseini-Nami, S.; Mehrzadi, S.; Shakeri-Zadeh, A.; Kamrava, S. K. Nanotechnology in Hyperthermia Cancer Therapy: From Fundamental Principles to Advanced Applications. *J. Controlled Release* **2016**, *235*, 205–221. https://doi.org/10.1016/j.jconrel.2016.05.062.
(10) Overchuk, M.; Weersink, R. A.; Wilson, B. C.; Zheng, G. Photodynamic and Photothermal Therapies: Synergy Opportunities for Nanomedicine. *ACS Nano* **2023**, *17* (9), 7979–8003. https://doi.org/10.1021/acsnano.3c00891.
(11) Morales-Dalmau, J. From Cells to Tissues, Microscopy to Modeling: Towards Precise, Data-Driven Photothermal Therapy with Gold Nanorods, Universitat Politecnica de Catalunya (UPC), 2018.
(12) Sommer, C. M.; Sommer, S. A.; Mokry, T.; Gockner, T.; Gnutzmann, D.; Bellemann, N.; Schmitz, A.; Radeleff, B. A.; Kauczor, H. U.; Stampfl, U.; Pereira, P. L. Quantification of Tissue Shrinkage and Dehydration Caused by Microwave Ablation: Experimental Study in Kidneys for the Estimation of Effective Coagulation Volume. *J. Vasc. Interv. Radiol.* **2013**, *24* (8), 1241–1248. https://doi.org/10.1016/j.jvir.2013.04.008.
(13) Frandon, J.; Akessoul, P.; Kammoun, T.; Dabli, D.; de Forges, H.; Beregi, J.-P.; Greffier, J. Microwave Ablation of Liver, Kidney and Lung Lesions: One-Month Response and Manufacturer's Charts' Reliability in Clinical Practice. *Sensors* **2022**, *22* (11), 3973. https://doi.org/10.3390/s22113973.
(14) Ren, Y.; Yan, Y.; Qi, H. Photothermal Conversion and Transfer in Photothermal Therapy: From Macroscale to Nanoscale. *Adv. Colloid Interface Sci.* **2022**, *308*, 102753. https://doi.org/10.1016/j.cis.2022.102753.
(15) Bruggmoser, G. Some Aspects of Quality Management in Deep Regional Hyperthermia. *Int. J. Hyperthermia* **2012**, *28* (6), 562–569. https://doi.org/10.3109/02656736.2012.714049.
(16) *Cancer today*. http://gco.iarc.fr/today/home (accessed 2024-01-23).
(17) Baffou, G. *Thermoplasmonics*; Cambridge University Press, 2017.
(18) Hirsch, L. R.; Stafford, R. J.; Bankson, J. A.; Sershen, S. R.; Rivera, B.; Price, R. E.; Hazle, J. D.; Halas, N. J.; West, J. L. Nanoshell-Mediated near-Infrared Thermal Therapy of Tumors under Magnetic Resonance Guidance. *Proc. Natl. Acad. Sci.* **2003**, *100* (23), 13549–13554. https://doi.org/10.1073/pnas.2232479100.
(19) O'Neal, D. P.; Hirsch, L. R.; Halas, N. J.; Payne, J. D.; West, J. L. Photo-Thermal Tumor Ablation in Mice Using near Infrared-Absorbing Nanoparticles. *Cancer Lett.* **2004**, *209* (2), 171–176. https://doi.org/10.1016/j.canlet.2004.02.004.
(20) de Melo-Diogo, D.; Pais-Silva, C.; Dias, D. R.; Moreira, A. F.; Correia, I. J. Strategies to Improve Cancer Photothermal Therapy Mediated by Nanomaterials. *Adv. Healthc. Mater.* **2017**, *6* (10), 1–20. https://doi.org/10.1002/adhm.201700073.
(21) Baffou, G.; Quidant, R.; Girard, C. Heat Generation in Plasmonic Nanostructures: Influence of Morphology. *Appl. Phys. Lett.* **2009**, *94* (15), 1–3. https://doi.org/10.1063/1.3116645.
(22) Riley, R. S.; Day, E. S. Gold Nanoparticle-Mediated Photothermal Therapy: Applications and Opportunities for Multimodal Cancer Treatment. *WIREs Nanomedicine Nanobiotechnology* **2017**, *9* (4), 1–16. https://doi.org/10.1002/wnan.1449.
(23) Huang, X.; El-Sayed, M. A. Plasmonic Photo-Thermal Therapy (PPTT). *Alex. J. Med.* **2011**, *47* (1), 1–9. https://doi.org/10.1016/j.ajme.2011.01.001.
(24) Vliet, F. F. J. Discovery of the Near-Infrared Window into the Body and the Early Development of near-Infrared Spectroscopy. *J. Biomed. Opt.* **1999**, *4* (4), 392–396. https://doi.org/10.1117/1.429952.
(25) Pattani, V. P.; Tunnell, J. W. Nanoparticle-Mediated Photothermal Therapy: A Comparative Study of Heating for Different Particle Types. *Lasers Surg. Med.* **2012**, *44* (8), 675–684. https://doi.org/10.1002/lsm.22072.

(26) Zhou, R.; Zhang, M.; Xi, J.; Li, J.; Ma, R.; Ren, L.; Bai, Z.; Qi, K.; Li, X. Gold Nanorods-Based Photothermal Therapy: Interactions Between Biostructure, Nanomaterial, and Near-Infrared Irradiation. *Nanoscale Res. Lett.* **2022**, *17* (1), 68. https://doi.org/10.1186/s11671-022-03706-3.
(27) Khalili Fard, J.; Jafari, S.; Eghbal, M. A. A Review of Molecular Mechanisms Involved in Toxicity of Nanoparticles. *Adv. Pharm. Bull.* **2015**, *5* (4), 447–454. https://doi.org/10.15171/apb.2015.061.
(28) Kinnear, C.; Moore, T. L.; Rodriguez-Lorenzo, L.; Rothen-Rutishauser, B.; Petri-Fink, A. Form Follows Function: Nanoparticle Shape and Its Implications for Nanomedicine. *Chem. Rev.* **2017**, *117* (17), 11476–11521. https://doi.org/10.1021/acs.chemrev.7b00194.
(29) Zhang, Y.; Xu, D.; Li, W.; Yu, J.; Chen, Y. Effect of Size, Shape, and Surface Modification on Cytotoxicity of Gold Nanoparticles to Human HEp-2 and Canine MDCK Cells. *J. Nanomater.* **2012**, *2012*. https://doi.org/10.1155/2012/375496.
(30) Carnovale, C.; Bryant, G.; Shukla, R.; Bansal, V. Identifying Trends in Gold Nanoparticle Toxicity and Uptake : Size , Shape , Capping Ligand , and Biological Corona. *ACS Omega* **2019**, *4*, 242–256. https://doi.org/10.1021/acsomega.8b03227.
(31) Naha, P. C.; Chhour, P.; Cormode, D. P. Systematic in Vitro Toxicological Screening of Gold Nanoparticles Designed for Nanomedicine Applications. *Toxicol. In Vitro* **2015**, *29* (7), 1445–1453. https://doi.org/10.1016/j.tiv.2015.05.022.
(32) Choi, W. I.; Kim, J. Y.; Kang, C.; Byeon, C. C.; Kim, Y. H.; Tae, G. Tumor Regression in Vivo by Photothermal Therapy Based on Gold-Nanorod-Loaded, Functional Nanocarriers. *ACS Nano* **2011**, *5* (3), 1995–2003. https://doi.org/10.1021/nn103047r.
(33) Morales-Dalmau, J.; Vilches, C.; Sanz, V.; de Miguel, I.; Rodríguez-Fajardo, V.; Berto, P.; Martínez-Lozano, M.; Casanovas, O.; Durduran, T.; Quidant, R. Quantification of Gold Nanoparticle Accumulation in Tissue by Two-Photon Luminescence Microscopy. *Nanoscale* **2019**, *11* (23), 11331–11339. https://doi.org/10.1039/C9NR01198F.
(34) Gad, S. C.; Sharp, K. L.; Montgomery, C.; Payne, J. D.; Goodrich, G. P. Evaluation of the Toxicity of Intravenous Delivery of Auroshell Particles (Gold–Silica Nanoshells). *Int. J. Toxicol.* **2012**, *31* (6), 584–594. https://doi.org/10.1177/1091581812465969.
(35) Ali, M. R. K.; Ali, H. R.; Rankin, C. R.; El-Sayed, M. A. Targeting Heat Shock Protein 70 Using Gold Nanorods Enhances Cancer Cell Apoptosis in Low Dose Plasmonic Photothermal Therapy. *Biomaterials* **2016**, *102*, 1–8. https://doi.org/10.1016/j.biomaterials.2016.06.017.
(36) Mooney, R.; Roma, L.; Zhao, D.; Van Haute, D.; Garcia, E.; Kim, S. U.; Annala, A. J.; Aboody, K. S.; Berlin, J. M. Neural Stem Cell-Mediated Delivery of Gold Nanorods Improves Intratumoral Photothermal Therapy. *ACS Nano* **2014**, *8* (12), 12450–12460. https://doi.org/10.1021/nn505147w.
(37) Liu, Y.; Yang, M.; Zhang, J.; Zhi, X.; Li, C.; Zhang, C.; Pan, F.; Wang, K.; Yang, Y.; Martinez De La Fuentea, J.; Cui, D. Human Induced Pluripotent Stem Cells for Tumor Targeted Delivery of Gold Nanorods and Enhanced Photothermal Therapy. *ACS Nano* **2016**, *10* (2), 2375–2385. https://doi.org/10.1021/acsnano.5b07172.
(38) Nikoobakht, B.; El-Sayed, M. A. Preparation and Growth Mechanism of Gold Nanorods (NRs) Using Seed-Mediated Growth Method. *Chem. Mater.* **2003**, *15* (10), 1957–1962. https://doi.org/10.1021/cm020732l.
(39) Pérez-Juste, J.; Pastoriza-Santos, I.; Liz-Marzán, L. M.; Mulvaney, P. Gold Nanorods: Synthesis, Characterization and Applications. *Coord. Chem. Rev.* **2005**, *249* (17-18 SPEC. ISS.), 1870–1901. https://doi.org/10.1016/j.ccr.2005.01.030.
(40) Choi, B. S.; Iqbal, M.; Lee, T.; Kim, Y. H.; Tae, G. Removal of Cetyltrimethylammonium Bromide to Enhance the Biocompatibility of Au Nanorods Synthesized by a Modified Seed Mediated Growth Process. *J. Nanosci. Nanotechnol.* **2008**, *8* (9), 4670–4674. https://doi.org/10.1166/jnn.2008.IC18.
(41) Shi, X.; Perry, H. L.; Wilton-Ely, J. D. E. T. Strategies for the Functionalisation of Gold Nanorods to Reduce Toxicity and Aid Clinical Translation. *Nanotheranostics* **2021**, *5* (2), 155–165. https://doi.org/10.7150/ntno.56432.
(42) Soenen, S. J.; Manshian, B. B.; Abdelmonem, A. M.; Montenegro, J. M.; Tan, S.; Balcaen, L.; Vanhaecke, F.; Brisson, A. R.; Parak, W. J.; De Smedt, S. C.; Braeckmans, K. The Cellular Interactions of PEGylated Gold Nanoparticles: Effect of PEGylation on Cellular Uptake and Cytotoxicity. *Part. Part. Syst. Charact.* **2014**, *31* (7), 794–800. https://doi.org/10.1002/ppsc.201300357.
(43) Lassenberger, A.; Bixner, O.; Gruenewald, T.; Lichtenegger, H.; Zirbs, R.; Reimhult, E. Evaluation of High-Yield Purification Methods on Monodisperse PEG-Grafted Iron Oxide Nanoparticles. *Langmuir* **2016**, *32* (17), 4259–4269. https://doi.org/10.1021/acs.langmuir.6b00919.
(44) Huang, X.; Peng, X.; Wang, Y.; Wang, Y.; Shin, D. M.; El-Sayed, M. A.; Nie, S. A Reexamination of Active and Passive Tumor Targeting by Using Rod-Shaped Gold Nanocrystals and Covalently Conjugated Peptide Ligands. *ACS Nano* **2010**, *4* (10), 5887–5896. https://doi.org/10.1021/nn102055s.
(45) Wolfe, T.; Chatterjee, D.; Lee, J.; Grant, J. D.; Bhattarai, S.; Tailor, R.; Goodrich, G.; Nicolucci, P.; Krishnan, S. Targeted Gold Nanoparticles Enhance Sensitization of Prostate Tumors to Megavoltage Radiation Therapy

in Vivo. *Nanomedicine Nanotechnol. Biol. Med.* **2015**, *11* (5), 1277–1283. https://doi.org/10.1016/j.nano.2014.12.016.
(46) Guerrini, L.; Alvarez-Puebla, R. A.; Pazos-Perez, N. Surface Modifications of Nanoparticles for Stability in Biological Fluids. *Materials* **2018**, *11* (7), 1154. https://doi.org/10.3390/ma11071154.
(47) Sanati, M.; Khodagholi, F.; Aminyavari, S.; Ghasemi, F.; Gholami, M.; Kebriaeezadeh, A.; Sabzevari, O.; Hajipour, M. J.; Imani, M.; Mahmoudi, M.; Sharifzadeh, M. Impact of Gold Nanoparticles on Amyloid β-Induced Alzheimer's Disease in a Rat Animal Model: Involvement of STIM Proteins. *ACS Chem. Neurosci.* **2019**, *10* (5), 2299–2309. https://doi.org/10.1021/acschemneuro.8b00622.
(48) Ruhoff, V. T.; Arastoo, M. R.; Moreno-Pescador, G.; Bendix, P. M. Biological Applications of Thermoplasmonics. *Nano Lett.* **2024**. https://doi.org/10.1021/acs.nanolett.3c03548.
(49) Wilson, A. M.; Mazzaferri, J.; Bergeron, É.; Patskovsky, S.; Marcoux-Valiquette, P.; Costantino, S.; Sapieha, P.; Meunier, M. In Vivo Laser-Mediated Retinal Ganglion Cell Optoporation Using KV1.1 Conjugated Gold Nanoparticles. *Nano Lett.* **2018**, *18* (11), 6981–6988. https://doi.org/10.1021/acs.nanolett.8b02896.
(50) Ribera, J.; Vilches, C.; Sanz, V.; de Miguel, I.; Portolés, I.; Córdoba-Jover, B.; Prat, E.; Nunes, V.; Jiménez, W.; Quidant, R.; Morales-Ruiz, M. Treatment of Hepatic Fibrosis in Mice Based on Targeted Plasmonic Hyperthermia. *ACS Nano* **2021**, *15* (4), 7547–7562. https://doi.org/10.1021/acsnano.1c00988.
(51) de Miguel, I.; Prieto, I.; Albornoz, A.; Sanz, V.; Weis, C.; Turon, P.; Quidant, R. Plasmon-Based Biofilm Inhibition on Surgical Implants. *Nano Lett.* **2019**, *19* (4), 2524–2529. https://doi.org/10.1021/acs.nanolett.9b00187.
(52) nanoComposix. *Nanobiotechnology*. nanoComposix. https://nanocomposix.com/pages/bionanotechnology (accessed 2024-02-05).
(53) Harris, T. J.; Kim, A. A. C. Hair Removal with Nanoparticles. US8821941B2, September 2, 2014. https://patents.google.com/patent/US8821941B2/en (accessed 2024-02-05).
(54) Paithankar, D. Y.; Meyer, T. J.; Blomgren, R. D.; Faupel, L. J.; Lando, A. V.; Anderson, R. R. Acne Treatment Based on Selective Photothermolysis of Sebaceous Follicles with Topically Delivered Gold Plasmonic Particles. **2016**.
(55) Rastinehad, A. R.; Anastos, H.; Wajswol, E.; Winoker, J. S.; Sfakianos, J. P.; Doppalapudi, S. K.; Carrick, M. R.; Knauer, C. J.; Taouli, B.; Lewis, S. C.; Tewari, A. K.; Schwartz, J. A.; Canfield, S. E.; George, A. K.; West, J. L.; Halas, N. J. Gold Nanoshell-Localized Photothermal Ablation of Prostate Tumors in a Clinical Pilot Device Study. *Proc. Natl. Acad. Sci.* **2019**, *116* (37), 18590–18596. https://doi.org/10.1073/pnas.1906929116.
(56) Zhu, L.; Altman, M. B.; Laszlo, A.; Straube, W.; Zoberi, I.; Hallahan, D. E.; Chen, H. ULTRASOUND HYPERTHERMIA TECHNOLOGY FOR RADIOSENSITIZATION. *Ultrasound Med. Biol.* **2019**, *45* (5), 1025–1043. https://doi.org/10.1016/j.ultrasmedbio.2018.12.007.
(57) Gongalsky, M.; Gvindzhiliia, G.; Tamarov, K.; Shalygina, O.; Pavlikov, A.; Solovyev, V.; Kudryavtsev, A.; Sivakov, V.; Osminkina, L. A. Radiofrequency Hyperthermia of Cancer Cells Enhanced by Silicic Acid Ions Released During the Biodegradation of Porous Silicon Nanowires. *ACS Omega* **2019**, *4* (6), 10662–10669. https://doi.org/10.1021/acsomega.9b01030.
(58) Radiofrequency and Microwave Hyperthermia in Cancer Treatment. In *Principles and Technologies for Electromagnetic Energy Based Therapies*; Academic Press, 2022; pp 281–311. https://doi.org/10.1016/B978-0-12-820594-5.00007-1.
(59) Zhao, Q.-L.; Fujiwara, Y.; Kondo, T. Mechanism of Cell Death Induction by Nitroxide and Hyperthermia. *Free Radic. Biol. Med.* **2006**, *40* (7), 1131–1143. https://doi.org/10.1016/j.freeradbiomed.2005.10.064.
(60) Huilgol, N. G.; Gupta, S.; C. R., S. Hyperthermia with Radiation in the Treatment of Locally Advanced Head and Neck Cancer: A Report of Randomized Trial. *J. Cancer Res. Ther.* **2010**, *6* (4), 492. https://doi.org/10.4103/0973-1482.77101.
(61) Jiang, X.; Wang, X. Cytochrome ***C*** -Mediated Apoptosis. *Annu. Rev. Biochem.* **2004**, *73* (1), 87–106. https://doi.org/10.1146/annurev.biochem.73.011303.073706.
(62) Kannan, K.; Jain, S. K. Oxidative Stress and Apoptosis. *Pathophysiol. Off. J. Int. Soc. Pathophysiol.* **2000**, *7* (3), 153–163. https://doi.org/10.1016/s0928-4680(00)00053-5.
(63) Ma, Z.; Zhang, Y.; Zhang, J.; Zhang, W.; Foda, M. F.; Dai, X.; Han, H. Ultrasmall Peptide-Coated Platinum Nanoparticles for Precise NIR-II Photothermal Therapy by Mitochondrial Targeting. *ACS Appl. Mater. Interfaces* **2020**, *12* (35), 39434–39443. https://doi.org/10.1021/acsami.0c11469.
(64) Ahmed, K.; Tabuchi, Y.; Kondo, T. Hyperthermia: An Effective Strategy to Induce Apoptosis in Cancer Cells. *Apoptosis* **2015**, *20* (11), 1411–1419. https://doi.org/10.1007/s10495-015-1168-3.
(65) Mocan, T.; Matea, C. T.; Cojocaru, I.; Ilie, I.; Tabaran, F. A.; Zaharie, F.; Iancu, C.; Bartos, D.; Mocan, L. Photothermal Treatment of Human Pancreatic Cancer Using PEGylated Multi-Walled Carbon Nanotubes Induces Apoptosis by Triggering Mitochondrial Membrane Depolarization Mechanism. *J. Cancer* **2014**, *5* (8), 679–688. https://doi.org/10.7150/jca.9481.
(66) Redza-Dutordoir, M.; Averill-Bates, D. A. Activation of Apoptosis Signalling Pathways by Reactive Oxygen Species. *Biochim. Biophys. Acta BBA - Mol. Cell Res.* **2016**, *1863* (12), 2977–2992. https://doi.org/10.1016/j.bbamcr.2016.09.012.

(67) Jones, M. C.; Zha, J.; Humphries, M. J. Connections between the Cell Cycle, Cell Adhesion and the Cytoskeleton. *Philos. Trans. R. Soc. B Biol. Sci.* **2019**, *374* (1779), 20180227. https://doi.org/10.1098/rstb.2018.0227.
(68) Coakley, W. T. Hyperthermia Effects on the Cytoskeleton and on Cell Morphology. *Symp. Soc. Exp. Biol.* **1987**, *41*, 187–211.
(69) Wang, Z.; Cai, F.; Chen, X.; Luo, M.; Hu, L.; Lu, Y. The Role of Mitochondria-Derived Reactive Oxygen Species in Hyperthermia-Induced Platelet Apoptosis. *PLoS ONE* **2013**, *8* (9), 1–14. https://doi.org/10.1371/journal.pone.0075044.
(70) Luchetti, F.; Canonico, B.; Felice, M. D.; Burattini, S.; Battistelli, M.; Papa, S.; Falcieri, E. Hyperthermia Triggers Apoptosis and Affects Cell Adhesiveness in Human Neuroblastoma Cells. *Histol. Histopathol.* **2003**, *18* (4), 1041–1052.
(71) Ludwig, B. S.; Kessler, H.; Kossatz, S.; Reuning, U. RGD-Binding Integrins Revisited: How Recently Discovered Functions and Novel Synthetic Ligands (Re-)Shape an Ever-Evolving Field. *Cancers* **2021**, *13* (7), 1711. https://doi.org/10.3390/cancers13071711.
(72) Ali, M. R. K.; Wu, Y.; Tang, Y.; Xiao, H.; Chen, K.; Han, T.; Fang, N.; Wu, R.; El-Sayed, M. A. Targeting Cancer Cell Integrins Using Gold Nanorods in Photothermal Therapy Inhibits Migration through Affecting Cytoskeletal Proteins. *Proc. Natl. Acad. Sci.* **2017**, *114* (28), E5655–E5663. https://doi.org/10.1073/pnas.1703151114.
(73) Peng, F.; Setyawati, M. I.; Tee, J. K.; Ding, X.; Wang, J.; Nga, M. E.; Ho, H. K.; Leong, D. T. Nanoparticles Promote in Vivo Breast Cancer Cell Intravasation and Extravasation by Inducing Endothelial Leakiness. *Nat. Nanotechnol.* **2019**. https://doi.org/10.1038/s41565-018-0356-z.
(74) Alberts, B.; Johnson, A.; Lewis, J.; Morgan, D.; Raff, M.; Roberts, K.; Walter, P. *Molecular Biology of the Cell*, 6th ed.; Taylor & Francis Group, 2015.
(75) Katschinski, D. M.; Wiedemann, G. J.; Longo, W.; d'Oleire, F. R.; Spriggs, D.; Robins, H. I. Whole Body Hyperthermia Cytokine Induction: A Review, and Unifying Hypothesis for Myeloprotection in the Setting of Cytotoxic Therapy. *Cytokine Growth Factor Rev.* **1999**, *10* (2), 93–97. https://doi.org/10.1016/S1359-6101(99)00006-4.
(76) Li, Z.; Deng, J.; Sun, J.; Ma, Y. Hyperthermia Targeting the Tumor Microenvironment Facilitates Immune Checkpoint Inhibitors. *Front. Immunol.* **2020**, *11*.
(77) Heled, Y.; Fleischmann, C.; Epstein, Y. Cytokines and Their Role in Hyperthermia and Heat Stroke. *J. Basic Clin. Physiol. Pharmacol.* **2013**, *24* (2), 85–96. https://doi.org/10.1515/jbcpp-2012-0040.
(78) Xu, D.; Tang, W.-J.; Zhu, Y.-Z.; Liu, Z.; Yang, K.; Liang, M.-X.; Chen, X.; Wu, Y.; Tang, J.-H.; Zhang, W. Hyperthermia Promotes Exosome Secretion by Regulating Rab7b While Increasing Drug Sensitivity in Adriamycin-Resistant Breast Cancer. *Int. J. Hyperthermia* **2022**, *39* (1), 246–257. https://doi.org/10.1080/02656736.2022.2029585.
(79) Sen, K.; Sheppe, A. E. F.; Singh, I.; Hui, W. W.; Edelmann, M. J.; Rinaldi, C. Exosomes Released by Breast Cancer Cells under Mild Hyperthermic Stress Possess Immunogenic Potential and Modulate Polarization in Vitro in Macrophages. *Int. J. Hyperth. Off. J. Eur. Soc. Hyperthermic Oncol. North Am. Hyperth. Group* **2020**, *37* (1), 696–710. https://doi.org/10.1080/02656736.2020.1778800.
(80) Toraya-Brown, S.; Fiering, S. Local Tumour Hyperthermia as Immunotherapy for Metastatic Cancer. *Int. J. Hyperthermia* **2014**, *30* (8), 531–539. https://doi.org/10.3109/02656736.2014.968640.
(81) Zhou, J.; Wang, X.; Du, L.; Zhao, L.; Lei, F.; OuYang, W.; Zhang, Y.; Liao, Y.; Tang, J. Effect of Hyperthermia on the Apoptosis and Proliferation of CaSki Cells. *Mol. Med. Rep.* **2011**, *4* (1), 187–191. https://doi.org/10.3892/mmr.2010.401.
(82) Petrova, N. V.; Velichko, A. K.; Razin, S. V.; Kantidze, O. L. Early S-Phase Cell Hypersensitivity to Heat Stress. *Cell Cycle Georget. Tex* **2016**, *15* (3), 337–344. https://doi.org/10.1080/15384101.2015.1127477.
(83) Elmore, S. Apoptosis: A Review of Programmed Cell Death. *Toxicol. Pathol.* **2007**, *35* (4), 495–516. https://doi.org/10.1080/01926230701320337.
(84) Porter, A. G.; Jänicke, R. U. Emerging Roles of Caspase-3 in Apoptosis. *Cell Death Differ.* **1999**, *6* (2), 99–104. https://doi.org/10.1038/sj.cdd.4400476.
(85) Silva, M. T. Secondary Necrosis: The Natural Outcome of the Complete Apoptotic Program. *FEBS Lett.* **2010**, *584* (22), 4491–4499. https://doi.org/10.1016/j.febslet.2010.10.046.
(86) Galluzzi, L.; Kroemer, G. Secondary Necrosis: Accidental No More. *Trends Cancer* **2017**, *3* (1), 1–2. https://doi.org/10.1016/j.trecan.2016.12.001.
(87) Galluzzi, L.; Vitale, I.; Aaronson, S. A.; Abrams, J. M.; Adam, D.; Agostinis, P.; Alnemri, E. S.; Altucci, L.; Amelio, I.; Andrews, D. W.; Annicchiarico-Petruzzelli, M.; Antonov, A. V.; Arama, E.; Baehrecke, E. H.; Barlev, N. A.; Bazan, N. G.; Bernassola, F.; Bertrand, M. J. M.; Bianchi, K.; Blagosklonny, M. V.; Blomgren, K.; Borner, C.; Boya, P.; Brenner, C.; Campanella, M.; Candi, E.; Carmona-Gutierrez, D.; Cecconi, F.; Chan, F. K. M.; Chandel, N. S.; Cheng, E. H.; Chipuk, J. E.; Cidlowski, J. A.; Ciechanover, A.; Cohen, G. M.; Conrad, M.; Cubillos-Ruiz, J. R.; Czabotar, P. E.; D'Angiolella, V.; Dawson, T. M.; Dawson, V. L.; De Laurenzi, V.; De Maria, R.; Debatin, K. M.; Deberardinis, R. J.; Deshmukh, M.; Di Daniele, N.; Di Virgilio,

F.; Dixit, V. M.; Dixon, S. J.; Duckett, C. S.; Dynlacht, B. D.; El-Deiry, W. S.; Elrod, J. W.; Fimia, G. M.; Fulda, S.; García-Sáez, A. J.; Garg, A. D.; Garrido, C.; Gavathiotis, E.; Golstein, P.; Gottlieb, E.; Green, D. R.; Greene, L. A.; Gronemeyer, H.; Gross, A.; Hajnoczky, G.; Hardwick, J. M.; Harris, I. S.; Hengartner, M. O.; Hetz, C.; Ichijo, H.; Jäättelä, M.; Joseph, B.; Jost, P. J.; Juin, P. P.; Kaiser, W. J.; Karin, M.; Kaufmann, T.; Kepp, O.; Kimchi, A.; Kitsis, R. N.; Klionsky, D. J.; Knight, R. A.; Kumar, S.; Lee, S. W.; Lemasters, J. J.; Levine, B.; Linkermann, A.; Lipton, S. A.; Lockshin, R. A.; López-Otín, C.; Lowe, S. W.; Luedde, T.; Lugli, E.; MacFarlane, M.; Madeo, F.; Malewicz, M.; Malorni, W.; Manic, G.; Marine, J. C.; Martin, S. J.; Martinou, J. C.; Medema, J. P.; Mehlen, P.; Meier, P.; Melino, S.; Miao, E. A.; Molkentin, J. D.; Moll, U. M.; Muñoz-Pinedo, C.; Nagata, S.; Nuñez, G.; Oberst, A.; Oren, M.; Overholtzer, M.; Pagano, M.; Panaretakis, T.; Pasparakis, M.; Penninger, J. M.; Pereira, D. M.; Pervaiz, S.; Peter, M. E.; Piacentini, M.; Pinton, P.; Prehn, J. H. M.; Puthalakath, H.; Rabinovich, G. A.; Rehm, M.; Rizzuto, R.; Rodrigues, C. M. P.; Rubinsztein, D. C.; Rudel, T.; Ryan, K. M.; Sayan, E.; Scorrano, L.; Shao, F.; Shi, Y.; Silke, J.; Simon, H. U.; Sistigu, A.; Stockwell, B. R.; Strasser, A.; Szabadkai, G.; Tait, S. W. G.; Tang, D.; Tavernarakis, N.; Thorburn, A.; Tsujimoto, Y.; Turk, B.; Vanden Berghe, T.; Vandenabeele, P.; Vander Heiden, M. G.; Villunger, A.; Virgin, H. W.; Vousden, K. H.; Vucic, D.; Wagner, E. F.; Walczak, H.; Wallach, D.; Wang, Y.; Wells, J. A.; Wood, W.; Yuan, J.; Zakeri, Z.; Zhivotovsky, B.; Zitvogel, L.; Melino, G.; Kroemer, G. Molecular Mechanisms of Cell Death: Recommendations of the Nomenclature Committee on Cell Death 2018. *Cell Death Differ.* **2018**, *25* (3), 486–541. https://doi.org/10.1038/s41418-017-0012-4.

(88) Ahmed, K.; Zaidi, S. F. Treating Cancer with Heat: Hyperthermia as Promising Strategy to Enhance Apoptosis. *J Pak Med Assoc* **2013**, *63* (4), 504–508.

(89) Cui, Z.-G.; Piao, J.-L.; Rehman, M. U. R.; Ogawa, R.; Li, P.; Zhao, Q.-L.; Kondo, T.; Inadera, H. Molecular Mechanisms of Hyperthermia-Induced Apoptosis Enhanced by Withaferin A. *Eur. J. Pharmacol.* **2014**, *723*, 99–107. https://doi.org/10.1016/j.ejphar.2013.11.031.

(90) Hou, C. H.; Lin, F. L.; Hou, S. M.; Liu, J. F. Hyperthermia Induces Apoptosis through Endoplasmic Reticulum and Reactive Oxygen Species in Human Osteosarcoma Cells. *Int. J. Mol. Sci.* **2014**, *15* (10), 17380–17395. https://doi.org/10.3390/ijms151017380.

(91) Milleron, R. S.; Bratton, S. B. 'Heated' Debates in Apoptosis. *Cell. Mol. Life Sci.* **2007**, *64* (18), 2329–2333. https://doi.org/10.1007/s00018-007-7135-6.

(92) Ali, M. R. K.; Wu, Y.; El-Sayed, M. A. Gold Nanoparticle-Assisted Plasmonic Photothermal Therapy Advances Towards Clinical Application. *J. Phys. Chem. C* **2019**, *123*, acs.jpcc.9b01961. https://doi.org/10.1021/acs.jpcc.9b01961.

(93) Richter, K.; Haslbeck, M.; Buchner, J. The Heat Shock Response: Life on the Verge of Death. *Mol. Cell* **2010**, *40* (2), 253–266. https://doi.org/10.1016/j.molcel.2010.10.006.

(94) Bettaieb, A.; Averill-Bates, D. A. Thermotolerance Induced at a Mild Temperature of 40 Degrees C Protects Cells against Heat Shock-Induced Apoptosis. *J. Cell. Physiol.* **2005**, *205* (1), 47–57. https://doi.org/10.1002/jcp.20386.

(95) Concannon, C. G.; Gorman, A. M.; Samali, A. On the Role of Hsp27 in Regulating Apoptosis. *Apoptosis* **2003**, *8* (1), 61–70. https://doi.org/10.1023/A:1021601103096.

(96) Beere, H. M. `The Stress of Dying': The Role of Heat Shock Proteins in the Regulation of Apoptosis. *J. Cell Sci.* **2004**, *117* (13), 2641–2651. https://doi.org/10.1242/jcs.01284.

(97) Albany, C.; Hahn, N. Heat Shock Proteins and Apoptosis as Therapeutic Targets in Prostate Cancer. *Asian J. Androl.* **2014**, *16*. https://doi.org/10.4103/1008-682X.126400.

(98) Ciocca, D.; Cappello, F.; Cuello-Carrión, F.; Arrigo, A. Molecular Approaches to Target Heat Shock Proteins for Cancer Treatment. In *Frontiers in Clinical Drug Research - Anti-Cancer Agents*; 2015; Vol. 2, pp 3–47.

(99) Sauvage, F.; Messaoudi, S.; Fattal, E.; Barratt, G.; Vergnaud-Gauduchon, J. Heat Shock Proteins and Cancer: How Can Nanomedicine Be Harnessed? *J. Controlled Release* **2017**, *248*, 133–143. https://doi.org/10.1016/j.jconrel.2017.01.013.

(100) Skitzki, J. J.; Repasky, E. A.; Evans, S. S. Hyperthermia as an Immunotherapy Strategy for Cancer. *Curr. Opin. Investig. Drugs Lond. Engl. 2000* **2009**, *10* (6), 550–558. https://doi.org/10.1016/j.pestbp.2011.02.012.Investigations.

(101) *1. What is nanotechnology?* https://ec.europa.eu/health/scientific_committees/opinions_layman/en/nanotechnologies/l-3/1-introduction.htm#0p0 (accessed 2024-02-12).

(102) Wang, F.; Li, Y.; Chen, L.; Chen, D.; Wu, X.; Wang, H. Mapping of Hyperthermic Tumor Cell Death in a Microchannel under Unidirectional Heating. *Biomicrofluidics* **2012**, *6* (1), 1–12. https://doi.org/10.1063/1.3694252.

(103) Yang, T.; Peng, J.; Shu, Z.; Sekar, P. K.; Li, S.; Gao, D. Determination of the Membrane Transport Properties of Jurkat Cells with a Microfluidic Device. *Micromachines* **2019**, *10* (12), 832. https://doi.org/10.3390/mi10120832.

(104) Thalhammer, S.; Schneider, M. F.; Wixforth, A. Integrated Lab-on-a-Chip System in Life Sciences. In *Nanoscale Phenomena: Fundamentals and Applications*; Hahn, H., Sidorenko, A., Tiginyanu, I., Eds.;

NanoScience and Technology; Springer: Berlin, Heidelberg, 2009; pp 161–190. https://doi.org/10.1007/978-3-642-00708-8_15.
(105) Đorđević, S.; Gonzalez, M. M.; Conejos-Sánchez, I.; Carreira, B.; Pozzi, S.; Acúrcio, R. C.; Satchi-Fainaro, R.; Florindo, H. F.; Vicent, M. J. Current Hurdles to the Translation of Nanomedicines from Bench to the Clinic. *Drug Deliv. Transl. Res.* **2022**, *12* (3), 500–525. https://doi.org/10.1007/s13346-021-01024-2.
(106) U.S. Department of Health and Human Services Food and Drug Administration. Guidance for Industry on Drug Products, Including Biological Products, That Contain Nanomaterials - Guidance for Indutry. *Food Drug Adm. FDA* **2017**, No. December. https://doi.org/10.1002/jgm.
(107) *What is nanomedicine?*. ETPN. https://etp-nanomedicine.eu/about-nanomedicine/what-is-nanomedicine/ (accessed 2024-02-12).
(108) Ventola, C. L. The Nanomedicine Revolution. *Pharm. Ther.* **2012**, *37* (9), 512–525.
(109) Satalkar, P.; Elger, B. S.; Shaw, D. M. Defining Nano, Nanotechnology and Nanomedicine: Why Should It Matter? *Sci. Eng. Ethics* **2016**, *22* (5), 1255–1276. https://doi.org/10.1007/s11948-015-9705-6.
(110) Namiot, E. D.; Sokolov, A. V.; Chubarev, V. N.; Tarasov, V. V.; Schiöth, H. B. Nanoparticles in Clinical Trials: Analysis of Clinical Trials, FDA Approvals and Use for COVID-19 Vaccines. *Int. J. Mol. Sci.* **2023**, *24* (1), 787. https://doi.org/10.3390/ijms24010787.
(111) Peón-Díaz, F. J.; Iriarte-Mesa, C.; Cao-Milán, R. NIR-Triggered Doxorubicin Photorelease Using CuS @ Albumin Composites and in-Vitro e Ff Ect over HeLa Cells. *J. Drug Deliv. Sci. Technol.* **2020**, *57* (March), 101642. https://doi.org/10.1016/j.jddst.2020.101642.
(112) Desai, N. Nanoparticle Albumin-Bound Paclitaxel (Abraxane®). In *Albumin in Medicine: Pathological and Clinical Applications*; Otagiri, M., Chuang, V. T. G., Eds.; Springer: Singapore, 2016; pp 101–119. https://doi.org/10.1007/978-981-10-2116-9_6.
(113) Mitchell, M. J.; Billingsley, M. M.; Haley, R. M.; Wechsler, M. E.; Peppas, N. A.; Langer, R. Engineering Precision Nanoparticles for Drug Delivery. *Nat. Rev. Drug Discov.* **2021**, *20* (2), 101–124. https://doi.org/10.1038/s41573-020-0090-8.
(114) Sepúlveda, B.; Angelomé, P. C.; Lechuga, L. M.; Liz-Marzán, L. M. LSPR-Based Nanobiosensors. *Nano Today* **2009**, *4* (3), 244–251. https://doi.org/10.1016/j.nantod.2009.04.001.
(115) Durr, N. J.; Larson, T.; Smith, D. K.; Korgel, B. A.; Sokolov, K.; Ben-Yakar, A. Two-Photon Luminescence Imaging of Cancer Cells Using Molecularly Targeted Gold Nanorods. *Nano Lett.* **2007**, *7* (4), 941–945. https://doi.org/10.1021/nl062962v.
(116) Metselaar, J. M.; Lammers, T. Challenges in Nanomedicine Clinical Translation. *Drug Deliv. Transl. Res.* **2020**, *10* (3), 721–725. https://doi.org/10.1007/s13346-020-00740-5.
(117) Guidolin, K.; Zheng, G. Nanomedicines Lost in Translation. *ACS Nano* **2019**, *13* (12), 13620–13626. https://doi.org/10.1021/acsnano.9b08659.
(118) Vilches, C.; Quidant, R. Targeted Hyperthermia with Plasmonic Nanoparticles. In *Frontiers of Nanoscience*; Elsevier Ltd, 2020; Vol. 16, pp 307–352. https://doi.org/10.1016/B978-0-08-102828-5.00012-7.
(119) Faria, M.; Björnmalm, M.; Thurecht, K. J.; Kent, S. J.; Parton, R. G.; Kavallaris, M.; Johnston, A. P. R.; Gooding, J. J.; Corrie, S. R.; Boyd, B. J.; Thordarson, P.; Whittaker, A. K.; Stevens, M. M.; Prestidge, C. A.; Porter, C. J. H.; Parak, W. J.; Davis, T. P.; Crampin, E. J.; Caruso, F. Minimum Information Reporting in Bio–Nano Experimental Literature. *Nat. Nanotechnol.* **2018**, *13* (9), 777–785. https://doi.org/10.1038/s41565-018-0246-4.
(120) Villuendas, H.; Vilches, C.; Quidant, R. Standardization of In Vitro Studies for Plasmonic Photothermal Therapy. *ACS Nanosci. Au* **2023**, *3* (5), 347–352. https://doi.org/10.1021/acsnanoscienceau.3c00011.
(121) Bucharskaya, A. B.; Maslyakova, G. N.; Chekhonatskaya, M. L.; Terentyuk, G. S.; Navolokin, N. A.; Khlebtsov, B. N.; Khlebtsov, N. G.; Bashkatov, A. N.; Genina, E. A.; Tuchin, V. V. Plasmonic Photothermal Therapy: Approaches to Advanced Strategy. *Lasers Surg. Med.* **2018**, No. June, 1–9. https://doi.org/10.1002/lsm.23001.
(122) Sharifi, M.; Attar, F.; Saboury, A. A.; Akhtari, K.; Hooshmand, N.; Hasan, A.; El-Sayed, M. A.; Falahati, M. Plasmonic Gold Nanoparticles: Optical Manipulation, Imaging, Drug Delivery and Therapy. *J. Controlled Release* **2019**, *311–312*, 170–189. https://doi.org/10.1016/j.jconrel.2019.08.032.
(123) Huang, X.; El-Sayed, M. A. Gold Nanoparticles: Optical Properties and Implementations in Cancer Diagnosis and Photothermal Therapy. *J. Adv. Res.* **2010**, *1* (1), 13–28. https://doi.org/10.1016/j.jare.2010.02.002.
(124) Baffou, G.; Cichos, F.; Quidant, R. Applications and Challenges of Thermoplasmonics. *Nat. Mater.* **2020**, *19* (9), 946–958. https://doi.org/10.1038/s41563-020-0740-6.
(125) Prasad, P. N. *Introduction to Biophotonics*; Wiley-Interscience: Hoboken, NJ, 2003.
(126) Wang, T.; Halaney, D.; Ho, D.; Feldman, M. D.; Milner, T. E. Two-Photon Luminescence Properties of Gold Nanorods. *Biomed. Opt. Express* **2013**, *4* (4), 584–595. https://doi.org/10.1364/BOE.4.000584.

(127) Kang, B.-H.; Lee, Y.; Yu, E.-S.; Na, H.; Kang, M.; Huh, H. J.; Jeong, K.-H. Ultrafast and Real-Time Nanoplasmonic On-Chip Polymerase Chain Reaction for Rapid and Quantitative Molecular Diagnostics. *ACS Nano* **2021**, *15* (6), 10194–10202. https://doi.org/10.1021/acsnano.1c02154.
(128) Morales-Dalmau, J.; Vilches, C.; De Miguel, I.; Sanz, V.; Quidant, R. Optimum Morphology of Gold Nanorods for Light-Induced Hyperthermia. *Nanoscale* **2018**, *10* (5), 2632–2638. https://doi.org/10.1039/c7nr06825e.
(129) Niidome, T.; Yamagata, M.; Okamoto, Y.; Akiyama, Y.; Takahashi, H.; Kawano, T.; Katayama, Y.; Niidome, Y. PEG-Modified Gold Nanorods with a Stealth Character for in Vivo Applications. *J. Controlled Release* **2006**, *114* (3), 343–347. https://doi.org/10.1016/j.jconrel.2006.06.017.
(130) Bhamidipati, M.; Fabris, L. Multiparametric Assessment of Gold Nanoparticle Cytotoxicity in Cancerous and Healthy Cells: The Role of Size, Shape, and Surface Chemistry. *Bioconjug. Chem.* **2017**, *28* (2), 449–460. https://doi.org/10.1021/acs.bioconjchem.6b00605.
(131) Liu, J.; Abshire, C.; Carry, C.; Sholl, A. B.; Mandava, S. H.; Datta, A.; Ranjan, M.; Callaghan, C.; Peralta, D. V.; Williams, K. S.; Lai, W. R.; Abdel-Mageed, A. B.; Tarr, M.; Lee, B. R. Nanotechnology Combined Therapy: Tyrosine Kinase-Bound Gold Nanorod and Laser Thermal Ablation Produce a Synergistic Higher Treatment Response of Renal Cell Carcinoma in a Murine Model. *BJU Int.* **2017**, *119* (2), 342–348. https://doi.org/10.1111/bju.13590.
(132) Vetten, M. A.; Yah, C. S.; Singh, T.; Gulumian, M. Challenges Facing Sterilization and Depyrogenation of Nanoparticles: Effects on Structural Stability and Biomedical Applications. *Nanomedicine Nanotechnol. Biol. Med.* **2014**, *10* (7), 1391–1399. https://doi.org/10.1016/j.nano.2014.03.017.
(133) Gomez, L.; Cebrian, V.; Martin-Saavedra, F.; Arruebo, M.; Vilaboa, N.; Santamaria, J. Stability and Biocompatibility of Photothermal Gold Nanorods after Lyophilization and Sterilization. *Mater. Res. Bull.* **2013**, *48* (10), 4051–4057. https://doi.org/10.1016/j.materresbull.2013.06.034.
(134) Kim, J.; Cho, H.; Lim, D.-K.; Joo, M. K.; Kim, K. Perspectives for Improving the Tumor Targeting of Nanomedicine via the EPR Effect in Clinical Tumors. *Int. J. Mol. Sci.* **2023**, *24* (12), 10082. https://doi.org/10.3390/ijms241210082.
(135) Yang, W.; Liang, H.; Ma, S.; Wang, D.; Huang, J. Gold Nanoparticle Based Photothermal Therapy: Development and Application for Effective Cancer Treatment. *Sustain. Mater. Technol.* **2019**, *22*, e00109. https://doi.org/10.1016/j.susmat.2019.e00109.
(136) Stabile, J.; Najafali, D.; Cheema, Y.; Inglut, C. T.; Liang, B. J.; Vaja, S.; Sorrin, A. J.; Huang, H. C. *Engineering Gold Nanoparticles for Photothermal Therapy, Surgery, and Imaging*; Elsevier Inc., 2020. https://doi.org/10.1016/B978-0-12-816662-8.00012-6.
(137) Polo, E.; Collado, M.; Pelaz, B.; Del Pino, P. Advances toward More Efficient Targeted Delivery of Nanoparticles in Vivo: Understanding Interactions between Nanoparticles and Cells. *ACS Nano* **2017**, *11* (3), 2397–2402. https://doi.org/10.1021/acsnano.7b01197.
(138) Wilhelm, S.; Tavares, A. J.; Dai, Q.; Ohta, S.; Audet, J.; Dvorak, H. F.; Chan, W. C. W.; Chatterley, A.; Group, W. Analysis of Nanopar.Cle Delivery to Tumours. *Nat. Rev. Mater.* **2016**, *1* (1), 16014. https://doi.org/10.1038/natrevmats.2016.14.
(139) Casals, E.; Pfaller, T.; Duschl, A.; Oostingh, G. J.; Puntes, V. Time Evolution of the Nanoparticle Protein Corona. *ACS Nano* **2010**, *4* (7), 3623–3632. https://doi.org/10.1021/nn901372t.
(140) Almeida, M. S. de; Susnik, E.; Drasler, B.; Taladriz-Blanco, P.; Petri-Fink, A.; Rothen-Rutishauser, B. Understanding Nanoparticle Endocytosis to Improve Targeting Strategies in Nanomedicine. *Chem. Soc. Rev.* **2021**, *50* (9), 5397–5434. https://doi.org/10.1039/D0CS01127D.
(141) Nel, A. E.; Mädler, L.; Velegol, D.; Xia, T.; Hoek, E. M. V.; Somasundaran, P.; Klaessig, F.; Castranova, V.; Thompson, M. Understanding Biophysicochemical Interactions at the Nano-Bio Interface. *Nat. Mater.* **2009**, *8* (7), 543–557. https://doi.org/10.1038/nmat2442.
(142) Rennick, J. J.; Johnston, A. P. R.; Parton, R. G. Key Principles and Methods for Studying the Endocytosis of Biological and Nanoparticle Therapeutics. *Nat. Nanotechnol.* **2021**, *16* (3), 266–276. https://doi.org/10.1038/s41565-021-00858-8.
(143) Park, S.; Ha, M. K.; Lee, Y.; Song, J.; Yoon, T. H. Effects of Immune Cell Heterogeneity and Protein Corona on the Cellular Association and Cytotoxicity of Gold Nanoparticles: A Single-Cell-Based, High-Dimensional Mass Cytometry Study. *ACS Nanosci. Au* **2023**, *3* (4), 323–334. https://doi.org/10.1021/acsnanoscienceau.3c00001.
(144) Jain, P.; Pawar, R. S.; Pandey, R. S.; Madan, J.; Pawar, S.; Lakshmi, P. K.; Sudheesh, M. S. In-Vitro in-Vivo Correlation (IVIVC) in Nanomedicine: Is Protein Corona the Missing Link? *Biotechnol. Adv.* **2017**, *35* (7), 889–904. https://doi.org/10.1016/j.biotechadv.2017.08.003.
(145) Jauffred, L.; Samadi, A.; Klingberg, H.; Bendix, P. M.; Oddershede, L. B. Plasmonic Heating of Nanostructures. *Chem. Rev.* **2019**. https://doi.org/10.1021/acs.chemrev.8b00738.
(146) Chen, W.-H.; Luo, G.-F.; Lei, Q.; Hong, S.; Qiu, W.-X.; Liu, L.-H.; Cheng, S.-X.; Zhang, X.-Z. Overcoming the Heat Endurance of Tumor Cells by Interfering with the Anaerobic Glycolysis Metabolism

for Improved Photothermal Therapy. *ACS Nano* **2017**, *11* (2), 1419–1431. https://doi.org/10.1021/acsnano.6b06658.

(147) Younis, M. R.; Wang, C.; An, R.; Wang, S.; Younis, M. A.; Li, Z. Q.; Wang, Y.; Ihsan, A.; Ye, D.; Xia, X. H. Low Power Single Laser Activated Synergistic Cancer Phototherapy Using Photosensitizer Functionalized Dual Plasmonic Photothermal Nanoagents. *ACS Nano* **2019**, *13* (2), 2544–2557. https://doi.org/10.1021/acsnano.8b09552.

(148) Schildkopf, P.; Ott, O. J.; Frey, B.; Wadepohl, M.; Sauer, R.; Fietkau, R.; Gaipl, U. S. Biological Rationales and Clinical Applications of Temperature Controlled Hyperthermia--Implications for Multimodal Cancer Treatments. *Curr. Med. Chem.* **2010**, *17* (27), 3045–3057. https://doi.org/10.2174/092986710791959774.

(149) Hirsch, C.; Schildknecht, S. In Vitro Research Reproducibility: Keeping up High Standards. *Front. Pharmacol.* **2019**, *10* (December), 1–9. https://doi.org/10.3389/fphar.2019.01484.

(150) Xu, L.; Xu, M.; Sun, X.; Feliu, N.; Feng, L.; Parak, W. J.; Liu, S. Quantitative Comparison of Gold Nanoparticle Delivery via the Enhanced Permeation and Retention (EPR) Effect and Mesenchymal Stem Cell (MSC)-Based Targeting. *ACS Nano* **2023**, *17* (3), 2039–2052. https://doi.org/10.1021/acsnano.2c07295.

(151) Johnston, H. J.; Hutchison, G.; Christensen, F. M.; Peters, S.; Hankin, S.; Stone, V. A Review of the in Vivo and in Vitro Toxicity of Silver and Gold Particulates: Particle Attributes and Biological Mechanisms Responsible for the Observed Toxicity. *Crit. Rev. Toxicol.* **2010**, *40* (4), 328–346. https://doi.org/10.3109/10408440903453074.

(152) Jensen, C.; Teng, Y. Is It Time to Start Transitioning From 2D to 3D Cell Culture? *Front. Mol. Biosci.* **2020**, *7*.

(153) Xavier, M.; Parente, I. A.; Rodrigues, P. M.; Cerqueira, M. A.; Pastrana, L.; Goncalves, C. Safety and Fate of Nanomaterials in Food The Role of in Vitro Tests. *Trends Food Sci. Technol.* **2021**, *109*, 593–607. https://doi.org/10.1016/j.tifs.2021.01.050.

(154) Guggenheim, E. J.; Milani, S.; Röttgermann, P. J. F.; Dusinska, M.; Saout, C.; Salvati, A.; Rädler, J. O.; Lynch, I. Refining in Vitro Models for Nanomaterial Exposure to Cells and Tissues. *NanoImpact* **2018**, *10* (February), 121–142. https://doi.org/10.1016/j.impact.2018.02.008.

(155) Ghasemi, M.; Turnbull, T.; Sebastian, S.; Kempson, I. The MTT Assay: Utility, Limitations, Pitfalls, and Interpretation in Bulk and Single-Cell Analysis. *Int. J. Mol. Sci.* **2021**, *22* (23), 12827. https://doi.org/10.3390/ijms222312827.

(156) Strober, W. Trypan Blue Exclusion Test of Cell Viability. *Curr. Protoc. Immunol.* **2015**, *111*, A3.B.1-A3.B.3. https://doi.org/10.1002/0471142735.ima03bs111.

(157) Rees, P.; Wills, J. W.; Brown, M. R.; Barnes, C. M.; Summers, H. D. The Origin of Heterogeneous Nanoparticle Uptake by Cells. *Nat. Commun.* **2019**, *10* (1), 2341. https://doi.org/10.1038/s41467-019-10112-4.

(158) Kettler, K.; Veltman, K.; van de Meent, D.; van Wezel, A.; Hendriks, A. J. Cellular Uptake of Nanoparticles as Determined by Particle Properties, Experimental Conditions, and Cell Type. *Environ. Toxicol. Chem.* **2014**, *33* (3), 481–492. https://doi.org/10.1002/etc.2470.

(159) Alkilany, A. M.; Murphy, C. J. Toxicity and Cellular Uptake of Gold Nanoparticles: What We Have Learned so Far? *J. Nanoparticle Res.* **2010**, *12* (7), 2313–2333. https://doi.org/10.1007/s11051-010-9911-8.

(160) Ke, P. C.; Lin, S.; Parak, W. J.; Davis, T. P.; Caruso, F. A Decade of the Protein Corona. *ACS Nano* **2017**, *11* (12), 11773–11776. https://doi.org/10.1021/acsnano.7b08008.

(161) Wang, H.; Huff, T. B.; Zweifel, D. A.; He, W.; Low, P. S.; Wei, A.; Cheng, J.-X. In Vitro and in Vivo Two-Photon Luminescence Imaging of Single Gold Nanorods. *Proc. Natl. Acad. Sci.* **2005**, *102* (44), 15752–15756. https://doi.org/10.1073/pnas.0504892102.

(162) So, P. T. Two-Photon Fluorescence Light Microscopy. In *Encyclopedia of Life Sciences*; John Wiley & Sons, Ltd, 2001. https://doi.org/10.1038/npg.els.0002991.

(163) Norouzi, H.; Khoshgard, K.; Akbarzadeh, F. In Vitro Outlook of Gold Nanoparticles in Photo-Thermal Therapy: A Literature Review. *Lasers Med. Sci.* **2018**, *33* (4), 917–926. https://doi.org/10.1007/s10103-018-2467-z.

(164) Kim, H. S.; Lee, D. Y. Photothermal Therapy with Gold Nanoparticles as an Anticancer Medication. *J. Pharm. Investig.* **2017**, *47* (1), 19–26. https://doi.org/10.1007/s40005-016-0292-6.

(165) Duval, K.; Grover, H.; Han, L.-H.; Mou, Y.; Pegoraro, A. F.; Fredberg, J.; Chen, Z. Modeling Physiological Events in 2D vs. 3D Cell Culture. *Physiology* **2017**, *32* (4), 266–277. https://doi.org/10.1152/physiol.00036.2016.

(166) Yim, W.; Zhou, J.; Sasi, L.; Zhao, J.; Yeung, J.; Cheng, Y.; Jin, Z.; Johnson, W.; Xu, M.; Palma-Chavez, J.; Fu, L.; Qi, B.; Retout, M.; Shah, N. J.; Bae, J.; Jokerst, J. V. 3D-Bioprinted Phantom with Human Skin Phototypes for Biomedical Optics. *Adv. Mater.* **2023**, *35* (3), 2206385. https://doi.org/10.1002/adma.202206385.

(167) Torras, N.; García-Díaz, M.; Fernández-Majada, V.; Martínez, E. Mimicking Epithelial Tissues in Three-Dimensional Cell Culture Models. *Front. Bioeng. Biotechnol.* **2018**, *6* (DEC), 1–7. https://doi.org/10.3389/fbioe.2018.00197.
(168) Fratoddi, I.; Venditti, I.; Cametti, C.; Russo, M. V. How Toxic Are Gold Nanoparticles? The State-of-the-Art. *Nano Res.* **2015**, *8* (6), 1771–1799. https://doi.org/10.1007/s12274-014-0697-3.
(169) Kilkenny, C.; Browne, W. J.; Cuthill, I. C.; Emerson, M.; Altman, D. G. Improving Bioscience Research Reporting: The Arrive Guidelines for Reporting Animal Research. *PLoS Biol.* **2010**, *8* (6), 6–10. https://doi.org/10.1371/journal.pbio.1000412.
(170) Kim, H. S.; Lee, D. Y. Near-Infrared-Responsive Cancer Photothermal and Photodynamic Therapy Using Gold Nanoparticles. *Polymers* **2018**, *10* (9), 1–14. https://doi.org/10.3390/polym10090961.
(171) Almada, M.; Leal-Martínez, B. H.; Hassan, N.; Kogan, M. J.; Burboa, M. G.; Topete, A.; Valdez, M. A.; Juárez, J. Photothermal Conversion Efficiency and Cytotoxic Effect of Gold Nanorods Stabilized with Chitosan, Alginate and Poly(Vinyl Alcohol). *Mater. Sci. Eng. C* **2017**, *77*, 583–593. https://doi.org/10.1016/j.msec.2017.03.218.
(172) Sykes, E. A.; Chen, J.; Zheng, G.; Chan, W. C. W. Investigating the Impact of Nanoparticle Size on Active and Passive Tumor Targeting Efficiency. *ACS Nano* **2014**, *8* (6), 5696–5706. https://doi.org/10.1021/nn500299p.
(173) Tonigold, M.; Simon, J.; Estupiñán, D.; Kokkinopoulou, M.; Reinholz, J.; Kintzel, U.; Kaltbeitzel, A.; Renz, P.; Domogalla, M. P.; Steinbrink, K.; Lieberwirth, I.; Crespy, D.; Landfester, K.; Mailänder, V. Pre-Adsorption of Antibodies Enables Targeting of Nanocarriers despite a Biomolecular Corona. *Nat. Nanotechnol.* **2018**, *13* (September), 1–8. https://doi.org/10.1038/s41565-018-0171-6.
(174) Huang, X.; Jain, P. K.; El-Sayed, I. H.; El-Sayed, M. A. Plasmonic Photothermal Therapy (PPTT) Using Gold Nanoparticles. *Lasers Med. Sci.* **2008**, *23* (3), 217–228. https://doi.org/10.1007/s10103-007-0470-x.
(175) Abadeer, N. S.; Murphy, C. J. Recent Progress in Cancer Thermal Therapy Using Gold Nanoparticles. *J. Phys. Chem. C* **2016**, *120* (9), 4691–4716. https://doi.org/10.1021/acs.jpcc.5b11232.
(176) Baffou, G.; Quidant, R.; Girard, C. Heat Generation in Plasmonic Nanostructures: Influence of Morphology. *Appl. Phys. Lett.* **2009**, *94* (15), 1–3. https://doi.org/10.1063/1.3116645.
(177) de Melo-Diogo, D.; Pais-Silva, C.; Dias, D. R.; Moreira, A. F.; Correia, I. J. Strategies to Improve Cancer Photothermal Therapy Mediated by Nanomaterials. *Adv. Healthc. Mater.* **2017**, *6* (10). https://doi.org/10.1002/adhm.201700073.
(178) Neutelings, T.; Lambert, C. A.; Nusgens, B. V.; Colige, A. C. Effects of Mild Cold Shock (25°C) Followed by Warming Up at 37°C on the Cellular Stress Response. *PLoS ONE* **2013**, *8* (7), 1–15. https://doi.org/10.1371/journal.pone.0069687.
(179) Villuendas, H.; Vilches, C.; Quidant, R. Influence of Cell Type on the Efficacy of Plasmonic Photothermal Therapy. *ACS Nanosci. Au* **2022**, *2* (6), 494–502. https://doi.org/10.1021/acsnanoscienceau.2c00023.
(180) Melamed, J. R.; Edelstein, R. S.; Day, E. S. Elucidating the Fundamental Mechanisms of Cell Death Triggered by Photothermal Therapy. *ACS Nano* **2015**, *9* (1), 6–11. https://doi.org/10.1021/acsnano.5b00021.
(181) Yang, X.; Su, L.-J.; La Rosa, F. G.; Smith, E. E.; Schlaepfer, I. R.; Cho, S. K.; Kavanagh, B.; Park, W.; Flaig, T. W. The Antineoplastic Activity of Photothermal Ablative Therapy with Targeted Gold Nanorods in an Orthotopic Urinary Bladder Cancer Model. *Bladder Cancer* **2017**, *3* (3), 201–210. https://doi.org/10.3233/BLC-170096.
(182) Xu, W.; Qian, J.; Hou, G.; Wang, Y.; Wang, J.; Sun, T.; Ji, L.; Suo, A.; Yao, Y. PEGylated Hydrazided Gold Nanorods for PH-Triggered Chemo/Photodynamic/Photothermal Triple Therapy of Breast Cancer. *Acta Biomater.* **2018**, *18*. https://doi.org/S1742706118306184.
(183) Kim, D.; Kim, H. Optimization of Photothermal Therapy Treatment Effect under Various Laser Irradiation Conditions. *Int. J. Mol. Sci.* **2022**, *23* (11), 5928. https://doi.org/10.3390/ijms23115928.
(184) Astashkina, A. I.; Jones, C. F.; Thiagarajan, G.; Kurtzeborn, K.; Ghandehari, H.; Brooks, B. D.; Grainger, D. W. Nanoparticle Toxicity Assessment Using an Invitro 3-D Kidney Organoid Culture Model. *Biomaterials* **2014**, *35* (24), 6323–6331. https://doi.org/10.1016/j.biomaterials.2014.04.060.
(185) Gormley, A. J.; Greish, K.; Ray, A.; Robinson, R.; Gustafson, J. A.; Ghandehari, H. Gold Nanorod Mediated Plasmonic Photothermal Therapy: A Tool to Enhance Macromolecular Delivery. *Int. J. Pharm.* **2011**, *415* (1–2), 315–318. https://doi.org/10.1016/j.ijpharm.2011.05.068.
(186) Leber, B.; Mayrhauser, U.; Leopold, B.; Koestenbauer, S.; Tscheliessnigg, K.; Stadlbauer, V.; Stiegler, P. Impact of Temperature on Cell Death in a Cell-Culture Model of Hepatocellular Carcinoma. *Anticancer Res.* **2012**, *32* (3), 915–921.
(187) Tortiglione, C.; Iachetta, R. Playing with Nanoparticle Shapes and Laser Powers to Decide Which Route to Take during Photothermal Therapy: Apoptosis or Necrosis? *Ann. Transl. Med.* **2016**, *4* (S1), S51–S51. https://doi.org/10.21037/atm.2016.10.09.
(188) Park, M. V. D. Z.; Lankveld, D. P. K.; van Loveren, H.; de Jong, W. H. The Status of in Vitro Toxicity Studies in the Risk Assessment of Nanomaterials. *Nanomed.* **2009**, *4* (6), 669–685. https://doi.org/10.2217/nnm.09.40.

(189) Richardson, H. H.; Carlson, M. T.; Tandler, P. J.; Hernandez, P.; Govorov, A. O. Experimental and Theoretical Studies of Light-to-Heat Conversion and Collective Heating Effects in Metal Nanoparticle Solutions. *Nano Lett.* **2009**, *9* (3), 1139–1146. https://doi.org/10.1021/nl8036905.
(190) Huang, X.; El-Sayed, I. H.; Qian, W.; El-Sayed, M. A. Cancer Cell Imaging and Photothermal Therapy in the Near-Infrared Region by Using Gold Nanorods. *J. Am. Chem. Soc.* **2006**, *128* (6), 2115–2120. https://doi.org/10.1021/ja057254a.
(191) Li, Z.; Huang, H.; Tang, S.; Li, Y.; Yu, X. F.; Wang, H.; Li, P.; Sun, Z.; Zhang, H.; Liu, C.; Chu, P. K. Small Gold Nanorods Laden Macrophages for Enhanced Tumor Coverage in Photothermal Therapy. *Biomaterials* **2016**, *74*, 144–154. https://doi.org/10.1016/j.biomaterials.2015.09.038.
(192) Talamini, L.; Violatto, M. B.; Cai, Q.; Monopoli, M. P.; Kantner, K.; Krpetić, Ž.; Perez-Potti, A.; Cookman, J.; Garry, D.; Silveira, C. P.; Boselli, L.; Pelaz, B.; Serchi, T.; Cambier, S.; Gutleb, A. C.; Feliu, N.; Yan, Y.; Salmona, M.; Parak, W. J.; Dawson, K. A.; Bigini, P. Influence of Size and Shape on the Anatomical Distribution of Endotoxin-Free Gold Nanoparticles. *ACS Nano* **2017**, *11* (6), 5519–5529. https://doi.org/10.1021/acsnano.7b00497.
(193) 3RCC. *The 3Rs Principle*. Swiss 3R Competence Center. https://swiss3rcc.org/description-on-the-3rs (accessed 2024-01-31).
(194) Hubrecht, R. C.; Carter, E. The 3Rs and Humane Experimental Technique: Implementing Change. *Anim. Open Access J. MDPI* **2019**, *9* (10), 754. https://doi.org/10.3390/ani9100754.
(195) Nasri, A.; Foisset, F.; Ahmed, E.; Lahmar, Z.; Vachier, I.; Jorgensen, C.; Assou, S.; Bourdin, A.; De Vos, J. Roles of Mesenchymal Cells in the Lung: From Lung Development to Chronic Obstructive Pulmonary Disease. *Cells* **2021**, *10* (12), 3467. https://doi.org/10.3390/cells10123467.
(196) Mohtar, N.; Parumasivam, T.; Gazzali, A. M.; Tan, C. S.; Tan, M. L.; Othman, R.; Fazalul Rahiman, S. S.; Wahab, H. A. Advanced Nanoparticle-Based Drug Delivery Systems and Their Cellular Evaluation for Non-Small Cell Lung Cancer Treatment. *Cancers* **2021**, *13* (14), 3539. https://doi.org/10.3390/cancers13143539.
(197) Fröhlich, E. The Role of Surface Charge in Cellular Uptake and Cytotoxicity of Medical Nanoparticles. *Int. J. Nanomedicine* **2012**, *7*, 5577–5591. https://doi.org/10.2147/IJN.S36111.
(198) Xia, Q.; Huang, J.; Feng, Q.; Chen, X.; Liu, X.; Li, X.; Zhang, T.; Xiao, S.; Li, H.; Zhong, Z.; Xiao, K. Size- and Cell Type-Dependent Cellular Uptake, Cytotoxicity and in Vivo Distribution of Gold Nanoparticles. *Int. J. Nanomedicine* **2019**, *14*, 6957–6970. https://doi.org/10.2147/IJN.S214008.
(199) Carnovale, C.; Bryant, G.; Shukla, R.; Bansal, V. Identifying Trends in Gold Nanoparticle Toxicity and Uptake : Size , Shape , Capping Ligand , and Biological Corona. *ACS Omega* **2019**, *4*, 242–256. https://doi.org/10.1021/acsomega.8b03227.
(200) Claudia, M.; Kristin, Ö.; Jennifer, O.; Eva, R.; Eleonore, F. Comparison of Fluorescence-Based Methods to Determine Nanoparticle Uptake by Phagocytes and Non-Phagocytic Cells in Vitro. *Toxicology* **2017**, *378*, 25–36. https://doi.org/10.1016/j.tox.2017.01.001.
(201) Kim, J.; Chun, S. H.; Amornkitbamrung, L.; Song, C.; Yuk, J. S. Gold Nanoparticle Clusters for the Investigation of Therapeutic Efficiency against Prostate Cancer under near - Infrared Irradiation. *Nano Converg.* **2020**, *7* (5), 1–9. https://doi.org/10.1186/s40580-019-0216-z.
(202) Amaral, M.; Charmier, A. J.; Afonso, R. A.; Catarino, J.; Faísca, P.; Carvalho, L.; Ascensão, L.; Coelho, J. M. P.; Manuela Gaspar, M.; Reis, C. P. Gold-Based Nanoplataform for the Treatment of Anaplastic Thyroid Carcinoma: A Step Forward. *Cancers* **2021**, *13* (6), 1–24. https://doi.org/10.3390/cancers13061242.
(203) Bhamidipati, M.; Fabris, L. Multiparametric Assessment of Gold Nanoparticle Cytotoxicity in Cancerous and Healthy Cells: The Role of Size, Shape, and Surface Chemistry. *Bioconjug. Chem.* **2017**, *28* (2), 449–460. https://doi.org/10.1021/acs.bioconjchem.6b00605.
(204) Alkilany, A. M.; Murphy, C. J. Toxicity and Cellular Uptake of Gold Nanoparticles: What We Have Learned so Far? *J. Nanoparticle Res.* **2010**, *12* (7), 2313–2333. https://doi.org/10.1007/s11051-010-9911-8.
(205) Zhao, P.; Chen, X.; Wang, Q.; Zou, H.; Xie, Y.; Liu, H.; Zhou, Y.; Liu, P.; Dai, H. Differential Toxicity Mechanism of Gold Nanoparticles in HK-2 Renal Proximal Tubular Cells and 786-0 Carcinoma Cells. *Nanomed.* **2020**, *15* (11), 1079–1096. https://doi.org/10.2217/nnm-2019-0417.
(206) Baffou, G.; Berto, P.; Bermúdez Ureña, E.; Quidant, R.; Monneret, S.; Polleux, J.; Rigneault, H. Photoinduced Heating of Nanoparticle Arrays. *ACS Nano* **2013**, *7* (8), 6478–6488. https://doi.org/10.1021/nn401924n.
(207) Morales-Dalmau, J.; Vilches, C.; De Miguel, I.; Sanz, V.; Quidant, R. Optimum Morphology of Gold Nanorods for Light-Induced Hyperthermia. *Nanoscale* **2018**, *10* (5), 2632–2638. https://doi.org/10.1039/c7nr06825e.
(208) Qi, G.; Zhang, Y.; Xu, S.; Li, C.; Wang, D.; Li, H.; Jin, Y. Nucleus and Mitochondria Targeting Theranostic Plasmonic Surface-Enhanced Raman Spectroscopy Nanoprobes as a Means for Revealing Molecular Stress Response Differences in Hyperthermia Cell Death between Cancerous and Normal Cells. *Anal. Chem.* **2018**, *90* (22), 13356–13364. https://doi.org/10.1021/acs.analchem.8b03034.

(209) Zhang, Y.; Zhan, X.; Xiong, J.; Peng, S.; Huang, W.; Joshi, R.; Cai, Y.; Liu, Y.; Li, R.; Yuan, K.; Zhou, N.; Min, W. Temperature-Dependent Cell Death Patterns Induced by Functionalized Gold Nanoparticle Photothermal Therapy in Melanoma Cells. *Sci. Rep.* **2018**, *8* (1), 1–9. https://doi.org/10.1038/s41598-018-26978-1.

(210) Guerrero-Florez, V.; Mendez-Sanchez, S. C.; Patrón-Soberano, O. A.; Rodríguez-González, V.; Blach, D.; Fernando Martínez, O. Gold Nanoparticle-Mediated Generation of Reactive Oxygen Species during Plasmonic Photothermal Therapy: A Comparative Study for Different Particle Sizes, Shapes, and Surface Conjugations. *J. Mater. Chem. B* **2020**, *8* (14), 2862–2875. https://doi.org/10.1039/d0tb00240b.

(211) Liu, Y.; Yang, M.; Zhang, J.; Zhi, X.; Li, C.; Zhang, C.; Pan, F.; Wang, K.; Yang, Y.; Martinez De La Fuentea, J.; Cui, D. Human Induced Pluripotent Stem Cells for Tumor Targeted Delivery of Gold Nanorods and Enhanced Photothermal Therapy. *ACS Nano* **2016**, *10* (2), 2375–2385. https://doi.org/10.1021/acsnano.5b07172.

(212) Wu, Y.; Ali, M. R. K.; Dong, B.; Han, T.; Chen, K.; Chen, J.; Tang, Y.; Fang, N.; Wang, F.; El-Sayed, M. A. Gold Nanorod-Photothermal Therapy Alters Cell Junctions and Actin Network in Inhibiting Cancer Cell Collective Migration. *ACS Nano* **2018**, *12* (9), 9279–9290. https://doi.org/10.1021/acsnano.8b04128.

(213) Liu, Y.; Xu, M.; Zhao, Y.; Chen, X.; Zhu, X.; Wei, C.; Zhao, S.; Liu, J.; Qin, X. Flower-like Gold Nanoparticles for Enhanced Photothermal Anticancer Therapy by the Delivery of Pooled SiRNA to Inhibit Heat Shock Stress. *J. Mater. Chem. B* **2019**, *3* (7), 586–597. https://doi.org/10.1039/c8tb02418a.

(214) Ali, M. R. K.; Wu, Y.; El-Sayed, M. A. Gold Nanoparticle-Assisted Plasmonic Photothermal Therapy Advances Towards Clinical Application. *J. Phys. Chem. C* **2019**, *123*, acs.jpcc.9b01961. https://doi.org/10.1021/acs.jpcc.9b01961.

(215) Sun, X.; Gamal, M.; Nold, P.; Said, A.; Chakraborty, I.; Pelaz, B.; Schmied, F.; von Pückler, K.; Figiel, J.; Zhao, Y.; Brendel, C.; Hassan, M.; Parak, W. J.; Feliu, N. Tracking Stem Cells and Macrophages with Gold and Iron Oxide Nanoparticles – The Choice of the Best Suited Particles. *Appl. Mater. Today* **2019**, *15*, 267–279. https://doi.org/10.1016/j.apmt.2018.12.006.

(216) Ramos, T. I.; Villacis-Aguirre, C. A.; López-Aguilar, K. V.; Padilla, L. S.; Altamirano, C.; Toledo, J. R.; Vispo, N. S. The Hitchhiker's Guide to Human Therapeutic Nanoparticle Development. *Pharmaceutics* **2022**, *14* (2), 1–49. https://doi.org/10.3390/pharmaceutics14020247.

(217) Vilches, C.; Quidant, R. Targeted Hyperthermia with Plasmonic Nanoparticles. In *Frontiers of Nanoscience*; Elsevier Ltd, 2020; Vol. 16, pp 307–352. https://doi.org/10.1016/B978-0-08-102828-5.00012-7.

(218) Brentnall, M.; Rodriguez-Menocal, L.; De Guevara, R. L.; Cepero, E.; Boise, L. H. Caspase-9, Caspase-3 and Caspase-7 Have Distinct Roles during Intrinsic Apoptosis. *BMC Cell Biol.* **2013**, *14* (1), 32. https://doi.org/10.1186/1471-2121-14-32.

(219) Noël, C.; Simard, J. C.; Girard, D. Gold Nanoparticles Induce Apoptosis, Endoplasmic Reticulum Stress Events and Cleavage of Cytoskeletal Proteins in Human Neutrophils. *Toxicol. In Vitro* **2016**, *31*, 12–22. https://doi.org/10.1016/j.tiv.2015.11.003.

(220) Poon, S.; Treweek, T. M.; Wilson, M. R.; Easterbrook-Smith, S. B.; Carver, J. A. Clusterin Is an Extracellular Chaperone That Specifically Interacts with Slowly Aggregating Proteins on Their Off-Folding Pathway. *FEBS Lett.* **2002**, *513* (2–3), 259–266. https://doi.org/10.1016/S0014-5793(02)02326-8.

(221) Junho, C. V. C.; Azevedo, C. A. B.; da Cunha, R. S.; de Yurre, A. R.; Medei, E.; Stinghen, A. E. M.; Carneiro-Ramos, M. S. Heat Shock Proteins: Connectors between Heart and Kidney. *Cells* **2021**, *10* (8), 1939. https://doi.org/10.3390/cells10081939.

(222) Bruey, J.-M.; Ducasse, C.; Bonniaud, P.; Ravagnan, L.; Susin, S. A.; Diaz-Latoud, C.; Gurbuxani, S.; Arrigo, A.-P.; Kroemer, G.; Solary, E.; Garrido, C. Hsp27 Negatively Regulates Cell Death by Interacting with Cytochrome c. *Nat. Cell Biol.* **2000**, *2* (9), 645–652. https://doi.org/10.1038/35023595.

(223) Chen, F.; Bao, H.; Xie, H.; Tian, G.; Jiang, T. Heat Shock Protein Expression and Autophagy after Incomplete Thermal Ablation and Their Correlation. *Int. J. Hyperth. Off. J. Eur. Soc. Hyperthermic Oncol. North Am. Hyperth. Group* **2018**, 1464–5157. https://doi.org/10.1080/02656736.2018.1536285.

(224) Matsushima-Nishiwaki, R.; Takai, S.; Adachi, S.; Minamitani, C.; Yasuda, E.; Noda, T.; Kato, K.; Toyoda, H.; Kaneoka, Y.; Yamaguchi, A.; Kumada, T.; Kozawa, O. Phosphorylated Heat Shock Protein 27 Represses Growth of Hepatocellular Carcinoma via Inhibition of Extracellular Signal-Regulated Kinase*. *J. Biol. Chem.* **2008**, *283* (27), 18852–18860. https://doi.org/10.1074/jbc.M801301200.

(225) Bukau, B.; Horwich, A. L. The Hsp70 and Hsp60 Chaperone Machines. *Cell* **1998**, *92* (3), 351–366. https://doi.org/10.1016/S0092-8674(00)80928-9.

(226) Chaudhuri (Chattopadhyay), P.; Rashid, N. HSP60 as Modulators of Apoptosis. In *Heat Shock Protein 60 in Human Diseases and Disorders*; Asea, A. A. A., Kaur, P., Eds.; Heat Shock Proteins; Springer International Publishing: Cham, 2019; pp 41–55. https://doi.org/10.1007/978-3-030-23154-5_4.

(227) Tang, H.; Chen, Y.; Liu, X.; Wang, S.; Lv, Y.; Wu, D.; Wang, Q.; Luo, M.; Deng, H. Downregulation of HSP60 Disrupts Mitochondrial Proteostasis to Promote Tumorigenesis and Progression in Clear Cell Renal Cell Carcinoma. *Oncotarget* **2016**, *7* (25), 38822–38834. https://doi.org/10.18632/oncotarget.9615.

(228) Humphreys, D. T.; Carver, J. A.; Easterbrook-Smith, S. B.; Wilson, M. R. Clusterin Has Chaperone-like Activity Similar to That of Small Heat Shock Proteins *. *J. Biol. Chem.* **1999**, *274* (11), 6875–6881. https://doi.org/10.1074/jbc.274.11.6875.
(229) Matukumalli, S. R.; Tangirala, R.; Rao, C. M. Clusterin: Full-Length Protein and One of Its Chains Show Opposing Effects on Cellular Lipid Accumulation. *Sci. Rep.* **2017**, *7* (1), 41235. https://doi.org/10.1038/srep41235.
(230) Zhang, H.; Kim, J. K.; Edwards, C. A.; Xu, Z.; Taichman, R.; Wang, C.-Y. Clusterin Inhibits Apoptosis by Interacting with Activated Bax. *Nat. Cell Biol.* **2005**, *7* (9), 909–915. https://doi.org/10.1038/ncb1291.
(231) Zha, J.; Harada, H.; Osipov, K.; Jockel, J.; Waksman, G.; Korsmeyer, S. J. BH3 Domain of BAD Is Required for Heterodimerization with BCL-XL and Pro-Apoptotic Activity*. *J. Biol. Chem.* **1997**, *272* (39), 24101–24104. https://doi.org/10.1074/jbc.272.39.24101.
(232) Czabotar, P. E.; Lessene, G.; Strasser, A.; Adams, J. M. Control of Apoptosis by the BCL-2 Protein Family: Implications for Physiology and Therapy. *Nat. Rev. Mol. Cell Biol.* **2014**, *15* (1), 49–63. https://doi.org/10.1038/nrm3722.
(233) Kale, J.; Osterlund, E. J.; Andrews, D. W. BCL-2 Family Proteins: Changing Partners in the Dance towards Death. *Cell Death Differ.* **2018**, *25* (1), 65–80. https://doi.org/10.1038/cdd.2017.186.
(234) Warren, C. F. A.; Wong-Brown, M. W.; Bowden, N. A. BCL-2 Family Isoforms in Apoptosis and Cancer. *Cell Death Dis.* **2019**, *10* (3), 1–12. https://doi.org/10.1038/s41419-019-1407-6.
(235) Taghiyev, A. F.; Guseva, N. V.; Harada, H.; Knudson, C. M.; Rokhlin, O. W.; Cohen, M. B. Overexpression of BAD Potentiates Sensitivity to Tumor Necrosis Factor-Related Apoptosis-Inducing Ligand Treatment in the Prostatic Carcinoma Cell Line LNCaP1. *Mol. Cancer Res.* **2003**, *1* (7), 500–507.
(236) Idogawa, M.; Adachi, M.; Minami, T.; Yasui, H.; Imai, K. Overexpression of BAD Preferentially Augments Anoikis. *Int. J. Cancer* **2003**, *107* (2), 215–223. https://doi.org/10.1002/ijc.11399.
(237) Martinez-Ruiz, G.; Maldonado, V.; Ceballos-Cancino, G.; Grajeda, J. P. R.; Melendez-Zajgla, J. Role of Smac/DIABLO in Cancer Progression. *J. Exp. Clin. Cancer Res.* **2008**, *27* (1), 48. https://doi.org/10.1186/1756-9966-27-48.
(238) Du, C.; Fang, M.; Li, Y.; Li, L.; Wang, X. Smac, a Mitochondrial Protein That Promotes Cytochrome c–Dependent Caspase Activation by Eliminating IAP Inhibition. *Cell* **2000**, *102* (1), 33–42. https://doi.org/10.1016/S0092-8674(00)00008-8.
(239) Creagh, E. M.; Murphy, B. M.; Duriez, P. J.; Duckett, C. S.; Martin, S. J. Smac/Diablo Antagonizes Ubiquitin Ligase Activity of Inhibitor of Apoptosis Proteins *. *J. Biol. Chem.* **2004**, *279* (26), 26906–26914. https://doi.org/10.1074/jbc.M313859200.
(240) Yang, Q.-H.; Church-Hajduk, R.; Ren, J.; Newton, M. L.; Du, C. Omi/HtrA2 Catalytic Cleavage of Inhibitor of Apoptosis (IAP) Irreversibly Inactivates IAPs and Facilitates Caspase Activity in Apoptosis. *Genes Dev.* **2003**, *17* (12), 1487–1496. https://doi.org/10.1101/gad.1097903.
(241) Vande Walle, L.; Lamkanfi, M.; Vandenabeele, P. The Mitochondrial Serine Protease HtrA2/Omi: An Overview. *Cell Death Differ.* **2008**, *15* (3), 453–460. https://doi.org/10.1038/sj.cdd.4402291.
(242) Ow, Y.-L. P.; Green, D. R.; Hao, Z.; Mak, T. W. Cytochrome c: Functions beyond Respiration. *Nat. Rev. Mol. Cell Biol.* **2008**, *9* (7), 532–542. https://doi.org/10.1038/nrm2434.
(243) Santucci, R.; Sinibaldi, F.; Cozza, P.; Polticelli, F.; Fiorucci, L. Cytochrome c: An Extreme Multifunctional Protein with a Key Role in Cell Fate. *Int. J. Biol. Macromol.* **2019**, *136*, 1237–1246. https://doi.org/10.1016/j.ijbiomac.2019.06.180.
(244) Eleftheriadis, T.; Pissas, G.; Liakopoulos, V.; Stefanidis, I. Cytochrome c as a Potentially Clinical Useful Marker of Mitochondrial and Cellular Damage. *Front. Immunol.* **2016**, *7*.
(245) Cong, H.; Xu, L.; Wu, Y.; Qu, Z.; Bian, T.; Zhang, W.; Xing, C.; Zhuang, C. Inhibitor of Apoptosis Protein (IAP) Antagonists in Anticancer Agent Discovery: Current Status and Perspectives. *J. Med. Chem.* **2019**, *62* (12), 5750–5772. https://doi.org/10.1021/acs.jmedchem.8b01668.
(246) Cetraro, P.; Plaza-Diaz, J.; MacKenzie, A.; Abadía-Molina, F. A Review of the Current Impact of Inhibitors of Apoptosis Proteins and Their Repression in Cancer. *Cancers* **2022**, *14* (7), 1671. https://doi.org/10.3390/cancers14071671.
(247) Berthelet, J.; Dubrez, L. Regulation of Apoptosis by Inhibitors of Apoptosis (IAPs). *Cells* **2013**, *2* (1), 163–187. https://doi.org/10.3390/cells2010163.
(248) Wolf, P. Inhibitor of Apoptosis Proteins as Therapeutic Targets in Bladder Cancer. *Front. Oncol.* **2023**, *13*.
(249) Altieri, D. C. Validating Survivin as a Cancer Therapeutic Target. *Nat. Rev. Cancer* **2003**, *3* (1), 46–54. https://doi.org/10.1038/nrc968.
(250) Varfolomeev, E.; Goncharov, T.; Fedorova, A. V.; Dynek, J. N.; Zobel, K.; Deshayes, K.; Fairbrother, W. J.; Vucic, D. C-IAP1 and c-IAP2 Are Critical Mediators of Tumor Necrosis Factor α (TNFα)-Induced NF-KB Activation. *J. Biol. Chem.* **2008**, *283* (36), 24295–24299. https://doi.org/10.1074/jbc.C800128200.

(251) Xu, L.; Zhu, J.; Hu, X.; Zhu, H.; Kim, H. T.; LaBaer, J.; Goldberg, A.; Yuan, J. C-IAP1 Cooperates with Myc by Acting as a Ubiquitin Ligase for Mad1. *Mol. Cell* **2007**, *28* (5), 914–922. https://doi.org/10.1016/j.molcel.2007.10.027.
(252) Obexer, P.; Ausserlechner, M. J. X-Linked Inhibitor of Apoptosis Protein – A Critical Death Resistance Regulator and Therapeutic Target for Personalized Cancer Therapy. *Front. Oncol.* **2014**, *4*.
(253) Kumar, R.; Herbert, P. E.; Warrens, A. N. An Introduction to Death Receptors in Apoptosis. *Int. J. Surg.* **2005**, *3* (4), 268–277. https://doi.org/10.1016/j.ijsu.2005.05.002.
(254) Wong, S. H. M.; Kong, W. Y.; Fang, C.-M.; Loh, H.-S.; Chuah, L.-H.; Abdullah, S.; Ngai, S. C. The TRAIL to Cancer Therapy: Hindrances and Potential Solutions. *Crit. Rev. Oncol. Hematol.* **2019**, *143*, 81–94. https://doi.org/10.1016/j.critrevonc.2019.08.008.
(255) Schneider, P.; Thome, M.; Burns, K.; Bodmer, J.-L.; Hofmann, K.; Kataoka, T.; Holler, N.; Tschopp, J. TRAIL Receptors 1 (DR4) and 2 (DR5) Signal FADD-Dependent Apoptosis and Activate NF-KB. *Immunity* **1997**, *7* (6), 831–836. https://doi.org/10.1016/S1074-7613(00)80401-X.
(256) Deng, D.; Shah, K. TRAIL of Hope Meeting Resistance in Cancer. *Trends Cancer* **2020**, *6* (12), 989–1001. https://doi.org/10.1016/j.trecan.2020.06.006.
(257) Lee, E.-W.; Seo, J.; Jeong, M.; Lee, S.; Song, J. The Roles of FADD in Extrinsic Apoptosis and Necroptosis. *BMB Rep.* **2012**, *45* (9), 496–508. https://doi.org/10.5483/bmbrep.2012.45.9.186.
(258) Liu, Y.; Li, X.; Zhou, X.; Wang, J.; Ao, X. FADD as a Key Molecular Player in Cancer Progression. *Mol. Med.* **2022**, *28* (1), 132. https://doi.org/10.1186/s10020-022-00560-y.
(259) Bi, R.; Deng, Y.; Tang, C.; Xuan, L.; Xu, B.; Du, Y.; Wang, C.; Wei, W. Andrographolide Sensitizes Human Renal Carcinoma Cells to TRAIL-Induced Apoptosis through Upregulation of Death Receptor 4. *Oncol. Rep.* **2020**, *44* (5), 1939–1948. https://doi.org/10.3892/or.2020.7737.
(260) Yoo, J.; Kim, H.-R. C.; Lee, >Yong J. Hyperthermia Enhances Tumour Necrosis Factor-Related Apoptosis-Inducing Ligand (TRAIL)-Induced Apoptosis in Human Cancer Cells. *Int. J. Hyperthermia* **2006**, *22* (8), 713–728. https://doi.org/10.1080/02656730601074052.
(261) Morlé, A.; Garrido, C.; Micheau, O. Hyperthermia Restores Apoptosis Induced by Death Receptors through Aggregation-Induced c-FLIP Cytosolic Depletion. *Cell Death Dis.* **2015**, *6* (2), e1633–e1633. https://doi.org/10.1038/cddis.2015.12.
(262) Ohara, G.; Okabe, K.; Toyama, N.; Ohta, Y.; Xinman, S.; Ichimura, N.; Sato, K.; Urata, Y.; Hibi, H. Hyperthermia Maintains Death Receptor Expression and Promotes TRAIL-Induced Apoptosis. *J. Oral Pathol. Med. Off. Publ. Int. Assoc. Oral Pathol. Am. Acad. Oral Pathol.* **2023**, *52* (8), 718–726. https://doi.org/10.1111/jop.13457.
(263) Katschinski, D. M.; Boos, K.; Schindler, S. G.; Fandrey, J. Pivotal Role of Reactive Oxygen Species as Intracellular Mediators of Hyperthermia-Induced Apoptosis. *J. Biol. Chem.* **2000**, *275* (28), 21094–21098. https://doi.org/10.1074/jbc.M001629200.
(264) Gao, L.; Liu, R.; Gao, F.; Wang, Y.; Jiang, X.; Gao, X. Plasmon-Mediated Generation of Reactive Oxygen Species from near-Infrared Light Excited Gold Nanocages for Photodynamic Therapy in Vitro. *ACS Nano* **2014**, *8* (7), 7260–7271. https://doi.org/10.1021/nn502325j.
(265) Sendoel, A.; Hengartner, M. O. Apoptotic Cell Death Under Hypoxia. *Physiology* **2014**, *29* (3), 168–176. https://doi.org/10.1152/physiol.00016.2013.
(266) Greijer, A. E.; van der Wall, E. The Role of Hypoxia Inducible Factor 1 (HIF-1) in Hypoxia Induced Apoptosis. *J. Clin. Pathol.* **2004**, *57* (10), 1009–1014. https://doi.org/10.1136/jcp.2003.015032.
(267) Guo, K.; Searfoss, G.; Krolikowski, D.; Pagnoni, M.; Franks, C.; Clark, K.; Yu, K. T.; Jaye, M.; Ivashchenko, Y. Hypoxia Induces the Expression of the Pro-Apoptotic Gene BNIP3. *Cell Death Differ.* **2001**, *8* (4), 367–376. https://doi.org/10.1038/sj.cdd.4400810.
(268) Vallelian, F.; Deuel, J. W.; Opitz, L.; Schaer, C. A.; Puglia, M.; Lönn, M.; Engelsberger, W.; Schauer, S.; Karnaukhova, E.; Spahn, D. R.; Stocker, R.; Buehler, P. W.; Schaer, D. J. Proteasome Inhibition and Oxidative Reactions Disrupt Cellular Homeostasis during Heme Stress. *Cell Death Differ.* **2015**, *22* (4), 597–611. https://doi.org/10.1038/cdd.2014.154.
(269) Campbell, N. K.; Fitzgerald, H. K.; Dunne, A. Regulation of Inflammation by the Antioxidant Haem Oxygenase 1. *Nat. Rev. Immunol.* **2021**, *21* (7), 411–425. https://doi.org/10.1038/s41577-020-00491-x.
(270) Chiang, S.-K.; Chen, S.-E.; Chang, L.-C. The Role of HO-1 and Its Crosstalk with Oxidative Stress in Cancer Cell Survival. *Cells* **2021**, *10* (9), 2401. https://doi.org/10.3390/cells10092401.
(271) Abe, K.; Ikeda, S.; Nara, M.; Kitadate, A.; Tagawa, H.; Takahashi, N. Hypoxia-Induced Oxidative Stress Promotes Therapy Resistance via Upregulation of Heme Oxygenase-1 in Multiple Myeloma. *Cancer Med.* **2023**, *12* (8), 9709–9722. https://doi.org/10.1002/cam4.5679.
(272) Luu Hoang, K. N.; Anstee, J. E.; Arnold, J. N. The Diverse Roles of Heme Oxygenase-1 in Tumor Progression. *Front. Immunol.* **2021**, *12*.
(273) Fujiki, Y.; Miyata, N.; Mukai, S.; Okumoto, K.; Cheng, E. H. BAK Regulates Catalase Release from Peroxisomes. *Mol. Cell. Oncol.* **2017**, *4* (3), e1306610. https://doi.org/10.1080/23723556.2017.1306610.

(274) Manco, G.; Porzio, E.; Carusone, T. M. Human Paraoxonase-2 (PON2): Protein Functions and Modulation. *Antioxidants* **2021**, *10* (2), 256. https://doi.org/10.3390/antiox10020256.
(275) Witte, I.; Altenhöfer, S.; Wilgenbus, P.; Amort, J.; Clement, A. M.; Pautz, A.; Li, H.; Förstermann, U.; Horke, S. Beyond Reduction of Atherosclerosis: PON2 Provides Apoptosis Resistance and Stabilizes Tumor Cells. *Cell Death Dis.* **2011**, *2* (1), e112. https://doi.org/10.1038/cddis.2010.91.
(276) Altenhöfer, S.; Witte, I.; Teiber, J. F.; Wilgenbus, P.; Pautz, A.; Li, H.; Daiber, A.; Witan, H.; Clement, A. M.; Förstermann, U.; Horke, S. One Enzyme, Two Functions: PON2 PREVENTS MITOCHONDRIAL SUPEROXIDE FORMATION AND APOPTOSIS INDEPENDENT FROM ITS LACTONASE ACTIVITY*. *J. Biol. Chem.* **2010**, *285* (32), 24398–24403. https://doi.org/10.1074/jbc.M110.118604.
(277) Pucci, B.; Kasten, M.; Giordano, A. Cell Cycle and Apoptosis. *Neoplasia N. Y. N* **2000**, *2* (4), 291–299.
(278) Kreis, N.-N.; Louwen, F.; Yuan, J. The Multifaceted P21 (Cip1/Waf1/CDKN1A) in Cell Differentiation, Migration and Cancer Therapy. *Cancers* **2019**, *11* (9), 1220. https://doi.org/10.3390/cancers11091220.
(279) Kuang, Y.; Kang, J.; Li, H.; Liu, B.; Zhao, X.; Li, L.; Jin, X.; Li, Q. Multiple Functions of P21 in Cancer Radiotherapy. *J. Cancer Res. Clin. Oncol.* **2021**, *147* (4), 987–1006. https://doi.org/10.1007/s00432-021-03529-2.
(280) Hiromura, K.; Pippin, J. W.; Fero, M. L.; Roberts, J. M.; Shankland, S. J. Modulation of Apoptosis by the Cyclin-Dependent Kinase Inhibitor $P27^{Kip1}$. *J. Clin. Invest.* **1999**, *103* (5), 597–604. https://doi.org/10.1172/JCI5461.
(281) Abbastabar, M.; Kheyrollah, M.; Azizian, K.; Bagherlou, N.; Tehrani, S. S.; Maniati, M.; Karimian, A. Multiple Functions of P27 in Cell Cycle, Apoptosis, Epigenetic Modification and Transcriptional Regulation for the Control of Cell Growth: A Double-Edged Sword Protein. *DNA Repair* **2018**, *69*, 63–72. https://doi.org/10.1016/j.dnarep.2018.07.008.
(282) Supriatno, null; Harada, K.; Hoque, M. O.; Bando, T.; Yoshida, H.; Sato, M. Overexpression of P27(Kip1) Induces Growth Arrest and Apoptosis in an Oral Cancer Cell Line. *Oral Oncol.* **2002**, *38* (7), 730–736. https://doi.org/10.1016/s1368-8375(02)00011-8.
(283) Katner, A. L.; Gootam, P.; Hoang, Q. B. L.; Gnarra, J. R.; Rayford, W. A Recombinant Adenovirus Expressing P7(Kip1) Induces Cell Cycle Arrest and Apoptosis in Human 786-0 Renal Carcinoma Cells. *J. Urol.* **2002**, *168* (2), 766–773.
(284) Aubrey, B. J.; Kelly, G. L.; Janic, A.; Herold, M. J.; Strasser, A. How Does P53 Induce Apoptosis and How Does This Relate to P53-Mediated Tumour Suppression? *Cell Death Differ.* **2018**, *25* (1), 104–113. https://doi.org/10.1038/cdd.2017.169.
(285) Lim, Y.; Dorstyn, L.; Kumar, S. The P53-Caspase-2 Axis in the Cell Cycle and DNA Damage Response. *Exp. Mol. Med.* **2021**, *53* (4), 517–527. https://doi.org/10.1038/s12276-021-00590-2.
(286) Yogosawa, S.; Yoshida, K. Tumor Suppressive Role for Kinases Phosphorylating P53 in DNA Damage-Induced Apoptosis. *Cancer Sci.* **2018**, *109* (11), 3376–3382. https://doi.org/10.1111/cas.13792.
(287) Pitolli, C.; Wang, Y.; Candi, E.; Shi, Y.; Melino, G.; Amelio, I. P53-Mediated Tumor Suppression: DNA-Damage Response and Alternative Mechanisms. *Cancers* **2019**, *11* (12), 1983. https://doi.org/10.3390/cancers11121983.
(288) Castrogiovanni, C.; Waterschoot, B.; De Backer, O.; Dumont, P. Serine 392 Phosphorylation Modulates P53 Mitochondrial Translocation and Transcription-Independent Apoptosis. *Cell Death Differ.* **2018**, *25* (1), 190–203. https://doi.org/10.1038/cdd.2017.143.
(289) Feng, L.; Hollstein, M.; Xu, Y. Ser46 Phosphorylation Regulates P53-Dependent Apoptosis and Replicative Senescence. *Cell Cycle* **2006**, *5* (23), 2812–2819. https://doi.org/10.4161/cc.5.23.3526.
(290) Diesing, K.; Ribback, S.; Winter, S.; Gellert, M.; Oster, A. M.; Stühler, V.; Gläser, E.; Adler, F.; Hartwig, C.; Scharpf, M.; Bedke, J.; Burchardt, M.; Schwab, M.; Lillig, C. H.; Kroeger, N. P53 Is Functionally Inhibited in Clear Cell Renal Cell Carcinoma (CcRCC): A Mechanistic and Correlative Investigation into Genetic and Molecular Characteristics. *J. Cancer Res. Clin. Oncol.* **2021**, *147* (12), 3565–3576. https://doi.org/10.1007/s00432-021-03786-1.
(291) Wang, X.; Zou, L.; Lu, T.; Bao, S.; Hurov, K. E.; Hittelman, W. N.; Elledge, S. J.; Li, L. Rad17 Phosphorylation Is Required for Claspin Recruitment and Chk1 Activation in Response to Replication Stress. *Mol. Cell* **2006**, *23* (3), 331–341. https://doi.org/10.1016/j.molcel.2006.06.022.
(292) Post, S.; Weng, Y.-C.; Cimprich, K.; Chen, L. B.; Xu, Y.; Lee, E. Y.-H. P. Phosphorylation of Serines 635 and 645 of Human Rad17 Is Cell Cycle Regulated and Is Required for G1/S Checkpoint Activation in Response to DNA Damage. *Proc. Natl. Acad. Sci.* **2001**, *98* (23), 13102–13107. https://doi.org/10.1073/pnas.231364598.
(293) Smits, V. A. J.; Cabrera, E.; Freire, R.; Gillespie, D. A. Claspin – Checkpoint Adaptor and DNA Replication Factor. *FEBS J.* **2019**, *286* (3), 441–455. https://doi.org/10.1111/febs.14594.
(294) Hsiao, H.-W.; Yang, C.-C.; Masai, H. Roles of Claspin in Regulation of DNA Replication, Replication Stress Responses and Oncogenesis in Human Cells. *Genome Instab. Dis.* **2021**, *2* (5), 263–280. https://doi.org/10.1007/s42764-021-00049-8.

(295) Clarke, C. A. L.; Bennett, L. N.; Clarke, P. R. Cleavage of Claspin by Caspase-7 during Apoptosis Inhibits the Chk1 Pathway*. *J. Biol. Chem.* **2005**, *280* (42), 35337–35345. https://doi.org/10.1074/jbc.M506460200.
(296) Semple, J. I.; Smits, V. a. J.; Fernaud, J.-R.; Mamely, I.; Freire, R. Cleavage and Degradation of Claspin during Apoptosis by Caspases and the Proteasome. *Cell Death Differ.* **2007**, *14* (8), 1433–1442. https://doi.org/10.1038/sj.cdd.4402134.
(297) Garcia, M. P.; Cavalheiro, J. R. T.; Fernandes, M. H. Acute and Long-Term Effects of Hyperthermia in B16-F10 Melanoma Cells. *PLoS ONE* **2012**, *7* (4), 1–9. https://doi.org/10.1371/journal.pone.0035489.
(298) Zhang, Y.; Zhan, X.; Xiong, J.; Peng, S.; Huang, W.; Joshi, R.; Cai, Y.; Liu, Y.; Li, R.; Yuan, K.; Zhou, N.; Min, W. Temperature-Dependent Cell Death Patterns Induced by Functionalized Gold Nanoparticle Photothermal Therapy in Melanoma Cells. *Sci. Rep.* **2018**, *8* (1), 1–9. https://doi.org/10.1038/s41598-018-26978-1.
(299) Häcker, G.; Haimovici, A. Sub-Lethal Signals in the Mitochondrial Apoptosis Apparatus: Pernicious by-Product or Physiological Event? *Cell Death Differ.* **2023**, *30* (2), 250–257. https://doi.org/10.1038/s41418-022-01058-0.
(300) Martini, H.; Passos, J. F. Cellular Senescence: All Roads Lead to Mitochondria. *FEBS J.* **2023**, *290* (5), 1186–1202. https://doi.org/10.1111/febs.16361.
(301) Kumar, B. V.; Connors, T.; Farber, D. L. Human T Cell Development, Localization, and Function throughout Life. *Immunity* **2018**, *48* (2), 202–213. https://doi.org/10.1016/j.immuni.2018.01.007.
(302) Abraham, R. T.; Weiss, A. Jurkat T Cells and Development of the T-Cell Receptor Signalling Paradigm. *Nat. Rev. Immunol.* **2004**, *4* (4), 301–308. https://doi.org/10.1038/nri1330.
(303) Carrasco-Padilla, C.; Aguilar-Sopeña, O.; Gómez-Morón, A.; Alegre-Gómez, S.; Sánchez-Madrid, F.; Martín-Cófreces, N. B.; Roda-Navarro, P. T Cell Activation and Effector Function in the Human Jurkat T Cell Model. *Methods Cell Biol.* **2023**, *178*, 25–41. https://doi.org/10.1016/bs.mcb.2022.09.012.
(304) Schutte, R. J.; Parisi-Amon, A.; Reichert, W. M. Cytokine Profiling Using Monocytes/Macrophages Cultured on Common Biomaterials with a Range of Surface Chemistries. *J. Biomed. Mater. Res. A* **2009**, *88* (1), 128–139. https://doi.org/10.1002/jbm.a.31863.
(305) Deckers, J.; Anbergen, T.; Hokke, A. M.; de Dreu, A.; Schrijver, D. P.; de Bruin, K.; Toner, Y. C.; Beldman, T. J.; Spangler, J. B.; de Greef, T. F. A.; Grisoni, F.; van der Meel, R.; Joosten, L. A. B.; Merkx, M.; Netea, M. G.; Mulder, W. J. M. Engineering Cytokine Therapeutics. *Nat. Rev. Bioeng.* **2023**, *1* (4), 286–303. https://doi.org/10.1038/s44222-023-00030-y.
(306) Zynda, E. R.; Grimm, M. J.; Yuan, M.; Zhong, L.; Mace, T. A.; Capitano, M.; Ostberg, J. R.; Lee, K. P.; Pralle, A.; Repasky, E. A. A Role for the Thermal Environment in Defining Co-Stimulation Requirements for CD4+ T Cell Activation. *Cell Cycle* **2015**, *14* (14), 2340–2354. https://doi.org/10.1080/15384101.2015.1049782.
(307) Bear, A. S.; Kennedy, L. C.; Young, J. K.; Perna, S. K.; Almeida, J. P. M.; Lin, A. Y.; Eckels, P. C.; Drezek, R. A.; Foster, A. E. Elimination of Metastatic Melanoma Using Gold Nanoshell-Enabled Photothermal Therapy and Adoptive T Cell Transfer. *PLOS ONE* **2013**, *8* (7), e69073. https://doi.org/10.1371/journal.pone.0069073.
(308) Israelsson, P.; Dehlin, E.; Nagaev, I.; Lundin, E.; Ottander, U.; Mincheva-Nilsson, L. Cytokine MRNA and Protein Expression by Cell Cultures of Epithelial Ovarian Cancer—Methodological Considerations on the Choice of Analytical Method for Cytokine Analyses. *Am. J. Reprod. Immunol.* **2020**, *84* (1), e13249. https://doi.org/10.1111/aji.13249.
(309) Remtulla, A. H. K. Reactive Oxygen Species in Protein Sulphenic Acid Formation during T Cell Activation; Implications for Rheumatoid Arthritis.
(310) Minagawa, K.; Wakahashi, K.; Kawano, H.; Nishikawa, S.; Fukui, C.; Kawano, Y.; Asada, N.; Sato, M.; Sada, A.; Katayama, Y.; Matsui, T. Posttranscriptional Modulation of Cytokine Production in T Cells for the Regulation of Excessive Inflammation by TFL. *J. Immunol.* **2014**, *192* (4), 1512–1524. https://doi.org/10.4049/jimmunol.1301619.
(311) Oh, B.-R.; Chen, P.; Nidetz, R.; McHugh, W.; Fu, J.; Shanley, T. P.; Cornell, T. T.; Kurabayashi, K. Multiplexed Nanoplasmonic Temporal Profiling of T-Cell Response under Immunomodulatory Agent Exposure. *ACS Sens.* **2016**, *1* (7), 941–948. https://doi.org/10.1021/acssensors.6b00240.
(312) Sullivan, K. E.; Cutilli, J.; Piliero, L. M.; Ghavimi-Alagha, D.; Starr, S. E.; Campbell, D. E.; Douglas, S. D. Measurement of Cytokine Secretion, Intracellular Protein Expression, and MRNA in Resting and Stimulated Peripheral Blood Mononuclear Cells. *Clin. Diagn. Lab. Immunol.* **2000**, *7* (6), 920–924.
(313) Benson, J. C.; Romito, O.; Abdelnaby, A. E.; Xin, P.; Pathak, T.; Weir, S. E.; Kirk, V.; Castaneda, F.; Yoast, R. E.; Emrich, S. M.; Tang, P. W.; Yule, D. I.; Hempel, N.; Potier-Cartereau, M.; Sneyd, J.; Trebak, M. A Multiple-Oscillator Mechanism Underlies Antigen-Induced Ca2+ Oscillations in Jurkat T-Cells. *J. Biol. Chem.* **2023**, *299* (11), 105310. https://doi.org/10.1016/j.jbc.2023.105310.
(314) Finnerty, C. C.; Przkora, R.; Herndon, D. N.; Jeschke, M. G. Cytokine Expression Profile over Time in Burned Mice. *Cytokine* **2009**, *45* (1), 20–25. https://doi.org/10.1016/j.cyto.2008.10.005.

(315) Bucharskaya, A. B.; Maslyakova, G. N.; Terentyuk, G. S.; Afanasyeva, G. A.; Navolokin, N. A.; Zakharova, N. B.; Khlebtsov, B. N.; Khlebtsov, N. G.; Bashkatov, A. N.; Genina, E. A.; Tuchin, V. V. The Inflammation Markers in Serum of Tumor-Bearing Rats after Plasmonic Photothermal Therapy. In *Biophotonics and Immune Responses XIII*; SPIE, 2018; Vol. 10495, pp 96–101. https://doi.org/10.1117/12.2289369.

(316) Zhou, J.; Lu, Z.; Zhu, X.; Wang, X.; Liao, Y.; Ma, Z.; Li, F. NIR Photothermal Therapy Using Polyaniline Nanoparticles. *Biomaterials* **2013**, *34* (37), 9584–9592. https://doi.org/10.1016/j.biomaterials.2013.08.075.

(317) Choi, J.-H.; Lee, J.; Shin, W.; Choi, J.-W.; Kim, H. J. Priming Nanoparticle-Guided Diagnostics and Therapeutics towards Human Organs-on-Chips Microphysiological System. *Nano Converg.* **2016**, *3* (1), 24. https://doi.org/10.1186/s40580-016-0084-8.

(318) Cunin, P.; Beauvillain, C.; Miot, C.; Augusto, J.-F.; Preisser, L.; Blanchard, S.; Pignon, P.; Scotet, M.; Garo, E.; Fremaux, I.; Chevailler, A.; Subra, J.-F.; Blanco, P.; Wilson, M. R.; Jeannin, P.; Delneste, Y. Clusterin Facilitates Apoptotic Cell Clearance and Prevents Apoptotic Cell-Induced Autoimmune Responses. *Cell Death Dis.* **2016**, *7* (5), e2215–e2215. https://doi.org/10.1038/cddis.2016.113.

(319) Jaiswal, P. K.; Goel, A.; Mittal, R. D. Survivin: A Molecular Biomarker in Cancer. *Indian J. Med. Res.* **2015**, *141* (4), 389–397. https://doi.org/10.4103/0971-5916.159250.

(320) Altieri, D. C. Molecular Circuits of Apoptosis Regulation and Cell Division Control: The Survivin Paradigm. *J. Cell. Biochem.* **2004**, *92* (4), 656–663. https://doi.org/10.1002/jcb.20140.

(321) Song, Z.; Yao, X.; Wu, M. Direct Interaction between Survivin and Smac/DIABLO Is Essential for the Anti-Apoptotic Activity of Survivin during Taxol-Induced Apoptosis*. *J. Biol. Chem.* **2003**, *278* (25), 23130–23140. https://doi.org/10.1074/jbc.M300957200.

(322) Sah, N. K.; Khan, Z.; Khan, G. J.; Bisen, P. S. Structural, Functional and Therapeutic Biology of Survivin. *Cancer Lett.* **2006**, *244* (2), 164–171. https://doi.org/10.1016/j.canlet.2006.03.007.

(323) Ma, L.; Huang, Y.; Song, Z.; Feng, S.; Tian, X.; Du, W.; Qiu, X.; Heese, K.; Wu, M. Livin Promotes Smac/DIABLO Degradation by Ubiquitin–Proteasome Pathway. *Cell Death Differ.* **2006**, *13* (12), 2079–2088. https://doi.org/10.1038/sj.cdd.4401959.

(324) Abd-Elrahman, I.; Hershko, K.; Neuman, T.; Nachmias, B.; Perlman, R.; Ben-Yehuda, D. The Inhibitor of Apoptosis Protein Livin (ML-IAP) Plays a Dual Role in Tumorigenicity. *Cancer Res.* **2009**, *69* (13), 5475–5480. https://doi.org/10.1158/0008-5472.CAN-09-0424.

(325) Abd-Elrahman, I.; Nassar, T.; Khairi, N.; Perlman, R.; Benita, S.; Ben Yehuda, D. Novel Targeted MtLivin Nanoparticles Treatment for Disseminated Diffuse Large B-Cell Lymphoma. *Oncogene* **2021**, *40* (2), 334–344. https://doi.org/10.1038/s41388-020-01529-z.

(326) Szliszka, E.; Mazur, B.; Zydowicz, G.; Czuba, Z. P.; Król, W. TRAIL-Induced Apoptosis and Expression of Death Receptor TRAIL-R1 and TRAIL-R2 in Bladder Cancer Cells. *Folia Histochem. Cytobiol.* **2009**, *47* (4), 579–585. https://doi.org/10.2478/v10042-009-0111-2.

(327) Li, H.-S.; Zhou, Y.-N.; Li, L.; Li, S.-F.; Long, D.; Chen, X.-L.; Zhang, J.-B.; Feng, L.; Li, Y.-P. HIF-1α Protects against Oxidative Stress by Directly Targeting Mitochondria. *Redox Biol.* **2019**, *25*, 101109. https://doi.org/10.1016/j.redox.2019.101109.

(328) Kang, M. Y.; Kim, H.-B.; Piao, C.; Lee, K. H.; Hyun, J. W.; Chang, I.-Y.; You, H. J. The Critical Role of Catalase in Prooxidant and Antioxidant Function of P53. *Cell Death Differ.* **2013**, *20* (1), 117–129. https://doi.org/10.1038/cdd.2012.102.

Annex A

The information contained in this annex complements the data and text presented in Chapter 5 of this dissertation. All graphs and data featured in this annex are referenced in the main text. The content provided here serves as supplementary material to the figures shown in the main body.

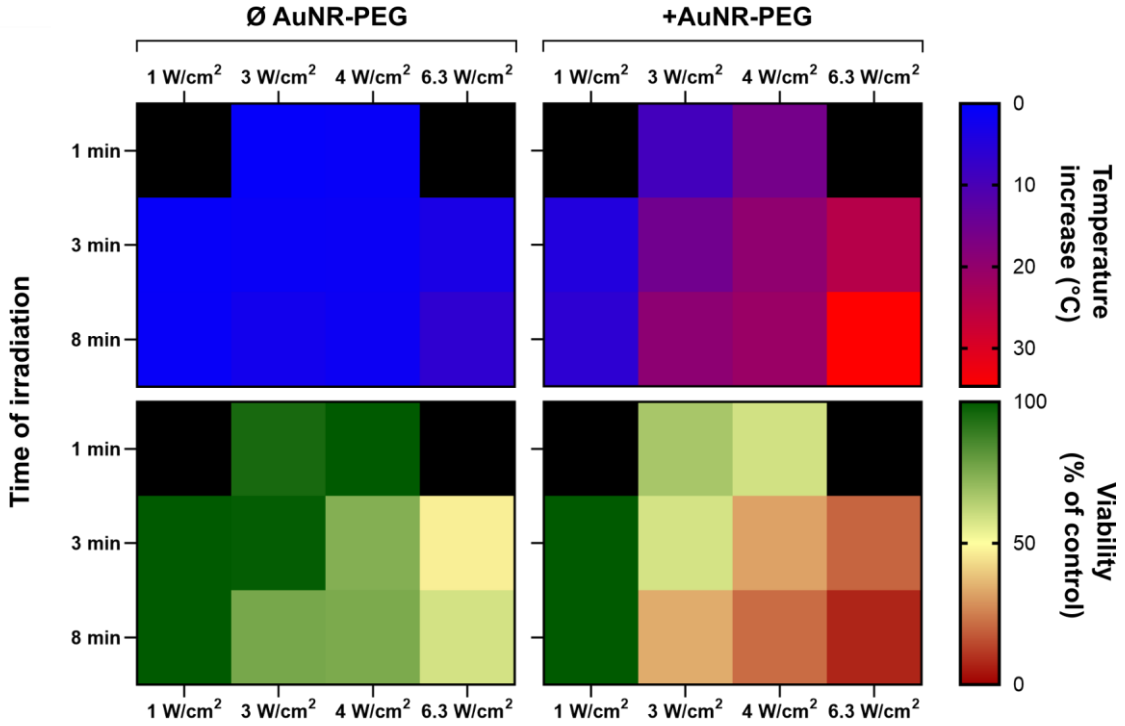

Figure S.5. 1. Cellular viability (%) and temperature increase (°C) of cells with (+AuNR-PEG) and without (ØAuNR-PEG) irradiated. Cellular viability (%) was measured with MTT relative to controls (not irradiated, ØAuNR-PEG). Temperature increase calculated as difference from initial temperature to maximum temperature achieved.

Annex B

The information contained in this annex complements the data and text presented in Chapter 6 of this dissertation. All graphs and data featured in this annex are referenced in the main text. The content provided here serves as supplementary material to the figures shown in the main body.

A

1 nM	786-0	A549	HepG2	Hek293	NL20
A549	0.018				
HepG2	0.127	0.165			
Hek293	0.018	0.018	0.018		
NL20	0.011	0.011	0.011	0.018	
THLE-3	0.302	0.040	0.071	0.429	0.714

2 nM	786-0	A549	HepG2	Hek293	NL20
A549	0.011				
HepG2	0.042	0.519			
Hek293	0.020	0.020	0.020		
NL20	0.277	0.011	0.011	0.020	
THLE-3	0.208	0.040	0.040	0.078	0.714

5 nM	786-0	A549	HepG2	Hek293	NL20
A549	0.039				
HepG2	0.032	1.000			
Hek293	0.024	0.024	0.024		
NL20	0.011	0.011	0.011	0.143	
THLE-3	0.277	0.039	0.039	0.091	0.631

B

786-0			p-val
0 nM	vs	1 nM	0.009
1 nM	vs	2 nM	>0.05
2 nM	vs	5 nM	<0.0001

Hek293			p-val
0 nM	vs	1 nM	>0.05
1 nM	vs	2 nM	>0.05
2 nM	vs	5 nM	>0.05

A549			p-val
0 nM	vs	1 nM	0.028
1 nM	vs	2 nM	0.041
2 nM	vs	5 nM	0.006

NL20			p-val
0 nM	vs	1 nM	0.023
1 nM	vs	2 nM	0.004
2 nM	vs	5 nM	0.004

HepG2			p-val
0 nM	vs	1 nM	0.045
1 nM	vs	2 nM	>0.05
2 nM	vs	5 nM	<0.0001

THLE-3			p-val
0 nM	vs	1 nM	>0.05
1 nM	vs	2 nM	>0.05
2 nM	vs	5 nM	0.047

Figure S.6. 1 Tables showcasing statistics on uptake differences. A) Differences on uptake as a function of the cell type. The flag highlights those comparisons that are statistically significant.B) Differences on uptake as a function of concentration within each cell type.

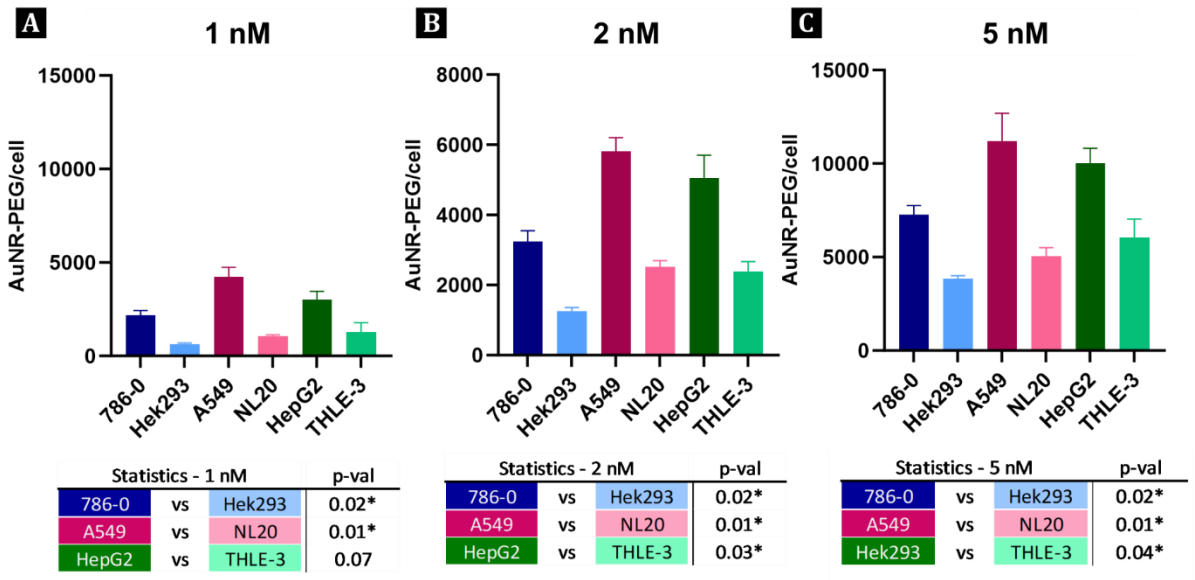

*Figure S.6.2. Uptake of AuNRPEG at 1 nM, 2 nM and 5 nM (52, 104 and 260 ug/mL gold). *p<0.05, **p<0.01, ***p<0.001. Error bars represent SEM (n=3-6).*

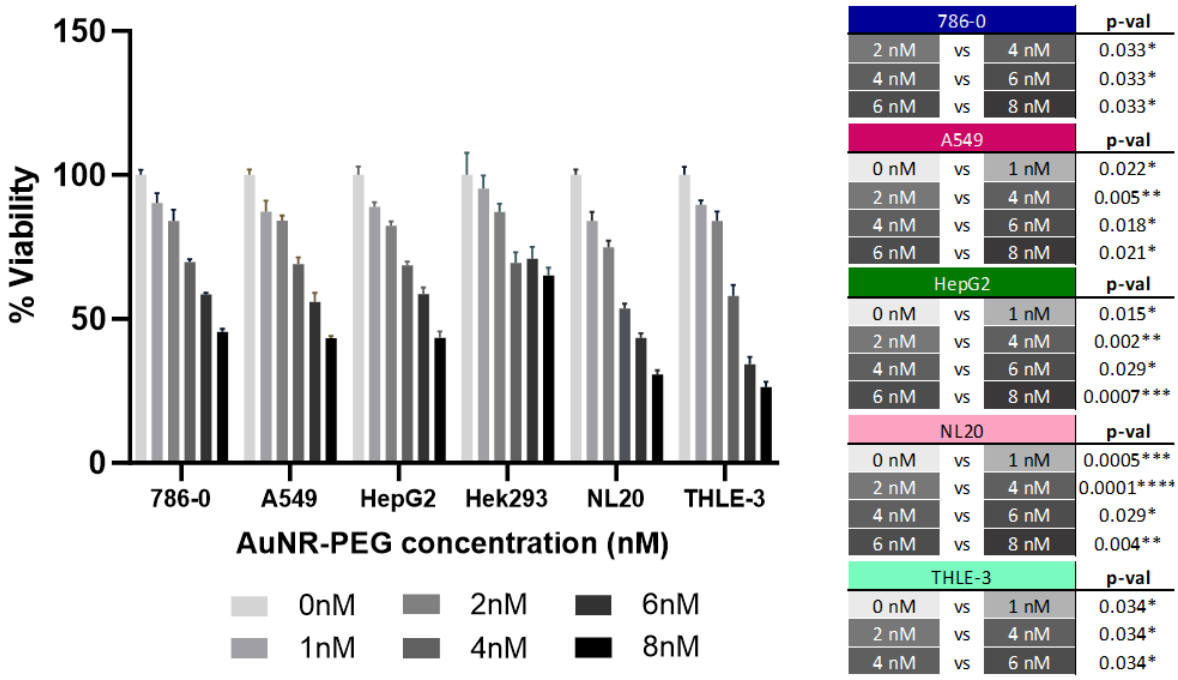

*Figure S.6.3. Effect of AuNR-PEG concentration on cellular viability. Error bars represent SEM (n=4). Table displays the statistical comparison within each cell line of the different concentrations. Only statistically and clinically relevant data is shown. *p ≤ 0.05; **p ≤ 0.01; ***p ≤ 0.001*

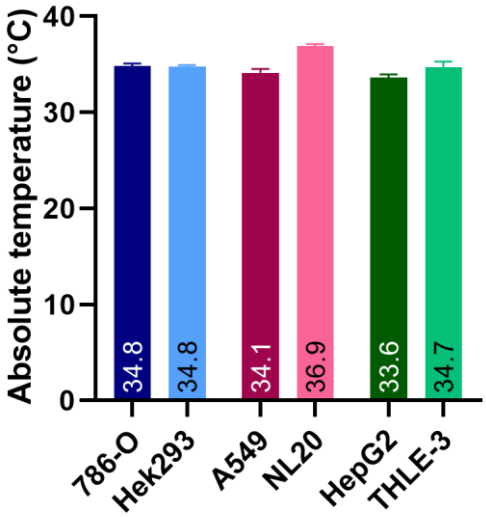

Figure S.6.6. Averaged absolute increases of temperature of cells without AuNR-PEG. Cell lines were irradiated with a 808 nm laser light at 3 W/cm² during 3 minutes.

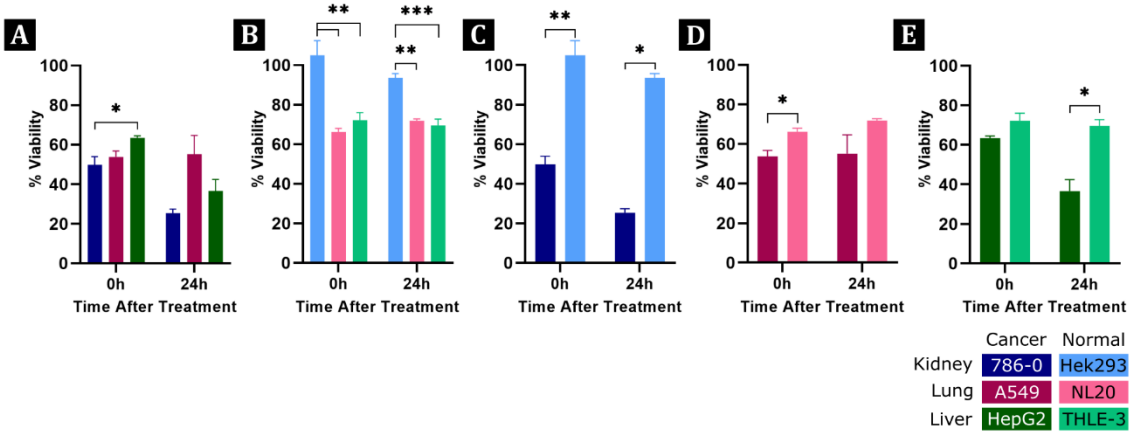

*Figure S.6.5. Cellular viability (%) after treatment assessed with MTT assay. A) Cancer cell lines, B) non-cancerous cell lines, C) kidney, D) lung and E) liver cellular viability for + AuNR-PEG cells at 0 and 24 hours after treatment. Statistical comparisons were made using Tukey/Wilcox post hoc tests. *p ≤ 0.05; **p ≤ 0.01; ***p ≤ 0.001; n.s.: not significant.*

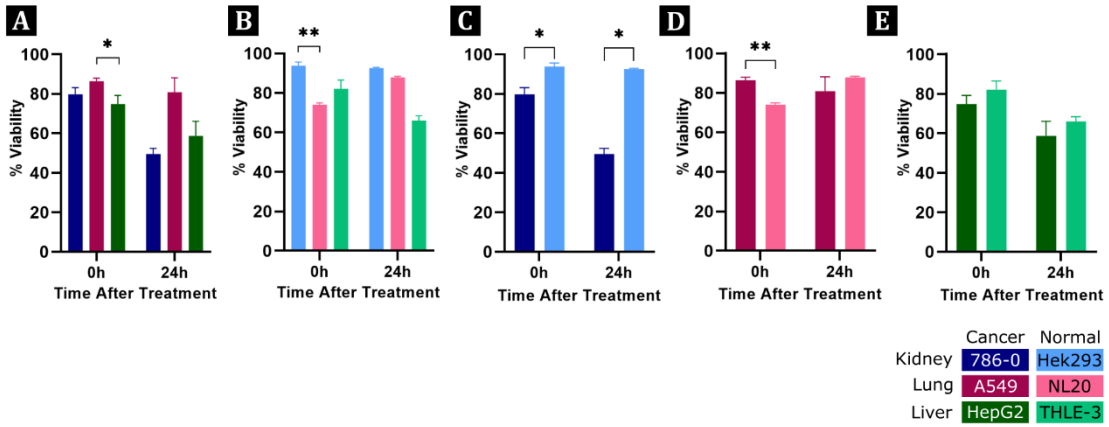

*Figure S.6.4. Cellular viability (%) after treatment assessed with TB assay. A) Cancer cell lines, B) non-cancerous cell lines, C) kidney, D) lung and E) liver cellular viability for + AuNR-PEG cells at 0 and 24 hours after treatment. Statistical comparisons were made using Tukey/Wilcox post hoc tests. *p ≤ 0.05; **p ≤ 0.01; ***p ≤ 0.001; n.s.:*

Annex C

The information contained in this annex complements the data and text presented in Chapter 7 of this dissertation. All graphs and data featured in this annex are referenced in the main text. The content provided here serves as supplementary material to the figures shown in the main body.

7.1.2.1. Hsp27

Small Hsps (<40 kDa), such as Hsp27, usually do not directly interfere with protein folding, but stabilise other proteins during stressful conditions to prevent protein precipitation.[7,93] Hsp27 prevents downstream mitochondrial damage and formation of the apoptosome by binding to cytochrome C and regulating mitochondrial stability.[97,221]

Additionally, it also interferes with Fas-mediated apoptosis signalling, part of the extrinsic pathway of apoptosis, binding to Fas receptors and preventing their interaction with other pro-apoptotic proteins.[95] Hsp27 works very closely with Hsp70 and Hsp90, and their interactions are crucial for their functionality.

7.1.2.2. Hsp60

Hsp60, also known as chaperonin or GroEL, functions as cytoprotective chaperone upon protein denaturation. Hsp60 forms an inner ring in which unfolded proteins have an opportunity to correctly assemble, essential in crowded cytosolic environments.[225]

Although Hsp60 is mainly considered to be anti-apoptotic, the interaction between Hsp60 and other proteins in specific cell types and situations (e.g. Jurkat cells) is believed to be pro-apoptotic by forming a complex with caspase 3 that leads to its maturation.[98,226] In the case of clear cell renal carcinoma (ccRCC), Hsp60 is downregulated, triggering ROS production and tumour progression.[227] The function of Hsp60 is highly discussed in normal healthy cells vs cancerous cells, being considered anti-apoptotic in the first group, but apoptotic in cancerous cells.

7.1.2.3. Hsp70

In addition to the core roles stated in the main text, Hsp70 also interferes with the extrinsic pathway of apoptosis by disturbing death receptor-mediated apoptosis through interaction with TRAIL-1 and TRAIL-2 receptors, blocking the recruitment of caspase 8 and activation of initiator caspases.[98]

Therefore, Hsp70 is an essential chaperone during a stress event and cellular recovery, as it mediates cellular survival and allows adaptation to stressful and lethal conditions[221] by controlling protein traffic and degradation of denatured proteins. Hsp70 is largely considered an anti-apoptotic protein.

7.1.2.4. Clusterin

Clusterin is a secreted multifunctional protein that upon stress-induced precipitation of unfolded proteins, it acts as a chaperone.[228,229] Although it does not have an active role in refolding proteins, clusterin forms a high molecular weight complex that allows stressed proteins in their non-native state to be solubilised and recovered by associating with Hsp70.[220] Clusterin can bind to a wide range of molecules, participating in controlling cell proliferation and apoptosis.[318] As Hsp70, clusterin interferes with Bax activation, blocking its pro-apoptotic effects.[230]

Upon chemical or heat-induced stress, clustering avoids aggregation of proteins *in vitro*, but this effect is mostly observed in slowly aggregating proteins, indicating that chaperons acting as chaperones recognise preferentially partially unfolded proteins.[220] Moreover, clustering can improve the clearance of late apoptotic cells by phagocytosis by macrophages, binding to histones that work as “eat-me” signals.[318]

Clusterin potentiates a rapid and efficient efferocytosis (process by which dying or dead cells are removed by phagocytic cells, preventing and inflammation response and promoting tissue homeostasis), avoiding the development of secondary necrotic cells and maintaining self-tolerance. The absence of phagocytosis of apoptotic cells develops to secondary necrosis, allowing antigen presenting cells (APCs) to produce inflammatory mediators. Lack of clusterin decreases tolerance to self-antigens, as APCs will present apoptotic cell antigens.[318]

7.1.4.1. Smac/Diablo

Smac/Diablo obtains its name from the initials of its main roles within the cell: Second mitochondria-derived activator of caspase (Smac)[61] and Direct inhibitor of apoptosis-binding protein with low pI (Diablo).[237] In homeostasis, Smac is found inside the mitochondria, but when an apoptotic signal is detected by the cell, and the MOMP is formed, it is released into the cytoplasm.

Smac neutralises the effect of inhibitor of apoptosis (IAP) proteins, preventing their interaction with caspases and releasing them to form the apoptosome and activate executor caspase 3.[237] Its method of action is to physically bind to IAPs, lowering the intrinsic ubiquitin-ligase function of these inhibitors.[239] This reduces the targeting and destruction of caspases. Therefore, an increase in the expression of Smac/Diablo is representative of apoptosis, as it lowers the apoptotic threshold for cells after a death stimulus.[238] Overexpression of Smac/Diablo sensitises cells to chemotherapeutic drugs.[239]

7.1.4.2. Htra2/Omi

Htra2/Omi, or high temperature requirement protein A2, is a pro-apoptotic protein that reduces the activity of IAPs by incapacitating them. Htra2/Omi is a serine protease that can cleave IAPs, reducing their capacity to inhibit caspases In contrast to Smac/Diablo, which labelled IAPs for elimination, Htra2/Omi directly cleaves IAPs and disables them irreversibly.[240,241] This protein, when released into to the cytoplasm, recognises IAPs through their IAP-binding motif. Upon contact, it unleashes its proteolytic function and cleaves IAPs. Increases of Htra2/Omi are associated with apoptosis promotion, as it efficiently removes their inhibitors, rendering cells susceptible to death signals and drugs.[240,241]

7.1.5.2. Survivin and Livin

Survivin can exert its anti-apoptotic functions and suppressing cell death in a variety of ways. Its expression highly correlates with aggressive tumours and poor therapeutical outcomes, whereas healthy tissues almost have no expression of survivin, making it an attractive target for cancer diagnostic and treatment.[319]

Survivin prevents apoptosis by targeting caspases and preventing the formation of the apoptosome, interacting with XIAP to increase its stability, and sequestering Smac/Diablo (Figure S.7.1-A).[319–321] On top of the caspase dependent and independent methods to block apoptosis, survivin is a direct target of p53, who represses its actions. p53 downregulates the anti-apoptotic action of surviving, so p53 loss results in an upregulation of surviving expression, although this activity is still poorly understood.[249,319,322] The role of survivin on chromosome segregation during cell division is to ensure that dividing cells preserve an anti-apoptotic environment.

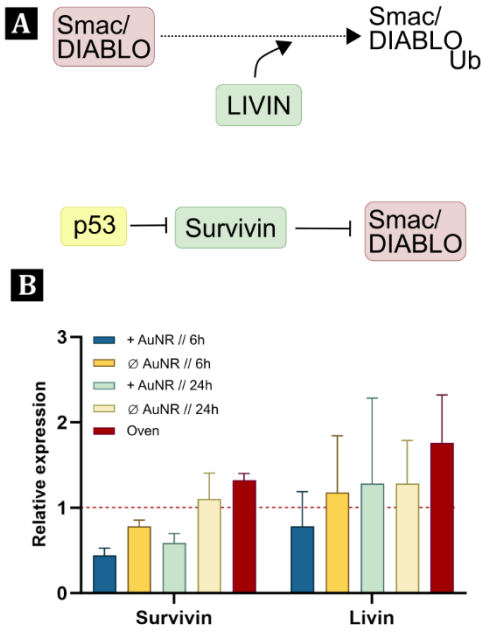

Figure S.7.1. Survivin and Livin role in apoptosis A) Schematic representation of the interaction of Survivin and Livin with pro-apoptotic proteins. B) Graph depicting relative expression of Bad, Bax and Bcl-2. No statistically significant differences were detected.

After an hyperthermic event, the expression of survivin is reduced when hyperthermia is induced by PPTT, but slightly increased if it happens in an oven. ($p \geq 0.05$). Cells without AuNR-PEG irradiated experienced a decrease in expression 6 hours after illumination but normalised 24 hours later. Overall, the expression of surviving is not indicative of a clear pro- or anti-apoptotic profile after PPTT or oven hyperthermia, indicating that other anti-apoptotic proteins may have more relevant roles after exposure to elevated temperatures.

In CaSki cells,[81] survivin expression markedly decreased 6 and 24 hours after conventional hyperthermia at 45-47°C, correlating with an increase of up-regulation of caspase 3 and increase on the expression of Smac/Diablo. In our case, we do not observe this same trend, indicating that PPTT cell affects the apoptotic pathway in a distinct way.

Livin is a protein with a reduced half-term life, estimated to be of 4 hours. It has E3-ubiquitine ligase activity, able to directly target Smac/Diablo for proteasomal degradation. Its own instability is the result of auto-ubiquitination, promoted by the RING domain on livin.[323] Although its main roles are anti-apoptotic, upon a strong apoptotic stimuli, livin can be cleaved by caspases, forming a truncated form that has the capacity to induce both apoptosis, and necrosis on different cell lines.[324,325]

Livin shows relatively consistent expression between all studied samples and controls, with no statistically significant differences between any of them ($p \geq 0.05$). This could be due to its relatively short-term half-life, which may explain the enormous differences on expression within the same conditions (Figure S.7.1-B)

7.1.6. Receptors involved in extrinsic apoptosis

Of the four receptors analysed in the human apoptosis kit, three of them (TRAIL R1/DR4, TRAIL R2/DR5 and Fas/TNRFRSF6/CD95) are direct activators of apoptosis upon binding of their respective ligands, TRAIL (TNF Receptor Apoptosis-Inducing Ligand) and FasL. On the other hand, TNF R1/TNFRSF1A (TNFR1 for short) can exert both pro- and anti-apoptotic effects depending on which downstream proteins are activated or stabilised.[83,87,253]

TRAIL R1 and TRAIL R2 are type II transmembrane proteins. TRAIL R1 and R2 are type II transmembrane proteins. Binding of TRAIL results in trimerization of R1 and R2, forming the DISC complex (death-inducing signalling complex), capable of FADD (Fas-associated protein death domain) recruitment and posterior activation of initiator caspases, such as Caspase-8 (Figure 7.1.). Formation of the DISC (death-inducing signalling complex) recruits other pro-caspases and signals downstream for apoptosis induction. The activation of caspase-8 can at the same time lead to truncation of Bid, allowing them to interact with Bcl-2 protein family members and intensifying the intrinsic apoptotic pathway by taking part in the permeabilization of the mitochondria.[254,255]

These two proteins interactions are very similar, involving the enrolment of FADD, expressing functional redundancy upon binding their ligand.[255] TRAIL R1 and R2 are stress-induced genes, and their protein expression is upregulated with increased expression of certain transcription factors, such as p53. Increases in the expression of p53 sensitise cancer cells to apoptosis.[256] On the other hand, lack of expression of these receptors render cells insensitive to TRAIL-induced extrinsic apoptosis.[254,326]

Fas receptor activates very similarly to TRAIL R1 and R2. Upon binding of FasL (Fas Ligand), there is a trimerization of the receptor, recruiting FADD and allowing the formation of the DISC together with caspase-8. FADD is therefore a key mediator for death receptor apoptosis, acting as a bridge between receptors being activated after ligand binding and recruitment of initiator caspases and other associated proteins.[257,258]

FADD is also involved in the activation of TNFR1 mediated apoptosis. Upon TNFα binding to the receptor, trimerization occurs and creation of a platform for recruitment of several proteins (Figure7.7-A) and formation of the complex I. Within this complex, TRADD can activate the NF-κB pathway

which leads to apoptosis blockage by a complex interaction of several proteins. Nonetheless, if RIPK1, a protein from complex I is deubiquitinated and its expression stabilised, complex I shifts to complex II and recruits FADD, leading to apoptosis activation. TNFR1 signal transduction contains a checkpoint in case signalling with complex I - NF-κB signalling pathway fails to be activated, cell death is triggered via complex II.

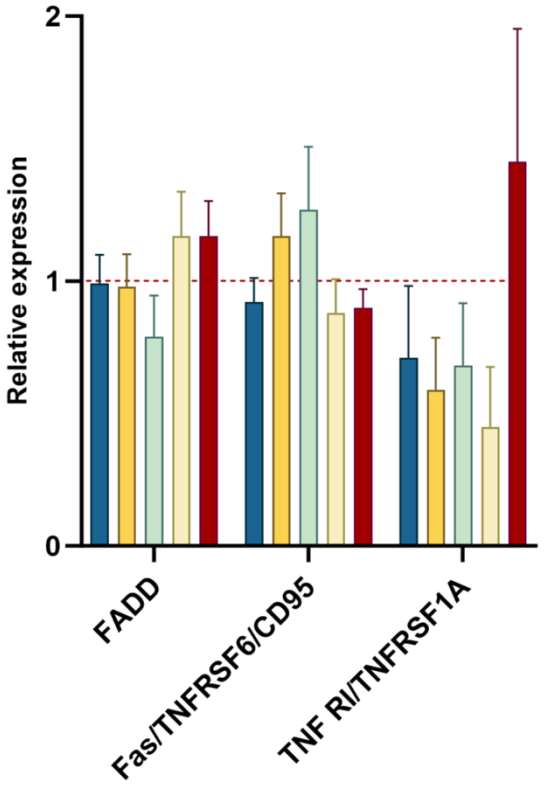

*Figure S.7. 2. Graphs depicting the expression levels of FADD, Fas/TNFRSF6/CD95 and TNFR1/TNFRSF1A.. Only statistically and clinically relevant differences are shown, with symbols denoting significance: * indicates significance vs control samples, & indicates significance vs oven samples, and # indicates significance vs other samples. *p<0.05, **p<0.01, ***p<0.001, ****p<0.0001*

7.1.7.1. HIF-1α

HIF-1α also interacts with p53 and activates its pro-apoptotic functions on Bcl-2, although this is slightly controversial.[265] In some instances, HIF-1 can translocate to the mitochondria after exposure to hypoxia. If hypoxic preconditioning had occurred before the hypoxic event, down-regulation of specific miRNAs maintained the mitochondrial membrane potential and blocked apoptosis.[327]

7.1.7.3. Catalase

Catalase and p53 have very tight interactions, in which cells overexpressing p53 lower catalase activity in stressed cells. This function of p53 is a pro-oxidant activity and pro-apoptotic effect on cells, making p53 a crucial regulator of intracellular ROS.[328]

7.1.8.1. p21/CIP/CDKN1A

Irradiation causes fluctuations in the expression of p21, being able to upregulate apoptosis (e.g. after photodynamic therapy on A431 cell line) or suppress programmed cell death (e.g. γ-irradiation on MCF-7 cell line).[279] In studies where p21 is involved in apoptotic inhibition, it does so by its direct interaction with pro-caspase 3 (preventing its activation) and blocking Fas receptor stimulation of apoptosis.[278,279] In the cases where p21 is considered pro-apoptotic, associated protein pRB must be mutated, then cell cycle is not arrested and signalling leads to apoptosis.[277]

7.1.8.3. p53

The p53 tumour suppressor protein and its gene, TP53, are among the most studied components in cancer biology due to their high mutation rate in most human cancers. Given this prevalence, it has been a focal point in cancer therapy for many years. p53 can bind to more than 500 genes, playing a pivotal role in regulating numerous cellular pathways, resulting in a highly complex pattern of interactions with genes and proteins.[284]

Regulation of p53 is mainly performed by ubiquitin ligase Mdm2, targeting p53 for proteasomal degradation in normal homeostatic conditions.[284–287] Low levels of p53 within the cell do not activate the transcription of apoptosis related genes and allows the cellular cycle to take place. If p53 is mutated, the cell cycle may proceed unchecked and facilitates the progression of cancer in the body.

However, in non-mutated instances, when the cell in under stress, p53 is phosphorylated (pp53) and can avoid Mdm2-mediated ubiquitination. In this case, p53 increases its half-life and can act as a transcriptional factor in the nucleus (Figure 11A). pp53 can activate the expression of pro-apoptotic genes and inhibit cellular proliferation, by upregulating p21 (Figure 10A).[284–287] However, phosphorylation of p53 at different sites modulates their interactions with the cell cycle and apoptosis.

7.1.8.5. Claspin

When replication stress is detected, claspin can be phosphorylated and act as an adaptor protein that passes the replication stress signal detected by sensor kinases, to Chk1 to facilitate a checkpoint arrest.[293,294] Phosphorylated claspin has major affinity for Chk1. If apoptosis has been triggered, claspin can be cleaved by Caspase-7, influencing the decision between cell cycle arrest and apoptosis.[295] Activation of Chk1 is vital in cellular response to genotoxic stress, but if claspin is not phosphorylated and cleaved by caspases, it cannot activate the checkpoint arrest and cells will undergo apoptosis (Figure 7.11).[295,296]

When replication stress is detected, claspin is phosphorylated and acts as an adaptor protein that passes the replication stress signal to Chk1 to facilitate a checkpoint arrest.[293,294] If apoptosis has been triggered, claspin can be cleaved by Caspase-7, influencing the decision between cell cycle arrest and apoptosis.[295] Activation of Chk1 is vital in cellular response to genotoxic stress, but if claspin is not phosphorylated and cleaved by caspases, it cannot activate the checkpoint arrest and cells will undergo apoptosis.[295,296]

Annex D

The information contained in this annex complements the data and text presented in Chapter 8 of this dissertation. All data featured in this annex are referenced in the main text. The content provided here serves as supplementary material to the figures shown in the main body.

IL-1			
+AuNR			p-val
30 min	vs	90 min	0.0001***
30 min	vs	6 h	0.0036**
60 min	vs	90 min	0.0093**
90 min	vs	4 h	0.0178*

IL-2			
+AuNR			p-val
2 h	vs	4 h	0.0265*
2 h	vs	6 h	0.0061**
3 h	vs	6 h	0.0240*

TNFα			
ØAuNR			p-val
2 h	vs	4 h	0.0240*
2 h	vs	6 h	0.0125*

IL-6			
CTL			p-val
30 min	vs	2 h	<0.0001****
		3 h	0.0005***
		4 h	0.0028**
60 min	vs	2 h	<0.0001****
		3 h	0.001**
		4 h	0.006**
90 min	vs	2 h	<0.0001****
		3 h	0.0033**
		4 h	0.0174*
2 h	vs	3h	0.0071**
		4 h	0.0012**
		6 h	<0.0001****

Table S 1. Statistical analysis results after PPTT for different cytokines. These tables present the results of the statistical analysis comparing different timepoints. Only statistically significant differences are shown, highlighting conditions where differences were observed for any of the studied timepoints. The corresponding graphs and detailed data can be found in Figure 4.